

CRANFIELD UNIVERSITY

CARLOS GÓMEZ-ARMAYONES

MODELLING THE AGRONOMIC AND ENVIRONMENTAL  
IMPACTS OF IRRIGATION MANAGEMENT ON TURFGRASS FOR  
GOLF GREENS IN NORTHERN EUROPE

SCHOOL OF WATER, ENERGY AND ENVIRONMENT  
Research Degree

Doctor of Philosophy (PhD)  
Academic Year: 2015 - 2018

Supervisor: Prof Jerry W. Knox and Dr Paul J. Burgess  
June 2018



CRANFIELD UNIVERSITY

SCHOOL OF WATER, ENERGY AND ENVIRONMENT  
Research Degree

PhD

Academic Year 2015 - 2018

CARLOS GOMEZ ARMAYONES

Supervisor: Prof Jerry W. Knox and Dr Paul J. Burgess  
June 2018

This thesis is submitted in partial fulfilment of the requirements for  
the degree of Doctor of Philosophy

© Cranfield University 2018. All rights reserved. No part of this  
publication may be reproduced without the written permission of the  
copyright owner.





## ABSTRACT

Irrigation is an essential component of turfgrass management for golf. During dry periods, it helps maintain turf health, stimulates nitrogen uptake, promotes germination, reduces canopy temperature, as well as assures high standards of quality for playability. In recent years, rising competition for water coupled with new environmental regulations has exerted pressure on water allocations for golf. Improving water efficiency and water management in golf have become major industry priorities.

The aim of this thesis was to understand and assess the relationships between irrigation management and turfgrass water use, soil water availability, dry matter production, drainage and nitrate leaching in golf greens under Northern European climate conditions. The research combined published science and industry evidence with field and experimental data, in order to calibrate and validate an irrigation ballistics-based model and a biophysical crop model (STICS). From this, an integrated model (BalliSTICS) was developed and used to simulate the impacts of irrigation uniformity on turfgrass growth and development and leaching risks, under contrasting management and climate scenario.

The modelling showed that system design plays a crucial role in achieving high irrigation uniformity, particularly sprinkler position and spacing. A larger spacing between sprinklers resulted in a decrease in irrigation rates and a significant decrease in uniformity, particularly when wind speeds exceeded  $2 \text{ m s}^{-1}$ . Surprisingly, the range of pressure and nozzle sizes investigated did not significantly impact on irrigation uniformity. Non-uniform irrigation was found to have a considerable impact on the spatial variability in turf growth, soil moisture content, drainage and leaching. Under northern European climate conditions, irrigation strategy had a more significant impact on turfgrass response than irrigation uniformity. A moderate deficit strategy (replacement of 60% potential evapotranspiration) was sufficient to achieve the highest growth values ( $233 \pm 10.6 \text{ g m}^{-2} \text{ season}^{-1}$ ). This strategy resulted in not only a reduction of irrigation water use but also minimised the amount of nitrate leached in drainage.

However, an inadequate irrigation schedule combined with poor irrigation uniformity ( $CU < 60\%$ ) led to a threefold increase in water use, and an average 114% and 50% increase in drainage and nitrate leaching, respectively. Inadequate irrigation practices had little impact on turfgrass growth, which could be misleading as excessive irrigation might not affect plant growth and visual quality but would mask poor irrigation uniformities, lead to excessive water use and an increase in risks of groundwater contamination from leaching. The research provides valuable and novel insights into better understanding the combined impacts of irrigation performance and management on turfgrass. The findings will support greenkeepers and the turfgrass industry and increase awareness of the importance of irrigation.

**Keywords:** Irrigation scheduling, irrigation uniformity, leaching, modelling, turfgrass

## **ACKNOWLEDGEMENTS**

First, I would like to acknowledge and thank my primary supervisor Prof. Jerry Knox for giving me the opportunity of being part of this exciting and challenging research. Thank you for all your guidance, support, suggestions, patience and encouragement throughout these three years. I would like to also acknowledge Dr Paul Burgess in his role of secondary supervisor, advice and useful critiques.

I would also like to extend the thanks to Dr Andre Daccache for all his appraisal regarding irrigation simulation. I want to express my sincere gratitude to Dr Trygve Aamlid for all his supportive feedback and technical support, for sharing with me his expertise on turfgrass, and for his hospitality during the weeks spent at Landvik, Norway. I also want to express my gratitude to the Nibio-Landvik team, especially to Agnar Kvalbein and Tatsiana Espevig, who made me feel like at home in Norway, where I met amazing people and discovered a wonderful country.

Thanks to the Scandinavian Turfgrass and Environment Research Foundation (STERF) for funding this research, in particular to Maria Strandberg. This work would not have been possible without the assistance from many research and industry specialists. Thanks to Thomas Pihl (Furesø GK), Albert Holmgeirsson (Oslo GK) and Gary Kenny (Ashford Manor GC) for all their help and support given during the fieldwork activities and for allowing me to access their sites and use of their facilities to conduct my trials. I would also like to thank Torben Kastrup Petersen, Edwin Roald, Mikael Frisk and Peter Edman for their translation assistance. Thank also to Samuel Buis and the STICS team for the invaluable help in model calibration; to Nigel Janes for technical support; and to Douglas Bomford Trust, Stuart Tate and Paul Shute (Xylem Lowara) for financial and logistics assistance.

I also wish to thank to my Cranfield colleagues and friends who have made my PhD experience a lifetime opportunity. Thank you for all the unforgettable moments, laughs and, from time to time, endless research conversations. Finally, and especially, thank you to my family and Silvia, that always supported my

decisions with endless love, and without whose encouragement this three-year journey would have been almost impossible.

# TABLE OF CONTENTS

ABSTRACT.....	i
ACKNOWLEDGEMENTS .....	iii
LIST OF FIGURES .....	viii
LIST OF TABLES .....	xv
LIST OF ABBREVIATIONS.....	xvii
1 INTRODUCTION .....	1
1.1 Background.....	1
1.2 Research definition.....	5
1.3 Aim and objectives .....	5
1.4 Thesis structure .....	6
1.4.1 Outline chapter content .....	8
2 LITERATURE REVIEW .....	11
2.1 Golf course fundamentals .....	11
2.1.1 Golf course layout .....	12
2.2 Turfgrass for golf .....	15
2.2.1 Turfgrass management practices .....	16
2.3 Golf course irrigation systems.....	20
2.3.1 Irrigation system performance and efficiency .....	20
2.3.2 Factors influencing irrigation uniformity .....	22
2.4 Modelling irrigation in turfgrass systems.....	24
2.4.1 Simulation models based on the ballistics theory.....	24
2.4.2 Other irrigation models .....	27
2.4.3 Crop models applied to turfgrass .....	28
2.4.4 Modelling impacts of irrigation uniformity on crop systems.....	31
3 METHODOLOGY OVERVIEW .....	35
3.1 Methodological framework requirements.....	35
4 ASSESSING EVIDENCE ON THE AGRONOMIC AND ENVIRONMENTAL IMPACTS OF TURFGRASS IRRIGATION MANAGEMENT .....	39
4.1 Introduction .....	39
4.2 Methodology .....	40
4.3 Results and discussion.....	45
4.3.1 Effects of irrigation management on turfgrass visual quality .....	45
4.3.2 Effects of irrigation management on root development.....	52
4.3.3 Effects of irrigation management on turfgrass growth rate.....	54
4.3.4 Effects of irrigation management on nitrogen fate.....	56
4.3.5 Methodological limitations .....	59
4.4 Summary .....	60
5 SIMULATING IRRIGATION HETEROGENEITY BASED ON BALLISTICS THEORY.....	63
5.1 Methodology .....	63
5.1.1 Field tests .....	63
5.1.2 Irrigation model development.....	70
5.1.3 Model calibration and validation.....	82
5.2 Results .....	84

5.2.1	Field tests .....	84
5.2.2	Calibration and validation of the irrigation model.....	90
5.2.3	Validation of overlapped patterns .....	98
5.3	Discussion .....	103
6	SIMULATING TURFGRASS GROWTH, WATER BALANCE AND LEACHING: STICS CROP MODEL SENSITIVITY ANALYSIS, CALIBRATION AND PERFORMANCE EVALUATION .....	111
6.1	Methodology .....	111
6.1.1	Study site and field data .....	112
6.1.2	Model selection for simulating turfgrass performance.....	115
6.1.3	STICS model overview.....	117
6.1.4	STICS model pre-parameterisation and assumptions.....	121
6.1.5	Sensitivity analysis .....	124
6.1.6	Model calibration .....	131
6.1.7	Model evaluation .....	134
6.2	Results .....	136
6.2.1	Sensitivity analysis .....	136
6.2.2	Model calibration .....	142
6.2.3	Model evaluation .....	144
6.3	Discussion .....	158
6.3.1	Performance evaluation of STICS model for turfgrass.....	158
6.3.2	Model limitations and opportunities for improvement.....	165
7	DEVELOPING AN INTEGRATED MODELLING FRAMEWORK TO SIMULATE IMPACTS OF IRRIGATION HETEROGENEITY ON TURFGRASS.....	169
7.1	Description of modelling framework.....	169
7.2	Model application - Simulated irrigation system performance.....	176
7.2.1	Methodology .....	176
7.2.2	Results .....	178
7.2.3	Discussion .....	185
7.3	Model application – Simulated impacts of irrigation strategy on turfgrass agronomy.....	189
7.3.1	Methodology .....	189
7.3.2	Results .....	190
7.3.3	Discussion .....	201
7.4	Model application – Simulated impacts of irrigation management on turfgrass agronomy.....	206
7.4.1	Methodology .....	206
7.4.2	Results .....	208
7.4.3	Discussion .....	223
8	DISCUSSION .....	229
8.1	Implications of the research .....	229
8.2	Integrated modelling approach.....	231
8.3	Implications for improving irrigation efficiency .....	233
8.4	Further research .....	241
9	CONCLUSIONS .....	243
	REFERENCES .....	249

ANNEXES.....	263
--------------	-----

## LIST OF FIGURES

Figure 1.1 Typical distribution of irrigation depths in sprinkler irrigation, where $H_R$ is required depth, $H_{max}$ is maximum depth, $H_{min}$ is minimum depth, $H_D$ is the depth of the water deficit, and $H_E$ is the fraction of the over-irrigated area. Figure adapted from Li (1998).....	4
Figure 1.2 Flow diagram of the thesis structure.....	7
Figure 2.1 Trend in number of golf courses and registered players in Europe between 1984 and 2016 (KPMG, 2017).....	11
Figure 2.2 Number of golf courses and registered players by country in Europe in 2016 (KPMG, 2017) .....	12
Figure 2.3 Different parts of a golf hole.....	13
Figure 2.4 Simplified nitrogen cycle in turfgrass systems adapted from Brown (2005) 18	
Figure 3.1 Overview of the methodology, results and discussion thesis chapters .....	36
Figure 4.1 Decision diagram for document inclusion/exclusion in the systematic review .....	44
Figure 4.2 Reported variation in turf quality depending on different irrigation amounts based three scheduling approaches (Epan, ETo, ETp) for cool- and warm-turfgrass species. The box and whisker plots display the quartiles and median values. Red crosses display outliers from the turfgrass quality values in the interquartile range (IQR) $\times$ 1.5. The minimum acceptable turfgrass quality 5 and 6 is highlighted (horizontal lines) (n = 555). ***p < 0.05 .....	46
Figure 4.3 Reported average turfgrass quality scores in relation to irrigation frequency (day) for (a) cool- and (b) warm-season turfgrasses. *Average scores for Kentucky bluegrass, tall fescue, junegrass [ <i>Koeleria macrantha</i> (Ledeb.) J.A. Schultes] and buffalograss.....	50
Figure 4.4 Reported variation in dry matter production in clippings (DMP) within treatments for different irrigation applications expressed as a percentage of irrigation applied (data extracted from seven studies) for (a) cool-season (n = 59) and (b) warm-season turfgrasses (n = 103). Circles display outliers for turfgrass quality values in the interquartile range (IQR) $\times$ 1.5, and stars display outliers beyond the IQR $\times$ 3.....	55
Figure 4.5 Reported relationships between N uptake ( $g\ N\ m^{-2}\ d^{-1}$ ) and dry matter production in clippings (DMP, $g\ m^{-2}\ d^{-1}$ ). *Results shown for Paré et al. (2006) are for clippings and shoot .....	55
Figure 4.6 Comparison of different nitrogen application rates ( $kg\ ha^{-1}$ ) on quantity leached when different irrigation amounts were applied in three different studies	57
Figure 4.7 Reported relationships between N fertiliser application rates per season/year/treatment ( $kg\ N\ ha^{-1}$ ) during the study period and N uptake ( $g\ N\ m^{-2}\ d^{-1}$ ) for (a) cool-season and (b) warm-season turfgrasses.....	59



Figure 5.1 Flow diagram of the methodology developed for the irrigation modelling ...	64
Figure 5.2 Location of the irrigation sprinkler test site .....	65
Figure 5.3 Close-up of the rotor sprinkler RainBird 751 SERIES.....	65
Figure 5.4 (a) View of the sprinkler stand installed in field. 1: Sprinkler RainBird 751 Series; 2: Pressure gauge; 3: Valve to control flow/pressure. (b) View of the pump station. 1: Pump Lowara 5SV14; 2: Flowmeter GPI A109LMA100IA1; 3: Pressure gauge. ....	66
Figure 5.5 Position of catchcans in the radial leg tests under 'no-wind' conditions. ....	68
Figure 5.6 Irrigation during the radial leg tests .....	68
Figure 5.7 Position of catchcans in tests under windy conditions .....	69
Figure 5.8 Panoramic view of the catchcan grid during an irrigation test .....	69
Figure 5.9 Variation in wind speed at different heights in turfgrass and wheat for wind 3 m s <sup>-1</sup> measured at 2 m height .....	76
Figure 5.10 Derived relationship between the percentage of evaporation losses (%) and droplet diameter (mm) based on equation proposed by Carrión et al. (2001b).....	77
Figure 5.11 Simulated trajectories (height and distance travelled) for four different droplet diameters ( $D_i$ ) from the exit of a sprinkler to the canopy based on ballistics theory. T: time travelled.....	78
Figure 5.12 Simulated trajectory of water droplets 5 mm in diameter at 4.2 bar pressure, with a wind speed of 3.5 m s <sup>-1</sup> . (a) X-Y view (b) Y-Z view (c) X-Z view .....	80
Figure 5.13 Distribution of different $D_i$ thrown every 10° under windy conditions (black dots) over a virtual squared mesh of pluviometers (blue dots) .....	81
Figure 5.14 Radial leg test conducted on 10 <sup>th</sup> June 2016. Sprinkler RainBird 751 Series, nozzle "#28 white" operating at 4.2 bar .....	84
Figure 5.15 Radial leg test conducted on 10 <sup>th</sup> 25 <sup>th</sup> October 2016. Sprinkler RainBird 751 Series, nozzle "#28 white" operating at 4.2 bar .....	84
Figure 5.16 Discharge radial curves for the RainBird 751 sprinkler using nozzles #28 (white) and #40 (orange) at operating pressures of 4.2 and 6.0 bar (Source: RainBird) .....	85
Figure 5.17 Windrose (left panel) and simulated wetting patterns (right panel) measured in two sprinkler tests. Upper panels (a,b) show results from a test with a high <i>WSU</i> . The lower panels (c,d) show results from a test with a low <i>WSU</i> . The black dots represent the catchcans and red dot the sprinkler location. ....	87
Figure 5.18 Correlation between simulated and measured WDEL (%) .....	89
Figure 5.19 (a) Reshaped sprinkler radial curve (mm h <sup>-1</sup> ) and (b) reshaped radial sprinkler flow (L h <sup>-1</sup> ); before and after applying WDEL .....	90
Figure 5.20 Influence of the corrector coefficients $K_1$ and $K_2$ on simulated distribution patterns. ....	92

Figure 5.21 Impacts of wind on measured wetted area and centre of gravity displacement (a) Variation of the wetted area by a single sprinkler for different wind speeds; (b) Variation of distance from sprinkler to the centre of gravity of the wetted area for different wind speeds. ....	93
Figure 5.22 Distortion of the sprinkler jet due to wind. ....	94
Figure 5.23 Simulated against observed (a) Christiansen’s Uniformity Coefficient (CU) and (b) Irrigation rate (IR) for the validation dataset .....	100
Figure 5.24 IR distribution of solid-set test simulation (upper panels) and overlapping of measured single sprinkler (lower panels) for test 10. Right panels present a zoom- in of its respective left panel. Red dots represent sprinkler location, and yellow lines limit the area on which irrigation CU. Values of CU were calculated for the catchcans inside the green. MAE = 2.9, RMSE = 3.8. ....	101
Figure 5.25 (a) Comparison of the irrigation rate ( $\text{mm h}^{-1}$ ) in each catchcan and average precipitation rate (dotted lines) for measured and simulated test 10 with sprinkler spacing $17.5 \times 17.5$ m. (b) Comparison of the cumulative distribution curves of water collected in the catchcans for simulated and measured overlapped irrigation. ...	102
Figure 5.26 IR distribution of solid-set test simulation (upper panels) and overlapping of measured single sprinkler (lower panels) for test 50. Right panels present a zoom- in of its respective left panel. Red dots represent sprinkler location, and yellow lines limit the area on which irrigation CU. Values of CU were calculated for the catchcans inside the green. MAE=3.3, RMSE=4.2 .....	102
Figure 5.27 (a) Comparison of the irrigation rate ( $\text{mm h}^{-1}$ ) in each catchcan and average precipitation rate (dotted lines) for measured and simulated test 50 with sprinkler spacing $20 \times 20$ m. (b) Comparison of the cumulative distribution curves of water collected in the catchcans for simulated and measured overlapped irrigation. ...	103
Figure 5.28 Nozzles #28 (white) and #40 (orange) used in the sprinkler RainBird 751 .....	108
Figure 5.29 Jet formation in the RainBird 751 sprinkler fitted with the nozzle #28. ....	109
Figure 6.1 Flowchart showing steps for model sensitivity analysis, calibration, validation and evaluation of STICS crop growth model for turfgrass. ....	111
Figure 6.2 Average monthly rainfall, reference evapotranspiration (ET <sub>o</sub> ) and temperature for Landvik from 1997 to 2016. Error bars represent the standard deviation. ....	112
Figure 6.3 Sequential steps followed as part of the STICS sensitivity analysis.....	125
Figure 6.4 Illustration of the eFAST sampling for one input parameter $Z_i$ , $w_i=5$ and $N=100$ samples .....	128
Figure 6.5 Illustration of the eFAST sampling for two input parameters, with $w_i=40$ and 800 samples per parameter .....	129
Figure 6.6 First order and total sensitivity indexes for cumulative evapotranspiration ( $ce_t$ ) at the end of the simulation period (30 <sup>th</sup> Sept), under non-water limiting (a) and water limiting conditions (b) conditions.....	137

Figure 6.7 Evolution of the first order and total sensitivity indexes for three input parameters on cumulative evapotranspiration ( <i>ce<sub>t</sub></i> ) over the simulation period for (a) non-water and (b) water limiting conditions.....	138
Figure 6.8 First order and total sensitivity indexes for average stomatic water stress index ( <i>swfac1moy</i> ) at the of the simulation period (30th Sept), under non-limiting (a) and limiting water (b) conditions. ....	139
Figure 6.9 First order and total sensitivity indexes for the cumulative dry matter in clippings ( <i>rendementsec</i> ) at the end of the simulation period (30th Sept), under (a) non-water limiting and (b) water limiting conditions. ....	140
Figure 6.10 First order and total sensitivity indexes for the cumulative NO <sub>3</sub> <sup>-</sup> -N in leaching ( <i>Q<sub>les</sub></i> ) (a); and average nitrogen nutrition index ( <i>inn1moy</i> ) (b) at the end of the simulation period (30th Sept), under non-water limiting conditions. ....	141
Figure 6.11 STICS simulated and measured gravimetric soil water content (GSWC, % w w <sup>-1</sup> ), irrigation applied and simulated drainage for 2013 (validation), 2014 (calibration) and 2015 (validation) for Treatments 1 to 3. ....	147
Figure 6.12 Comparison of simulated versus measured dry matter production (DMP) in clippings (left panel), analysis of the residuals against DMP simulation (centre panel), and distribution of the residuals (right panel). The upper panel corresponds to individual observation events (n=54), and lower panel represents the accumulated DMP in each simulated year (n=54). ....	149
Figure 6.13 Comparison between simulated and measured monthly accumulated dry matter production (DMP) in clippings (a) and accumulated DMP (b) for 2014 (calibration) and <i>treatment 1</i> .....	150
Figure 6.14 Comparison between simulated and measured monthly accumulated dry matter production (DMP) in clippings (a) and accumulated DMP in the simulated period (b), for 2015 (validation) and <i>treatment 1</i> .....	150
Figure 6.15 Comparison between simulated and measured monthly accumulated dry matter production (DMP) in clippings (a) and accumulated DMP in the simulated period (b), for 2015 and <i>treatment 3</i> .....	151
Figure 6.16 Comparison between simulated and measured cumulative dry matter production (DMP) in clippings at the end of each treatment in 2013, 2014 and 2015. ....	151
Figure 6.17 Simulated gravimetric (GSWC, % w w <sup>-1</sup> ) soil water content, irrigation applied, rainfall and drainage from 2007 to 2009 for treatments 4 and 5. ....	153
Figure 6.18 Comparison of measured against simulated water drainage (left panel), analysis of the residuals against drainage simulation (centre panel) and distribution of the residuals (right panel). The upper graphs correspond to monthly measurement events (n=21), and lower graphs represent the accumulated drainage in each simulated year (n=21). ....	155
Figure 6.19 Comparison of measured and simulated leaching (left panels), analysis of the residuals against leaching simulation (centre panels), and distribution of the residuals (right graphs). The upper graphs correspond to monthly measurement events (n=21), and lower graphs represent the cumulative leaching in each simulated year (n=21). ....	157

Figure 6.20 Monthly simulated and measured leaching ( $\text{g NO}_3^- \text{-N m}^{-2}$ ) in 2013, 2014 and 2015 for treatments 4 and 5.....	157
Figure 6.21 Simulated daily variation in $LAI_{(t)}$ for turfgrass using the STICS model. ...	163
Figure 7.1 Example of water distribution on a golf green, with a wind speed of $3 \text{ m s}^{-1}$ . (a) Histogram showing the distribution of irrigation rate. The red line corresponds to the lognormal distribution. (b) Cumulative distribution function (CDF) of irrigation rate .....	171
Figure 7.2 Flowchart summarising the BalliSTICS model links, inputs and outputs ...	174
Figure 7.3 Steps followed by the BalliSTICS model .....	175
Figure 7.4 Example of the combinations of sprinkler locations on green “Furesø F9”. .....	178
Figure 7.5 Modelled relationship between sprinkler set-up, sprinkler spacing and average irrigation rate. ....	181
Figure 7.6 Relationship between sprinkler set-up, sprinkler spacing and average irrigation rate. Variation in each boxplot is due to wind speed, wind direction and green shape. ....	181
Figure 7.7 Percentage variation in irrigation rate (IR) with respect to irrigation under no wind conditions for different wind speeds and sprinkler location. ....	183
Figure 7.8 Average values of the simulated Christiansen’s Uniformity Coefficient (CU, %) for wind speed from 0 to $5 \text{ m s}^{-1}$ considering (a) sprinkler set-up and (b) sprinkler displacement .....	184
Figure 7.9 Modelled variation in CU (%) due to wind direction and wind speed $5 \text{ m s}^{-1}$ for each simulated green.....	185
Figure 7.10 Boxplots showing irrigation applied (mm) between May and September for each irrigation depth strategy (ETp). Each boxplot is representative of different years and irrigation frequencies. ....	191
Figure 7.11 Comparison between irrigation needs and $ET_a$ by the plant for simulations considering rainfall (red dots, dashed line) and no rainfall (green dots, continuous line).....	193
Figure 7.12 Boxplots of seasonal available water content (SAWC, mm) between May to September for different irrigation depth strategy. Each boxplot is representative of different years and irrigation frequencies. ....	194
Figure 7.13 Accumulated drainage between May and September for irrigation strategies from 0 to 1.0 ETp and irrigation frequencies of 1, 2, 3 and 7 irrigation events per week. Each dot represents the average drainage for all irrigation treatments within each year (1997 to 2016). Error lines represent the standard deviation within each year. ....	195
Figure 7.14 Curve fitting of the simulated drainage in relation to irrigation amount and frequency between 1997 and 2016. Grey envelope shows the 95% confidence interval of the regression curve. Dots represent the results of individual simulations .....	196

Figure 7.15 Boxplots showing accumulated dry matter production in clippings (DMP, g m <sup>-2</sup> ) between May and September for different ETp treatments. Each boxplot is representative of different years and irrigation frequencies.....	197
Figure 7.16 Comparison between irrigation needs and simulated DMP in clippings for simulations considering rainfall (red dots, dashed line), and no rainfall (green dots, continuous line).....	198
Figure 7.17 Curve fitting of the simulated leaching in relation to irrigation level and irrigation frequency during the period 1997-2016. Grey area behind lines show the 95% confidence interval of the regression curve. Dots represent the results of individual simulations .....	199
Figure 7.18 Relationship between leaching and dry matter in clippings according to ETp strategy between 1997 and 2016. Numbers correspond to ETp strategy and error bars represent the standard deviation of each variable .....	200
Figure 7.19 Conceptual relationship between dry matter production (DMP), drainage, leaching and DMP/leaching rates for different irrigation depth strategies (ETp) under Northern European climate conditions. ....	205
Figure 7.20 Variation in water applied inside the green with respect to 100 % CU as affected by non-uniform irrigation for (a) IS <sub>AVE</sub> and (b) IS <sub>DRIEST</sub> scheduling methods .....	208
Figure 7.21 Seasonal available water content (SAWC) across the green for different irrigation strategies and irrigation heterogeneities when using the IS <sub>AVE</sub> scheduling method. (a) No rain; (b) Average year; (c) Dry year; (d) Wet year. ....	210
Figure 7.22 Seasonal available water content (SAWC) across the green for different irrigation strategies and irrigation heterogeneities when using the IS <sub>DRIEST</sub> scheduling method. (a) No rain; (b) Average year; (c) Dry year; (d) Wet year....	211
Figure 7.23 Variation in drainage across the green with respect to perfect irrigation uniformity, for different climate years, irrigation strategies and irrigation uniformities. Red lines indicate the average values across the green. (a) IS <sub>AVE</sub> scheduling method. (b) IS <sub>DRIEST</sub> scheduling method .....	214
Figure 7.24 Dry matter production in clippings across the green for different irrigation strategies and irrigation heterogeneities when using the IS <sub>AVE</sub> scheduling method. (a) No rain; (b) Average year; (c) Dry year; (d) Wet year.....	216
Figure 7.25 Dry matter production in clippings across the green for different irrigation strategies and irrigation heterogeneities when using the IS <sub>DRIEST</sub> scheduling method. (a) No rain; (b) Average year; (c) Dry year; (d) Wet year.....	217
Figure 7.26 Variation rate of nitrate leaching respect perfect irrigation uniformity, for different climate years, irrigation strategies and irrigation uniformities. Red lines indicate the average values across the green. (a) IS <sub>AVE</sub> scheduling method. (b) IS <sub>DRIEST</sub> scheduling method.....	219
Figure 7.27 Hourly wind speed, averaged by month, recorded at Landvik between 1997 and 2016 .....	221

Figure 7.28 Comparison of the simulated daily Christiansen's Uniformity Coefficients (CU, %) for morning and afternoon irrigation in from May to September between 1997 and 2006 at Landvik .....	222
Figure 7.29 Simulated wind drift and evaporation losses (WDEL) for morning and afternoon irrigations and operating pressures 4.2 and 6.0 bar .....	223
Figure 8.1 Relationships between golf practice, agronomic and sustainability aspects in turf irrigation management .....	234
Figure 8.2 Schematic for proposing improvements in turfgrass irrigation efficiency...	236

## LIST OF TABLES

Table 1.1 Matrix of the relationship between individual thesis chapters and each research objective. ....	8
Table 2 Quality rating for $DU_{LQ}$ (Mecham, 2004) .....	22
Table 5.1 Performance of the RainBird 751 sprinkler under test conditions (source: RainBird). ....	66
Table 5.2 Summary of weather and operating conditions for single sprinkler tests under windy conditions. Standard deviation values given in brackets. ....	86
Table 5.3 Pearson's correlation coefficients and $p$ -value of the measured WDELm and measured variables in field, for selected weather variables .....	88
Table 5.4 Proposed WDEL equations based on the multivariate linear regression.....	89
Table 5.5 Mean values for the corrector coefficients of $K_1$ and $K_2$ and the similitude parameters of the single sprinkler and different set-ups for the calibration dataset .....	95
Table 5.6 Similitude parameters for the single sprinkler and different set-ups derived for the calibration dataset.....	98
Table 5.7 Average CU from measured ( $CU_{meas}$ ) and simulated ( $CU_{sim}$ ) sprinkler overlapping, average errors between measured and simulated CU ( $CU_e$ , %), and average MAE and RMSE within tests. Results presented for each sprinkler set-up and distance. Standard deviation values are shown in brackets.....	99
Table 6.1 Penman-Monteith ETo and irrigation applied (mm) by treatment and year ( <i>Study 1</i> ).....	114
Table 6.2 Pan evaporation, rainfall and irrigation applied (mm) in <i>Study 2</i> .....	115
Table 6.3. Selected crop models and main features .....	116
Table 6.4 Initial assumptions of plant parameter values used in the pre-parameterisation of turfgrass, compared against default values for forage crops tall fescue, ryegrass, and grass provided in STICS.....	123
Table 6.5 Parameters selected for sensitivity analysis and uncertainty ranges used for sensitivity sampling .....	126
Table 6.6 Steps, parameters and datasets used in the parameter calibration phase.	132
Table 6.7 Datasets and years used for model calibration and validation.....	132
Table 6.8 Results from the parameter calibration for the water balance and biomass production modules in <i>Study 1</i> .....	143
Table 6.9 Results from the parameter calibration for the water balance and leaching modules for <i>Study 2</i> .....	143

Table 6.10 Number of measurements (n), mean bias error (MBE) and root mean square error (RMSE) for prediction of gravimetric soil water content (GSWC, % w w <sup>-1</sup> ) for the calibration and validation datasets in <i>Study 1</i> .....	146
Table 6.11 Number of measurements (n), mean bias error (MBE) and root mean square error (RMSE) in the prediction of the dry matter production in clippings (g m <sup>-2</sup> ) for the calibration (2014) and validation (2013, 2015) datasets in <i>Study 1</i> .....	148
Table 6.12 Number of measurements (n), mean bias error (MBE) and root mean square error (RMSE) in the prediction of the monthly and annual drainage for the calibration (2008) and validation (2007, 2009) datasets in <i>Study 1</i> .....	154
Table 6.13 Number of measurements (n), model efficiency (ME), mean bias error (MBE) and root mean square error (RMSE) in the prediction of the monthly and annual leaching for the calibrated and validated datasets in <i>Study 2</i> .....	156
Table 7.1 Output variables from STICS used for the assessment of turfgrass growth and performance .....	172
Table 7.2 Options available in BalliSTICS and their relation to each sub-model.....	173
Table 7.3 Golf greens characteristics used in simulations .....	177
Table 7.4 Summary of BalliSTICS simulations to assess irrigation heterogeneity impacts on golf greens .....	177
Table 7.5 Irrigation rate (IR, mm h <sup>-1</sup> ) and CU (%) under ‘no-wind’ conditions and original sprinkler location, for each sprinkler set-up and simulated green.....	179
Table 7.6 Irrigation rate (IR, mm h <sup>-1</sup> ), and CU (%) under ‘no-wind’ conditions for different sprinkler locations .....	180
Table 7.7 Number of simulations of turfgrass agronomy for perfect irrigation uniformity .....	190
Table 7.8 Ranked Summer irrigation needs (mm) for a 1.0 ET <sub>p</sub> strategy, ET <sub>o</sub> , May to September rainfall and number of rainfall events between 1997-2016. Numbers in brackets are standard deviation for different irrigation frequencies.....	192
Table 7.9 Number of simulations of turfgrass agronomy regarding different irrigation strategies, different irrigation heterogeneity profiles and rain patterns.....	207
Table 7.10 Average SAWC uniformity (CU <sub>SAWC</sub> ,%) for high irrigation CU (82%) and low irrigation CU (50%), rain patterns and irrigation scheduling methods .....	212



## LIST OF ABBREVIATIONS

CDF	Cumulative distribution function of irrigation applied
CU	Christiansen's Uniformity Coefficient (%)
CU <sub>SAWC</sub>	Seasonal available water content uniformity (%)
DMP	Dry matter production in clippings ( $\text{g m}^{-2}$ , $\text{g m}^{-2} \text{d}^{-1}$ )
DU <sub>LQ</sub>	Lower quarter distribution uniformity (%)
Epan	Pan evaporation (mm)
ET	Evapotranspiration (mm)
ETa	Actual evapotranspiration (mm)
ETo	Reference evapotranspiration (mm)
ETp	Potential evapotranspiration (mm)
GSWC	Gravimetric soil water content ( $\% \text{ w w}^{-1}$ )
IDE	Irrigation discharge efficiency (%)
IF	Irrigation frequency
IL	Irrigation level
IR	Irrigation rate
IU	Irrigation uniformity
Kc	Crop coefficient
LAI	Leaf Area Index ( $\text{m}^2 \text{ m}^{-2}$ )
MAE	Mean absolute error
MBE	Mean bias error
N	Nitrogen
RMSE	Root mean squared error
SAWC	Seasonal available water content (mm)
SR	Systematic Review
SWC	Soil water content (mm)
TQ	Turfgrass quality
VSWC	Volumetric soil water content ( $\% \text{ v v}^{-1}$ )
WD	Wind direction (degrees)
WDEL	Wind drift and evaporation losses (%)
WS	Wind speed ( $\text{m s}^{-1}$ )
WSU	Wind speed uniformity (%)



# 1 INTRODUCTION

This chapter introduces the context for the research and the importance of irrigation as a major component in improving water efficiency and turfgrass management for golf. The terms irrigation management, efficiency, accuracy and uniformity, which all need clear explanation, are also defined. Finally, the research problem, aim and objectives and thesis structure are provided.

## 1.1 BACKGROUND

In recent decades, golf has increased in popularity due to the multiple benefits offered by this sport. Despite golf courses having had a poor reputation for being harmful to the environment, several investigations highlight that well-managed golf courses can provide considerable benefits to the environment, enhancing landscape beauty, improving mental and physical human health and supporting national economies (Stier et al., 2013). In 2016, there were reported to be 6,924 golf courses in Europe, with 4.22 million registered players; this constitutes more than double the number of golf courses and almost three times more registered players than thirty years ago (KPMG, 2017).

This major increase in popularity has been accompanied by a corresponding demand for year-round high-quality playing areas. Golf courses areas are mainly comprised of fine turfgrass, in addition to trees, natural vegetation and obstacles such as lakes and bunkers. The importance of turfgrass in golf relies not only on its ornamental and environmental functionality but also on its impact on golf playability (Beard, 2000). This is influenced by a number of factors including turfgrass uniformity, density, smoothness and firmness; which must allow the ball to bounce and roll without plugging into the turf (Moeller, 2013). Those proprieties are particularly crucial on greens. Although greens only comprise about 2% of the total on a golf course (Beard, 2002), they are the areas that receive the most traffic and hence intense management on the whole course (McClellan et al., 2009). Management activities on greens include frequent and short mowing, fertiliser and pesticide applications, aeration, sand capping and irrigation.

Irrigation helps to meet turf water requirements during periods of drought stress or low rainfall, as well as maximising turf playability, improving nutrient use efficiency, reducing canopy temperature and is an important component in turf seeding and re-establishment. Thus, water is a critical element for successful turfgrass management. However, water is becoming a scarce resource, even in humid and temperate regions where rainfall is abundant (Daccache et al., 2012). In recent years, population growth in Europe coupled with changing long-term availability and the short-term variability of water resources is adding further pressure on water allocations (Olmstead, 2014; Rey et al., 2018). Under this scenario, competition for water between agriculture, public and leisure water supply coupled with new environmental regulations have become a major concern for the golf industry (Strandberg et al., 2012).

Rising improvements in irrigation management to enhance turf quality while reducing water consumption and negative environmental impacts have become “driver for change” in turfgrass management. According to the United States Department of Agriculture (USDA, 2006 p. 1) irrigation management is “the process of determining and controlling the volume, frequency and application rate of irrigation water in a planned, efficient manner”. In this research, we refer to irrigation management as the sum of actions at the golf green scale that involve irrigation system performance and irrigation strategy. Hence, the concept of irrigation management is linked to questions including: *how much water should I apply?* and *how often should irrigation be applied?* Poor or inadequate irrigation management reduces turf quality and can lead to water and energy wastage and groundwater contamination from nutrient and pesticide leaching and run-off (Shuman, 2002a; Branham, 2006). It is therefore essential to meet the exact turf water requirements whilst also ensuring that any negative environmental impacts are minimised.

Successful irrigation management therefore relies on knowing how much water is required by plants, how much water needs to be provided during each irrigation event, and how much water is supplied by the irrigation system. Failure in any of these steps will inevitably lead to inefficient irrigation. In this research, irrigation

efficiency relies on the ability of the irrigation system to deliver a desired water amount; and the heterogeneity in water application across the irrigated area. These concepts are addressed by the terms *irrigation adequacy* and *irrigation uniformity*, and are embraced by the irrigation management practices. Irrigation adequacy indicates the ability of an irrigation system to deliver the required amount of water that can be stored in the effective root zone and meet the crop water requirement (Dinka, 2016). Irrigation heterogeneity relates to the spatial variability in irrigation water application across the irrigated area.

All irrigation systems apply water non-uniformly to varying degrees. In this research, this characteristic is referred to as irrigation heterogeneity and quantified by the use of irrigation uniformity indexes. According to Pereira (1999), factors affecting irrigation uniformity include the operating pressure, sprinkler spacing, nozzle size, water distribution pattern of the sprinkler and wind speed. Thus, irrigation uniformity is influenced by system design and environmental factors. Although irrigation adequacy provides essential information on the performance of the system, irrigation heterogeneity is also considered a critical indicator of system performance (Maroufpoor et al., 2010).

Low irrigation uniformities will result in areas that are either under-watered or over-watered. A conceptual distribution of water across an irrigated area as affected by irrigation heterogeneity is shown in Figure 1.1. Low values of irrigation uniformity lead to an increase in the difference in water applied between areas receiving more and areas receiving less water, which are represented by  $H_{\max}$  and  $H_{\min}$ , respectively. Plants may experience water stress in areas that are under watered ( $H_D$ ), whilst regions receiving more water ( $H_E$ ) than required will be more prone to drainage and, when the infiltration rate is low, to losses through surface runoff (Odhiambo et al., 2011).

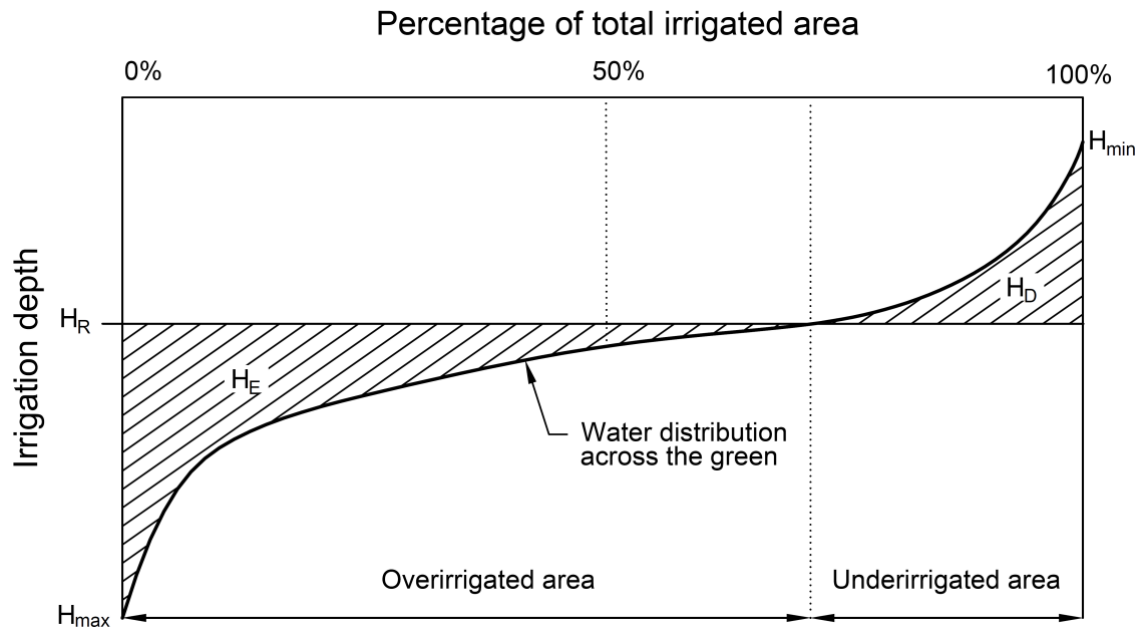


**Figure 1.1** Typical distribution of irrigation depths in sprinkler irrigation, where  $H_R$  is required depth,  $H_{max}$  is maximum depth,  $H_{min}$  is minimum depth,  $H_D$  is the depth of the water deficit, and  $H_E$  is the fraction of the over-irrigated area. Figure adapted from Li (1998).

To date, studies investigating the links between irrigation uniformity on crop growth have been limited to agricultural crops (eg Pérez-Ortolá et al. (2016), González-Perea et al. (2017)) and mainly used biophysical crop modelling approaches. The main reason for the use of crop models is the difficulty and cost in assessing the impacts of irrigation uniformity on crop development under field conditions. Numerous studies have reported that lower irrigation uniformity leads to higher water consumption (Mantovani et al., 1995), lower yields, an increase of production costs (Brennan, 2008) and an increased risk of nitrogen leaching (Pang et al., 1997). However, the impacts of irrigation heterogeneity on turfgrass systems has not been studied.

The use of models allows pilot investigations to be conducted and to speed up research, as well as to generate infinite sampling conditions that would be impractical to recreate in field conditions (Li et al., 2012). In addition to their ability to predict crop yields, water consumption or nitrogen fixation under defined environmental and management conditions, models are also useful tools for improving decision-making, the planning and allocation of water resources, the evaluation of economic and environmental performance of farming systems, and

for assessing the impacts of climate change and droughts on a particular crop type (Jones et al., 2017a).

To date, there has been research on modelled turfgrass systems to evaluate the implications of different management practices on nitrogen balances (Qian et al., 2003; Zhang et al., 2013b); water and/or nitrogen transport in golf soils (McCoy and McCoy, 2009; Filipović et al., 2014); to estimate nitrogen leaching (King and Balogh, 1999; Jackson and Estes, 2007; Zhang et al., 2013b) and carbon budgets (Bandaranayake et al., 2003; Milesi et al., 2005; Bartlett and James, 2011a) and on turfgrass quality (Wilkerson et al., 2015). However, none of these studies considered the effects of water heterogeneity on turfgrass performance. Studying the impacts of irrigation management on turfgrass systems will help the sportsturf industry have a deeper understanding on this topic and support adoption of new strategies that maximise water use efficiency and reduce the environmental risks associated with turf irrigation.

## **1.2 RESEARCH DEFINITION**

The research question in this thesis was: How does irrigation management on golf greens affect turfgrass performance and the environment? To assess the existing links between irrigation management, turfgrass agronomy and environmental impacts; and to provide the necessary evidence to address this question, a combined approach involving literature review, field data collection and ballistic and biophysical modelling has been completed. The research was mainly based at Cranfield University, with occasional trips to Norway and Denmark for data collection for model calibration, and to conduct irrigation evaluations and interview golf industry stakeholders.

## **1.3 AIM AND OBJECTIVES**

The aim of this thesis was to understand and assess the relationships between irrigation management and turfgrass water use, soil water availability, dry matter production, drainage and nitrate leaching in golf greens under Northern European climate conditions.

To achieve the aim of this research, four research objectives were setup:

- i) To critically review and synthesise existing science and industry evidence on the links between irrigation management, turfgrass agronomy and environmental impacts;
- ii) To develop, calibrate and validate a ballistics-based model to simulate irrigation system performance under contrasting environmental and irrigation design conditions;
- iii) To calibrate and validate a biophysical crop growth model to simulate changes in dry matter production, water use and nutrient leaching for fine turf under varying environmental conditions, and;
- iv) To simulate a range of irrigation management strategies on turfgrass agronomy and their environmental impacts through the development of an integrated irrigation-crop modelling framework.

## **1.4 THESIS STRUCTURE**

This thesis is organised in seven sections and split into ten chapters. The whole thesis is composed of an *introduction*, followed by a *literature review*, *methodology*, *results*, *discussion*, *conclusions* and *references*. The methodology contains four chapters to reflect the complex approach which was developed. Figure 1.2 provides a schematic summarising the thesis structure. The relation between each chapter and their relevance to the thesis objectives is shown in Table 1.1.



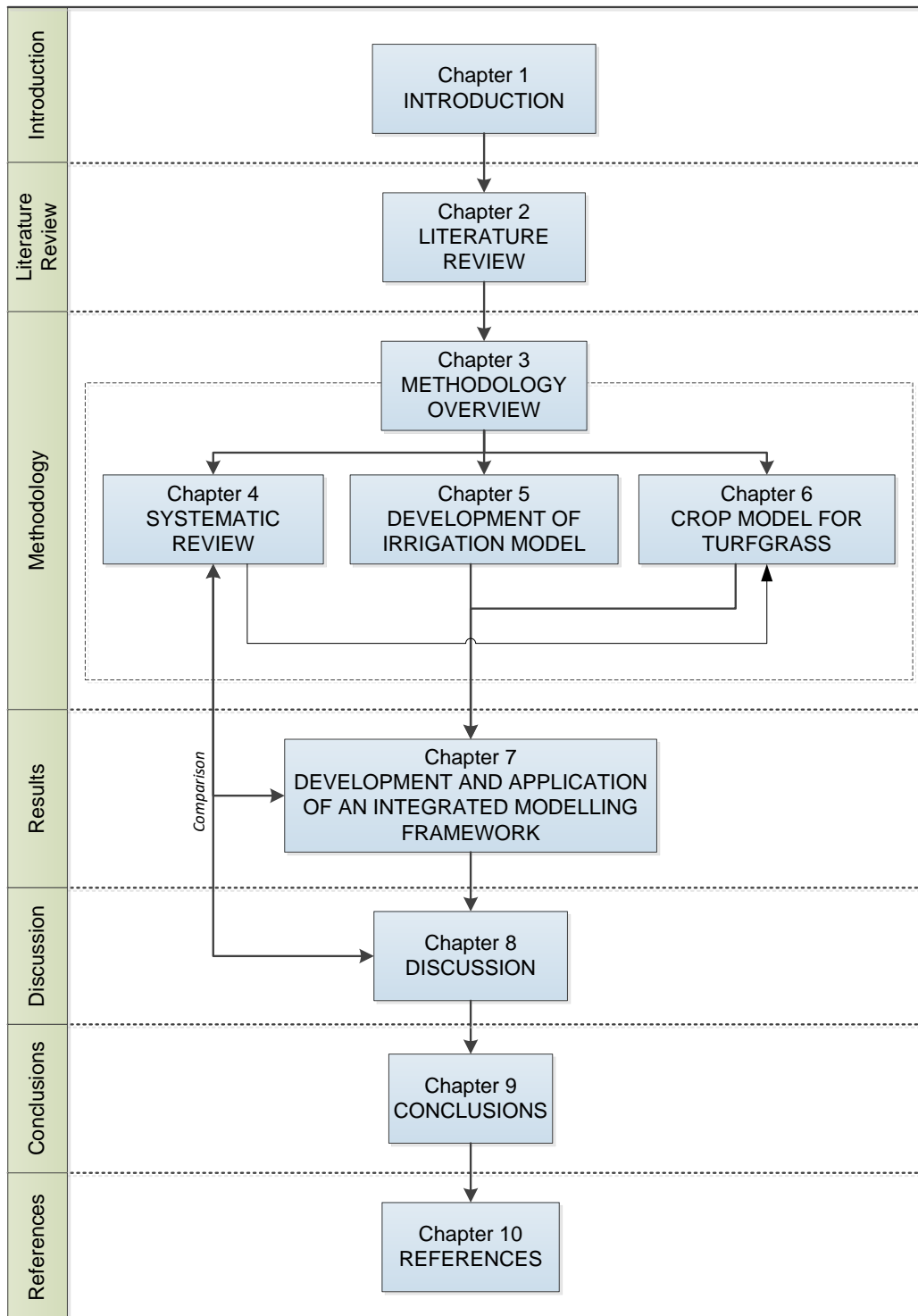


**Figure 1.2** Flow diagram of the thesis structure

**Table 1.1** Matrix of the relationship between individual thesis chapters and each research objective.

Chapter	Objective			
	i	ii	iii	iv
1. Introduction				
2. Literature review				
3. Methodology overview				
4. Systematic review				
5. Development of an irrigation model				
6. Crop model for turfgrass				
7. Integrated modelling framework				
8. Discussion				
9. Conclusions				

### 1.4.1 Outline chapter content

A brief description of each chapter is presented below:

**Chapter 1** outlines the background of the research and introduces the topic of the problem investigated. The aim and objectives are presented, specifying the links between chapters and objectives.

**Chapter 2** provides a brief review of golf course turfgrass maintenance and management including irrigation system design and the factors affecting irrigation efficiency. Irrigation and process-based crop models are also reviewed.

**Chapter 3** presents the research framework methodology and outlines the rationale for data collection and development of an integrated modelling approach. It explains how the individual methodologies developed in Chapters 4 to 6 are related.

**Chapter 4** synthesises the results from a systematic review of published evidence of irrigation impacts on turfgrass and the environment. The findings are later used to complement the discussion of the integrated modelling approach presented in Chapter 7.

**Chapter 5** describes the approach to develop a model that simulates irrigation heterogeneity on golf greens using ballistics theory under windy and non-windy conditions.

**Chapter 6** evaluates and discusses the STICS crop growth model for simulating water balance, dry matter production in clippings and nitrogen leaching in turfgrass on greens.

**Chapter 7** details the steps followed in the development of a model framework that couples the irrigation model (Chapter 5) with the crop model (Chapter 6). A number of scenarios were defined which combine different irrigation system configurations, irrigation strategies and weather conditions. The model outcomes are presented, providing data to quantify the impacts of irrigation management on the water balance, turfgrass growth and nitrogen leaching in greens. The results from the modelling framework are critically evaluated and discussed.

**Chapter 8** evaluates the results from the integrated modelling process, linking the findings from different chapters. Key findings to address the question *How does irrigation management in golf greens affect turfgrass performance and the environment?* are presented. The methodology is also critically discussed highlighting the advantages and limitations. An approach for improving golf irrigation efficiency and best management practices in Nordic countries are defined; as well as the potential implications of the research on the Nordic golf industry. Finally, areas for further research are identified and described.

**Chapter 9** summarises the key findings and main conclusions of the research linked to the objectives identified in Chapter 1.

**Chapter 10** includes a detailed bibliography of references used in the research.



## 2 LITERATURE REVIEW

This chapter provides a review of golf course turfgrass maintenance and management including irrigation system design and the factors affecting irrigation efficiency. Irrigation and process-based crop models are also reviewed.

### 2.1 GOLF COURSE FUNDAMENTALS

According to the Rules of Golf (R&A and USGA, 2016), the game of golf consists of playing a ball with a club from the teeing ground into the hole by a stroke or successive strokes. The game originated during the 14<sup>th</sup> century on the British coastal areas. Today golf courses are designed to emulate the natural conditions from which the game originated (R&A, 2017).

In recent decades, the number of golf courses around the world has increased significantly. According to the R&A (2017) in 2016 golf was played on 33,161 courses in 208 countries with Europe having 6,924 courses and more than 4 million registered players. Assuming an average size of 62 ha per course (Kuiper, 1997), the estimated area occupied by golf courses in Europe is 4,293 km<sup>2</sup>. The popularity of golf in Europe increased from the 1980s until the mid-2000s but the trend has stabilised since then (Figure 2.1). From 1984 to 2016, the number of registered players in Europe has tripled while the number of golf courses has more than doubled.

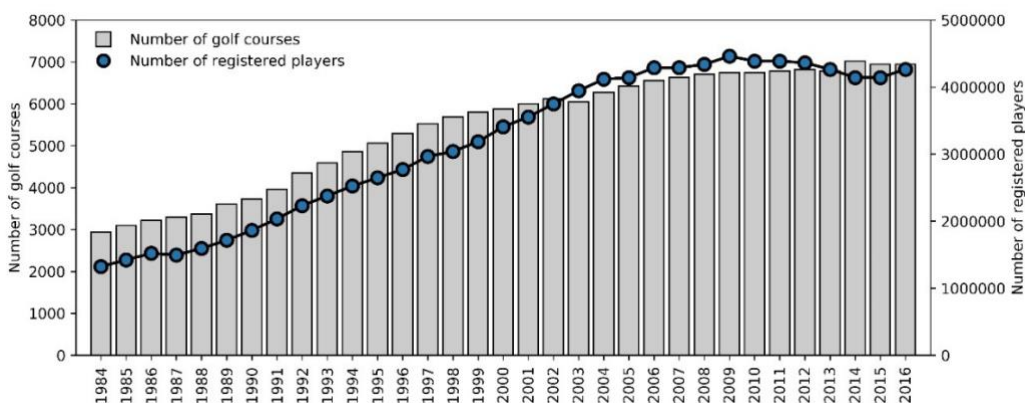


**Figure 2.1** Trend in number of golf courses and registered players in Europe between 1984 and 2016 (KPMG, 2017)

Figure 2.2 shows the number of golf courses and registered players for 20 countries in Europe (KPMG, 2017). England has the greatest popularity for golf,

with 1,907 courses and 694,623 players, followed by Germany, France, Scotland, Sweden and Ireland. The countries with a larger number of courses are located within temperate oceanic and continental climates, with rainfall spread throughout the year and a large seasonal variation in temperature.

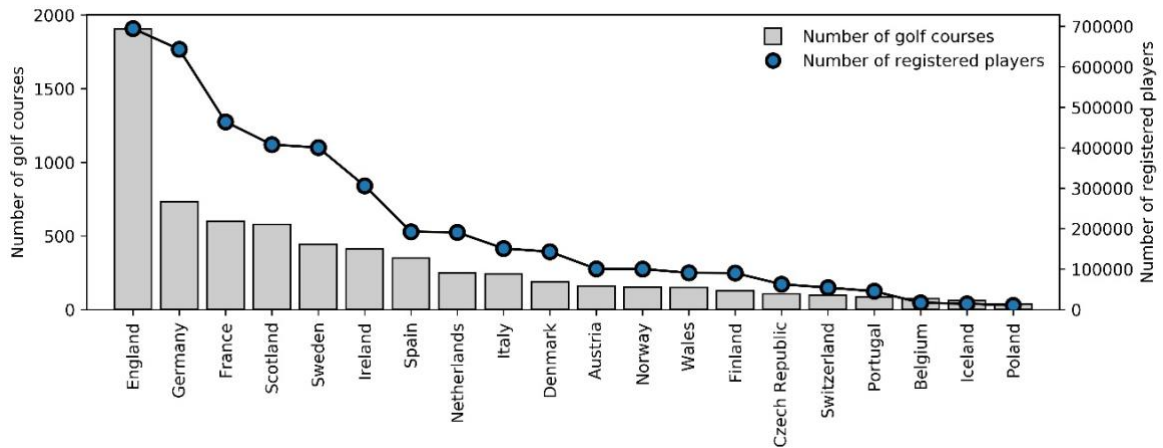


**Figure 2.2** Number of golf courses and registered players by country in Europe in 2016 (KPMG, 2017)

### 2.1.1 Golf course layout

A well-designed golf course aims to deliver a beautiful site which is aesthetically pleasing and enjoyable to play (Beard, 2002). Its design should balance with the constraints given by the local topography and aspects of design such as surface and subsurface drainage, the natural environment, soil and selection of turfgrasses and other vegetation (Kuiper, 1997). Its design must allow maintenance of the course for high quality playing conditions whilst ensuring its management is economically viable (McCarty, 2005). Golf courses are usually composed of 9, 18 or 27 holes. The aim of golf is to use the least number of strokes on all holes. Most of the area where the game occurs is covered by turfgrass which requires intense management. The parts of a hole are shown in Figure 2.3 and described in detail below.

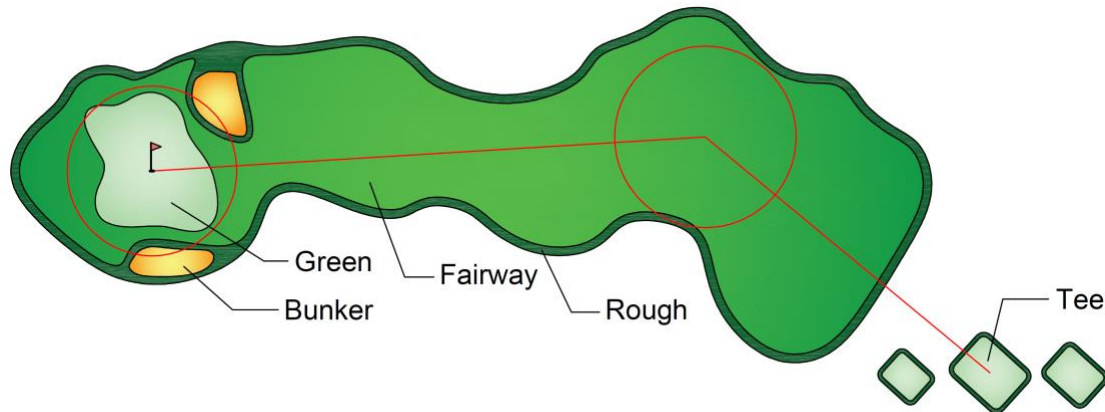


**Figure 2.3** Different parts of a golf hole.

### Green

According to the Rules of Golf (2016 p. 41), a “green or putting green is all ground of the hole being played which is specially prepared for putting or otherwise defined as such by the committee”. These areas are covered by fine leaf turfgrass mowed at very short heights (Beard, 2002). Each green is unique in shape and size. They can be flat, sloped, ranging in contour, and with an area generally comprised between 300 and 700 m<sup>2</sup>. Despite their small size compared with other areas, greens are the most critical area on the course. A green should be large enough to provide a variable surface, offer a challenge to the golfer and provide flexibility in hole placement and the associated rotation of traffic. Greens require intense maintenance to reduce plant stresses produced by the short mowing heights and high levels of soil compaction from the intense traffic of players and turf machinery.

Hartwiger (2014) described three characteristics of green surfaces which impact on golf playability: surface firmness, green speed and green slope. The surface firmness influences the reaction of the ball to a shot landing on the green. When the green surface is less firm, the ball does not move as far from where it lands. Green speed influences how far a ball rolls on a flat surface and is governed by the resistance of the surface to ball roll. The slope around the hole location influences the difficulty of the putt. Another essential playability quality is turfgrass resilience (Adams and Gibbs, 1994), which is the capacity of the turfgrass to return to its original position after the ball strikes the surface.

All these playability proprieties are closely linked with the level of thatch-mat in the root zone. Thatch is composed of accumulated dead (thatch) and living (mat) stems and roots hidden below the green vegetation (Gaussoin et al., 2013). An excessive thatch is related with poor playability, low water infiltration, increased localised dry spots, reduced tolerance to cold temperatures, increased disease and insect problems and reduced pesticide effectiveness (Callahan et al., 1997; McCarty et al., 2007; Carley et al., 2011). An excessive thatch layer is usually related to too intense growth rates, and therefore plant tissue development rate is quicker than organic matter microbial decomposition (Christians et al., 2017). Thatch can be controlled by practices such as aeration, vertical cutting, sand capping or use of wetting agents (Callahan et al., 1997). Reducing the level of nitrogen fertilisation might also reduce the thatch layer as it reduces growth rates. Greenkeepers continually seek turf management practices that strike a balance between combating excessive thatch production, whilst ensuring enough growth for the turf to recover from traffic stresses.

To provide the appropriate surface firmness, avoid excessive thatch layer development and improve the infiltration rate of the soil, greens are usually built following the USGA (2004) rootzone construction specifications. This is characterised by a high-sand content built over a gravel layer that provides excellent internal drainage and minimises the risk of soil compaction (Beard, 2002). Despite the benefits of the USGA method, the sandy soil character of these types of construction along with shallow root depths on greens usually leads to a low soil water storage capacity. For this reason, well managed irrigation on greens is essential to keep healthy turfgrass during periods with high water demand and low rainfall.

### Tee

The tee is the starting place for the hole (R&A and USGA, 2016) and has an area that is specially prepared for hitting the first shot. According to Beard (2002), good turfgrass conditions in tees include a relatively flat and smooth surface, firm, dense, uniform, resilient and closely cut. Turfgrass species and management



strategies in tees are similar to greens, as turfgrass in those areas need to tolerate short mowing heights, divots and soil compaction from player wear.

### Fairway

The fairway is the area between the tee and green and consists of the part of the course with the largest playable surface. Fairways usually receive lower maintenance than tees and greens, as they are mowed less frequently and have higher cuts (10-20 mm). Building fairways on native soils is common practice.

### Rough

The rough surrounds the greens, tees and fairways and due to its non-playable nature receives low or no maintenance. Plants in roughs usually include native species. Rough areas can comprise up to 70% of the total area of a course (Beard, 2002).

## **2.2 TURFGRASS FOR GOLF**

According to the USGA (2018) turfgrass is a vegetative ground cover composed of close cut, thickly growing, intertwining stems and leaves of grass plants. Despite the large number of perennial grasses species, only a few perform adequately on greens. In these areas, turfgrass must provide features that differentiate them from other species used in grasslands or on domestic lawns. These are (i) the tolerance to frequent and close mowing, (ii) very high and uniform shoot density, (iii) fine leaves, (vi) tendency to produce erect leaves, and (v) good recovery from stresses associated with golf practice (Beard, 1973). In addition, the choice of species is driven by the local climate, and, to a lesser extent, by the budget of the course and required intensity of maintenance (McCarty, 2005; Aamlid and Molteberg, 2011). Based on their temperature requirements, turfgrasses are classified into cool and warm-season species.

Cool-season turfgrass species are characterised by the C<sub>3</sub> photosynthetic pathway and are better adapted to temperate and cold climates. The optimum temperature for cool-season species ranges between 15 to 24°C for shoots and between 10 to 18°C for roots (DaCosta et al., 2013). High temperatures are a

primary stress for these species (Huang et al., 2014), which lead to photosynthesis inhibition, to limited nutrient uptake and low growth rates (Fry and Huang, 2004; Du and Wang, 2009). At high temperatures, turfgrass respiration increases, resulting depletion of turfgrass storage pools of carbohydrate (Huang and Gao, 2000). This characteristic makes cool-season species a poor choice for hot or dry environments. The main species adapted to green management conditions are creeping bentgrass (*Agrostis stolonifera* L.), colonial bentgrass (*Agrostis capillaris* L.), velvet bentgrass (*Agrostis canina* L.), red fescue (*Festuca rubra* L.) and annual bluegrass (*Poa annua* L.).

Warm-season turfgrasses are characterised by the C<sub>4</sub> pathway which gives them a better performance under warm and dry climates (Hanna et al., 2013). The optimum temperature ranges between 27 to 35°C for shoots and between 24 to 29°C for roots (Beard, 1973). Owing to the C<sub>4</sub> pathway, warm-season turfgrasses can continue photosynthesising and producing carbohydrates even during hot, dry days, when stomata are closed and there is no intake of CO<sub>2</sub> into the leaves (Fry and Huang, 2004). These features make this group more tolerant to heat and drought than cool-season species, resulting in lower water consumption and higher water use efficiency. The main temperature stresses for warm-season turfgrasses are produced by cold. Below 10°C, warm-season species enter into dormancy (McCarty, 2005). The main warm-season species used on greens are hybrid bermudagrass (*Cynodon dactylon* L. × *C. transvaalensis* L.) and, to a lesser extent, Zoysia species (*Zoysia* ssp. Steud.) and seashore paspalum (*Paspalum vaginatum* Sw.).

### **2.2.1 Turfgrass management practices**

The demand for high-quality turfgrass has been a primary driver to improve turfgrass management practices in recent decades (Breuninger et al., 2013). Main management practices include irrigation, fertilisation, mowing, top-dressing, aeration and pest control (Carrow et al., 2010). One of the objectives of greenkeepers is to optimise these activities to avoid unnecessary expenditure, carry out the practices in a sustainable way and achieve high-quality turfgrass. The course design influences turf-grass management due to three main factors

(Blanco, 2012). Firstly, the different playable areas might have different soil structure. Secondly, the diverse parts of a course might be covered by different turfgrass species, and finally, each area is maintained at a different mowing height, which affects grass growth and development.

### Irrigation

Irrigation involves the application of water to meet plant requirements not satisfied by rain. In agricultural crops, irrigation is typically used to maximise yield or profitability. In contrast, the aim of irrigation in turfgrass is to deliver the necessary water that provides a healthy, high-quality and functional surface (Leinauer and Devitt, 2013). The decision to irrigate (when and how much) is influenced by several factors including the irrigation system and management strategies. A comprehensive review and synthesis of existing literature on the impacts of irrigation scheduling on turfgrass is included in Chapter 4. The components affecting irrigation system performance are presented in section 2.3.

### Nitrogen fertilisation

Nitrogen (N) is the most critical element in turfgrass quality and turfgrass management (Calvache, 2014). In sportsturf, N fertilisers are applied frequently to maintain colour, density and growth, with typically annual application rates ranging between 50 and 300 kg N ha<sup>-1</sup> year<sup>-1</sup> (Branham, 2006). Although N is essential for healthy and actively growing turfgrass, excessive application leads to excessive shoot growth and poor rooting (Ericsson et al., 2012c), greater sensitivity to attack from certain pathogens (Frank et al., 2013), and to an increased risk of groundwater contamination through leaching (Petrovic, 1990). Greens built according to the USGA specification (USGA, 2004) have a very restricted nutrient storage capacity. Therefore, excess fertilisation in those areas should be avoided from both an economic and environmental perspective (Frank et al., 2006; Ericsson et al., 2012a).

Nitrogen transformation in turfgrass is driven by a process called the “nitrogen cycle”. This is a complex of processes by which the N changes between forms that are available and unavailable for plants (Frank et al., 2013). Nitrogen

mineralisation and immobilisation are influenced by several factors such as temperature (Lee et al., 2001), soil moisture (Bowman et al., 1987), turf growth (Qian et al., 2003), soil organic matter (Ericsson et al., 2012a), fertiliser type (Guillard and Kopp, 2004) and turf age (Frank et al., 2006). The nitrogen cycle in turfgrass systems is presented in Figure 2.4, and the processes involved in N transformation are described below.

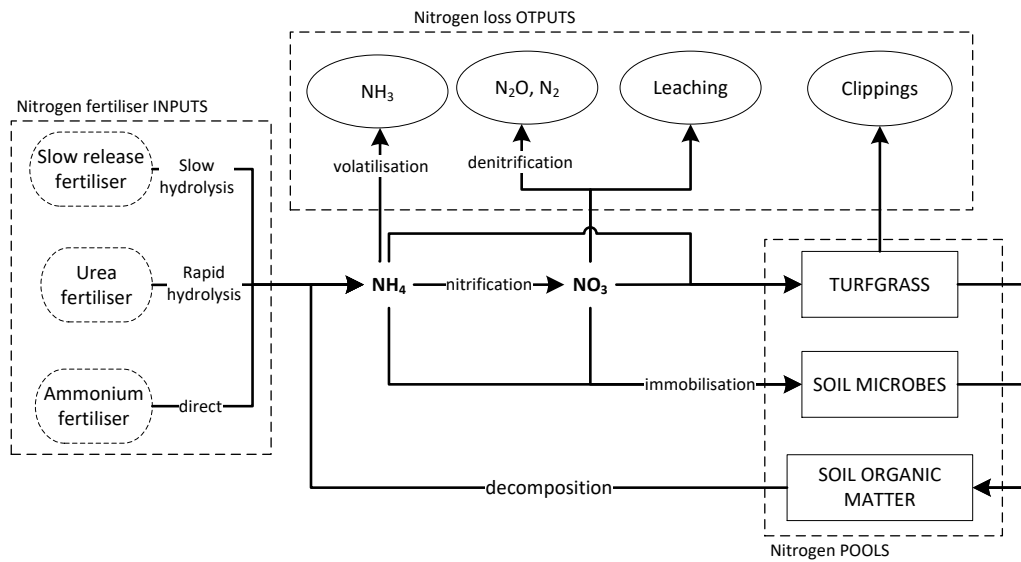


**Figure 2.4** Simplified nitrogen cycle in turfgrass systems adapted from Brown (2005)

- **Mineralisation.** Is the process through which organic N is transformed into the inorganic forms of ammonium and nitrate. This conversion is carried out through the processes of ammonification and nitrification. The levels of mineralisation on greens can vary between sites. Among other factors, it is affected by the age of the turfgrass and soil temperature (Lee et al., 2001; Shi et al., 2006).
- **Immobilisation.** Immobilisation is the opposite to mineralisation and consists of the process whereby mineral N is transformed into organic biomass that is not available to the plant. The rates of N applied immobilised varies between studies, ranging between 13% in bermudagrass (Wherley et al., 2009) to 37% in perennial ryegrass (Bristow et al., 1987), and from 31 to 62% in Kentucky bluegrass (Miltner et al., 1996). Greens with more thatch, with a higher content of organic matter

and microbial activity, can immobilise significant amounts of N within a few days of fertilisation (Bowman et al., 1989, 1998).

- **Denitrification.** The loss of N in the N<sub>2</sub> and N<sub>2</sub>O gaseous forms. Denitrification in turfgrass are positively related with high soil organic matter content, frequent irrigation and N fertilisation (Frank et al., 2013). When soils are not saturated and temperatures are not high, the typical N gas lost in turfgrass systems due to denitrification does not exceed 2 % of the total N applied (Mancino et al., 1988; Kaye et al., 2004; Bremer, 2006).
- **Volatilisation.** This phenomenon occurs when N is lost in the form of ammonia after applying urea fertiliser. Volatilisation in turfgrass is more prone to occur at high soil water contents, high wind speed, high temperature and high soil pH (Frank et al., 2013). In turfgrass systems, irrigation after fertilising can reduce the amount of N volatilised, from 40-60% to 1-2% of the total N applied (Bowman et al., 1987; Knight et al., 2007; Frank et al., 2013).
- **Nitrogen leaching.** The process by which soluble N (mainly in the form of nitrates) are lost with drainage. In general, well-managed turfgrass systems do not pose a major risk in terms of ground-water contamination, providing plants take up N actively, and N fertilisers are not over-used and that irrigation is not applied in excess (Barton and Colmer, 2006). A synthesis of literature on the relationships between leaching and irrigation management in turfgrass systems is discussed in Chapter 4.

### Mowing

Mowing involves cutting the turf to provide a desired canopy height. On greens, turfgrass is typically mowed at 3-6 mm height for aesthetic and playability requirements (Qian and Fu, 2005). Cuts are carried out daily or every other day, resulting in a constant biomass removal. This continuous reduction of biomass and height produces stress in plants which is manifested through physiological, developmental and morphological changes. As the cutting height is reduced, turfgrass shows a decrease in carbohydrate synthesis, leaf width and root depth

and an increase in shoot density (Beard, 1973). Closely mowed turfgrass on greens requires more intense maintenance, including lighter and more frequent irrigation (McCarty, 2005).

## **2.3 GOLF COURSE IRRIGATION SYSTEMS**

For golf, irrigation systems typically consists of one or more pumps, water distribution lines (piping), valves, controllers, sprinkler heads and nozzles (Emmons, 2008). Sprinkler heads and nozzles deliver water to the irrigated area. In modern golf irrigation systems, the pop-up rotor sprinklers heads are activated automatically through control valves which are operated from a centralised computer (Leinauer and Devitt, 2013).

### **2.3.1 Irrigation system performance and efficiency**

Efficient irrigation systems need to be designed to embrace the engineering (hydraulics of water transport and delivering) and biological (soil and plant) components of the irrigated area (Huck and Zoldoske, 2006). The concept of irrigation efficiency is contested in the literature and can be adressed in different ways. For example, it can be expressed as a function of technical efficiency (Aldous, 1999), economic efficiency, distribution efficiency, water use efficiency or technical cost efficiency (Pereira and Marques, 2017). The most common approach relates the water beneficially used by plant and water delivered by the system (Jensen, 2007). An improvement of irrigation efficiency must therefore consider the irrigation system and its management, while reducing leaching, runoff and evaporation losses during irrigation (Evelt and Tolk, 2009). In this research, irrigation efficiency is considered a function of the *irrigation adequacy* and *irrigation uniformity*. High irrigation efficiencies are only achieved by adopting proper irrigation management, which embrace not only the water application efficiency, but also the irrigation strategy adopted (*how much and how often should irrigation be applied?*).

- ***Irrigation strategy.*** An ideal irrigation strategy relies on understanding the water status in the soil, plant water requirements and irrigation decision-making. The irrigation strategy integrates the amount of water applied in each

irrigation event (irrigation depth) with its frequency. The irrigation depth can be adapted (i) to exceed water requirements in order to wash salts out from the root zone; (ii) to refill the maximum soil water storage capacity, irrigating up to the field capacity; or (iii) to apply water using a deficit irrigation strategy. In this research, deficit irrigation has been considered as deliberate underirrigate below the field capacity content of the soil, which generally results in water savings and an increase in water use efficiency (DaCosta and Huang, 2006a).

- **Water application efficiency.** Huck and Zoldoske (2006) described it as a function of *irrigation adequacy* and *irrigation uniformity* (or *heterogeneity*).
  - o **Irrigation adequacy** is related to the ability of the irrigation system to deliver the desired amount of water. Factors affecting irrigation adequacy are, for example, the variation in operating pressure of the sprinklers (Latif and Ahmad, 2008) or wind drift and evaporation losses (Playán et al., 2005). Water application (mm) is quantified by the irrigation rate provided by the system (IR, mm h<sup>-1</sup>) and the length of the irrigation event. The IR is controlled by the sprinkler head nozzle size, sprinkler head spacing and the type of sprinkler head (Beard, 2002). In golf, the IR should be as high as possible, but without exceeding the soil infiltration capacity.
  - o **Irrigation uniformity** (IU) is defined as the spatial variability of water applied to the irrigated area (Roberts, 2015). Under field conditions, irrigation systems never distribute water uniformly (Leinauer and Devitt, 2013). In sprinkler irrigation, the IU is commonly quantified using uniformity coefficients. These coefficients define the relationship between the variability in the irrigated water distribution and the mean water depth that reaches the soil. The two most commonly used coefficients to characterise irrigation are the Christiansen's Coefficient of Uniformity (CU) (Christiansen, 1942) and the Lower Quarter Distribution Uniformity (DU<sub>LQ</sub>). CU is defined as:

$$CU=1-\frac{\sum_{i=1}^N |x_i-\bar{x}|}{N \bar{x}}$$

where  $x_i$  is the water depth in a catchcan  $i$ ;  $\bar{x}$  is the average water collected in all catchcans in the studied area; and  $N$  is the total number of catchcans. Keller and Bliesner (1990) recommended values of CU of 85% for irrigation in horticultural crops, and a CU between 75% and 83% for crops with deeper roots.

The  $DU_{LQ}$  is defined as:

$$DU_{LQ} = \frac{\bar{x}_{LQ}}{\bar{x}}$$

where  $\bar{x}_{LQ}$  is the average water collected in the 25% of catchcans that collected the least water. Values of  $DU_{LQ}$  are generally lower than CU. Table 2 shows the rating of irrigation systems for landscapes based on the  $DU_{LQ}$  values (Mecham, 2004).

**Table 2** Quality rating for  $DU_{LQ}$  (Mecham, 2004)

$DU_{LQ}$	Quality of the irrigation system	Irrigation System Rating
> 85%	Exceptional	10
75-84%	Excellent	9
70-74%	Very Good	8
60 -69%	Good	7
50-59%	Fair	5
40-49%	Poor	3
< 40%	Fail	<3

### 2.3.2 Factors influencing irrigation uniformity

Pereira (1999) described IU in sprinkler systems as a function of multiple factors:

$$IU = f(P, \Delta P, S, d_n, WDP, WS)$$

where  $P$  is the available pressure in the sprinkler head;  $\Delta P$  is the variation of the pressure along the lateral;  $S$  is the spacing of the sprinklers along and between the laterals;  $d_n$  is the nozzle diameter;  $WDP$  is the water distribution pattern of the sprinkler;  $WS$  is the wind speed and direction.

These factors can be aggregated into three components:

- **Sprinkler set-up ( $P$ ,  $d_n$ ,  $WDP$ ):** The nozzle and operating pressure determine the (i) water distribution pattern, (ii) discharge rate of the sprinkler



( $L h^{-1}$ ), and (iii) how the water jet breaks up and how well water is distributed along the wetted radius. The placement of water throughout the pattern is controlled by the size and shape of the slots and the amount of turbulence generated while passing through the nozzle (Huck and Zoldoske, 2006). The sprinkler and associated nozzle usually are one of the most important elements of the irrigation system (and thereby irrigation uniformity) because they distribute the water.

The operating pressure impacts on the droplet size distribution (Kohl, 1974). Operating pressures below those recommended by the manufacturer result in the generation of larger droplet sizes at the exit of the sprinkler, which can produce a “doughnut” wetted pattern (Turgeon, 2008). Conversely, high pressures lead to a jet break up into small droplets. Small droplets cannot travel far from the sprinkler because of the influence of the air resistance forces. Therefore, high pressures result in higher irrigated rates close to the sprinkler head. In addition, smaller droplets are more prone to wind drift and evaporation. Molle et al. (2012) reported that evaporation losses for droplets below 0.4 mm vary between 10 and 75%, while for droplet diameters beyond 0.5 mm the evaporation losses drop towards zero as drop diameter is larger. The nozzles angle, height of the sprinkler, rotation speed and duration of the irrigation event also affect IU (Tarjuelo et al., 1999a; Tarjuelo, 2005).

- **Irrigation system design ( $\Delta P, S$ ):** Although Tarjuelo (2005) recommends squared, rectangular or triangular sprinkler layouts to achieve a high IU, in golf courses this is hard to accomplish due to the irregular irrigated shapes within each course (Vega and Hermosin, 2014). There is no consensus in the literature regarding the optimum sprinkler spacing to obtain a high IU, as it will vary from one sprinkler model to another (Sanchez et al., 2011). Keller and Bliesner (1990) reported that the optimum spacing depends mainly on the sprinkler model and how water is delivered. These authors suggested that the final sprinkler spacing will depend on the targeted irrigation rate, the combination of sprinkler-nozzle-pressure and the variability in wind speed.
- **Climatic factors ( $WS$ ):** Wind speed is considered as one of the main factors affecting the IU (Darko et al., 2017). In contrast to the irrigation design factors,

wind speed and direction are variables that cannot be controlled. The influence of wind on irrigation uniformity varies depending on the droplet size, jet trajectory and drag and evaporation losses (Tarjuelo, 2005). According to Regan (1987), wind speeds greater than  $1.3 \text{ m s}^{-1}$  often result in variable CU values. To reduce negative impacts of wind speed on IU, different authors recommended irrigating during the night or early morning, when wind speeds tend to be lower (Seginer et al., 1991; Playán et al., 2005; Turgeon, 2008).

## **2.4 MODELLING IRRIGATION IN TURFGRASS SYSTEMS**

### **2.4.1 Simulation models based on the ballistics theory**

Field measurements of IU are both difficult and expensive (Clemmens, 1991). Seginer et al. (1991) suggested the use of computer irrigation models as an inexpensive alternative. Compared with field tests, the main advantage of models is that the cost for computations are minimal, there is no need to carry out arduous field tests, and they provide a useful tool for the new design and improvement of irrigation systems (Nin, 2008). In recent decades, several researchers have focused on the use of models for simulating irrigation heterogeneity as affected by wind. One common approach for simulating irrigation is the use of ballistics-based models. This method applies ballistics theory to the water droplets that compose the water jet delivered by the sprinkler. These models simplify the process of jet break-out, assuming that the set of different drops with different sizes are generated at the exit of the nozzle. From the nozzle exit, droplets travel independently in the air until they reach the soil or crop canopy. During their travel, different resistance coefficients are applied to the droplets, which are function of the Reynold number (Fukui et al., 1980) and the droplet diameter (von Bernuth and Gilley, 1984). Another simplification assumed by this method is that each droplet size reaches the soil at different distances. Larger water droplets reach longer distances (Li et al., 1994). However, in reality, in each distance within the wetted radial curve<sup>1</sup> fall droplets with different diameters (Augier, 1996). Although factors such as jet break up or drop collision during their trajectory are

---

<sup>1</sup> The wetted radial curve relates the water discharged by a sprinkler rate with the distance from the sprinkler.

not considered, ballistics models have been applied successfully for simulating irrigation uniformity and wind drift and evaporation losses for agricultural impact sprinklers and fixed spray plates under windy conditions.

Due to the importance of droplet size in ballistics modelling, many studies have focused on the measurement of the water droplet distribution patterns using different techniques. The most common are those using photographic methods (Bautista-Capetillo et al., 2012; Márquez-villagrana, 2013; Ouazaa et al., 2014), using flour containers (Kohl, 1974; Li et al., 1994; Li and Kawano, 1995), or the more recent optical methods (Kincaid et al., 1996; Montero et al., 2003; King et al., 2010). Despite the effectiveness of those methods, measuring droplet size distribution is time consuming and expensive. Von Bernuth and Gilley (1984) proposed a modelling approach based on droplet ballistics, in which droplet size frequencies and distributions along the wetted radius were estimated from the water distribution radial curve. The water distribution radial curve is unique for each sprinkler model, nozzle configuration, working pressure and, to a lesser extent, the ambient conditions such as temperature or relative humidity. This method was used by Montero et al. (2001) in the SIRIAS model, whose underlying principles have been adopted in this research.

After the droplet size distribution is determined whether by measurement or estimation, ballistics theory is then applied to each individual droplet diameter, which has associated a discharge rate ( $L h^{-1}$ ). This process is applied to each drop size up to complete the circle (or partial circle) irrigated by the sprinkler. This process results in a set of points located over the plane. Each point has associated a discharge rate, and thereby a volume of water, which is aggregated in virtual pluviometers. When this process is repeated for multiple sprinklers, ballistics-based models can estimate the irrigation rates and irrigation uniformity across a given area.

#### SIRIAS model

The SIRIAS model (Carrión et al., 2001b; Montero et al., 2001) was developed following the ballistics equations proposed by Fukui et al (1980). To simulate the deformation of the sprinkler wetted patterns as affected by wind, the authors of

the SIRIAS model introduced the correction coefficients  $K_1$  and  $K_2$ , which correct for the air drag coefficient (Seginer et al., 1991; Tarjuelo et al., 1994). The correction of the air drag coefficient results in a windward shortened and leeward lengthening wetted pattern, providing a better fit between the model simulations and field measurements. The model was calibrated, validated and applied to agricultural impact sprinklers operating at pressures ranging between 2 and 3.5 bar, with different nozzle sizes, rising height, and irrigation spacing. The authors observed that the model performed better for block irrigation simulations than for single sprinklers. For block irrigation, the errors in the prediction of CU did not exceed 5%.

#### Ador-Sprinkler model

The Ador-Sprinkler model (Dechmi et al., 2004a; b) followed a similar methodology as proposed by Fukui et al. (1980) and Carrion et al. (2001b), varying the method to determine the water droplet distribution based on the equations proposed by Kincaid et al. (1996). These equations characterise two parameters ( $d_{50}$  and  $n$ ) proposed by Li et al. (1994), where  $d_{50}$  is the mean drop diameter, and  $n$  is a dimensionless exponent. These parameters were calibrated to obtain the relationship between the simulated and measured wetted radial curve for a given sprinkler. Once these parameters are adjusted, the discharge rate specific to each water droplet diameter is calculated. The authors observed that the Ador-Sprinkler model explained 87% of the variability in measured CU during a season. In their research, Dechmi et al. (2004a) coupled the Ador-Sprinkler model with the crop model Ador-Crop for simulating the impacts of irrigation heterogeneity on maize yield.

The Ador-Sprinkler model has been applied over the last decade by various authors. Playán et al. (2006) calibrated and validated the model for a wide variety of operating pressures and nozzle diameters, showing the efficacy of the model and expected CU for different combinations of sprinkler model, nozzle, operating pressure, sprinkler spacing and wind speeds. When integrated with other models, Zapata et al. (2013) used the Ador-Sprinkler model as a decision-making tool to automate irrigation scheduling. In more recent research, Ouazaa et al. (2016)

used a modified version of the Ador-Sprinkler for simulating irrigation performance of a partial-circle sprinkler and deflection plate sprinkler to analyse the differences between both types of sprinklers when used for irrigation field boundaries.

#### Model for simulation of fixed sprays

Ballistics simulation was also used by Ouazaa et al. (2014) to characterise and simulate the water droplet distribution in centre-pivot spray sprinklers. The characteristic of this type of sprinklers is that the main jet brakes up into a plate perpendicular to the main jet. Due to the different nature of those sprinklers, the droplet size was estimated for each sprinkler set-up using the photographic method as proposed by Salvador et al., (2009). This showed that with adequate model calibration and validation, ballistics modelling can be adapted to different sprinkler typologies.

### **2.4.2 Other irrigation models**

#### Richards and Weatherhead model of raingun application patterns in windy conditions

Richards and Weatherhead (1993) developed a semi empirical model for predicting the distortion of water applied by raingun as affected by wind speed. This model followed different principles to those based on the ballistics theory, assuming that wind speed influences  $\theta$  the flux of water and not on individual droplets. The different nature of this model in comparison to ballistics-based models relies on the obvious differences between sprinklers and rainguns. After applying the model, the authors reported an error in predicted irrigation rates of between 8.5 and 10.5% which is considered acceptable. The difficulty in applying the ballistics theory to simulate raingun irrigation meant some researchers adopted this semi-empirical method (Granier et al., 2003; Smith et al., 2008; Faria et al., 2009).

#### Model of sprinkler distribution patterns in windy conditions

Han et al. (1994) developed a model for simulating the water distribution of a sprinkler distorted by wind speed. The model used an ellipse to represent the

distortion of the water applied under windy conditions. In order to determine the shape of this ellipse, a series of parameters need to be determined experimentally. The model was calibrated with data from 170 trials, in which 78 combinations of sprinkler set-up were used. However, the authors found a low correlation between the shape factor of the ellipse and wind speed, with an average error in irrigation rate of 20.3%.

### 2.4.3 Crop models applied to turfgrass

Sinclair and Seligman (1996) defined crop models as the dynamic simulation of crop growth by numerical integration of constituent processes with the aid of computers. This comprises the design of computer programs that describe the dynamics of the growth of a crop and their interaction with the environment, in a defined time-step, providing outputs that describe the state of the crop system at different stages during the season. According to Van Ittersum et al. (2013) the outcomes of crop models in relation to crop production can be categorised into three groups, which must be estimated for a defined geographical area and time:

- **Potential yield**, which is the yield of a crop cultivar when grown with water and nutrients non-limiting and biotic stress effectively controlled, being therefore determined by climatic factors (CO<sub>2</sub>, radiation, temperature) and crop characteristics (Jones et al., 2017b). Although potential yield is rarely achieved in field conditions, its value can be used as baseline to study the impacts of other factors such as management or stresses on yield reduction.
- **Water and nutrient limited yields.** These outcomes consider a reduction in yield as affected by “limiting factors” of water and nutrients. Crop models that simulate water and/or nutrient-limitations must include water and nutrient balance submodules, with associated reduction in plant development when crops do not meet their “potential yield demands” (Jones et al., 2017b).
- **Actual yields**, which is defined as the yield actually achieved on the farm. The difference between the potential yield and the actual yield is known as the “exploitable yield gap” (Van Ittersum et al., 2013). This gap consists of

the reduction in yield due to the limiting factors water and nutrients, plus other factors affecting plant growth and development such as weeds, pests and diseases. The majority of crop models do not simulate yield reductions as influenced by such reducing factors (Jones et al., 2017b).

Crop models are presented as a useful tool to study the impact of contrasting environments, different management strategies and other stresses on plant development, yield and derived environmental risks such as leaching or drainage. Crop models can therefore be applied to different disciplines, including research, decision-support tools in crop system management, policy makers and education (Boote et al., 1996; Matthews, 2002). In the past 40 years crop models have been used to (i) represent, organise and summarise knowledge, (ii) to predict the evolution of systems under un-tested conditions, and (iii) to test hypotheses and generate new ideas to drive new research (Bergez et al., 2014). One of the main advantages of crop models is that they enable a large number of sampling conditions to be evaluated that would be impossible to reproduce in the field (Li et al., 2012). After adequate calibration, crop models can partially replace field experiments, helping to quantify some variables under controlled environment that otherwise would be difficult to measure in field conditions due to financial and time constraints (Graves et al., 2002). However, some limitations might be considered when using crop models. Boote et al. (1996) pointed out that the complexity of the processes involved in some crop models can make them difficult to understand, use and apply. These authors emphasized the large number of input parameters commonly required by crop models, which, in many cases, are impossible to obtain. The parameterisation therefore needs to be based on assumptions or estimations. They suggested that the limitations of obtaining good data include (i) the cost of obtaining that data to use as input in models, (ii) the spatial variability in the data collected, (iii) the theoretical knowledge required for some input parameters, (iv) the temporal variability of the crop system across the season, and (v) the quality of the data collection process as affected by experimental errors and poor calibration of measuring instruments. Mathews et al. (2002) also highlighted that data gathered in field under research conditions usually does not take into account spatial variability within the same

crop, as they consider perfect plant uniformity. Poor quality and quantity in data for parameterisation and model calibration will lead to poorer overall model performance.

#### Crop models applied to turfgrass

The use of crop models in turfgrass systems is a relatively recent concept with very few references in the literature. Crop models have been applied extensively in forage crops and grassland [e.g. Kiniry et al. (1995), Pérez-Ortolá et al. (2016), Steduto et al. (2009), Ruget et al. (2009), Persson et al. (2014)]. These crops present similar fundamental characteristics to turf. They can be considered perennial plants, which are subjected to a reduction in height and biomass through cuts, mowing or grazing (Adams and Gibbs, 1994). Plants in those type of systems have the ability to regrowth after a cut occur.

In comparison to other grass systems, turfgrass for golf is subjected to very intense maintenance, its canopy is maintained at a lower height and the plants receive multiple frequent cuts. Difficulties for simulating regrowth after cutting was previously reported by Jégo et al. (2013) when simulating timothy grass (*Phleum pratense* L.) with the STICS model. Whilst these authors reported average good model performance for the first cut, they also observed that the simulation of plant regrowth showed poor model efficiency. Similar results were obtained by Pérez-Ortolá et al. (2016) when using the DNDC model to simulate tall fescue (*Festuca arundinacea* L.) yields during successive years. These authors obtained good prediction of annual yield. However, they observed a much higher degree of variability in the predicted yield between individual cuts.

Regarding the application of crop models to turfgrass systems, Qian et al. (2003) predicted clippings on a monthly basis in Kentucky bluegrass (*Poa pratensis* L.) under home lawn conditions on a clay loam soil in Colorado using the CENTURY model. The authors reported that monthly clipping biomass presented high variation between measured and simulated values. However, when the simulated values of clippings were aggregated on an annual basis, the model was able to simulate satisfactory annual values of clipping for different managements in one year and underestimated annual clipping yields in other two years. Those authors



calculated the clipping removal on a weekly basis, mowing 4.7% of the standing aboveground biomass at each mowing. In other research in which the CENTURY model was used for simulating the same turfgrass species under fairway conditions (Bandaranayake et al., 2003), clipping was calculated on a monthly basis as a removal of a 30% of the aboveground tissue.

Zhang et al. (2012; 2013b) calibrated and validated successfully the DayCent model for simulating clipping yields, evapotranspiration (ET), deep percolation, nitrate leaching, and soil temperature in Kentucky bluegrass and tall fescue lawns. Overall, prediction of weekly ET and deep percolation of the three years was acceptable ( $r > 0.6$ ), while the simulated clipping presented an  $r$  value of 0.74 for seasonal values. However, in that research the authors deduced the calculated mowing as harvest events, leaving  $336.6 \text{ g m}^{-2}$  of verdure (aboveground biomass not subjected to mowing) after each cut but without specifying the frequency in clipping removal.

Wilkerson et al. (2015) developed a model for turf quality (from 1 to 9 visual scores) under irrigated and drought conditions for four cultivars of St. Augustinegrass (*Stenotaphrum secundatum* L.) and bermudagrass (*Cynodon dactylon* L.). Despite the model predicting turf quality successfully within a 95% confidence interval, the authors did not consider other processes such as cuts and plant re-growth. Other investigations have applied models to simulate turf systems but with different aims, such as the simulation of the soil water and/or nitrogen movement in golf green rootzones using the HYDRUS-2D model (McCoy and McCoy, 2009; Filipović et al., 2014), the estimation of nitrogen leaching (King and Balogh, 1999) the estimation of pesticides leaching (Jackson and Estes, 2007) and carbon budgets in turfgrass systems (Milesi et al., 2005; Bartlett and James, 2011b).

#### **2.4.4 Modelling impacts of irrigation uniformity on crop systems**

Despite the evidence published on the links between different irrigation strategies on turfgrass performance (Gómez-Armayones et al., 2018), the impacts of non-uniform irrigation on turfgrass development have not been fully investigated.

Leskys et al. (1999) observed significant interactions between leaching fractions and IU in tall fescue plots, as well as with clippings, evapotranspiration, tissue moisture content and canopy temperature. Other turfgrass has related IU and soil moisture uniformity. Dukes et al (2006) found that although irrigation uniformity and the soil moisture uniformity followed a linear relationship, the soil moisture uniformity presented values of  $DU_{LQ}$  up to a 20% higher than irrigation  $DU_{LQ}$ . Similar results were obtained by Kieffer and Huck (2008). However, those authors pointed out that their results might be biased by pre-existing soil moisture occurring between catch-can evaluations. In more recent research conducted on golf courses, Miller et al. (2014) observed that soil moisture  $DU_{LQ}$  presented values between 11 to 20% higher than irrigation  $DU_{LQ}$ . They concluded that IU should not be the only measure of irrigation system performance when assessing the soil water content.

To date, studies of irrigation uniformity on plant systems have been mainly limited to agricultural crops. The most common methodology used for this assessment is scenario modelling. Brennan (2008) related lower irrigation uniformities in lettuce with higher production costs and greater water consumption to achieve the maximum yield ( $6,270 \text{ m}^3 \text{ ha}^{-1}$  for IU equalling 90% and  $9,250 \text{ m}^3 \text{ ha}^{-1}$  for CU equalling 60%). Mantovani et al. (1995) reported that in order to achieve maximum yield in maize in south Spain, required irrigation depths doubled from 500 to 1000 mm when the CU decreased from 95% to 55%. In addition, these authors observed that when irrigation uniformity was low, errors in estimating the water required had greater impact on the net economic return of the maize production. In a similar study, Li (1998) observed that the water required to achieve a given level of yield was negatively correlated with CU values. Thus, maximum winter wheat yields required 330 mm, 430 mm and 1800 mm for CU 95%, 75%, and 55%, respectively. In research conducted on the impacts of non-uniform irrigation in onion in humid climate, Pérez-Ortolá et al. (2015) reported that in comparison with perfectly uniform irrigation, non-uniformity reduced simulated yields up to 10%, with yield reductions exacerbated during dry summers, while rainfall in wet years buffered the impacts of irrigation heterogeneity. Pang et al. (1997) reported that CU 75% not only reduced maize

yield in comparison with uniform irrigation, but also increased N leaching risks. In another research, the impacts of irrigation uniformity on alfalfa were studied (Montazar and Sadeghi, 2008) based on field observations. These authors concluded that the water distribution of a sprinkler irrigation system has a direct effect on alfalfa growth, hay yield, water productivity and water use efficiency.

In contrast to the results presented above, Dechmi et al. (2004a) concluded that the average CU during the crop season in maize were not relevant to final yield. Based on the application of the Ador-Sim model, the authors stated that irrigation depth (mm) was far more important than irrigation uniformity, responsible for up to 13.4% reduction in yield. Other studies also found low impacts of irrigation uniformity on average yield (Mateos et al., 1997; Allaire-Leung et al., 2001).

The use of a crop modelling approach applied to turfgrass systems could help to assess the impacts of irrigation heterogeneity and irrigation strategy on turfgrass systems. Further investigation is required to couple the links between the existing knowledge in irrigation systems performance and irrigation management on turfgrass growth, water use and potential environmental impacts. The study of these relationships would not only benefit the turfgrass research sector, but would also be beneficial for the sportsturf industry.



## **3 METHODOLOGY OVERVIEW**

This chapter describes the methodological framework developed in this thesis, including data collection for the development of an integrated modelling approach.

### **3.1 METHODOLOGICAL FRAMEWORK REQUIREMENTS**

Due to the multiple components developed in this research, a description of the methodology has been split into three specific chapters (4, 5 and 6) each containing a method description, results and discussion section. The justification for including these chapters in the methodology section, and not in the results chapter, was because they constitute the basis for understanding the components of the integrated modelling framework (Chapter 7).

The main components of methodological framework include:

1. Gathering baseline data to investigate current irrigation management practices and typical levels of irrigation system performance for selected golf courses in Northern Europe.
2. Synthesising evidence and data to investigate the biophysical links between irrigation management, turfgrass response (turf quality, growth and rooting) and environmental impacts (nitrogen fate) of golf irrigation.
3. Designing and building a sprinkler rig and conduct extensive experimental field tests to investigate irrigation sprinkler performance under contrasting environmental conditions. This data would support the development and calibration of a ballistics model to simulate irrigation heterogeneity.
4. Gathering data and information on turfgrass irrigation management with the purpose of calibrating and validating a biophysical crop growth model to simulate turfgrass agronomy.

Adopting a purely experimental approach to address the research aim taking into account different turfgrass, water and nutrient management strategies and irrigation systems would not be feasible due to resource and time constraints. Consequently, a combination approach was developed, involving coupling data

from both existing field experiments and new field tests, with extensive use of models to simulate a wide range of turfgrass-water-environment-management interactions. Significant effort was involved in model calibration and validation in order to develop an integrated approach that was robust for simulating multiple scenarios relating to turfgrass management.

In addition to simulating irrigation system performance and turfgrass growth and development independently, there was a requirement for the models (Chapters 5 and 6) to be combined within an integrated framework (Chapter 7) to allow assessment of the impacts of irrigation heterogeneity on turfgrass growth including water and nutrient fluxes. Figure 3.1 shows the links between the different components of the methodology, results and discussion and how these relate to specific thesis chapters.

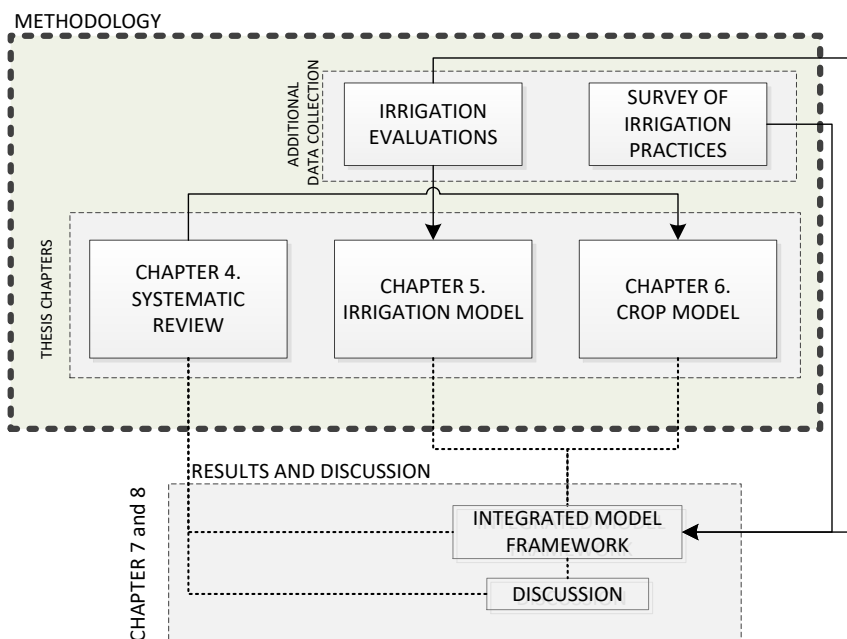


**Figure 3.1** Overview of the methodology, results and discussion thesis chapters

#### Chapter 4. Systematic review

The primary objective of conducting a systematic review was to identify and synthesise the available published data and information on the links between irrigation management, turfgrass performance and N fate. Published literature was selected following a systematic review methodology (CEBC, 2010) including search definition terms, inclusion and exclusion criteria, to finally extracting the

quantitative and qualitative data from 83 studies. These data were then combined in a database for meta- analysis. This chapter constitutes an essential component of data collection with information used to provide the baseline in the pre-parameterisation of the crop model (Chapter 6). The results in Chapter 4 were also used to support and compare the outputs from the application of the integrated modelling framework (Chapter 7).

#### Chapter 5. Irrigation ballistics model

This chapter relies on the need to develop a model capable of simulating irrigation heterogeneity on golf greens under contrasting climate (wind) and turf management (sprinkler configuration, irrigated area) conditions. This chapter includes description of (i) model development, (ii) data collection from field tests conducted on individual sprinklers, (iii) ballistics model calibration and validation, and (iv) discussion of model performance. This model was applied in Chapter 7 to study the impacts of the system design on irrigation performance, and coupled with the crop model (Chapter 6) to evaluate the implications of irrigation management on turfgrass.

#### Chapter 6. Biophysical crop model

The findings presented in Chapter 4 relating to the turfgrass responses to water were used to identify a suitable biophysical crop growth model capable of simulating (i) turf development and growth, (ii) water and N balances, and (iii) irrigation, fertilisation and mowing practices. Appropriate data for parameterising the model were gathered. Chapter 6 includes the results from model sensitivity analysis, calibration, validation, evaluation and discussion of model performance. In Chapter 7 the crop model is integrated with the ballistics model to assess the impacts of uniform and non-uniform irrigation on turfgrass management.

#### Additional data collection

The methodology has been supplemented with results from an industry survey of golf irrigation management practices in four Nordic countries, and data from irrigation evaluations conducted on three golf courses. The results from the online golf industry survey are presented in Annex-1. In total, 144 golf courses

representing 16% of courses registered with the Danish, Iceland, Norwegian and Swedish Golf federations in 2015 were involved. The survey aimed to produce a comprehensive understanding of the state of the irrigation systems and management strategies adopted by the golf sector in Scandinavia, as well as identifying research gaps and future opportunities for improvement. The survey results were also used to define the irrigation strategies (Chapter 7); key findings were also included to support thesis discussion (Chapter 8).

Summary results from the irrigation evaluations are presented in Annex-2. In total, 11 irrigation uniformity tests were conducted on three golf courses in the UK, Norway and Denmark. The site visits also provided an opportunity to interview course managers about the challenges of turf irrigation management. The results from these evaluations also provided practical knowledge on irrigation practices to support model parameterisation (Chapter 5). The nine green shapes and sprinkler positions from these courses were used for simulating irrigation performance (Chapter 7).



## **4 ASSESSING EVIDENCE ON THE AGRONOMIC AND ENVIRONMENTAL IMPACTS OF TURFGRASS IRRIGATION MANAGEMENT**

This chapter presents the synthesis of the results from a systematic review of published evidence on irrigation impacts on turfgrass agronomy and the environment. The methodology for inclusion and exclusion criteria of literature is described. Quantitative and qualitative data from 83 selected studies were then extracted and combined in a database for meta-analysis. This chapter has been published as a peer-reviewed paper in a scientific journal<sup>2</sup>.

### **4.1 INTRODUCTION**

Turfgrass has an important multifunctional role, contributing to urban development (green spaces) and supporting multiple environmental (ecosystems), societal and well-being (sports surfaces and leisure), and economic (source of direct and indirect employment) benefits (Beard and Green, 1994; Haydu et al., 2008). To maintain high-quality turf surfaces, a range of maintenance activities is required, including mowing, irrigation, aeration and the application of topdressing, fertiliser and pesticides (Beard, 1973). Adequate inputs of water and fertiliser are crucial for maintenance of high-quality standards in turfgrass, but inappropriate management can lead to an increase of nutrients and pesticides in ground and surface water through leaching (Branham, 2006) and run-off (Shuman, 2002a). It is therefore essential to understand the agronomic requirements for managing turf quality while ensuring that negative environmental impacts are minimised. Over the last 20 years, the focus of turf research has shifted away from improving aesthetic quality to reducing environmental impacts (Stier et al., 2013), mainly in response to concerns regarding diffuse pollution from nutrients and their impacts on the aquatic

---

<sup>2</sup> Gómez-Armayones, C., A. Kvalbein, T.S. Aamlid, and J.W. Knox. 2018. Assessing evidence on the agronomic and environmental impacts of turfgrass irrigation management. *J. Agron. Crop Sci.*: 1–14. DOI: 10.1111/jac.12265

environment (Carey et al., 2012; Strandberg et al., 2012). Rising competition for water between leisure, agriculture and residential water supply, coupled with new environmental regulations, is adding further pressure on the turfgrass sector (Carrow, 2006; Rodríguez Díaz et al., 2007). Improvements in irrigation management to enhance turf quality, while reducing water and energy consumption and environmental impacts, have become major “drivers for change” in the turfgrass industry.

The aim of this study was to critically review and assess published evidence on the links between irrigation management, turfgrass performance (turf quality, growth and rooting) and environmental impacts (N fate). A systematic review (SR) approach was adopted; this provides an internationally recognised highly robust technique for identifying, synthesising and evaluating published evidence from the scientific and grey literature (industry documents and technical reports that have not been subject to a peer-review process). Although originally developed for use in medical research, its application has spread into natural and environmental sciences [e.g., Knox et al. (2016)] to support decision-making and policy formulation.

## **4.2 METHODOLOGY**

A SR approach originally developed by the Collaboration for Environmental Evidence and Centre for Evidence Based Conservation (CEBC, 2010) was adopted. This included the drafting of a protocol to define the research method, followed by systematic search and selection of relevant literature based on a defined set of “inclusion criteria.” Methods for data reporting, synthesis and study quality assessment were also carefully defined. The underpinning element in a SR is the primary research question. For this study, the following question was formulated as follows: *Turfgrass irrigation management: what are the agronomic benefits and environmental impacts?* The primary question was split into four components referred to as PICO or PECO terms, which are acronyms for *Population, Intervention/Exposure, Comparator* and *Outcome*. For this SR, the targeted population was turfgrass; the intervention/exposure was irrigation and other turfgrass maintenance practices such as N fertilisation, mowing or

application of surfactants; comparators were turfgrass visual quality, growth, rooting, leaching and run-off; and as outcomes, we expected to find evidence on the most appropriate irrigation management strategies to maximise turf quality, growth and rooting and to minimise environmental impacts. The search strategy included drawing on evidence from a number of well-established scientific bibliographic databases (Web of Science, Scopus, Science Direct and Turfgrass Information File from Michigan State University, MSU) and grey literature from selected websites (turf federations, societies, associations). Searches were limited to publications in English. Following a number of trial searches, the final search term used for the SR was as follows: "TITLE-ABS-KEY ((turf\* OR golf) AND (irrigat\*) AND (management OR (irrigat\* AND (frequency OR calendar OR practic\*))) OR "water\* regime" OR sprinkler OR uniformity OR efficiency OR strategy OR drought OR deficit OR "irrig\* sched\*" OR mowing OR fertiliz\* OR surfact\*) AND (quality OR leaching OR "water consu\*" OR environ\* OR impact OR evapo\*) AND NOT wastewater)," where TITLE-ABS-KEY limits the scope of the search to the publication title, abstract and keywords; AND, OR are Boolean inclusion operators; and AND NOT is a Boolean exclusion operator.

All relevant literature was screened based on a set of inclusion criteria. These were first applied to the title, then to the abstract, and finally to the full text. Selected literature had to comply with the following requirements: (i) the population had to be turfgrass species, (ii) all papers had to be based on irrigated turf (not other grassland crops) and (iii) the research had to describe turfgrass performance as a response to irrigation and/or turf management, or related to environmental impacts such as nutrient leaching. The literature that focused on grasslands without frequent mowing (e.g., permanent leys and/or pastures), turf resistance to pests, run-off losses, pesticide fate, water quality or use of wastewater for turfgrass irrigation were all excluded. Justification on the exclusion of irrigation using wastewater is provided in the methodological limitations section. The literature preferably had to include quantitative data to allow comparison between individual studies. Quantitative and qualitative data were then extracted from each publication and a database created. Relevant data

embedded within published sources (figures) were extracted using WebPlotDigitizer (Rohatgi, 2017).

From each source, data relating to irrigation management, distinguishing between irrigation amount and frequency was extracted. Irrigation amount was expressed as a percentage (%) of either (i) water evaporated from a US Class A evaporation pan (Epan), (ii) reference evapotranspiration (ET<sub>o</sub>) or (iii) potential evapotranspiration (ET<sub>p</sub>) since the last irrigation. For ET<sub>p</sub>, water replaced was expressed as a percentage of water consumed by the plant under non-limiting water conditions (100% ET<sub>p</sub>). Data from ET<sub>p</sub> scheduled studies were those in which the irrigation amount was calculated as a function of weight loss by lysimeters or from measured soil water content, or based on the equation  $ET_c = K_c \times ET_o$ , where ET<sub>c</sub> is crop evapotranspiration, K<sub>c</sub> is a crop coefficient (Allen et al., 1998). This approach was used because it was the main expression of irrigation amount in the literature, and as it was assumed to be the most appropriate approach to compare results between studies. Using the total amount of water consumed by the plant or the soil water content depletion in absolute terms would not have allowed comparison of results between different studies. Data in which irrigation amount was expressed as Epan, ET<sub>o</sub> or ET<sub>p</sub> were analysed and presented separately as these values were derived from various scheduling approaches (Allen et al., 1998). The term “deficit irrigation” which is the practice of underirrigating turfgrass below its maximum water demand (Wherley, 2011) was used to refer to irrigations where water was supplied at a lower rate than 100% ET<sub>p</sub>. For irrigations below 100% Epan or ET<sub>o</sub>, the values are only expressed as “below 100%,” or the reported irrigation amount. Regarding irrigation frequency, two strategies are referred, either “light-frequent” or “deep-infrequent” irrigation. For “light-frequent,” less water was applied and on a shorter interval compared to “deep-infrequent” irrigation.

To assess turfgrass quality, it was used a visual quality index ranging from 1 to 9 was used, where 1 represented uneven and poor-quality turf, and 9 represented even (uniform) and ideal quality turf (Espevig and Aamlid, 2012). The minimum acceptable quality varied among the reported studies between 5 and 6 (Krans

and Morris, 2007). For this reason, scores of minimum acceptable turfgrass quality as being those values between 5 and 6 were considered. In research where other scales were used, turfgrass quality scores were converted to correspond to the 1–9 scale. Although it was used this scale to assess turfgrass quality, it is important to recognise other methods for quantifying turfgrass quality exist such as assessing ground cover, the use vegetation indices, turf hardness or ball roll. However, visual turfgrass quality scoring regime was used due to the lack of references reporting quantitative data on turf quality in relation to irrigation practices using the alternate approaches. Data presented in the results reflect the average value from each irrigation treatment. It was distinguished published data between cool and warm-season grasses and considered “treatment” as the different irrigation replacement levels in each study, for each species and variety. Turfgrass growth rate, total N leaching and N uptake by turf were expressed as the sum of samples from each irrigation treatment. Turfgrass growth rate was defined as the dry matter production (DMP) in clippings per day ( $\text{g m}^{-2}$ ,  $\text{g m}^{-2} \text{d}^{-1}$ ) or increment in canopy height per day ( $\text{mm d}^{-1}$ ). N uptake was defined as the amount of N in clippings ( $\text{g N m}^{-2}$ ) and was, where possible, expressed as a daily value ( $\text{g N m}^{-2} \text{d}^{-1}$ ). Data to describe root development were dry root biomass ( $\text{g m}^{-2}$ ) and root length ( $\text{cm cm}^{-3}$ ) as well as the distribution at different soil depths. For turfgrass growth, N uptake and N leaching, it was necessary to standardise the data extracted from the literature. Thus, to present the results from research as a daily rate ( $\text{g m}^{-2} \text{d}^{-1}$ ) for clippings and  $\text{g N m}^{-2} \text{d}^{-1}$  for N uptake and leaching), the published data were aggregated and then divided by the duration of each treatment to derive equivalent daily values.

To assess environmental impacts, only data relating to nutrient uptake by turfgrass and N losses via leaching was considered. Units were expressed as the total amount of nutrient taken up or lost ( $\text{g m}^{-2} \text{d}^{-1}$ ) or concentration of N in leachate ( $\text{mg L}^{-1}$ ). Due to the importance of other factors known to affect leaching from irrigated turfgrass, it was also considered research where fertilisation rates and dates, soil types or turfgrass age were included.

The SR methodology followed four discrete stages (Figure 4.1). Based on the search criteria, 653 articles were identified. The scientific and grey literature was then subjected to assessment using the inclusion criteria. Ultimately, 83 documents were selected, including 76 peer-reviewed papers and seven documents from the grey literature. Most articles stemmed from research conducted in the USA (79%), Australia (6%), Norway (6%) and Turkey (6 %). Other relevant studies were reported from Canada, Italy, Puerto Rico and Thailand (see Supplementary Information for the complete list of references included in the SR)<sup>3</sup>. The statistical analyses for the regression curves, fitting parameter ( $R^2$ ) and significance tests were conducted using the Statistics Toolbox in MATLAB R2014a software (MathWorks, 2014). The significance of the regressions was calculated for  $p < 0.05$ , where the null hypothesis was that there was no relationship between irrigation and the variable being studied.

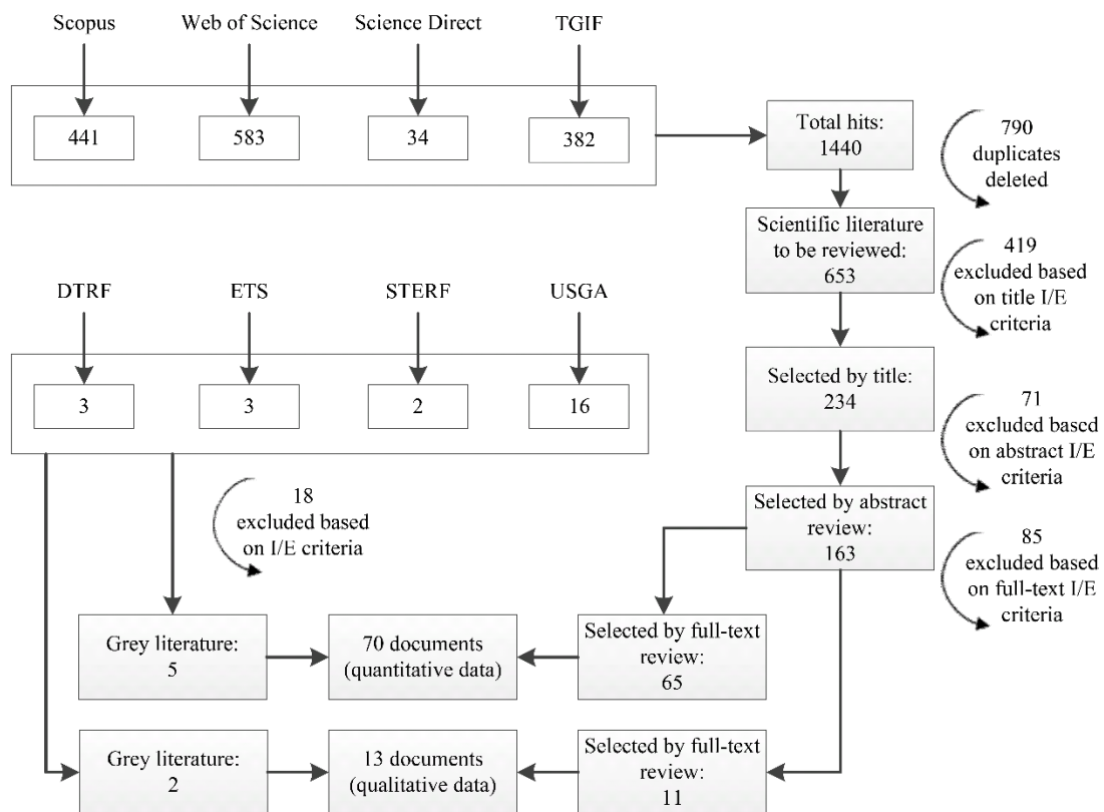


**Figure 4.1** Decision diagram for document inclusion/exclusion in the systematic review

<sup>3</sup> <https://goo.gl/Zyu3zg>

## 4.3 RESULTS AND DISCUSSION

### 4.3.1 Effects of irrigation management on turfgrass visual quality

The SR outputs confirmed that the approach adopted for scheduling irrigation can significantly impact turfgrass quality. It was observed a positive correlation between the amount of irrigation applied and turfgrass quality. When the reported turfgrass quality scores were compared between different irrigation scheduling methods for cool-season turfgrasses the  $R^2$  values for the logistic curve  $f(x) = \frac{a}{1+e^{-bx}}$ , where  $a = 9$ , were 0.77, 0.37 and 0.32 for Epan, ETo and ETp, respectively (Figure 4.2). For warm-season turfgrasses, the corresponding  $R^2$  values were 0.45, 0.34 and 0.44 for Epan, ETo and ETp. In all cases, the  $p$ -values for the regressions between irrigation amount and turfgrass quality were  $<.001$ . Based on the regression analyses, a stronger correlation was observed between irrigation amount and turf quality for Epan-based scheduling methods. Whilst a strong correlation based on irrigation using ETp might be expected, as these were mostly based on field measurements, the weak correlation was likely due to the inherent variability between individual studies rather than the method itself per se. Although the use of Epan and ETo to schedule irrigation are useful methods for comparing different irrigation amounts (ETo and Epan values are usually available to course managers), the application of incorrect crop coefficients ( $K_c$ ) can lead to overestimation in irrigation need and thus make these methods less reliable than ETp-based methods using soil moisture sensors or lysimeters. Although  $K_c$  values of 0.8 for cool-season turfgrass and 0.6 for warm-season turfgrass are widely accepted as industry standards, several studies report that  $K_c$  varies significantly depending on the site, local weather, seasons, turfgrass species, mowing height and N fertilisation (Meyer and Gibeault, 1986; Poro et al., 2016; Aamlid et al., 2016). Readers interested in crop coefficients for turfgrass are referred to Romero and Dukes (2016) who provide a recent updated review.

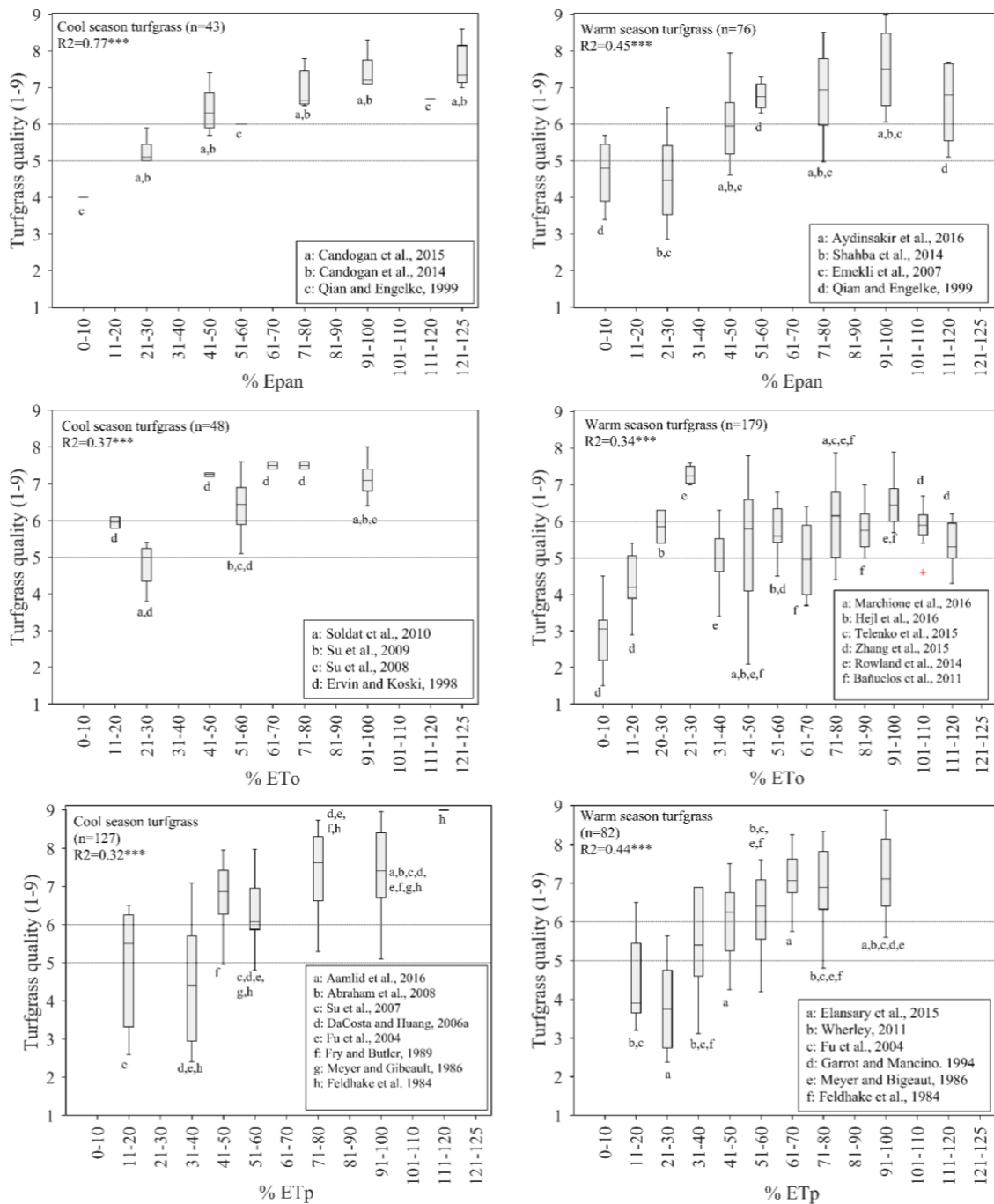


**Figure 4.2** Reported variation in turf quality depending on different irrigation amounts based three scheduling approaches (Epan, ETo, ETp) for cool- and warm-turfgrass species. The box and whisker plots display the quartiles and median values. Red crosses display outliers from the turfgrass quality values in the interquartile range (IQR)×1.5. The minimum acceptable turfgrass quality 5 and 6 is highlighted (horizontal lines) (n = 555). \*\*\*p < 0.05

Considering the points above, when variations in % Epan or ETo irrigation amount are reported in studies, they indicate a variation in water applied, but not necessarily in the amount of water consumed by the plant. Thus, irrigations below 100% Epan or ETo do not necessarily result in deficit irrigation. Thus, where there



are presented the impacts of different irrigation amounts on turfgrass expressed as % Epan or ETo, those results show the impact of different irrigation levels on turfgrass performance but do not indicate the amount of water consumed by the plant or if a deficit irrigation strategy was adopted. When deficit irrigation is used, only refers to % ETp.

It was found that both cool and warm-season turfgrasses followed a similar trend in their response of visual turfgrass quality to deficit irrigation. In general, the highest turfgrass quality was obtained for irrigation close to 100% ETp. Regarding Epan and ETo irrigation strategies, higher irrigation amounts also led to improved turfgrass quality scores. However, in most cases, an average acceptable turfgrass quality ( $\geq 6$ ) could also be maintained with deficit irrigation above 40% ETp. It was also observed that the irrigation amount required to maintain an acceptable turfgrass quality varied between studies, which in many cases was related to other factors such as the drought resistance of the species and variety, season and ambient weather conditions, turf management practices, including the use of soil surfactants or growth regulators, and the duration of the study. These factors explain the moderate  $R^2$  value when comparing different studies (Figure 4.2).

Differences in turfgrass quality among species and varieties became more noticeable as the irrigation amount was reduced. In two studies conducted in Turkey, Candogan et al. (2014, 2015) reported on the effects of irrigating perennial ryegrass (*Lolium perenne* L.) and tall fescue (*Festuca arundinacea* L.) at 25%, 50%, 75%, 100% and 125% Epan. In both studies, the average turfgrass quality over 5 months (May to September) did not fall below 6 for irrigation treatments above 50% Epan in tall fescue and above 75% Epan in the perennial ryegrass. However, only irrigations above 100% Epan for both species maintained a consistent turfgrass quality  $>6.0$ . In New Jersey (USA), DaCosta and Huang (2006b; a) reported that it was not necessary to irrigate to 100% ETp to maintain turfgrass quality in bentgrass (*Agrostis* spp.). However, they noted that different irrigation amounts were required to maintain acceptable turfgrass quality between species and different treatment years. During the growing

season in the first year, the irrigation amount varied from 80% to 100% ETp in colonial bentgrass (*Agrostis capillaris* L.), while for velvet (*Agrostis canina* L.) and creeping (*Agrostis stolonifera* L.) bentgrass the irrigation amounts varied between 60% and 80% ETp. In the second year, the irrigation amount to maintain turfgrass quality across all species studies was 60% ETp. In Colorado (USA), Feldhake et al. (1984) reported that there were no significant differences in turfgrass quality between Kentucky bluegrass (*Poa pratensis* L.) and tall fescue when irrigated at 80 and 100% ETp, respectively. However, when the turf was subjected to 40% and 60% ETp, tall fescue showed a higher turfgrass quality compared to Kentucky bluegrass. In a study in Kansas (USA), Fu et al. (2004) also showed that Kentucky bluegrass needs to be irrigated to 100% ETp to maintain an acceptable turfgrass quality, while tall fescue responded well to 60% in the first year and 80% in the second year trials.

Shahba et al. (2014) reported that irrigating three varieties of seashore paspalum (*Paspalum vaginatum* Sw.) at 100% ETp maintained a high turfgrass quality regardless of variety. However, reductions in irrigation to 75% and 50% ETp led to reductions in quality between varieties. In Texas (USA), for example, Qian and Engelke (1999) reported that the irrigation amount required to maintain a minimum acceptable turfgrass quality varied from 26% Epan in buffalograss (*Buchloe dactyloides* Engelm) to 68% Epan in zoysiagrass (*Zoysia japonica* Steud.). Other factors in combination with irrigation also influence turfgrass quality. Su et al. (2007) observed that in Kentucky bluegrass, hybrid bluegrass (*P. pratensis* L. × *Poa arachnifera* L.) and tall fescue, high temperatures severely reduced turfgrass quality when combined with drought stress (35/25°C and 60% ETp). Seasonal differences may also influence the impact of irrigation amount on turfgrass quality. For example, DaCosta and Huang (2006b) reported that during autumn, irrigation in bentgrass species could be reduced to 40% ETp without observing any severe decline in turfgrass quality. The higher water-stress resistance showed by turfgrass during autumn and winter seasons was mainly associated with lower temperatures and a reduction in activity, which resulted in lower water consumption and therefore lower and slower soil moisture depletion. These authors also observed greater water use efficiency during autumn for lower

irrigation amounts. Conversely, lower turf quality is usually observed during summer months under deficit irrigation (Su et al., 2009; Marchione and Fracchiolla, 2016), when hot and dry conditions make plants more susceptible to water shortages. Aydinsakir et al. (2016) reported a decline in bermudagrass (*Cynodon dactylon* L.) quality for 50% and 75% Epan, while in autumn months, when temperatures were lower, turfgrass quality recovered. This suggests that the aesthetic requirements of turfgrass might also be a contributory factor in determining the irrigation strategy adopted during the warmest months. In those areas where periods with lower turfgrass quality are acceptable, moderate deficit irrigation could be applied for limited periods. Although this might compromise turfgrass quality, this strategy can lead to lower water consumption compared to irrigating back to field capacity, and could be useful in regions where water is increasingly scarce and/or expensive.

No major impacts of cutting height on turf quality were identified in the literature when turfgrass was well-watered (25, 35 and 45 mm in seashore paspalum (Shahba et al., 2014); 20 and 50 mm in Kentucky bluegrass (Feldhake et al., 1984)). However, where low irrigation amounts were applied, higher mowing heights resulted in greater turfgrass quality compared to lower mowing. These findings differ from those reported by Su et al. (2009) who did not observe any significant differences due to the interaction between mowing height and irrigation amount for Hybrid and Kentucky bluegrass, based on mowing heights of 38 and 76 mm and irrigation of 60% and 100% ETo.

The use of soil surfactants was reported to enhance turfgrass quality at low irrigation amounts [30% ETp, Soldat et al. (2010)] compared to treatments with no surfactant. This was reportedly due to reductions in soil hydrophobicity and higher soil moisture uniformity. Candogan et al. (2014, 2015) and Wang et al. (2014) observed that turfgrass water consumption and the irrigation amounts required to produce acceptable turfgrass quality increased with increasing N fertilisation levels. Under non-limiting water conditions, turfgrass quality was more dependent on N than irrigation amount (Shaddox et al., 2016b). Other researchers reported that unfertilised turf leads to low turfgrass quality

irrespective of irrigation amount (Wu et al., 2010; Carey et al., 2012; Telenko et al., 2015), as N is the main limiting factor in turfgrass performance. The use of growth regulators also helped to maintain turf quality in Seashore paspalum (*P. vaginatum*) (Elansary and Yessoufou, 2015), especially under drought conditions (<50 ETp).

The impacts of irrigation frequency on turfgrass quality for cool and warm-season turfgrasses are summarised in Figure 4.3. Overall, no major turfgrass quality impact was reported for intervals of up to 4 days. In contrast, when the irrigation interval was longer, the average turfgrass quality declined as irrigation frequency was lower (Peacock and Dudeck, 1984; Fry and Butler, 1989; Baldwin et al., 2006). Both cool and warm-season turfgrasses followed a similar trend of declining turfgrass quality as the interval between irrigation events became longer. The differences in turfgrass quality between studies with the same irrigation interval as shown in Figure 4.3 were caused by different (i) irrigation amounts (Fry and Butler, 1989; Aamlid et al., 2012), (ii) varieties of the same species (Baldwin et al., 2006) and (iii) years of study (Fry and Butler, 1989; Jordan et al., 2003; Fu and Dernoeden, 2009a); this last factor possibly being related to both weather conditions and turf age.

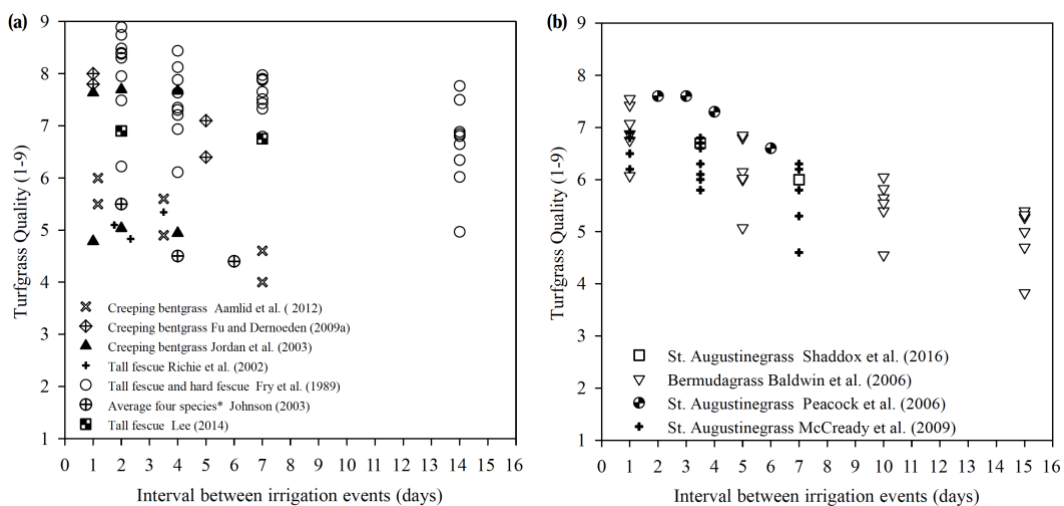


**Figure 4.3** Reported average turfgrass quality scores in relation to irrigation frequency (day) for (a) cool- and (b) warm-season turfgrasses. \*Average scores for Kentucky bluegrass, tall fescue, junegrass [*Koeleria macrantha* (Ledeb.) J.A. Schultes] and buffalograss

In two studies, turfgrass quality was reported to be higher with light-frequent irrigation compared to deep infrequent in the first year of treatment, while the

opposite effect occurred the following year (Fu and Dernoeden, 2009a; Espevig and Aamlid, 2012). This was reported to be due to turfgrass adaptation to wilt stress over time, allowing the plants to maintain a higher turfgrass quality during summer stress periods. Similar results were reported by Jordan et al. (2003) who found better turfgrass quality related to irrigation every 4 days compared with daily and alternate irrigation, which can be linked with an adaptation of creeping bentgrass to drier conditions when irrigation intervals were increased. When comparing irrigation on a weekly and two times per week cycle in three different locations, Shaddox et al. (2016b) only found significant differences between irrigation frequency and turfgrass quality in one location. In contrast to other studies, turfgrass quality was slightly higher for more infrequent irrigation treatments. Conducting research in Michigan (USA), Lee (2014) observed that during the hottest part of the season tall fescue performed better when irrigated twice weekly compared to once a week. From these studies, two deductions can be made: firstly, weekly or less frequent irrigation might not improve drought adaptation of turfgrass species, and secondly, that the impacts of irrigation frequency on turfgrass quality might be more evident in long-term trials, as irrigation frequency affects the adaptation of turfgrass to drought stress, rather than showing a direct response to varying the irrigation amount. However, further research is required to investigate irrigation frequency on turf performance.

Although light-frequent irrigation to field capacity appears to be the optimum strategy to achieve a high turfgrass quality, it also results in more water being transpired (Peacock and Dudeck, 1984; Aamlid et al., 2016). For example, in Norway, Aamlid et al. (2016) observed that water consumption of cool-season turfgrasses was more than double on the first day after irrigation to field capacity ( $K_c = 1.67\text{--}2.85$ ) compared to the following days (mean  $K_c = 0.76\text{--}0.99$ ). However, it must be recognised that the maximum values of  $K_c$  observed in that research were far higher than those reported in other studies. However, these findings suggest that the water consumption will be high if irrigation is applied at low deficits and with a frequent schedule, corroborating with research by DaCosta and Huang (2006b) and Aamlid et al. (2012). Achieving water savings whilst maintaining turfgrass quality may also be attained by selecting turfgrass species

and varieties well adapted to local climatic conditions (Huang, 2008), by improving the uniformity of soil moisture through the use of soil surfactants (Soldat et al., 2010; Cisar, 2012), using growth regulators (Elansary and Yessoufou, 2015) and/or by improving irrigation uniformity, accuracy and efficiency using new technology of irrigation controllers and sensors (McCready et al., 2009). Bell et al. (2013) also highlighted the potential opportunities for integrating new technologies adapted from precision agriculture into turfgrass irrigation management, including determining turfgrass quality derived from digital image analysis from small unmanned aerial vehicles (Phan et al., 2017), wireless soil moisture and climate sensors for computer-based irrigation monitoring (scheduling) and variable rate irrigation.

#### **4.3.2 Effects of irrigation management on root development**

Results showed that root development at moderate levels of reduction in irrigation amount is more related to the intrinsic drought resistance of different species and varieties than to the amount of irrigation applied per se (Bowman et al., 1998; Ervin and Koski, 1998; Su et al., 2007; Sinclair et al., 2011). Overall, no significant changes were observed in rooting at different irrigation amounts between 60% and 100% ET<sub>p</sub> (Fu et al., 2007; Su et al., 2007). However, under a more severe deficit irrigation regime (20% ET<sub>p</sub>), Fu et al. (2007) observed a greater number and length of roots, but this was accompanied by a reduction in turfgrass quality. For larger irrigation amounts applied to bermudagrass (140% vs. 70% Epan), Barton et al. (2006a; b) reported that the total root biomass decreased by 30% when the turf was overirrigated. In addition to the reported variation in rooting as a response to different irrigation treatments, the authors also observed that the total root biomass increased with time, up to ten times when comparing the first with the fourth treatment. Hejl et al. (2016) also reported an increase in root weight from the first to second year of study. In the second year, significant differences between irrigation treatments were found, but the maximum root dry weight did not coincide with the lowest irrigation amount: maximum root biomass was observed for 45% ET<sub>o</sub>, followed by 60% and 30%, respectively. Hejl et al. (2016) reported that the observed differences between treatments in root

biomass during the second year might be attributable to developmental changes in response to long-term exposure to contrasting irrigation treatments.

Several studies report on how moderate drought induced by an increase in irrigation interval can have a positive effect on root development (e.g., Fu and Dernoeden (2009b)). Thus, rooting at deeper soil layers can be stimulated by infrequent irrigation and periods of induced drought stress (Bowman et al., 1998). Infrequent irrigation allows turf to adapt to wilt stress over time, as a result of a more expansive root systems and improved carbohydrate status (Fu and Dernoeden, 2009a). However, those strategies, in addition to promoting deeper root systems, may also lead to a reduction in turfgrass quality. Baldwin et al. (2006) reported that the root biomass of bermudagrass (*Cynodon* spp.) was 46%, 61% and 78% greater when irrigated at 5, 10 and 15-day intervals compared to daily irrigation. However, setting these irrigation intervals also resulted in a decline in the average turfgrass quality between the 12 and 29% compared with plots irrigated on a daily basis. To maintain the balance between a good root system while maintaining turfgrass quality, Johnson (2003) recommended deep-infrequent irrigation to promote rooting, combined with more frequent irrigation to avoid adverse impacts of drought stress during hot periods.

In many cases, under limiting water conditions, those species and varieties that were able to develop deeper, more extensive root systems not only performed better in terms of turfgrass quality (Ervin and Koski, 1998; Fu et al., 2004) but also showed more rapid drought stress recovery (Qian and Fry, 1996; Jordan et al., 2003). High temperatures may also lead to less root biomass in cool-season species (Su et al., 2007; Abraham et al., 2008); during hot periods irrigation should be applied more lightly and frequently which helps to reduce canopy temperature (Ervin and Koski, 1998; Bañuelos et al., 2011) so that transpiration can be maintained. In addition to being able to keep healthy turf under more severe drought conditions, turf with deep, extensive root systems may reduce nitrate leaching risks due to greater N uptake (Bowman et al., 1998; Paré et al., 2006; Wu et al., 2007). Thus, irrigation schedules that promote rooting may also help to reduce N losses.

### 4.3.3 Effects of irrigation management on turfgrass growth rate

In contrast to most agricultural systems, for turfgrass, any reductions in shoot growth are perceived to be beneficial, as long as visual and functional quality are not significantly sacrificed (Wherley, 2011). As with turfgrass quality, turf irrigated with larger irrigation amounts showed higher DMP. It is important to highlight the positive correlation between turfgrass quality and daily DMP in irrigated turfgrass. Where both variables were recorded in the same study, it was observed a positive correlation, with  $R^2$  values for the logistic regression ranging between 0.60 and 0.97 (Qian et al., 2003; Su et al., 2007; Bañuelos et al., 2011; Wherley, 2011; Candogan et al., 2014, 2015; Lee, 2014; Telenko et al., 2015). This nonlinear relationship shows that although low or zero growth rates might compromise turf quality, maximum turf quality scores are achieved before DMP rates reach their maximum. Therefore, high visual turf quality can be achieved with reduced rates of turfgrass growth, providing the turfgrass is maintained in a healthy condition. The growth rates necessary to achieve high-quality scores will vary depending on other factors such as species, season and environment conditions.

The variation in DMP for low irrigation amounts depends on various factors such as site conditions, the turfgrass species/variety (Sinclair et al., 2011) and season (Candogan et al., 2014, 2015). Figure 4.4 shows the reported variation in DMP for studies where the irrigation amount was varied. By irrigating at 50% Epan or less, DMP decreased markedly (e.g., Candogan et al. (2014, 2015)). However, the variation in DMP for different irrigation amounts also differed between studies. For example, Su et al. (2007) observed 45%–48% less DMP when tall fescue, Kentucky bluegrass and hybrid bluegrass were irrigated at 60% compared to 100% ETp. Conversely, excessive irrigation may also lead to reduced DMP (Nektarios et al., 2014). Qian and Engelke (1999) also reported negative impacts of over irrigation (115% vs. 55% Epan) in buffalograss due to too poor tolerance of the species to high irrigations, while tall fescue, bermudagrass and St. Augustine grass (*Stenotaphrum secundatum*) produced more dry matter in their clippings under regimes with high irrigation amounts. Despite the positive relation between DMP and irrigation, turfgrass DMP is more closely dependent on levels of N fertilisation (Candogan et al., 2014, 2015). Figure 4.5 shows the positive



correlation between both variables based on reported observations from four studies. As expected, an increase in DMP leads to a proportional increase in N uptake. Thus, any reduction in growth rate induced by adopting a moderate deficit irrigation strategy would not only lead to a reduction in water use, but also a reduction in N fertilisation need and mowing.

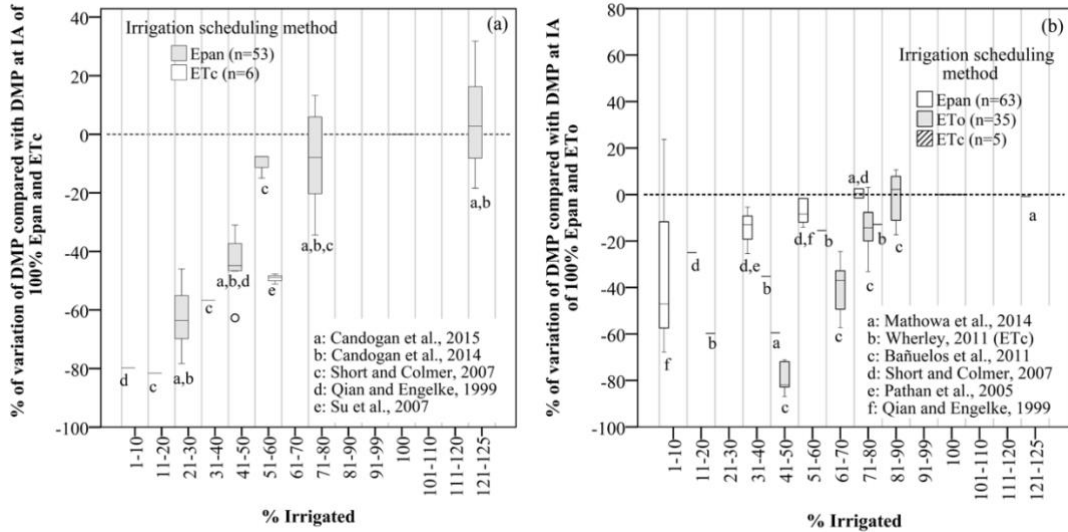


**Figure 4.4** Reported variation in dry matter production in clippings (DMP) within treatments for different irrigation applications expressed as a percentage of irrigation applied (data extracted from seven studies) for (a) cool-season (n = 59) and (b) warm-season turfgrasses (n = 103). Circles display outliers for turfgrass quality values in the interquartile range (IQR)  $\times$  1.5, and stars display outliers beyond the IQR  $\times$  3

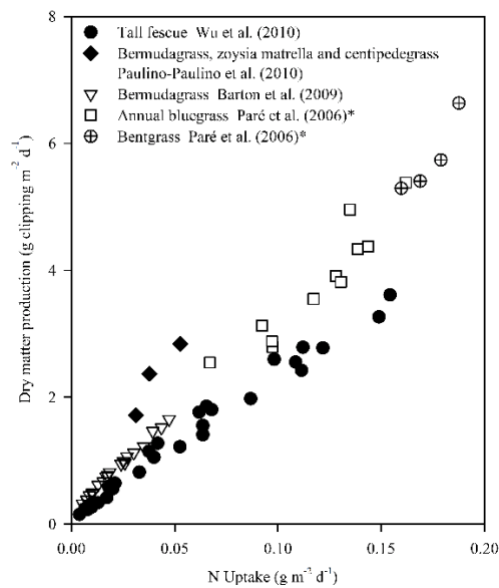


**Figure 4.5** Reported relationships between N uptake (g N m<sup>-2</sup> d<sup>-1</sup>) and dry matter production in clippings (DMP, g m<sup>-2</sup> d<sup>-1</sup>). \*Results shown for Paré et al. (2006) are for clippings and shoot

#### **4.3.4 Effects of irrigation management on nitrogen fate**

As expected, the evidence showed that an increase in irrigation amount resulted in higher drainage and hence an increase in total N losses in leachate. The data also showed a direct relationship between nutrient leaching and fertilisation rates which were evident when turf was overirrigated. In three cases (Morton et al., 1988; Shuman, 2002a; Barton et al., 2006b), no substantial changes in nutrient leaching were reported when fertiliser rates were increased but at a lower irrigation application amount (Figure 4.6). However, when irrigation increased and/or was applied beyond field capacity, a marked increase in leaching occurred. Scheduling irrigation to maximise N uptake and minimise N leaching also needs to consider irrigation frequency. Although deep-infrequent irrigation might lead to more N leaching because larger volumes of water are applied in a single event. Espevig and Aamlid (2012) reported that higher drainage volumes occurred when the same irrigation amount was given as light-frequent irrigation. They related this to the fact that light-frequent irrigation kept the soil water content closer to field capacity thus allowing less buffering capacity for natural rainfall. The effect of irrigation frequency on total N and nitrate leaching was, however, much less than that of rootzone composition. Trenholm et al. (2012) reported that light-frequent irrigations led to a slight increase in nitrate leaching, but with variations between species (zoysiagrass and St. Augustinegrass). Shaddox et al. (2016b) only found significant differences on N leached when comparing normal irrigation with over-irrigation. However, when turf was irrigated 26 mm per week applied in one or two irrigations, no significant differences between total  $\text{NO}_3^-$ -N in leachate and irrigation treatment were reported. Shaddox et al. (2016b) also reported an increase of  $\text{NO}_3^-$ -N leaching for stressed turfgrass (also related to low visual quality).

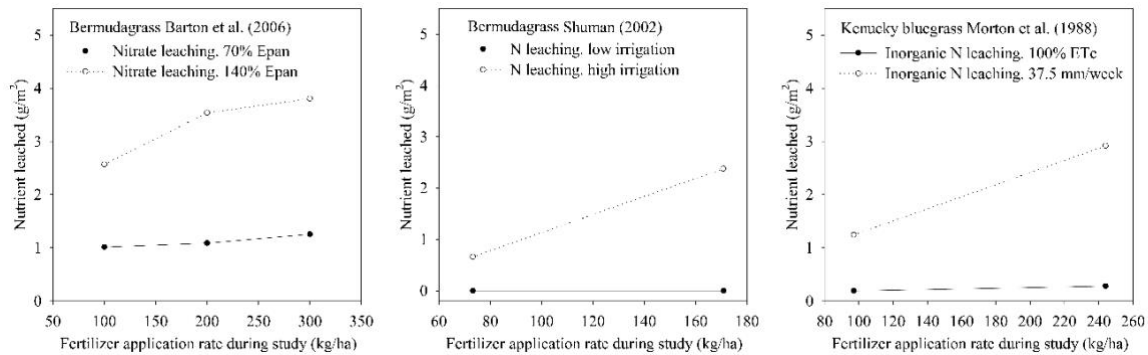


**Figure 4.6** Comparison of different nitrogen application rates ( $\text{kg ha}^{-1}$ ) on quantity leached when different irrigation amounts were applied in three different studies

In addition to irrigation, other factors were found to affect the amount of N lost in leachate. Bowman et al. (1998) observed that the proportion of N lost could be decreased by increasing the interval between the last fertilisation and the following irrigation (75%–100% reduction in N leached when irrigation was delayed by 3–5 days after fertilisation). This may be explained by an increasing residence time of N in the rootzone leading to greater absorption by the roots. Irrigating on sand-based golf greens may increase nitrate leaching risk. Sandy soils have lower water retention capacity, and usually lower organic matter content than more fine-textured soils (Nektarios et al., 2014). However, heavier soils with more organic matter and higher moisture retention will facilitate N denitrification, which may result in less leaching of  $\text{NO}_3^-$ -N (Nektarios et al., 2014). Sand-based rootzones with higher organic matter content may be attained by amending the sand with compost (Espevig and Aamlid, 2012), by having older turf with a deeper thatch-mat layer (Barton et al., 2009) or by maintaining a healthier, actively growing and denser canopy (Paré et al., 2006; Trenholm et al., 2012; Shaddox et al., 2016b), which promotes higher N uptake (Wu et al., 2010; Telenko et al., 2015). These results are consistent with Kvalbein and Aamlid (2014) who suggested that the risk of N leaching from dense and healthy golf greens is usually quite low, but that it may increase dramatically if the turfgrass cover becomes incomplete due to diseases, winter damage, wear or management. High amounts of  $\text{NO}_3^-$ -N in leachate from young or recently established turf may be related to a thinner thatch-mat layer containing less organic matter (Barton et al., 2009; Telenko et al., 2015), and therefore, less N is immobilised.

It was observed that higher growth rates were closely related with increased N uptake (Paré et al., 2006; Paulino-Paulino et al., 2008; Barton et al., 2009; Wu et al., 2010) (Figure 4.5) resulting in lower nitrate leaching (Paré et al., 2006). Evidence suggested that N uptake was less related to irrigation than to the maximum potential growth rates for different turfgrass species and varieties (Paré et al., 2006; Ericsson et al., 2012c). The maximum potential growth rate is the maximum possible plant growth under a favourable and healthy environment and non-limiting inputs. While applied N is not taken up by the plant, a portion that remains in the soil is susceptible to leaching, run-off and gaseous losses through volatilisation and denitrification. The gaseous N losses through denitrification are relatively higher when N fertilisation exceeds plant needs (Wang et al., 2014). The gaseous losses of N in turfgrass can also be affected by irrigation. Bowman et al. (1987) observed that irrigating after fertilisation reduces N losses by volatilisation, whilst recognising that volatilisation is also affected by soil pH. In contrast, an increase in soil water content, accompanied by high temperatures, might increase N gaseous losses by denitrification (Wang et al., 2014). Irrigation strategies where irrigation is applied frequently and back to field capacity might increase the risk of N losses due of denitrification.

Variations observed in N uptake for the same species, at the same fertiliser rate and in the same study (Figure 4.7), were related to other factors such as fertiliser source (Barton et al., 2006a; Wu et al., 2010), frequency of fertiliser application (Quiroga-Garza et al., 2001; Barton et al., 2009), turfgrass age (Barton et al., 2009), varieties within the same species (Paré et al., 2006) and year of treatment (Wu et al., 2010). Paulino-Paulino et al. (2008) reported that bermudagrass leached 8%–60% less  $\text{NO}_3^-$ -N compared to centipedegrass (*Eremochloa ophiuroides* Hack.) and manilagrass (*Zoysia matrella* L.) which coincided with higher N uptake and DMP in the former species. Most importantly, Wu et al. (2010) showed that the irrigation and N application rates ought to be reduced towards the end of the growing season because of the slowdown in turfgrass metabolism.

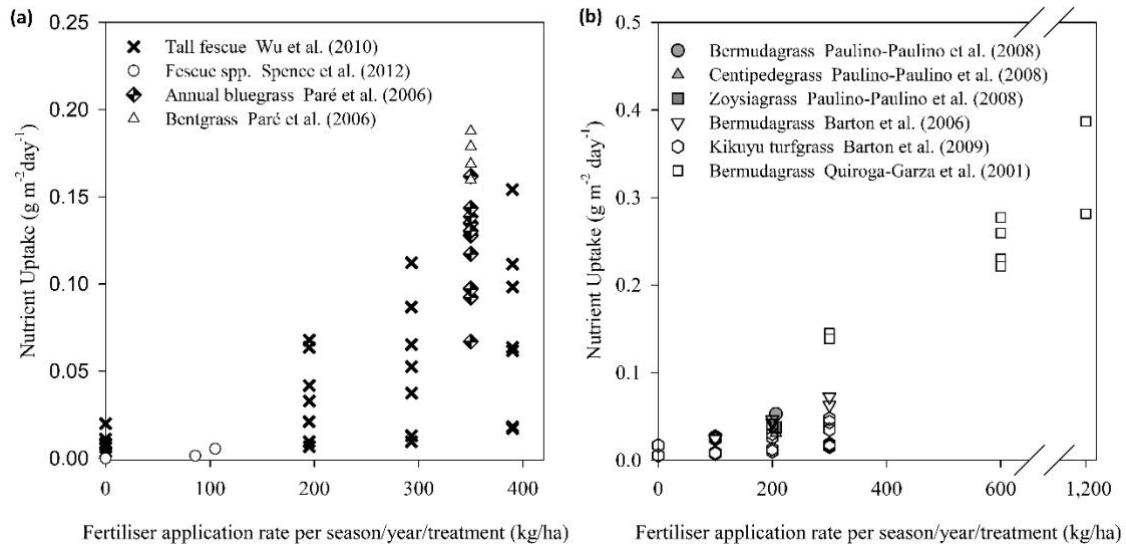


**Figure 4.7** Reported relationships between N fertiliser application rates per season/year/treatment (kg N ha<sup>-1</sup>) during the study period and N uptake (g N m<sup>-2</sup> d<sup>-1</sup>) for (a) cool-season and (b) warm-season turfgrasses

#### 4.3.5 Methodological limitations

This SR had a number of methodological limitations which need to be recognised. Some papers identified in the literature were not available; it was also difficult to source some conference papers. Although data were extracted from studies in which turf development was directly or indirectly influenced by irrigation, there were confounding factors, for example, the region and climate of the area where the research was conducted, trials using different turfgrass species, varieties, fertiliser rates and/or different methods for ET estimation. Although ET indicators can be directly related to irrigation need and are widely used in irrigation scheduling, their application is more suited to semi-arid environments rather than humid climates where irrigation is supplemental to rainfall. Some researchers have therefore developed drought stress indicators that combine both ET and rainfall to overcome this challenge (Haro-Monteagudo et al., 2017). Not all studies followed the same experimental design or methodology, and for turfgrass quality assessment, the duration of each experiment, turf maintenance, the use of rainout shelter and any bias in turfgrass quality scoring may all have influenced the synthesis of results. Some errors may also have been introduced into the metadatabase during data extraction from published data (graphs), but this is likely to be  $\leq \pm 10\%$ . There were also a range of so-called effect modifiers, which

present opportunities to convey a deeper understanding of the topic across a wide variety of environments but also had influence in the final analysis of the results. Those include different scheduling methods, irrigation strategies, turfgrass species, mowing height, fertilisation rates, wear stresses, weather/local conditions and treatment durations. Finally, although the use of wastewater is a growing trend in turfgrass irrigation, this topic was excluded to limit the impact of effect modifiers, one of which is water source. Understanding wastewater issues in the context of agronomic and environmental impacts in turf is worthy of a SR in its own right.

#### **4.4 SUMMARY**

This SR summarises evidence on the effects of irrigation management on turf performance and complements research by Barton and Colmer (2006) by synthesising recent evidence on the impacts of irrigation on turfgrass quality, rooting and its relationships with turf growth and N fate. In general, during the growing season, average visual turf quality can be maintained at an acceptable level through deficit irrigation (up to 40% ET<sub>p</sub>), while maximum turfgrass quality can be achieved with irrigation above 60%–80% ET<sub>p</sub>. However, it was found that it is difficult to define irrigation need precisely, as the impacts of irrigation on turfgrass quality also depend on other factors such as turfgrass species, location and year of study. Results from several studies showed that adverse effects of deficit irrigation on turfgrass quality are more evident when turf is subject to environmental and/ or management stresses such as long intervals between irrigation, short mowing heights or high temperatures. Moderate deficit irrigation strategies can be applied during the year without significantly compromising on turfgrass quality. However, during high-stress periods such as hot summer days or intense traffic, irrigation strategies should reflect the target use (sports, amenity, landscape) and accept there may be periods with reduced visual turfgrass quality. Deeper rooting was shown to be related to improved turfgrass quality particularly during drought events and faster recovery after drought stress. In contrast to most agricultural crops, high growth rates are not desirable in turfgrass as they lead to more frequent mowing and greater N and water

consumption. Evidence showed that well-watered and fertilised turfgrass results in good turfgrass quality. However, the relationship is not linear. Although greater irrigation amounts lead to increases in DMP, N fertilisation appeared to be a more important driver of turfgrass growth than irrigation. Thus, adequate irrigation scheduling becomes crucial as N leaching risks may also be minimised by avoiding irrigation applications beyond field capacity and by avoiding fertiliser applications when growth rates are reduced due to the impact of plant stress, or the recent establishment of turfgrass. By maintaining a healthy, actively growing turf cover, the nutrient leaching risk will be minimised. This SR not only provides a valuable synthesis for turfgrass agronomy researchers, but also useful insights for practitioners involved in turfgrass management, including greenkeepers and sports facility groundsmen.





## **5 SIMULATING IRRIGATION HETEROGENEITY BASED ON BALLISTICS THEORY**

This chapter describes the development of a model to simulate irrigation performance on golf greens. Field tests were undertaken to measure water distribution patterns for a typical golf sprinkler operating under ‘no-wind’ and ‘windy’ conditions. A ballistics-based model was then developed to simulate irrigation for a selected golf rotor sprinkler. Finally, the ballistics model was calibrated and validated with field data and its performance evaluated.

### **5.1 METHODOLOGY**

The methodology was split into three stages. Figure 5.1 summarises the individual stages and their linkages.

#### **5.1.1 Field tests**

Single sprinkler performance field tests were conducted between 10<sup>th</sup> June 2016 and 25<sup>th</sup> October 2016. The test site was located at Cranfield University, Bedfordshire, UK (Lat 52°05’N, Lon 0°38’W, 101 m.a.s.l.). The area was approximately 6000 m<sup>2</sup>, flat and covered with short-mown grass. The shape of the field was nearly rectangular with an NW-SE orientation along the longest side, surrounded by trees in the NE and SW edges and with free air circulation in the NW and SE sides (Figure 5.2). A pop-up rotor sprinkler RainBird 751 SERIES (Figure 5.3) was tested. This model was chosen as it is widely used on greens and fairways. In this sprinkler, water under pressure enters the base of the head through a stator, which produces a circular movement of the “nozzle assembly”. Through torque, this nozzle assembly provides the sprinkler with a relatively slow rotational speed required for excellent coverage and precipitation (Choate, 1994).

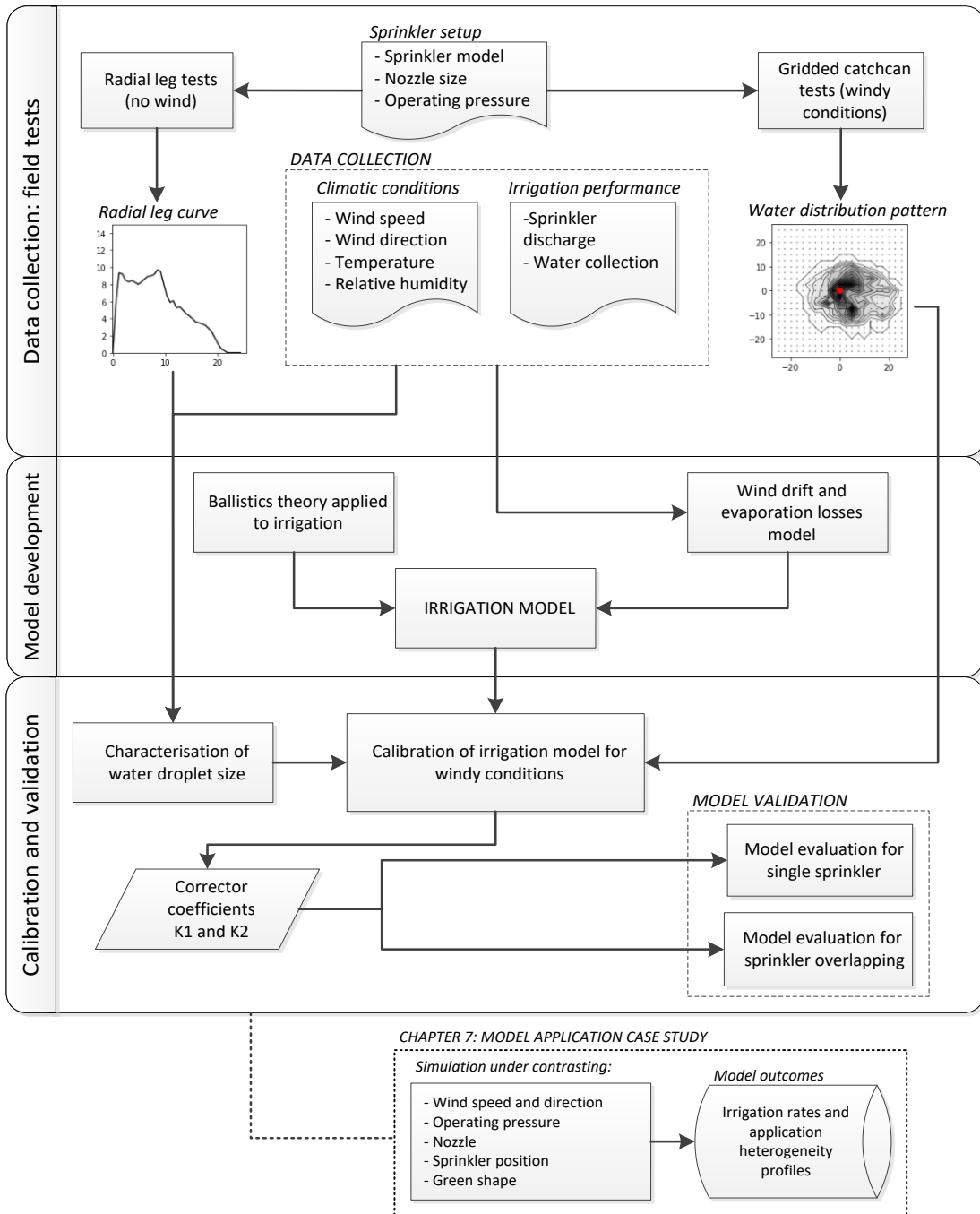


**Figure 5.1** Flow diagram of the methodology developed for the irrigation modelling

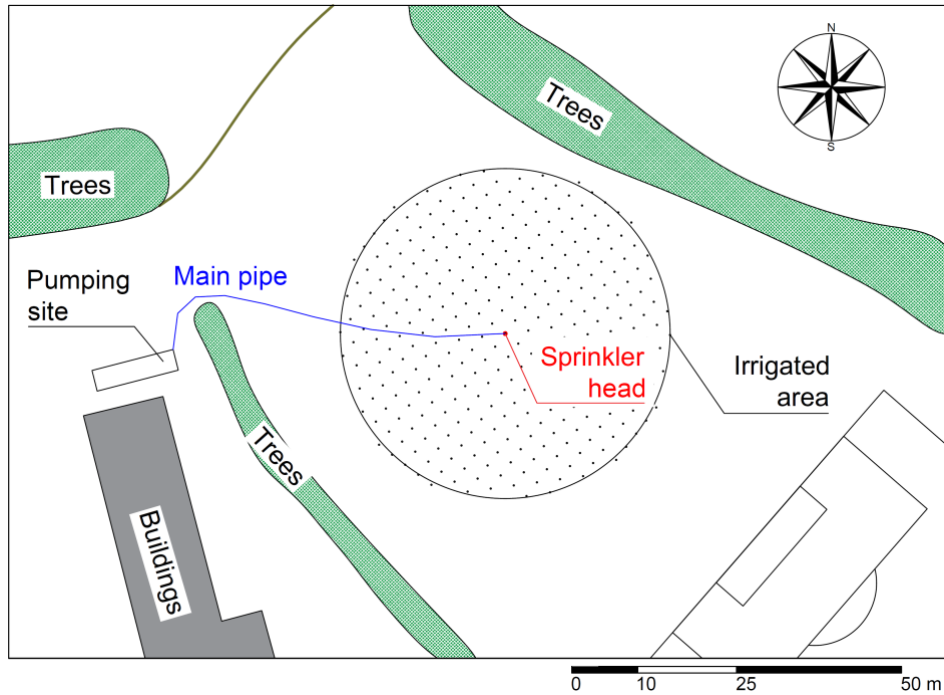


**Figure 5.2** Location of the irrigation sprinkler test site



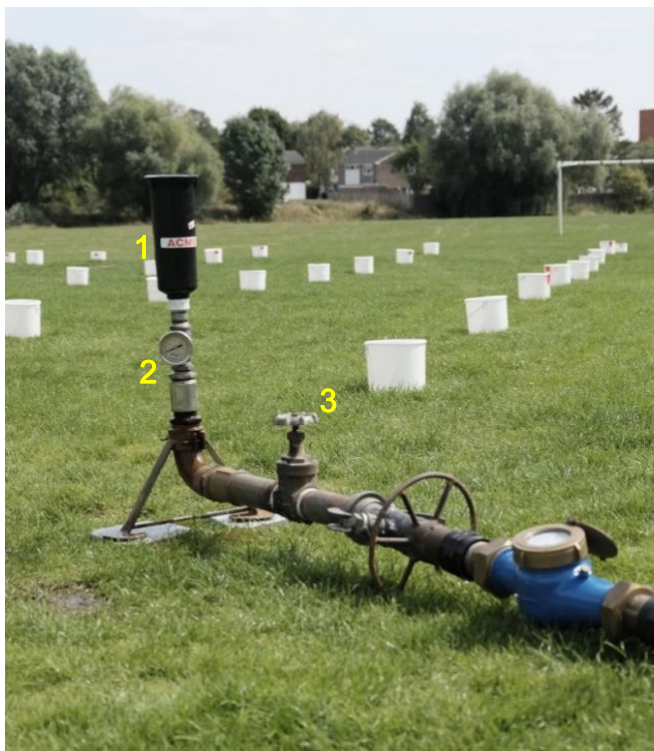
**Figure 5.3** Close-up of the rotor sprinkler RainBird 751 SERIES

Four sprinkler set-ups were used: nozzle size “#28 white” operating at pressures of 4.2 and 6.0 bar, and nozzle size “#40 orange” operating at pressures of 4.2 and 6.0 bar. According to the manufacturer, these set-ups provide flows that range between 64 and 108 L min<sup>-1</sup> and provide a wetted radius of 17.5 to 21.5 m under ‘no-wind’ conditions (Table 5.1).

**Table 5.1** Performance of the RainBird 751 sprinkler under test conditions (source: RainBird).

Nozzle	Pressure (bar)	Flow (L min <sup>-1</sup> )	Radius (m)
#28 White	4.2	64	17.5
	6.0	76	18.0
#40 Orange	4.2	90	20.5
	6.0	108	21.5

The sprinkler was mounted on a prefabricated stand, which placed the sprinkler nozzle (and therefore start position of the water jet) 0.79 m above ground level (Figure 5.4a). The system was pressurised using a 2.2 kW Lowara 5SV14 pump (Figure 5.4b), with the pressure controlled via a valve located on the delivery pipe to the sprinkler. The pressure was measured at the exit of the pump and between the valve and sprinkler. The volume of water used in each test and flowrate was measured using a flowmeter located on the discharge side of the pump. The flowmeter recordings were checked so as readings of flow and water use were consistent with values provided by the manufacturer for a given sprinkler set-up.



(a)



(b)

**Figure 5.4** (a) View of the sprinkler stand installed in field. 1: Sprinkler RainBird 751 Series; 2: Pressure gauge; 3: Valve to control flow/pressure. (b) View of the pump station. 1: Pump Lowara 5SV14; 2: Flowmeter GPI A109LMA100IA1; 3: Pressure gauge.

The run time for each test varied between 7 and 29 minutes, depending on the volume of water available in the 1.5 m<sup>3</sup> storage tank. Test duration was therefore limited by the available water flow for each sprinkler set-up. For each test, the 'initial' and 'final' jet position were the same so that all the catchcans were irrigated by the same number of sprinkler rotations.

All catchcans were identical and measured 0.19 m in height and 0.209 m in diameter. The water collected in each catchcan was measured using a graduated cylinder following each test. Evaporation during each test was estimated as the difference between the initial and final volume of water collected in a graduated rain gauge located outside the wetted test area. Hourly relative humidity data were obtained from a nearby weather station<sup>4</sup>.

Two types of tests were carried out to calibrate the sprinkler RainBird® 751 Series comprising (i) radial leg tests under 'no-wind' conditions and (ii) gridded catchcan tests under 'windy' conditions. These were conducted in accordance with the relevant standards from the American Society of Agricultural Engineers (ASAE) S398.1 (1985) and S436.1(1989).

#### Radial leg tests under 'no-wind' conditions

The first type of test was the radial leg test under 'no-wind' conditions. These tests aimed to characterise the radial curve of the sprinkler operating at different pressures and nozzle size. The tests consisted of setting out three radial legs of catchcans with each leg extending 25 m, and with the catchcans placed every 0.5 m (Figure 5.5 and Figure 5.6). The resultant radial leg data for each test was calculated as the average of the three lines. The output from these tests are radial leg curves for a specific sprinkler model, and operating pressure and nozzle set-up. This curve was necessary in order to characterise the water droplet size distribution along the wetted radius using ballistics theory. Four attempts of radial leg irrigation tests under 'no-wind' conditions were carried out between 10<sup>th</sup> June 2016 and 25<sup>th</sup> October 2016. Field tests were conducted in the early morning usually between 5 and 7 am due to calm conditions at that time of day.

---

<sup>4</sup> Cranfield Airport. [http://rp5.co.uk/Weather\\_in\\_Cranfield\\_\(airport\)](http://rp5.co.uk/Weather_in_Cranfield_(airport))

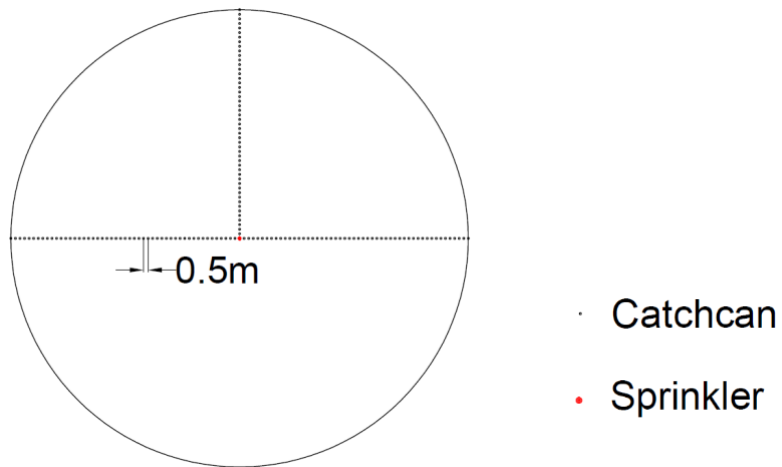


**Figure 5.5** Position of catchcans in the radial leg tests under ‘no-wind’ conditions.



**Figure 5.6** Irrigation during the radial leg tests

**Gridded catchcan tests under ‘windy’ conditions**

The second type of tests was conducted under windy conditions. The objective was to characterise the water distribution pattern over the plane distorted by wind speed and wind direction. Catchcans were placed on a 2.5 × 2.5 m grid with the sprinkler at the centre (Figure 5.7 and Figure 5.8). In total, 328 catchcans were used covering a circle with a radius of 25 m.

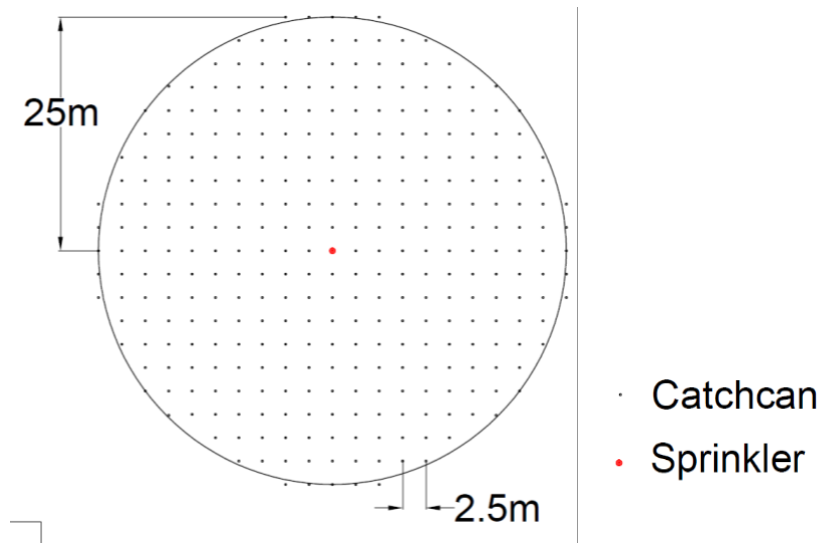


**Figure 5.7** Position of catchcans in tests under windy conditions



**Figure 5.8** Panoramic view of the catchcan grid during an irrigation test

Measurements of wind speed and direction were taken approximately every 60 seconds at 2 m height. Wind speed ( $\text{m s}^{-1}$ ) and air temperature were recorded using a hand-held anemometer HoldPeak HP-866B. Wind direction was measured by a wind monitor Young 05103. The average wind speed was calculated as the average of the vector wind  $\overline{\vec{W}_s}$ . Using  $\overline{\vec{W}_s}$  instead of the average of the scalar products of wind speeds improves the assessment of irrigation uniformity (Sanchez et al., 2011). To assess the variation in wind direction within each test, the wind speed uniformity (WSU, %) was calculated as:

$$\text{WSU} = \left( 1 - \frac{|\overline{\vec{W}_s}| - \overline{W_s}}{|\overline{\vec{W}_s}|} \right) \times 100$$

where  $\overline{|\vec{W}_s|}$  is the average of the scalar products of measured wind speed ( $\text{m s}^{-1}$ ); and  $\overline{\vec{W}_s}$  is the average of the vectors wind speed measured in field ( $\text{m s}^{-1}$ ).

For the calibration and validation of the ballistic model, only those tests with a WSU above 80% were used.

### Estimation of total water applied

The volume of water collected was measured and converted to an irrigation rate at each catchcan ( $\text{IR}_{\text{CC}}$ ,  $\text{mm h}^{-1}$ ):

$$\text{IR}_{\text{CC}} = \frac{\text{Water collected (ml)} \times 0.24}{\text{catchcan diameter}^2 (\text{m}^2) \times \pi \times \text{test duration (min)}} = \text{mm h}^{-1}$$

The  $\text{IR}_{\text{CC}}$  ( $\text{mm h}^{-1}$ ) was considered to be representative of the  $2.5 \times 2.5 \text{ m}^2$  surrounding them, with the catchcan in the centre. The  $\text{IR}_{\text{CC}}$  in the gridded tests were used to estimate the flow ( $F_{\text{CC}}$ ,  $\text{m}^3 \text{ h}^{-1}$ ) and total water ( $I_{\text{CC}}$ ,  $\text{m}^3$ ) collected in the catchcans; i.e., the total water that reached the canopy. The  $F_{\text{CC}}$  and  $I_{\text{CC}}$  were calculated:

$$F_{\text{CC}} (\text{m}^3 \text{ h}^{-1}) = \frac{\text{IR}_{\text{CC}} (\text{mm h}^{-1}) \times n \times [\text{Catchcan spacing (m)}]^2}{10^3}$$

$$I_{\text{CC}} (\text{m}^3) = \frac{\sum_1^N \text{Water collected (ml)} \times [\text{Catchcan spacing (m)}]^2}{10^3}$$

where  $n$  is the number of catchcans in which water was measured.

The difference between the volume of water that passes through the sprinkler and  $I_{\text{CC}}$  was then used to calculate the irrigation application efficiency ( $I_{\text{AE}}$ , %):

$$I_{\text{AE}} (\%) = \frac{I_{\text{CC}} (\text{m}^3)}{\text{volume measured before the sprinkler (m}^3)} \times 100$$

### **5.1.2 Irrigation model development**

In parallel to the field data collection, a model was developed for simulating irrigation heterogeneity on a green using ballistics theory. The individual steps which were adopted are presented below, building on previous work conducted



by Carrión et al. (2001b). Firstly, the equations used by the model to describe the water droplet trajectories are described. Secondly, the process of determining the droplet sizes along the radial leg curve under 'no-wind' conditions are explained, together with the method used to simulated full circle irrigation under windy conditions. Finally, the water applied by irrigation over the relevant area was aggregated. The model was calibrated and validated with data from the field tests and its performance evaluated.

The model was coded in Matlab® (The MathWorks Inc., 2010). The model interacts with input files that contain sprinkler data, green shape or meteorological conditions, and returns the wetted patterns of a single or overlapped set of sprinklers over the designated irrigated area.

#### Calculation of water droplet trajectories using ballistics theory

The basis of ballistics-based modelling applied to individual water droplets relies on the fact that water droplets thrown by sprinkler travel independently in the air from the nozzle to the crop canopy or the soil. Fukui et al. (1980) proposed the original equations described here, which have been applied successfully in further investigations (Seginer et al., 1991; Carrión et al., 2001b; Playán et al., 2006; Yan et al., 2010).

The starting point of the ballistic model is to know the initial droplet velocity at the exit of the nozzle, which is estimated by the discharge equation:

$$\vec{U}_0 = c \sqrt{2 g H}$$

where  $\vec{U}_0$  is the initial velocity of the droplet at the exit of the sprinkler nozzle in relation to the ground ( $\text{m s}^{-1}$ );  $c$  is the discharge coefficient (near 1);  $g$  is the value of the acceleration of the gravity ( $9.81 \text{ m s}^{-2}$ ); and  $H$  is the pressure of water (water metre column) in the nozzle.

$\vec{U}_0$  is the resultant of the components  $U_{0x}$ ,  $U_{0y}$  and  $U_{0z}$ . Components  $U_{0x}$  and  $U_{0y}$  are a function of the initial jet angle (which is determined by the nozzle) and the jet direction during the sprinkler rotation.  $U_{0z}$  is only a function of the initial jet

angle. The components of the initial droplet velocity can be therefore split as follows:

$$\begin{aligned}U_{0x} &= \cos(jd) \times \cos(ja) \times \overrightarrow{U_0} \\U_{0y} &= \sin(jd) \times \cos(ja) \times \overrightarrow{U_0} \\U_{0z} &= \sin(ja) \times \overrightarrow{U_0}\end{aligned}$$

where  $jd$  is the jet direction in the rotation (0 to 360 degrees); and  $ja$  is the initial jet angle relative to the soil (degrees).

In the absence of wind, the droplet velocity in relation to the air at the position  $i$  ( $\overrightarrow{U}_i$ ) is equal to the velocity relative to the air at the same position ( $\overrightarrow{V}_i$ ,  $m\ s^{-1}$ ). Under the influence of wind,  $\overrightarrow{V}_i$  is affected by the component horizontal of wind velocity relative to the ground ( $\overrightarrow{W}_i$ ) ( $m\ s^{-1}$ ). Thus, the components of  $\overrightarrow{V}_i$  are:

$$\begin{aligned}V_{ix} &= U_{ix} - W_{ix} \\V_{iy} &= U_{iy} - W_{iy} \\V_{iz} &= U_{iz}\end{aligned}$$

During their trajectory, the velocity of water droplets is altered due to the resistance force ( $F_R$ ), which is based on the drag force of the air. Fukui et al. (1980) proposed that  $F_R$  could be derived from the general drag equation:

$$F_R = \frac{1}{2} \rho u^2 C A = \frac{1}{8} \rho_a V^2 C \pi D^2$$

where  $\rho$  is the density of the fluid ( $kg\ m^{-3}$ );  $u$  is the speed of the object relative to the fluid ( $m\ s^{-1}$ );  $C$  is the drag coefficient,  $A$  is the cross-sectional area of the object ( $m^2$ );  $\rho_a$  is the density of the air ( $kg\ m^{-3}$ );  $V$  is the velocity of the water droplet relative to the air ( $m\ s^{-1}$ ); and  $D$  is the water droplet diameter (m).

For isolated water droplets,  $C$  is defined as a function of the Reynolds number ( $Re$ ) (Fukui et al., 1980; Seginer et al., 1991), as shown in the following equations:

$$Re = \frac{VD}{\nu}$$

$$\left\{ \begin{array}{l} \text{if } R_e \leq 128 \longrightarrow C = \frac{33.3}{R_e} - 0.0033R_e + 1.2 \\ \text{if } 128 \leq R_e \leq 1440 \longrightarrow C = \frac{72.2}{R_e} - 0.0000556R_e + 0.48 \\ \text{if } 1440 \leq R_e \longrightarrow C = 0.45 \end{array} \right.$$

where  $u$  is the kinematic viscosity of the air.

Seginer et al. (1991) proposed a different equation for  $F_R$  based on the mass of the water droplet:

$$F_R = m C_2 V^2 = \rho_w \frac{4}{3} \pi \frac{D^3}{8} C_2 V^2$$

where  $m$  is the mass of a drop of water (kg);  $C_2$  is the resistance coefficient; and  $\rho_w$  is the water density ( $\text{kg m}^{-3}$ ).

By equating the resistance force proposed by Fukui et al. (1980) and Seginer et al. (1991),  $C_2$  is isolated:

$$C_2 = \frac{4}{3} \frac{\rho_a}{\rho_w} \frac{C}{D}$$

When irrigation of a single sprinkler is simulated under 'windy' conditions using the previously defined resistance coefficients, the resultant water distribution pattern is almost circular. To solve this problem, the aerodynamic coefficient  $C$  was corrected as proposed by Tarjuelo et al. (1994). This modification consisted of narrowing the simulated water distribution in a perpendicular direction to the wind, as well as shortening the simulated water distribution to windward with an extension to leeward. The modification of the aerodynamic coefficient  $C$  depends on the corrector coefficients  $K_1$  and  $K_2$ :

$$C' = C (1 + K_1 \sin\beta - K_2 \cos\alpha)$$

where  $\beta$  is the angle comprised between the vectors  $\vec{V}_i$  and  $\vec{U}_i$ ; and  $\alpha$  is the angle comprised between the vectors  $\vec{V}_i$  and  $\vec{W}_i$ .

Corrector coefficients  $K_1$  and  $K_2$  modify the simulated water distribution pattern. Under no-wind conditions, the water distribution pattern is circular as  $C$  is equal to  $C'$ .

Variation of trajectory, velocity and acceleration of a water droplet in the air during its flight

Water droplet movement in the air is obtained from the conditions of their dynamic equilibrium (Carrión et al., 2001a). Considering the previous expressions to estimate  $F_R$ , components of acceleration might be expressed as shown in the differential equation:

$$A_x = \frac{d^2x}{dt^2} = -\frac{3}{4} \frac{\rho_a}{\rho_w} \frac{C}{D} V \left( \frac{dx}{dt} - W_x \right) = -C_2 V (U_x - W_x)$$

$$A_y = \frac{d^2y}{dt^2} = -\frac{3}{4} \frac{\rho_a}{\rho_w} \frac{C}{D} V \left( \frac{dy}{dt} - W_y \right) = -C_2 V (U_y - W_y)$$

$$A_z = \frac{d^2z}{dt^2} = -\frac{3}{4} \frac{\rho_a}{\rho_w} \frac{C}{D} V \frac{dz}{dt} - g = -C_2 V U_z - g$$

where  $A$  is the acceleration of the water droplet in the air ( $m\ s^{-2}$ );  $x, y, z$  are the Cartesian coordinates with origin in the sprinkler (m);  $\frac{dx}{dt}$ ,  $\frac{dy}{dt}$  and  $\frac{dz}{dt}$  are the components of  $\vec{U}_i$  ( $m\ s^{-1}$ ); and  $t$  is the time since the water droplet started to travel from the nozzle (seconds).

The differential equations presented above are solved using the fourth order Runge-Kutta numerical integration technique (Carrión et al., 2001b). For this it is necessary to know the initial droplet position (given by the  $x, y, z$  of the sprinkler nozzle), velocity (given by  $\vec{U}_0$ ) and time (zero seconds). This resolution method allows the water droplet position at each time interval  $\Delta t$ , which is dependent on the position, acceleration and velocity at the previous step  $t_{i-1}$  to then be determined. Lower time intervals or steps in the calculation lead to greater precision in the results in the simulation at the expense of increasing the time of resolution. The three components of the droplet velocity  $U_i$  in step  $i$  are expressed as:

$$U_{x(i)} = U_{x(i-1)} + A_{x(i-1)} \Delta t$$

$$U_{y(i)} = U_{y(i-1)} + A_{y(i-1)} \Delta t$$

$$U_{z(i)} = U_{z(i-1)} + A_{z(i-1)} \Delta t$$

And therefore, the position of the water droplet was determined by:

$$X_{(i)} = X_{(i-1)} + U_{x(i-1)} \Delta t$$

$$Y_{(i)} = Y_{(i-1)} + U_{y(i-1)} \Delta t$$

$$Z_{(i)} = Z_{(i-1)} + U_{z(i-1)} \Delta t$$

### Assessment of wind speed at different height

The variation of the horizontal component of the vector  $\overline{W}_i$  at different heights in relation to the plane (and hence its influence in droplet trajectory) was also estimated. The relation between wind speed and height follows a logarithmic relationship, with it being possible to relate wind measured ( $W_a$ ,  $m s^{-1}$ ) at height  $z_a$  (m) with wind velocity  $W_z$  at any other height  $z$  (Vories et al., 1987).

$$W_z = W_a \frac{\ln\left(\frac{z-d}{z_0}\right)}{\ln\left(\frac{z_a-d}{z_0}\right)}$$

where  $d$  is roughness height (m); and  $z_0$  is the roughness parameter (m).

Roughness height accounts for the shift of the logarithmic curve vertically over a crop canopy. Stanhill (1969) defined the roughness height ( $d$ ) as a function of the crop height ( $h$ , in m).

$$\log d = 0.9793 \log h - 0.1536$$

The roughness parameter is a way to describe the ground surface or plant canopy. Tanner and Pelton (1960) related the roughness parameter  $z_0$  to crop height ( $h$ ).

$$\log z_0 = 0.997 \log h - 0.883$$

Figure 5.9 shows an example of the estimated variation in wind speed at different heights for turfgrass and wheat, when a wind speed of  $3 m s^{-1}$  was measured at 2 m from the ground. For turfgrass, a height of 0.01 m was assumed and 0.7 m for wheat. It can be observed that the estimated variation in wind speed at different heights is lower for turfgrass compared to higher crops due to its lower roughness coefficient.

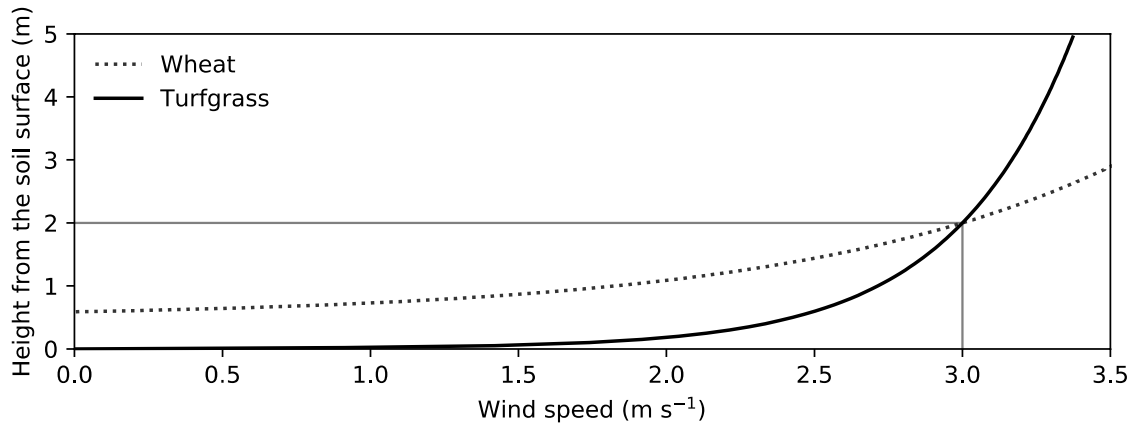


**Figure 5.9** Variation in wind speed at different heights in turfgrass and wheat for wind 3 m s<sup>-1</sup> measured at 2 m height

### Assessment of wind drift and evaporation losses (WDEL)

During sprinkler irrigation, some water thrown by sprinklers does not actually reach the crop canopy (Odhiambo et al., 2011). These losses are mainly derived from the action of wind drift and evaporation, and commonly known as Wind Drift and Evaporation Losses (WDEL). WDEL depends on environmental factors and the characteristics of the sprinkler. In this research, WDEL measured in field tests (from now WDEL<sub>m</sub>) were estimated as the ratio between the water collected by the catchcans (F<sub>CC</sub>) and water discharge rate entering the sprinkler (F<sub>spr</sub>):

$$WDEL_m(\%) = \frac{F_{spr}(L h^{-1}) - F_{CC} (L h^{-1})}{F_{spr} (L h^{-1})} \times 100 = 1 - I_{AE}$$

Various researchers have proposed predictive equations to determine simulated WDEL<sub>m</sub>; these are summarised and compared by Playán et al. (2005). However, in this research was developed a predictive model with better fitting to the sprinkler type and climate conditions measured during the tests. For this, a multivariable linear regression approach was used, where the dependent variable was WDEL<sub>m</sub> for each test, and the independent variables were operating pressure (bar), temperature (°C), relative humidity (%) and wind speed (m s<sup>-1</sup>) measured in the same test.

The derived equation was then used to predict WDEL (WDEL<sub>s</sub>) for each simulation. The WDEL<sub>s</sub> was used to correct the initial radial leg curve. This process followed three stages. Firstly, the percentage of evaporation losses

( $E_i$ , %) for each drop diameter ( $D_i$ , in mm) was calculated using the following equation proposed by Carrión et al. (2001b).

$$E_i = 1.8271 D^{-1.5379}$$

This equation is valid for droplet diameters greater than 0.2 mm, while for diameters larger than 2 mm, the percentages of water lost by evaporation were assumed to be negligible (Figure 5.10).

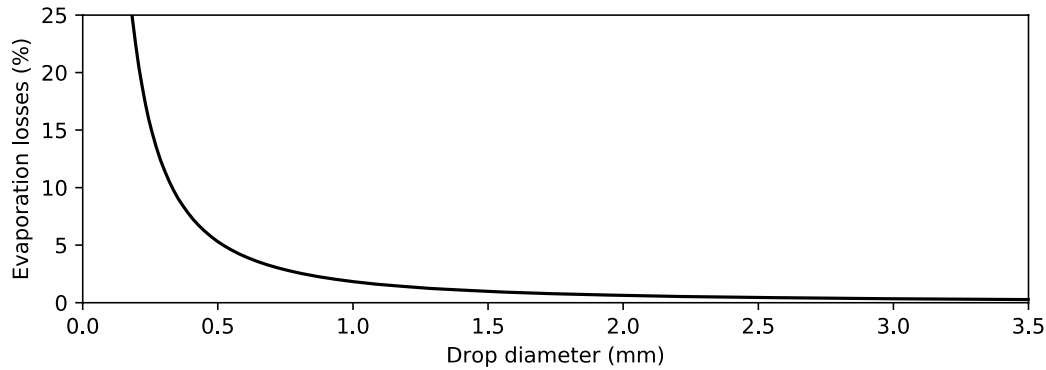


**Figure 5.10** Derived relationship between the percentage of evaporation losses (%) and droplet diameter (mm) based on equation proposed by Carrión et al. (2001b)

The total evaporation losses (EL,  $L h^{-1}$ ) were then calculated by aggregating the evaporated water along the radial curve. Each point of the radial curve had associated a drop diameter that reached at that point. The percentage of evaporation losses associated to each drop diameter (Figure 5.10) were then multiplied by the discharge rate associated to that point in the radial leg curve. This process is described as:

$$EL = \sum_{i=0.2} E_i Q_i = \sum_{i=0.2} E_i P_i \pi \left[ \left( r_i - \frac{r_i - r_{i-1}}{2} \right)^2 - \left( r_i + \frac{r_{i+1} - r_i}{2} \right)^2 \right]$$

where EL are total evaporation losses ( $L h^{-1}$ );  $Q_i$  is the flow discharged by the sprinkler at each point of the radial curve ( $L h^{-1}$ );  $P_i$  is the precipitation discharged by the sprinkler at each point of the radial curve ( $mm h^{-1}$ ); and  $r_i$  is the radius each point of the radial curve (m).

In the second stage, losses associated with wind drift were calculated by considering the evaporation losses corresponding to each point of the radial curve:

$$WD_i = \frac{Q_i}{\sum Q_i} [(\sum Q_i \times WDEL_s(\%)) - EL]$$

where  $WD_i$  are the drift losses at the point  $i$  of the radial curve, in  $L h^{-1}$ .

The last stage consisted of the correction of the radial curve with new precipitation rates. The following shows the procedure to obtain the corrected precipitation rates at each point ( $P_{ci}$ , in  $\text{mm h}^{-1}$ ).

$$P_{ci} = \frac{Q_i - (WD_i + E_i)}{\pi \left[ \left( r_i - \frac{r_i - r_{i-1}}{2} \right)^2 - \left( -r_i + \frac{r_{i+1} - r_i}{2} \right)^2 \right]}$$

Estimation of droplet size at each distance of the radial curve under ‘no-wind’ conditions

The equations presented above were used to determine a water flow associated with a given droplet diameter ( $D_i$ ). Firstly, the trajectory of different  $D_i$  under ‘no-wind’ conditions from the exit of the sprinkler nozzle to the turf canopy was characterised. This trajectory was estimated by using ballistics theory for given climate conditions, operating pressure and initial jet angle. The trajectories were calculated for a range of droplet diameters starting at  $D_i$  of 0.2 mm, with increments of 0.02 mm until a maximum  $D_i$ , was reached which was set as the  $D_i$  that exceeded the radius of the sprinkler radial leg curve. As the radius of the radial leg curve is intrinsic to each sprinkler model and sprinkler set-up, the value of the maximum  $D_i$  varied depending on each simulation.

Figure 5.11 shows an example of the trajectories of four  $D_i$  from the exit of the sprinkler (0.07 m in height) to the turf canopy (0.01 m height) at 0.01-second intervals. In this example, the simulated operating pressure was 6 bar and jet angle  $25^\circ$ . It is evident that the larger droplets travelled further and higher distances over a longer period of time.

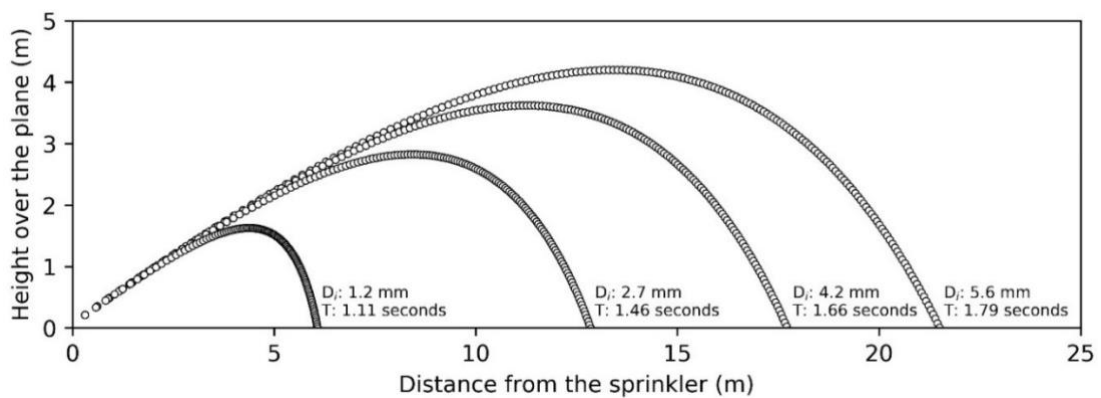


**Figure 5.11** Simulated trajectories (height and distance travelled) for four different droplet diameters ( $D_i$ ) from the exit of a sprinkler to the canopy based on ballistics theory. T: time travelled



When the distance at which each  $D_i$  reached the soil was known, a flow rate was assigned to each drop diameter at each  $r_i$  distance, based on the discharge rate ( $P_{ci}$ ,  $L h^{-1}$ ) at  $r_i$  in the irrigation radial leg curve. To do that, the average droplet diameter for all droplet sizes that fell between the distance  $r_i - \frac{r_i - r_{i-1}}{2}$  and  $r_i + \frac{r_{i+1} - r_i}{2}$  were calculated. The flow assigned to each  $D_i$  was then calculated as:

$$Q_{ci} = P_{ci} \pi \left[ \left( r_i + \frac{r_{i+1} - r_i}{2} \right)^2 - \left( r_i - \frac{r_i - r_{i-1}}{2} \right)^2 \right]$$

### Simulation of drop trajectories under windy conditions

Once the  $D_i$  and associated flow ( $Q_{ci}$ ) was characterised by a given sprinkler set-up and climatic conditions, the trajectories of  $D_i$  were simulated by considering the component wind ( $\vec{W}_i$ ). In the model, the input wind variables were wind speed ( $m s^{-1}$ ) and wind direction (degrees) which were transformed to the scalars  $W_{xi}$  and  $W_{yi}$ . The use of wind component in the two dimensions (x,y) made it necessary to add an extra coordinate axis to represent a three-dimensional droplet trajectory.

This process was repeated for each  $D_i$ . To reflect a sprinkler rotation, the simulations were executed for different directions with respect to the plane provided by the z plane, iterating from 0 to 360 degrees with a 10-degree increment. Figure 5.12 shows an example of the trajectory of water droplets of 5 mm in diameter, under 4.2 bar pressure and the influence of wind at  $3.5 m s^{-1}$ .

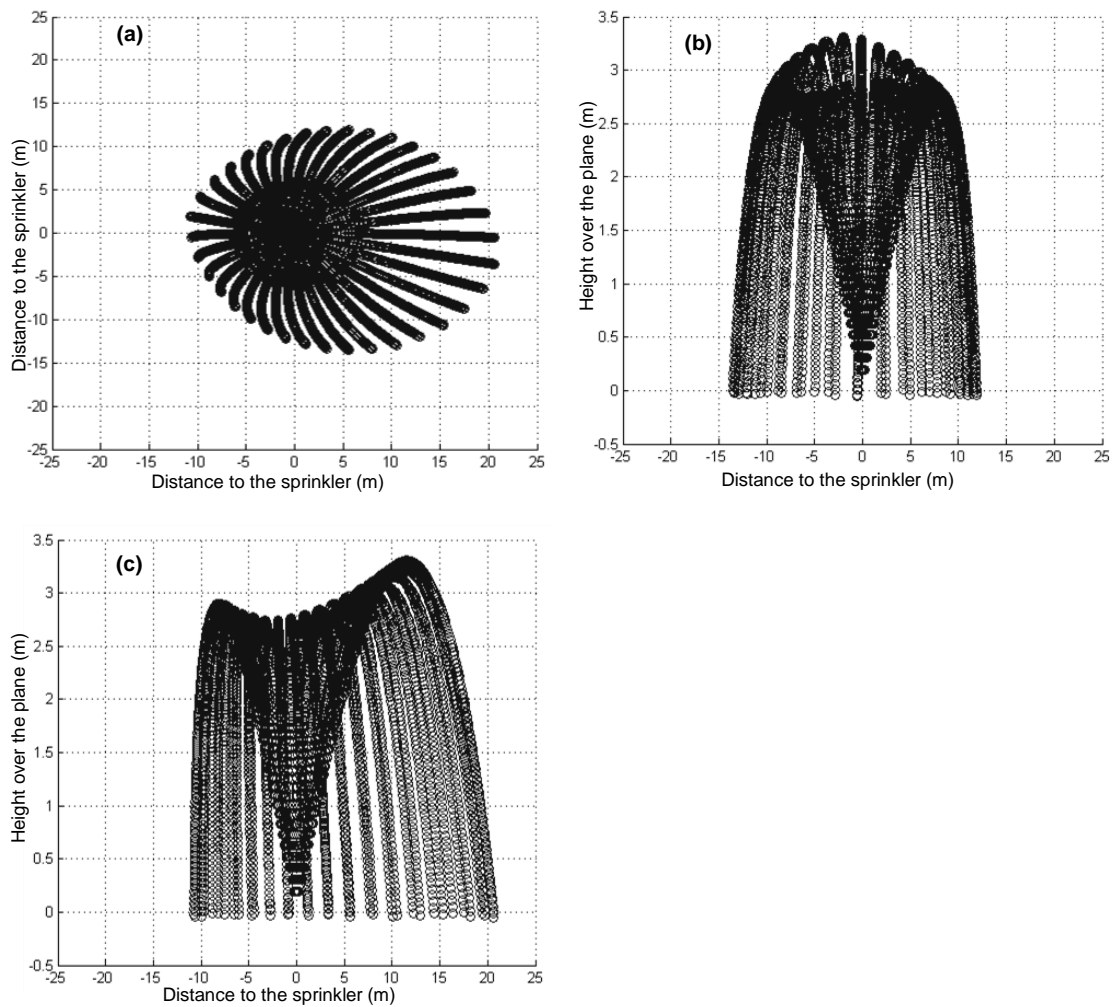


**Figure 5.12** Simulated trajectory of water droplets 5 mm in diameter at 4.2 bar pressure, with a wind speed of  $3.5 \text{ m s}^{-1}$ . (a) X-Y view (b) Y-Z view (c) X-Z view

The simulation of the full rotation of the sprinkler resulted in a set of points over the plane. Each point had  $x$ ,  $y$ ,  $z$  position values, where  $z$  was equal to the turf canopy height; and an associated  $D_i$ . Flows  $Q_{ci}$  corresponding to each point were then aggregated to the nearest point within a squared mesh of virtual pluviometers with an adjustable size (ranging from  $0.5 \times 0.5 \text{ m}$  to  $3 \times 3 \text{ m}$ ). Figure 5.13 shows an example of the simulation of water distribution under ‘windy’ conditions plotted over a virtual mesh of pluviometers distributed in a  $2.5 \times 2.5 \text{ m}$  grid. Droplets (or points) inside each square were aggregated to a central point (blue dot).

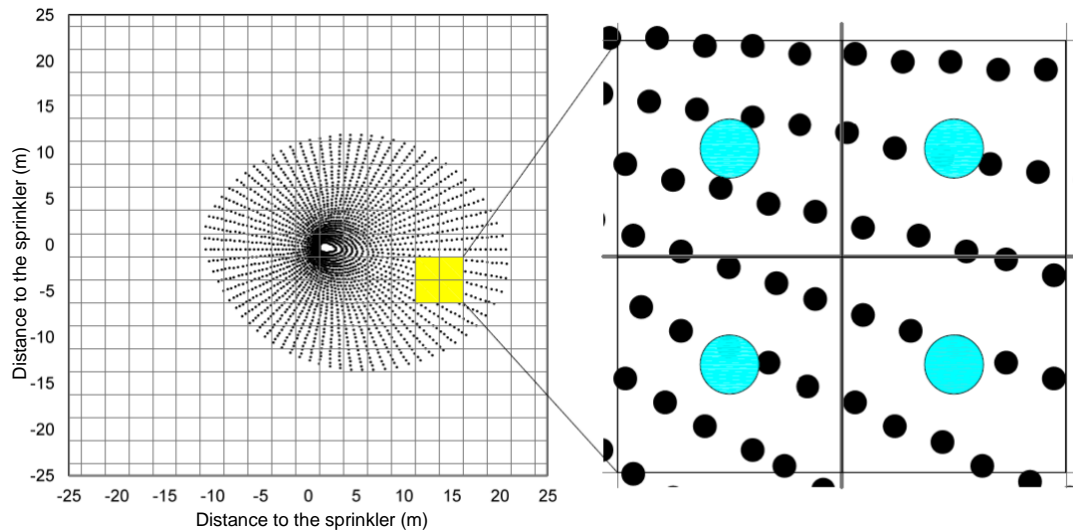


**Figure 5.13** Distribution of different  $D_i$  thrown every  $10^9$  under windy conditions (black dots) over a virtual squared mesh of pluviometers (blue dots)

Finally, from the aggregation of the water collected within each grid, a matrix with its  $x$  and  $y$  position in the plane, and the aggregated flow  $\Sigma Q_{ci}$  ( $L h^{-1}$ ) in each catchcan was generated. Precipitation rates ( $mm h^{-1}$ ) at each point were then calculated by dividing the  $\Sigma Q_{ci}$  in each virtual catchcan by the squared area of a virtual catchcan.

### *Sprinkler overlapping and assessment of irrigation heterogeneity*

The next step in irrigation model involved the calculation of the amount of water applied by the various sprinklers within a defined area. This was achieved by overlapping the wetted areas of single sprinklers. The final output from the sprinkler overlapping was to derive a dataset representing  $IR_{cc}$  across a delimited area, given by a defined sprinkler configuration (number, type and position) and local climate conditions. From all  $IR_{cc}$  within the irrigated, it was calculated the average IR and the Christiansen Uniformity Coefficient.

To generate the overlapped patterns, the model simulated the irrigation of single sprinklers but changing the starting jet position over the plane ( $y, x$  coordinates) at each iteration. The simulation of all sprinklers resulted in a set of points over the plane with  $x, y, z, D_i$  and associated  $Q_{ci}$ . Water was then aggregated to each virtual catchcan following the same procedure as described for a single sprinkler.

### 5.1.3 Model calibration and validation

Model calibration and validation were conducted with data from the single sprinkler tests using independent datasets. The model calibration aimed to find the  $K_1$  and  $K_2$  corrector coefficients that reduce the error between the test measurements and model simulations. For this comparison, different similitude parameters as proposed by Carrión (2001b) were used:

One-dimensional similitude parameter ( $\xi$ ), with optimum value 0:

$$\xi = \frac{|L_s - L_m|}{L_m}$$

where  $L_s$  is the distance from the sprinkler head to the centre of gravity of the simulated pattern (m); and  $L_m$  is the distance from the sprinkler head to the centre of gravity of the measured pattern (m).

Two-dimensional similitude parameter ( $\Phi$ ), with optimum value 1:

which is defined as the rate between the intersection ( $\cap$ ) of the areas and their unions ( $\cup$ ).

$$\Phi = \frac{S_m \cap S_s}{S_m \cup S_s}$$

where  $S_s$  is the simulated wetted area ( $m^2$ ); and  $S_m$  is the measured wetted area ( $m^2$ ).

Spatial similitude parameters, with optimum value 0:

The root mean squared error (RMSE) is one of the most widely used methods to determine the error between measurements and simulations. The use of squared differences implies that differences are heavily weighted but with the same units than evaluated data, which is useful to identify sources of error in the results (Wallach et al., 2006).

$$RMSE = \sqrt{\frac{\sum [P_{is} - P_{im}]^2}{N_u}}$$

where  $P_{is}$  is the simulated precipitation rate at each point ( $mm\ h^{-1}$ );  $P_{im}$  is the measured precipitation rate at each point ( $mm\ h^{-1}$ ); and  $N_u$  is the union of the wetted catchcans in measurements in field and wetted catchcans in simulations.

Another commonly used method to measure modelling or experimental error is the mean absolute error (MAE). The MAE is more appropriate than RMSE if the aim is merely to examine the overall model error.

$$\text{MAE} = \frac{\sum |P_{is} - P_{im}|}{N_u}$$

During calibration, water patterns measured in 22 field tests were compared with the equivalent simulated patterns. These results were used to calibrate the  $K_1$  and  $K_2$  corrector parameters. In each simulation, similar conditions to those used/observed during the tests were created. These included wind speed and wind direction, nozzle size, operating pressure, relative humidity and air temperature. Simulations were then repeated by combining differing values for  $K_1$ , from 0.5 to 4.0 at increments of 0.1, with values of  $K_2$ , ranging from 0 to 0.25 at increments of 0.01; resulting in 936 repetitions. For each simulated test in the calibration dataset, final  $K_1$  and  $K_2$  values were calculated as the average  $K_1$  and  $K_2$  obtained in the five simulations with the lowest RMSE and the five simulations with lowest MAE.

For each sprinkler set-up (nozzle size and operating pressure), the  $K_1$  and  $K_2$  corrector parameters were determined as the average of the selected values for each calibration test. The  $K_1$  and  $K_2$  values were then used to validate the model using data collected from 20 additional separate field tests. Spatial similitude coefficients were then calculated to evaluate the model outcomes for simulations of the wetted pattern of single sprinklers and overlapped sprinklers (solid-set irrigation). For the validation of the solid-set irrigation, sprinkler spacings of  $15 \times 15$  m,  $17.5 \times 7.5$  m,  $20 \times 20$  m, and  $22.5 \times 22.5$  m were used. In addition to MAE and RMSE, the Christiansen's Uniformity Coefficient measured ( $CU_m$ ) and simulated ( $CU_s$ ) were compared.

## 5.2 RESULTS

### 5.2.1 Field tests

#### Radial leg tests ('no-wind' conditions)

The results radial leg tests under 'no-wind' showed high variation in the volume of water collected and their distribution for each radial leg. Although tests were conducted on days on which the forecast wind speed was below  $1.34 \text{ m s}^{-1}$ , zero wind conditions were never recorded. During these tests, and despite the predominantly calm conditions, a few wind gusts between  $2$  and  $3 \text{ m s}^{-1}$  were recorded, which then distorted the profile radial leg curve. Figure 5.14 and Figure 5.15 summarise the results from two radial leg tests. It is evident that there was substantial variation in the volume of water collected between lines in the same test, as well as the average volume of water collected between separate tests.

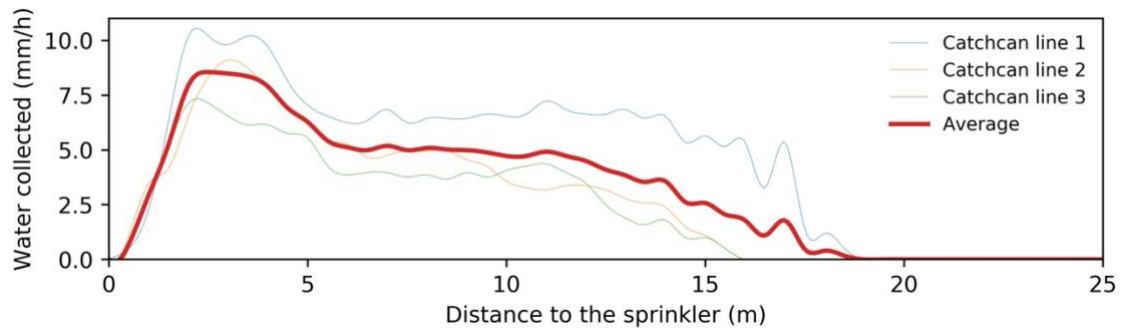


**Figure 5.14** Radial leg test conducted on 10<sup>th</sup> June 2016. Sprinkler RainBird 751 Series, nozzle “#28 white” operating at 4.2 bar

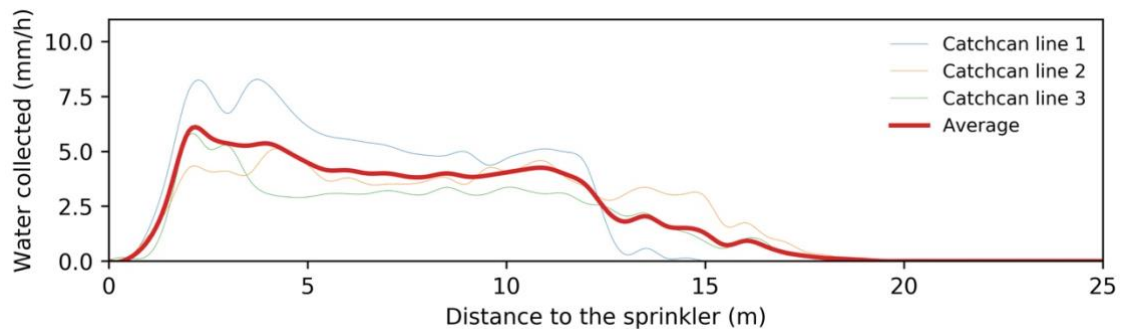


**Figure 5.15** Radial leg test conducted on 10<sup>th</sup> 25<sup>th</sup> October 2016. Sprinkler RainBird 751 Series, nozzle “#28 white” operating at 4.2 bar

In this research radial curve data for the sprinkler operating under 'no-wind' conditions provided by the sprinkler manufacturer were used in the simulations. These were based on sprinkler tests originally conducted at the Centre for

Irrigation Technology (CIT), in Fresno, USA under controlled indoor laboratory conditions. Radial leg data for the sprinkler operating at 6.0 bar was obtained by doing the weighted mean of the radial curves at 5.5 and 6.2 bar for both #28 and #40 nozzle sizes provided by the manufacturer. The radial curve data finally used for the model calibration and application are shown in Figure 5.16.

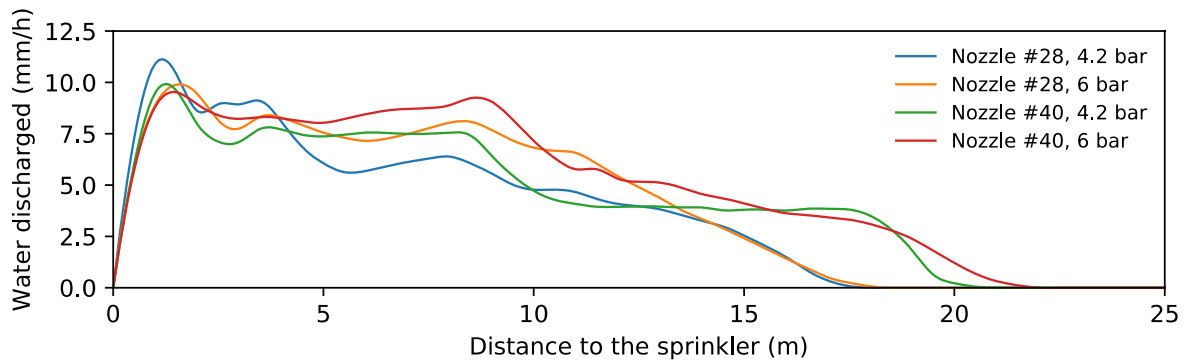


**Figure 5.16** Discharge radial curves for the RainBird 751 sprinkler using nozzles #28 (white) and #40 (orange) at operating pressures of 4.2 and 6.0 bar (Source: RainBird)

The water distribution of a golf irrigation sprinkler is directly related to the shape of the radial curve, which in turn is largely determined by sprinkler design (Sanchez et al., 2011), the nozzle shape and area and, to a lesser extent, the operating pressure. For the RainBird 751 sprinkler, the use of bigger nozzels and higher operating pressure resulted in higher flow rates and wetted radius (Table 5.1 and Figure 5.16).

One important factor to be considered was the difference in sprinkler height between the tests conducted at Cranfield University and those conducted at CIT. In the first step of the model calibration and validation, when the droplets sizes were determined, it was assumed that the jet nozzle was positioned 0.07 m above ground level. These measures coincide with the tests conducted at CIT. In the second step of the model calibration under windy conditions, an initial jet height of 0.78 m (sprinkler stand plus sprinkler height) was assumed. These measures coincide with the sprinkler location at tests conducted at Cranfield University.

#### Tests under windy conditions

In total, 63 single sprinkler tests under windy conditions were finalised. Forty tests were conducted using the “#28 orange” nozzle: 21 at 4.2 bar, 15 at 6 bar, 2 at 3 bar, and 1 at 5 and 7 bar, respectively. For the “#40 white” nozzle, 13 tests were

at 4.2 bar, and 10 at 6 bar. The average wind speed  $\overline{W_s}$  during the tests ranged from 0.3 to 4.1 m s<sup>-1</sup>. For higher average wind speeds (when wind gusts exceeded 7-8 m s<sup>-1</sup>), the tests were not completed because the catchcans were knocked over. Table 5.2 summarises the weather and operating conditions for each sprinkler test. Detailed results from all sprinkler tests are given in Annex-3.

**Table 5.2** Summary of weather and operating conditions for single sprinkler tests under windy conditions. Standard deviation values given in brackets.

Set-up	n	Duration (min)	Temp (°C)	RH (%)	F <sub>spr</sub> (L min <sup>-1</sup> )	F <sub>cc</sub> (L min <sup>-1</sup> )	I <sub>AE</sub> (%)	$\overline{ W_s }$ (m s <sup>-1</sup> )	$\overline{W_s}$ (m s <sup>-1</sup> )	WSU (%)
1	21	20.1(±4.2)	21(±2)	66(±11)	64.3(±0.9)	56.9(±2.7)	88.4(±4.2)	2.2(±0.5)	1.7(±0.8)	73.1(±23.8)
2	15	10.4(±1.2)	22(±2)	67(±10)	76.0(±0.3)	60.5(±3.6)	79.6(±4.6)	2.2(±0.7)	1.8(±1.0)	73.1(±24.2)
3	13	10.5(±1.0)	20(±2)	63(±13)	91.5(±0.3)	77.3(±4.4)	84.5(±4.8)	2.4(±0.9)	2.1(±0.9)	88.5(±11.2)
4	10	8.4(±0.9)	18(±2)	66(±12)	107.8(±1.1)	88.1(±4.0)	81.7(±4.1)	2.6(±0.8)	2.4(±0.8)	91.7(±2.4)

Set-ups: 1 – Nozzle #28, 4.2 bar; 2 – Nozzle #28, 6.0 bar; 3 – Nozzle #40, 4.2 bar; 4 – Nozzle #40, 6.0 bar

N: number of finished tests; F<sub>spr</sub>: Discharge measured at the entrance of the sprinkler; F<sub>cc</sub>: Discharge measured by catchcans;

I<sub>AE</sub>: Irrigation application efficiency

Overall, the wind speed uniformity (WSU) values were acceptable, with values above 80%. Tests with values of WSU below 80% (3 to 6, 15 to 20, 22, 23, 26 to 29, and 40, see Annex-3) where not used for model calibration as  $\overline{W_s}$  differed considerably from the  $\overline{|W_s|}$  due to the high variability in recorded wind direction. It is important to recognise that the wind speed and direction do not remain constant during a test but change continuously. Wind direction was more stable in most tests compared to wind speed which showed greater fluctuation. Thus, the wetted patterns were affected by the variation in wind speed and wind direction, as well as by the position of the water jet relative to the wind when a gust occurred.

Figure 5.17 shows two examples of tests conducted under different wind conditions. The upper panel shows results from a test with WSU 93% and average wind speed  $\overline{|W_s|}$  of 2.9 m s<sup>-1</sup>. The wind rose (Figure 5.17a) shows that wind speed and direction remained almost constant throughout the test (Figure 5.17b). The distortion of the wetting pattern due to wind is evident with a general shift in a leeward direction and a narrowing of its shape in the same direction to the wind.



In contrast, the lower panels (Figure 5.17c) show results from a test with great variability in speed and direction, and poor WSU (53%). The scalar average wind speed  $\overline{|\vec{W}_s|}$  was  $2.2 \text{ m s}^{-1}$ . However, due to the variation in wind direction, the average  $\overline{\vec{W}_s}$  was  $1.2 \text{ m s}^{-1}$ . The low WSU is reflected in the wetted pattern shown in Figure 5.17d, where there is evident wind distortion.

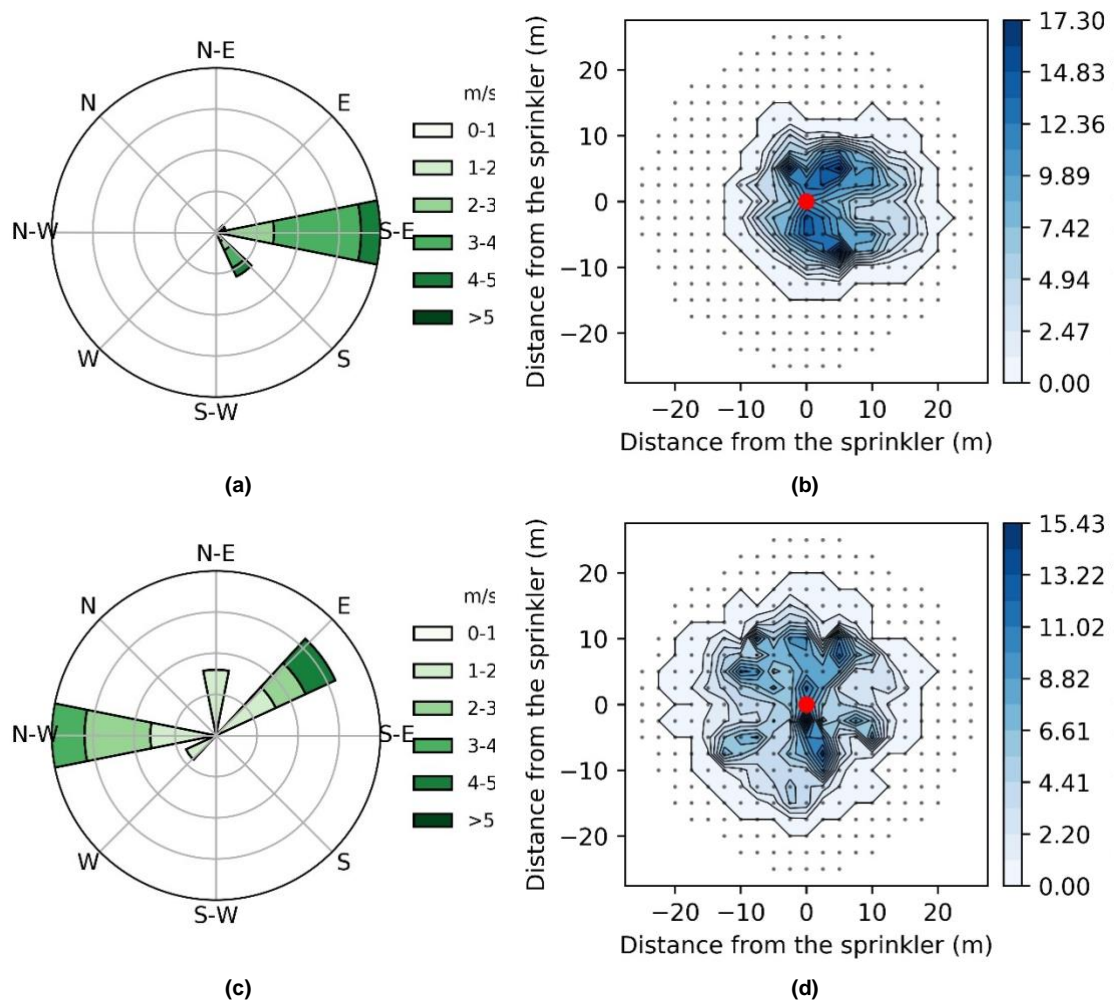


**Figure 5.17** Windrose (left panel) and simulated wetting patterns (right panel) measured in two sprinkler tests. Upper panels (a,b) show results from a test with a high *WSU*. The lower panels (c,d) show results from a test with a low *WSU*. The black dots represent the catchcans and red dot the sprinkler location.

The irrigation application efficiency ( $I_{AE}$ ) ranged between 80 and 88%. No evaporation losses from water collected in catchcans were recorded at any of the tests. Thus, all water lost between the sprinkler and that collected was attributed to wind drift and evaporation losses ( $WDEL$ ). These results coincide with Playán et al. (2005) who estimated that only <0.5% of water losses corresponded to

catchcan evaporation. The field measurements of WDEL were used to derive an equation for estimating WDEL in the irrigation simulations.

Estimating wind drift and evaporation losses (WDEL)

The wind drift and evaporation losses from field tests (WDEL<sub>m</sub>) were estimated as the rate between the water delivered to the sprinkler and the water collected in catchcans. The WDEL<sub>m</sub> ranged between 5.7 and 29%, with a mean 15.7%. To derive an equation that could predict WDEL, the variables of pressure (P), temperature (T), relative humidity (RH) and wind speed (WS) were compared with the WDEL<sub>m</sub> obtained in each test.

Table 5.3 shows the results from a Pearson coefficient analysis and test of significance (*p-values*) when individual variables were compared with WDEL<sub>m</sub>. In contrast to results reported by earlier research by Playán et al. (2005), wind speed (WS) did not affect WDEL<sub>m</sub> significantly. The slope of the correlation was almost zero, meaning no variation in WDEL<sub>m</sub> was observed for a varying WS. The impact of temperature (T) on WDEL<sub>m</sub> was moderate but significant ( $p < 0.05$ ), while the relationship between RH and P with WDEL<sub>m</sub> was stronger ( $p < 0.01$  and  $p < 0.001$ , respectively).

**Table 5.3** Pearson’s correlation coefficients and *p-value* of the measured WDEL<sub>m</sub> and measured variables in field, for selected weather variables

Explanatory variable	WDEL <sub>m</sub>	
	Pearson correlation coefficient.	p-value
RH	-0.357	0.006
P	0.543	0.000
WS	0.045	n.s.
T	0.282	0.03

For tests using an operating pressure of 4.2 bar, the average WDEL<sub>m</sub> was 12.8%; while for the higher pressure (6.0 bar), the average WDEL<sub>m</sub> was 19.5%. When all variables were combined (Table 5.4) neither WS nor T were statistically significant based on a multivariable linear regression analysis. Surprisingly, when WS was included in the predictive equation, it was expressed as a negative dependent variable, which is meaningless in practical terms. For these reasons, WS and T were not included in the predictive equation.

**Table 5.4** Proposed WDEL equations based on the multivariate linear regression

Equation	R <sup>2</sup>	p-value	Significance of dependent variables				
			Constant	P	RH	WS	T
8.645+3.517P-0.230RH-0.837WS+0.28T	0.493	0.000	0.270	0.000	0.000	n.s.	n.s.
3.598+3.390P-0.2RH+0.385T	0.481	0.000	0.578	0.000	0.000	-	n.s.
15.680+3.64P-0.251RH-1.159WS	0.480	0.000	0.002	0.000	0.000	n.s.	-
<b>11.791+3.511P-0.214RH</b>	<b>0.473</b>	<b>0.000</b>	<b>0.010</b>	<b>0.000</b>	<b>0.000</b>	-	-

The P and RH variables were therefore considered in the simulated WDEL equation (WDEL<sub>s</sub>).

Figure 5.18 shows a positive significant correlation between WDEL<sub>m</sub> and WDEL<sub>s</sub> from equation  $WDEL(\%) = 11.791+3.511P-0.214RH$ . Despite a reasonable correlation, this equation tends to over-estimate WDEL<sub>s</sub> for WDEL<sub>m</sub> below 15%, and under-estimate WDEL<sub>s</sub> for higher percentages of WDEL<sub>m</sub>.

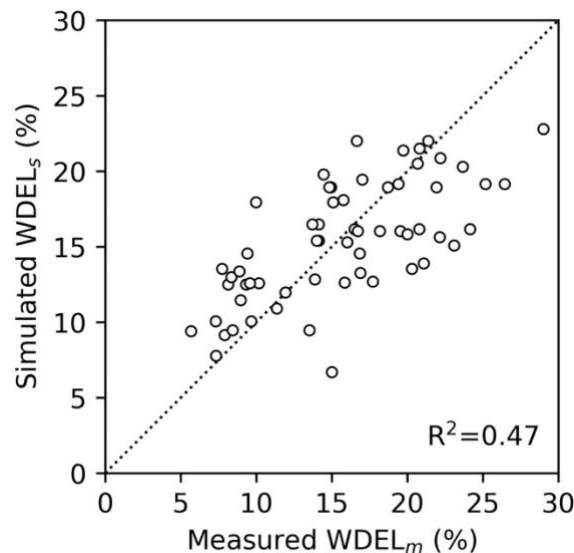


**Figure 5.18** Correlation between simulated and measured WDEL (%)

The WDEL<sub>s</sub> equation was then integrated into the irrigation model together with the evaporation losses equation, modifying the discharge water efficiency of the initial radial leg curve. For example, Figure 5.19 shows the variation of the radial leg curve (a) and radial sprinkler flow curve (b) before and after considering a WDEL of 17.9% for the RainBird 751 sprinkler with a nozzle “#40 Orange”, operating pressure of 6.0 bar and relative humidity of 70%. For the radial flow curve (a), the most significant reduction in discharge rate was observed in the first few metres of the irrigated radius. This is because of the higher evaporation

loses of the smaller droplets, which occur close to the sprinkler. Conversely, when water losses were expressed on the radial sprinkler flow data (b) this resulted in higher losses in the total amount of water at distances greater than 9.5 m. This is explained because of a greater amount of water applied at longer distances, as they cover a greater radial area.

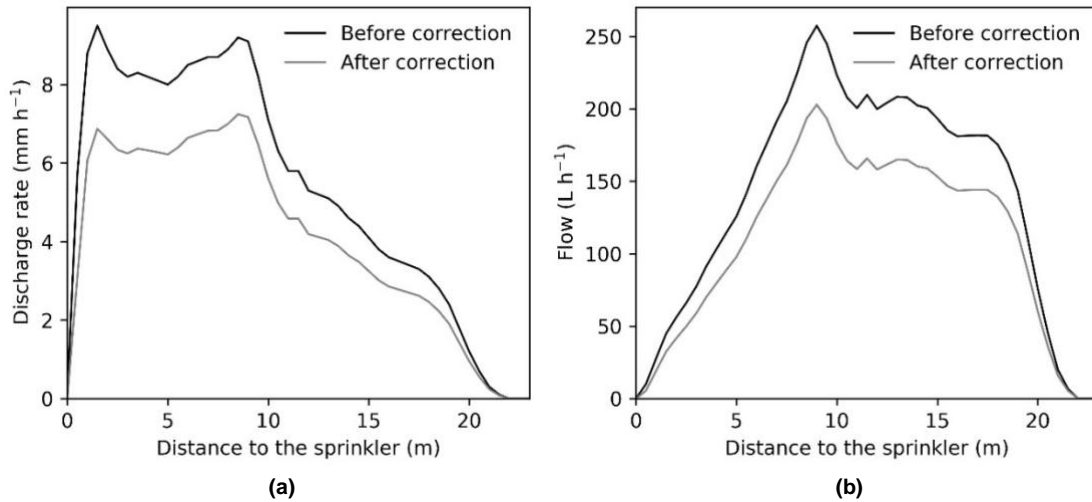


**Figure 5.19** (a) Reshaped sprinkler radial curve ( $\text{mm h}^{-1}$ ) and (b) reshaped radial sprinkler flow ( $\text{L h}^{-1}$ ); before and after applying WDEL

## 5.2.2 Calibration and validation of the irrigation model

### Influence of corrector coefficients $K_1$ and $K_2$ on water distribution

The correction of water distribution patterns under windy conditions using corrector coefficients ( $K_1$  and  $K_2$ ) to modify the air drag coefficient  $C$  was introduced by Seginer et al. (1991) and used successfully in later research when simulating irrigation uniformity. As an example, Figure 5.20 shows the impact of the combination of  $K_1$  and  $K_2$  coefficients by comparing the measured and simulated distribution patterns for the RainBird 751 sprinkler with nozzle size #40, and an operating pressure of 6.0 bar under a wind speed  $1.97 \text{ m s}^{-1}$  (N-NW direction). The impacts of  $K_1$  and  $K_2$  showed improvements in the simulated wetted pattern similar to those shown by Montero et al. (2001). This demonstrates the usefulness of using  $K_1$  and  $K_2$  coefficients to correct the shape of the wetted pattern for a golf sprinkler.

When no corrector coefficients were used (Figure 5.20a,  $K_1=0$  and  $K_2=0$ ), the simulated water pattern was circular, with a centre of gravity displaced from the

origin of the sprinkler in the same direction as the wind. However, the one-dimensional similitude parameter  $\xi$ , two-dimensional parameter  $\Phi$  and spatial similitude parameters MAE and RMSE showed poorer values compared to when the  $K_1$  and  $K_2$  correctors were used.

The  $K_1$  corrector coefficient shows a greater impact on the similitude between measured and simulated water distribution patterns. In Figure 5.20b where only the coefficient  $K_1$  ( $K_1=3.7$ ,  $K_2=0$ ) was used, a significant improvement in the similitude coefficients  $\Phi$ , and, to a lesser extent, to  $\xi$  is shown with a narrowing of the wetted pattern in line with the wind direction. An increase in the  $K_1$  parameter results in a narrower, more elliptical shape.

The  $K_2$  coefficient showed less influence compared to  $K_1$  in the simulation of a wetted pattern by a single sprinkler. When  $K_2$  was applied in isolation (Figure 5.20c,  $K_1=0$ ,  $K_2=0.18$ ) an improvement in the unidimensional similitude coefficient  $\xi$  is observed due to a more significant displacement of the centre of gravity in the simulated wetted pattern in the same direction as the wind. However, the  $K_2$  coefficient appears to have no impact on the narrowing of the water distribution shape, with negligible influence on  $\Phi$ , MAE and RMSE.

When  $K_1$  and  $K_2$  were used together (Figure 5.20d), it resulted in a simulated wetted pattern with an improved MAE and RMSE. Despite these improvements, the parameter  $\Phi$  was slightly lower than when  $K_2$  was not considered ( $\Phi$  from 0.86 to 0.82). Thus, the values of  $K_1$  and  $K_2$  to obtain the optimum similitude parameter ( $\xi \rightarrow 0$ ,  $\Phi \rightarrow 1$ , MAE and RMSE  $\rightarrow 0$ ) differed in many cases when simulated and measured wetted patterns were compared. That was due to the inherent variability in the field tests provided by variations in wind speed and direction, which, in many cases, led to a moderate change in the wetted pattern. In those cases, the selection of  $K_1$  and  $K_2$  parameters that resulted in better RMSE and MAE coefficients were considered due to their stronger influence on the values of simulated irrigation uniformity when sprinklers were overlapped. For the simulation of overlapping sprinklers, inaccuracies in the wetted points located at longer distances from the sprinkler had a low impact on irrigation uniformity

percentages. However, these errors might reduce the accuracy of the similitude coefficients.

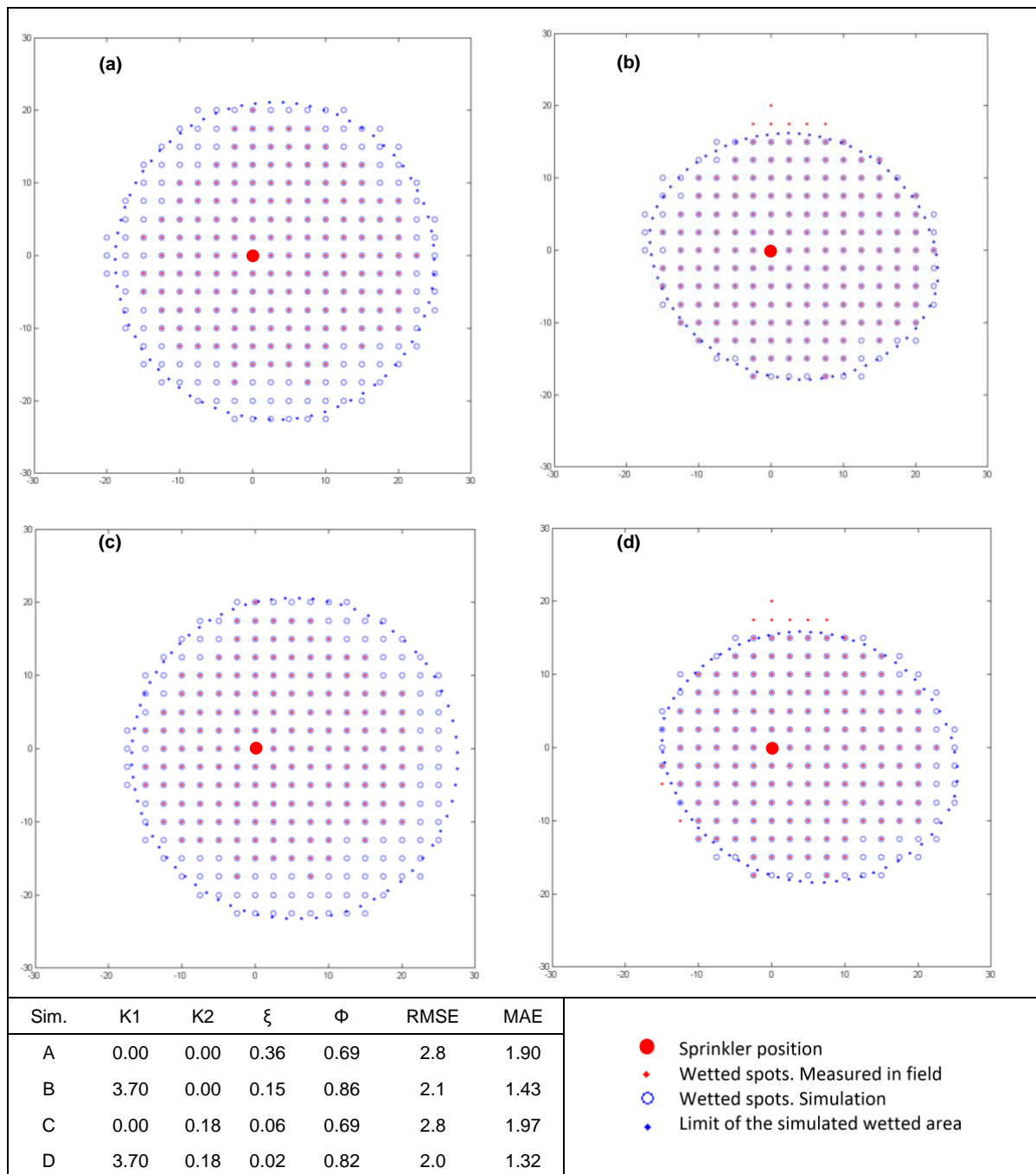


**Figure 5.20** Influence of the corrector coefficients  $K_1$  and  $K_2$  on simulated distribution patterns.

Figure 5.21a shows a comparison between wind speed and measured wetted area in field tests. For each sprinkler set-up, a negative linear correlation was observed between both variables. This illustrates the need of using the corrector coefficients  $K_1$  and  $K_2$ . The area wetted by a single sprinkler was reduced as the

wind speed increased, which resulted from the narrowing of the wetted pattern in the direction of the wind. Wetted area was also influenced by the sprinkler nozzle, but not by the operating pressure. This is explained because in the sprinkler model used, the irrigated radius is mainly given by the nozzle size rather than the operating pressure.

Figure 5.21b shows the relationship between the sprinkler and the centre of gravity of the measured wetted area. It was observed a greater displacement of the centre of gravity at higher operating pressure (6.0 bar) than when the pressure was lower (4.2 bar). This fact might be explained due to higher pressures results in a lower droplet size (De Wrachien and Lorenzini, 2006), which offers less aerodynamic resistance to wind speed. However, those differences were only evident when wind speeds were greater than 1 m s<sup>-1</sup>.

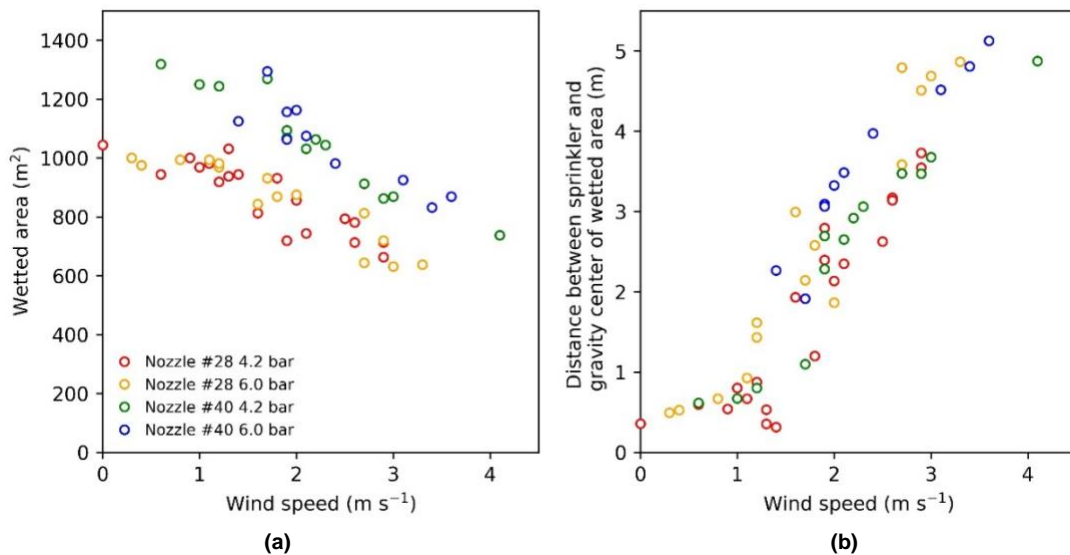


**Figure 5.21** Impacts of wind on measured wetted area and centre of gravity displacement (a) Variation of the wetted area by a single sprinkler for different wind speeds; (b) Variation of distance from sprinkler to the centre of gravity of the wetted area for different wind speeds.

Figure 5.22 shows the distortion of the sprinkler jet during the tests as affected by wind speed.

Wind direction



**Figure 5.22** Distortion of the sprinkler jet due to wind.

#### Model calibration for a single sprinkler

Table 5.5 shows the  $K_1$  and  $K_2$  corrector coefficients and similitude parameters for the calibration dataset. To estimate  $K_1$  and  $K_2$  coefficients, each field test was simulated 936 times, altering the values of the corrector coefficients for each iteration. Selected corrector coefficients for each sprinkler set-up consisted of the average coefficients for the defined sprinkler set-up.

Six field tests were used for calibration of the sprinkler with nozzle size #28 and an operating pressure 4.2 bar. The mean coefficients for this set-up were  $K_1=2.33$  and  $K_2=0.07$ , respectively. For nozzle size #28 at 6.0 bar, the corrector coefficients were  $K_1=1.80$  and  $K_2=0.04$  based on the results of five field tests; for the nozzle size #40 at 4.2 bar, the corrector coefficients were  $K_1=2.74$  and  $K_2=0.13$  based on results from six field tests; for nozzle size #40 at 6.0 bar, the corrector coefficients were  $K_1=2.84$  and  $K_2=0.10$  based on five field tests.



**Table 5.5** Mean values for the corrector coefficients of  $K_1$  and  $K_2$  and the similitude parameters of the single sprinkler and different set-ups for the calibration dataset

	Wind speed $\text{m s}^{-1}$	$K_1$	$K_2$	$\xi$	$\Phi$	MAE $\text{mm h}^{-1}$	RMSE $\text{mm h}^{-1}$
<b>nozzle #28 operated at 4.2 bar</b>							
	1.94	1.44	0.01	0.03	0.79	0.99	1.44
	2.02	2.06	0.06	0.12	0.77	1.19	1.87
	1.91	2.28	0.05	0.05	0.66	1.47	2.13
	2.14	2.52	0.15	0.16	0.73	1.45	2.07
	1.89	2.9	0.15	0.08	0.68	1.41	2.16
	2.55	2.76	0.03	0.01	0.65	1.44	2.79
<b>Mean</b>	<b>2.08</b>	<b>2.33</b>	<b>0.07</b>	<b>0.08</b>	<b>0.71</b>	<b>1.33</b>	<b>2.08</b>
<b>nozzle #28 operated at 6.0 bar</b>							
	1.95	1.16	0.01	0.28	0.74	1.14	1.71
	1.80	1.2	0.09	0.04	0.69	1.33	2.04
	3.29	1.68	0.05	0.06	0.62	1.56	2.64
	2.67	2.4	0.03	0.25	0.67	1.84	2.91
	1.64	2.58	0.04	0.30	0.75	1.49	2.34
<b>Mean</b>	<b>2.27</b>	<b>1.80</b>	<b>0.04</b>	<b>0.19</b>	<b>0.69</b>	<b>1.47</b>	<b>2.33</b>
<b>nozzle #40 operated at 4.2 bar</b>							
	1.02	1.4	0.05	0.46	0.83	1.06	1.36
	1.20	2.42	0.17	0.57	0.86	1.10	1.62
	2.15	3.3	0.13	0.07	0.75	1.64	2.57
	2.18	3.22	0.15	0.03	0.77	1.45	2.09
	2.96	3	0.18	0.07	0.70	1.62	2.45
	2.73	3.12	0.12	0.02	0.72	1.68	2.48
<b>Mean</b>	<b>2.04</b>	<b>2.74</b>	<b>0.13</b>	<b>0.20</b>	<b>0.77</b>	<b>1.42</b>	<b>2.10</b>
<b>nozzle #40 operated at 6.0 bar</b>							
	1.89	2.58	0.10	0.05	0.76	1.16	1.74
	1.97	3.46	0.13	0.02	0.79	1.21	1.87
	1.69	2.6	0.03	0.23	0.80	1.20	1.77
	3.13	2.64	0.07	0.03	0.73	1.48	2.39
	2.38	2.94	0.18	0.02	0.69	1.27	1.99
<b>Mean</b>	<b>2.21</b>	<b>2.84</b>	<b>0.10</b>	<b>0.07</b>	<b>0.76</b>	<b>1.26</b>	<b>1.95</b>

Tests using nozzle size #40 resulted in higher  $K_1$  and  $K_2$  values. One possible explanation for the higher  $K_1$  value was that the wetted radius was higher for this nozzle size. A larger irrigated radius means that some droplets travel a longer distance from the sprinkler, and during that time they are more exposed to wind distortion. For these cases, the wetted pattern is likely to be more affected compared to shorter trajectories of water droplets. However, the highest value of  $K_2$  obtained with nozzle #40 at 4.2 bar contradicts the field observations given in Figure 5.21b. The tests results showed a greater displacement of the centre of gravity at a higher pressure, and therefore  $K_2$  should be higher at 6.0 bar than 4.2 bar. A possible explanation for this might be that the algorithm that chooses the most suitable corrector coefficients was programmed to find the lowest value of the spatial similitude parameters MAE and RMSE, instead of the one and two-

dimensional parameters  $\xi$  and  $\Phi$ . The higher values of  $K_2$  at lower pressures for the same nozzle might be derived from errors from the estimation of the droplet diameters in the first few metres of the wetted radius. No relationship was found between wind speed and the corrector coefficients.

Regarding the similitude parameters, the parameter  $\Phi$  presented better scores than  $\xi$ , MAE and RMSE. Average  $\Phi$  values ranged from 0.69 to 0.77 which were considered acceptable. Those values relate the intersection and union wetted catchcans of both measured and simulated patterns. It could be considered that in all cases the approximation of the simulated wetted areas to the observed in field was correct. Looking at the literature, the only reference to this parameter was presented by Montero et al. (2001) when calibrating SIRIAS model. After applying  $K_1$  and  $K_2$  coefficients to the simulation of an agricultural impact sprinkler, operating at 3 bar and under the influence of wind speed  $4.15 \text{ m s}^{-1}$ , parameter  $\Phi$  was 0.9. One explanation for the errors obtained in the current research could be because of measurement errors that are inherent to field tests. Also, continuous changes in wind speed and direction might have introduced some error into the simulations, as the model runs considering a constant wind speed and direction.

The average values of the one-dimension similitude parameter  $\xi$  ranged from 0.07 to 0.20. Although for most of the calibrated tests  $\xi$  was acceptable, three simulations from the calibration dataset gave results above 0.30 (Table 5.5), which increased the average  $\xi$ . In this research, high values of  $\xi$  were produced due to three factors. Firstly, in two of the tests the wind speeds were relatively low and consequently the measured distances between the centre of gravity of the water collected and sprinkler ( $L_m$ ) and calculated ( $L_c$ ) were also low. Under those conditions, the difference  $|L_m - L_c|$  would produce a higher relative error for lower  $L_m$ . Secondly, the irregular measured distribution pattern in some tests due to wind variability made difficult to obtain similar  $L_m$  and  $L_c$ . Finally, the corrector coefficients were selected to obtain the most suitable spatial similitude in detriment of  $\xi$  and  $\Phi$ .

Regarding the spatial similitude parameters, the mean absolute error (MAE) and root mean squared error (RMSE), averages ranged from 1.26 to 1.47 mm h<sup>-1</sup>, and from 1.95 to 2.33 mm h<sup>-1</sup>, respectively. Average values of MAE presented by Montero et al. (2001) in the calibration of three sprinkler set-ups ranged from 0.43 to 0.66 mm h<sup>-1</sup>. However, the sprinklers analysed in that case presented an average precipitation rate of 2.41 to 2.59 mm h<sup>-1</sup>, while the precipitation rate for the RainBird 750 at the studied sprinkler set-ups ranged from 3.99 to 4.46. This higher precipitation rates may increase the absolute error between simulated and measured precipitation in catchcans. Nonetheless, the obtained MAE was still slightly worse than that presented by Montero et al. (2001).

#### Model validation for single sprinklers

The estimated corrector coefficients  $K_1$  and  $K_2$  obtained in the calibration step were then used to validate the irrigation model using data from the validation dataset. Table 5.6 summarises the results from validation. Overall, the mean values of the similitude parameters were similar to those obtained from the calibration. The greatest accuracy in the validation dataset was for nozzle #40 at 6.0 bar, with a MAE of 1.35 mm h<sup>-1</sup> and 37% coefficient of variation (CV). This CV value is very close to 36% which according to Montero et al. (2001) is considered acceptable, as it corresponds to the variation observed when comparing two single sprinkler tests with similar climate and operating conditions. Some sources of error are factors inherent to irrigation, such as the spatial and temporal variability in wind speed and direction, and the distribution of the different droplet sizes across the irrigated radius.

**Table 5.6** Similitude parameters for the single sprinkler and different set-ups derived for the calibration dataset

	<b>WS</b> <b>m s<sup>-1</sup></b>	<b>ξ</b>	<b>Φ</b>	<b>MAE</b> <b>mm h<sup>-1</sup></b>	<b>RMSE</b> <b>mm h<sup>-1</sup></b>
<b>nozzle #28 operating at 4.2 bar</b>					
	2.6	0.07	0.64	1.76	2.86
	1.62	0.11	0.77	1.15	1.63
	2.9	0.02	0.67	1.37	2.36
	2.9	0.07	0.70	1.16	1.92
	2.48	0.21	0.70	1.36	2.12
<b>Mean</b>	<b>2.50</b>	<b>0.10</b>	<b>0.70</b>	<b>1.36</b>	<b>2.18</b>
<b>nozzle #28 operating at 6.0 bar</b>					
	1.68	0.08	0.73	1.29	1.96
	2.86	0.13	0.66	1.42	2.63
	2.99	0.14	0.60	1.38	2.13
	2.68	0.03	0.71	1.52	2.32
<b>Mean</b>	<b>2.55</b>	<b>0.19</b>	<b>0.66</b>	<b>1.40</b>	<b>2.26</b>
<b>nozzle #40 operating at 4.2 bar</b>					
	1.7	0.57	0.67	1.35	1.76
	2.35	0.07	0.80	1.70	2.58
	1.92	0.18	0.76	1.34	2.00
	4.11	0.11	0.67	1.94	2.92
	2.85	0.14	0.70	1.65	2.40
	1.89	0.03	0.70	1.80	2.30
<b>Mean</b>	<b>2.47</b>	<b>0.18</b>	<b>0.72</b>	<b>1.63</b>	<b>2.33</b>
<b>nozzle #40 operating at 6.0 bar</b>					
	2.06	0.08	0.76	1.4	2.04
	1.95	0.04	0.74	1.35	1.98
	3.39	0.04	0.64	1.47	2.20
	3.61	0.03	0.70	1.48	2.36
	1.41	0.02	0.72	1.06	1.52
<b>Mean</b>	<b>2.48</b>	<b>0.04</b>	<b>0.71</b>	<b>1.35</b>	<b>2.02</b>

### 5.2.3 Validation of overlapped patterns

The field and simulated wetted patterns for a single sprinkler were then used to calculate irrigation uniformity for a typical irrigation system on a golf course at different spacings. Four sprinkler spacings were used: 15 × 15 m, 17.5 × 17.5 m, 20 × 20 m and 22.5 × 22.5 m; these reflect the range in distances typically found on golf greens. Irrigation uniformity values were calculated for both the measured data and simulated modelled overlaps. Table 5.7 shows the average CU using measured test data ( $CU_{meas}$ ), the average CU calculated from simulations ( $CU_{sim}$ ) and average errors between both ( $CU_e$ ). Similitude parameters MAE and RMSE for overlapped patterns within the irrigated area are also shown.

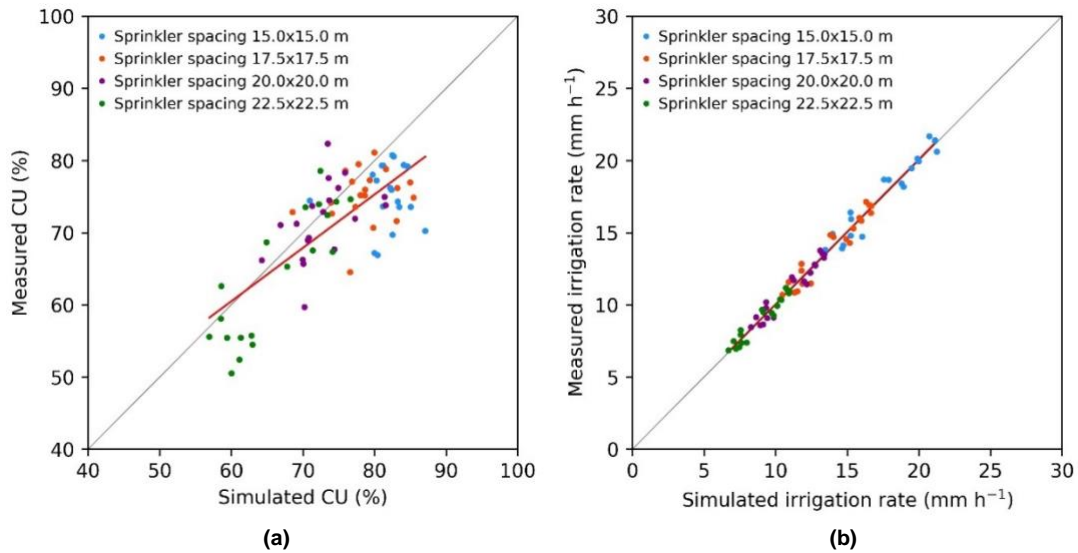
**Table 5.7** Average CU from measured ( $CU_{meas}$ ) and simulated ( $CU_{sim}$ ) sprinkler overlapping, average errors between measured and simulated CU ( $CU_e$ , %), and average MAE and RMSE within tests. Results presented for each sprinkler set-up and distance. Standard deviation values are shown in brackets.

Nozzle and pressure	15.0 x 15.0 m					17.5 x 17.5 m				
	$CU_{meas}$ (%)	$CU_{sim}$ (%)	$CU_e$ (%)	MAE (mm h <sup>-1</sup> )	RMSE (mm h <sup>-1</sup> )	$CU_{meas}$ (%)	$CU_{sim}$ (%)	$CU_e$ (%)	MAE (mm h <sup>-1</sup> )	RMSE (mm h <sup>-1</sup> )
#28 4.2 bar	78.1(±2)	81.6(±1)	3.5(±3.1)	3.3(±0.3)	4.4(±0.4)	77.9(±1)	79.3(±1)	1.5(±0.5)	2.8(±0.3)	3.8(±0.4)
#28 6.0 bar	69.9(±4)	81.3(±1)	11.4(±2.9)	4.2(±0.7)	5.3(±0.7)	71.3(±4)	80.0(±3)	8.7(±3.5)	3.7(±0.4)	4.8(±0.3)
#40 4.2 bar	76.9(±2)	80.4(±4)	3.5(±3.3)	5.5(±0.4)	6.8(±1.0)	76.2(±3)	75.7(±4)	0.6(±1.4)	4.4(±0.6)	5.7(±0.8)
#40 6.0 bar	75.2(±3)	84.1(±2)	8.9(±4.4)	4.5(±0.6)	5.7(±0.7)	74.5(±2)	80.5(±4)	6.0(±3.8)	3.9(±0.2)	4.8(±0.6)
Nozzle and pressure	20.0 x 20.0 m					22.5 x 22.5 m				
	$CU_{meas}$ (%)	$CU_{sim}$ (%)	$CU_e$ (%)	MAE (mm h <sup>-1</sup> )	RMSE (mm h <sup>-1</sup> )	$CU_{meas}$ (%)	$CU_{sim}$ (%)	$CU_e$ (%)	MAE (mm h <sup>-1</sup> )	RMSE (mm h <sup>-1</sup> )
#28 4.2 bar	70.1(±3)	70.9(±2)	0.8(±1.3)	2.7(±0.3)	3.4(±0.4)	58.2(±6)	60.7(±3)	2.6(±3.2)	2.4(±0.3)	3.2(±0.4)
#28 6.0 bar	67.6(±5)	74.3(±4)	6.6(±3.3)	3.3(±0.3)	4.4(±0.3)	57.4(±6)	64.9(±5)	7.5(±1.2)	3.1(±0.3)	4.1(±0.5)
#40 4.2 bar	74.8(±5)	71.7(±4)	3.1(±2.8)	3.9(±0.3)	5.1(±0.6)	69.9(±7)	69.3(±6)	0.7(±1.9)	3.3(±0.4)	4.4(±0.7)
#40 6.0 bar	72.5(±4)	74.3(±5)	1.8(±1.4)	3.3(±0.3)	4.3(±0.5)	66.9(±7)	68.3(±7)	1.5(±1.9)	2.9(±0.2)	3.9(±0.4)

The irrigation model tends to slightly overestimate CU values, which might indicate some degree of bias in the simulations. The error in the predictions of CU decreased as the distance between sprinklers was higher. On average, the  $CU_e$  values were acceptable for the set-ups #28 with 4.2 bar and #40 operating at 4.2 and 6.0 bar. In those cases,  $CU_e$  ranged between 0.6 and 8.9%. For the sprinkler set-up #28 operating at 6.0 bar pressure,  $CU_e$  doubled the value obtained with the other sprinkler set-ups. The better  $CU_e$  values in comparison with spatial similitude parameters MAE and RMSE indicates that the model predicted well the total variability of water application but presented some lack of precision predicting the spatial distribution of water; i.e., the water that is collected by each virtual catchcan.

Figure 5.23a compares  $CU_{sim}$  against  $CU_{meas}$ . Although measured and simulated data follow a positive correlation, it is evident that the simulated CU was often over-estimated. The fact that the  $CU_e$  did not present significant differences when comparing sprinkler spacings suggests that it was more related to errors inherent in individual tests than to the differences in sprinkler spacing. In contrast, the simulated and measured IR (average water applied across a green) showed a

strong correlation (Figure 5.23b). As expected, it was observed that there is a clear variation between the IR and sprinkler spacing and set-up. This highlights the importance in the selection of sprinkler set-up and spacing on irrigation adequacy, i.e., how much water an irrigation system applies over a given area.



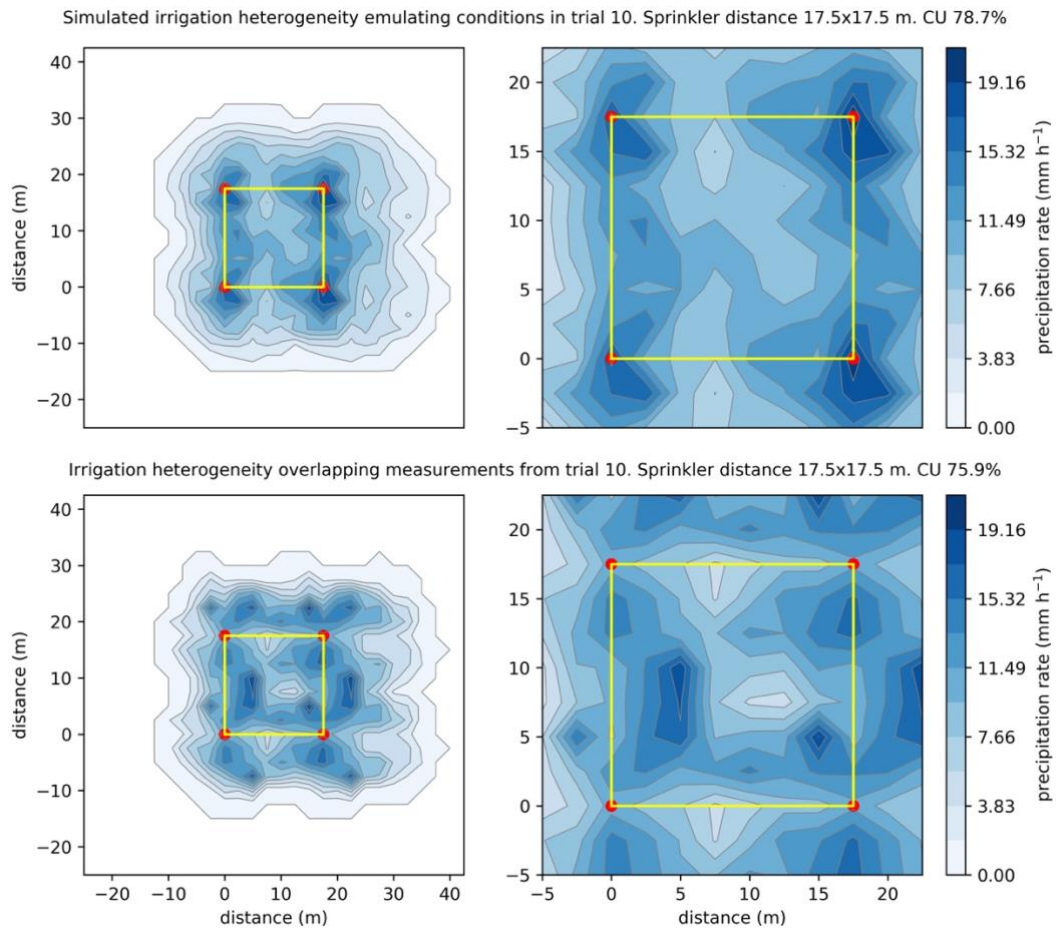
**Figure 5.23** Simulated against observed (a) Christiansen’s Uniformity Coefficient (CU) and (b) Irrigation rate (IR) for the validation dataset

Figure 5.24 and Figure 5.26 show two contrasting examples comparing the simulated and measured irrigation patterns. Simulations were intended to replicate the conditions observed in test 10 (17.5 × 17.5 m spacing) and 50 (20 × 20 m spacing). The measured and simulated wetted areas coincide in shape and, to a lesser extent, in their spatial variability (left panels in Figure 5.24 and Figure 5.26).

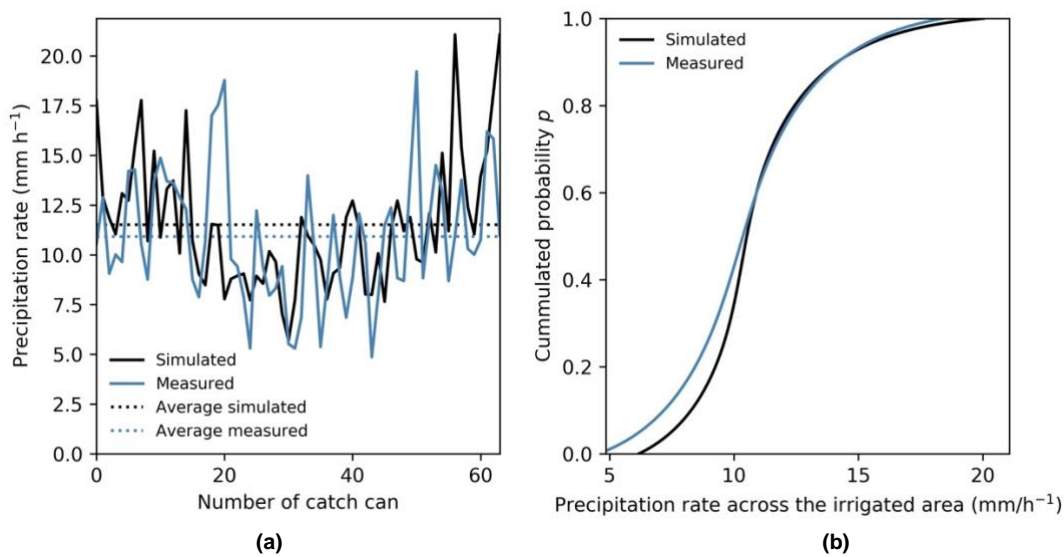
A comparison of the simulated and measured irrigation rates for each catchcan is shown in Figure 5.25a and Figure 5.27a for tests 10 and 50, respectively. The average amount of water collected was similar (dotted lines). However, the maximum and minimum peaks in precipitation rate did not always coincide with the same catchcans. This might explain the good CU<sub>e</sub> but poor spatial similitude parameters, MAE and RMSE.

Figure 5.25b and Figure 5.27b compare the simulated and measured IR<sub>CC</sub> (irrigation rates on each catchcan) in the form of cumulative distribution function. This function describes the probability that a given area, represented by  $p$ ,

receives less than or equal to a given amount of water. It is observed the use of the cumulative distribution function to characterise irrigation heterogeneity resulted in higher similarities between simulated and measured patterns. However, it is important to highlight that the use of this kind of distributions shows the general variability of the irrigation rate across a given surface, but do not consider the spatial distribution.



**Figure 5.24** IR distribution of solid-set test simulation (upper panels) and overlapping of measured single sprinkler (lower panels) for test 10. Right panels present a zoom-in of its respective left panel. Red dots represent sprinkler location, and yellow lines limit the area on which irrigation CU. Values of CU were calculated for the catchcans inside the green. MAE = 2.9, RMSE = 3.8.



**Figure 5.25** (a) Comparison of the precipitation rate ( $\text{mm h}^{-1}$ ) in each catchcan and average precipitation rate (dotted lines) for measured and simulated test 10 with sprinkler spacing  $17.5 \times 17.5$  m. (b) Comparison of the cumulative distribution curves of water collected in the catchcans for simulated and measured overlapped irrigation.

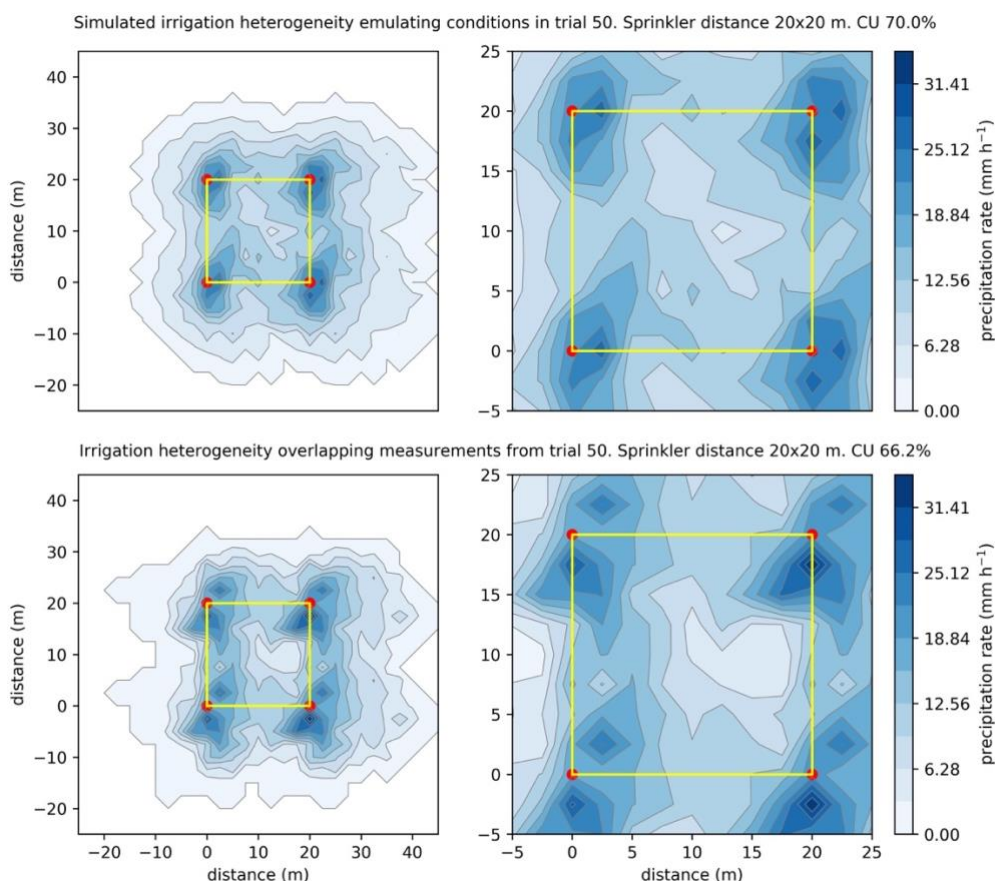


**Figure 5.26** IR distribution of solid-set test simulation (upper panels) and overlapping of measured single sprinkler (lower panels) for test 50. Right panels present a zoom-in of its respective left panel. Red dots represent sprinkler location, and yellow lines limit the area on which irrigation CU. Values of CU were calculated for the catchcans inside the green. MAE=3.3, RMSE=4.2



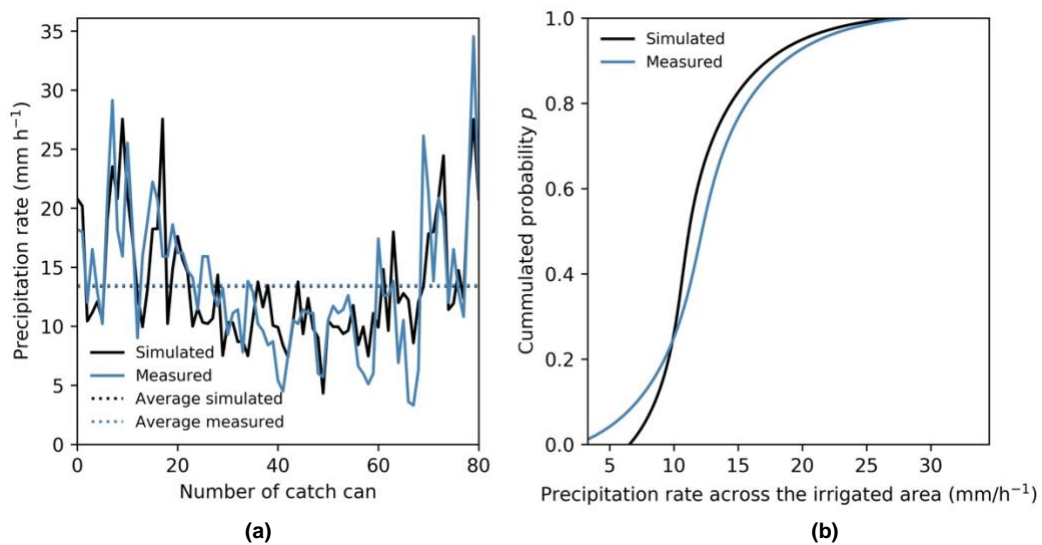


**Figure 5.27** (a) Comparison of the precipitation rate ( $\text{mm h}^{-1}$ ) in each catchcan and average precipitation rate (dotted lines) for measured and simulated test 50 with sprinkler spacing  $20 \times 20$  m. (b) Comparison of the cumulative distribution curves of water collected in the catchcans for simulated and measured overlapped irrigation.

### 5.3 DISCUSSION

In this section the results obtained from the field tests and model evaluation are critically discussed. The results are compared with findings reported by earlier research. Overall, the developed model provided excellent predictions of IR and acceptable predictions of CU. Sources of errors have been identified, and opportunities for improvement are pointed out. This is the first research to apply ballistics theory for simulating irrigation performance in golf rotor sprinklers.

#### Field test

Field test data were necessary to calibrate and evaluate the model and assess its performance. However, some methodological limitations in characterising the radial leg curve data under ‘no-wind’ conditions were experienced. These coincide with observations from Sanchez et al. (2011) who reported that several precautions must be required when radial leg tests are conducted outdoors. Even under low winds the radial leg curves for impact sprinklers can be significantly distorted, with wind speeds that exceed  $0.6 \text{ m s}^{-1}$  leading to erroneous results. Seginer et al. (1991) and Stambouli et al. (2014) reported similar errors when trying to evaluate radial leg curves. Ideally, the radial leg tests should have been conducted indoors but this facility was not available for this research.

Due to the challenges in characterising the radial leg curve, the manufacturer's data was used. It is important to point out that in the CIT tests the sprinkler height was different to that in the field tests conducted at Cranfield University. In this research, the sprinkler was placed on a stand, with the water jet set at 0.79 m above ground level, and water collected at 0.2 m, coinciding with the catchcan rim. Conversely, in tests conducted by the manufacturer, the difference between the jet and the water collection surface was 0.07 m. The difference of 0.52 m between the radial leg test conducted by the manufacturer and the field tests under wind conditions might have affected the estimation of droplet sizes.

The field tests under windy conditions were conducted successfully. The sprinkler wetted patterns were affected by wind speeds, displacing the centre of gravity of the wetted area and narrowing its shape towards the leeward side, coinciding with results reported by previous investigations (von Bernuth and Seginer, 1990; Tarjuelo et al., 1999a; Sanchez et al., 2011). A limitation observed in gridded catchcan tests was that the weather reduced the days available to conduct tests in optimum conditions, i.e., when wind is reasonably uniform. Also, during the tests, variations in wind speed and wind direction were common, with occasional wind gusts and periods of no-wind. This variability might have introduced some error in the estimation of irrigation distorted by wind. Due to the natural variability of the wind, the use of the average of the vector wind speeds seems to be appropriate than the use of the average of the scalar wind speed. However, it is important to highlight that in conditions with very low wind direction uniformities, the average of the wind vectors might reflect a value of average wind speed much lower than the one observed in field. In those conditions, the results from those tests should be rejected for its use in model calibration or the assessment of the impacts of wind speed on irrigation performance.

Wind gusts also limited field data collection notably when gusts exceeded 7 to 8  $\text{m s}^{-1}$  resulting in catchcans being knocked over. Thus, in future studies on the impacts of wind on irrigation, it also might be desirable to use heavier rain gauges or with some subjection to the soil that prevents from turning when strong wind gusts occur. This turning of the catchcans during some tests limited the number

of field tests finished with success, as well as the maximum average wind speed measured at which data was collected.

#### Estimation of wind drift and evaporation losses

Results from current research proved the impact of wind on the distortion of water distribution in golf sprinkler irrigation, but not its relationship with WDEL for the range of studied wind speeds. The limit of the maximum average wind speed measured in tests might be one of the reasons for which wind appeared to have no impact on the WDEL equation. These results contradict the results from previous research, which reported that wind speed not only influences WDEL, but also that is the most critical factor when predicting WDEL (Molle et al., 2012). However, a good correlation between wind speed and WDEL was found for higher wind speeds. For instance, Tarjuelo et al. (1999b) did not observe dramatic drops of WDEL when comparing irrigation under wind speeds from 0 to 4 m s<sup>-1</sup>. For higher wind speeds (4 to 4.6 m s<sup>-1</sup>), the application efficiency dropped by more than 10%. Dechmi et al. (2003a), Playán et al. (2005) and Yacoubi et al. (2012) observed a linear increase in WDEL for increments of wind speeds, particularly above 2 m s<sup>-1</sup>. However, results provided by those researchers were obtained under more arid conditions and using different sprinkler type, which might have influenced differently on WDEL.

The type of sprinkler used in the tests might also explain the non-significant influence of wind on WDEL for the range of wind speeds tested. The only reference found in the literature on WDEL on golf sprinklers (Latif and Ahmad, 2008) reported variations in WDEL in relation to sprinkler discharge (given by the combination of nozzle and operating pressure) and relative humidity; but not wind speed. However, only two of the tests conducted were under windy conditions, with a wind speed of 3.6 m s<sup>-1</sup>.

Despite the reported impact of wind on WDEL, the equations found in the literature varied between sources. Limitations of WDEL predicting equations were previously reported by Playán et al. (2005) and Sánchez et al. (2011). These authors observed that although many published WDEL equations yield good results when reproducing WDEL for the irrigation system for which they were

designed, in many instances the equations do not provide representative results when used with other irrigation systems and the independent variables used are out of the evaluated range. The difficulty in identifying and measuring the contribution of each parameter to the prediction model was also reported by De Wrachien and Lorenzini (2006). Thus, evidence suggests that the estimation of WDEL will vary depending on the sprinkler set-up and study location. In recent research, Al-Ghobari et al. (2018) obtained better predictions when applying neural network techniques than when used a classical regression approach, which highlights the complexity of the relationship between explanatory variables in the prediction of WDEL.

The WDEL equation proposed in this research should be used considering the studied sprinkler, ranges of relative humidity (47-88%, mean 64.6 %), pressure (3-7 bar), temperature (15-27°C, mean 20.5°C) and wind speed (0.3-4.1 m s<sup>-1</sup>). Simulations of irrigation using values outside these ranges might introduce additional error. Field results showed an overall increase in WDEL at higher operating pressures, which can be explained by a reduction in the resulting droplet diameters (Montero et al., 2003), which are more likely to be evaporated. However, comparison of the influence of the operating pressure on WDEL with results from other research is limited as these studies did not use operating pressures above 5 bar to assess WDEL. A positive correlation between WDEL and pressure was reported by Tarjuelo et al. (1999b). These authors observed that the average application efficiency decreased as the operating pressure increased from 2.1 to 4.8 bar. However, both maximum and minimum values of WDEL were found in tests where higher pressure was used, which indicates that WDEL is not only influenced by the operating pressure. That might be related to the lower influence of operating pressure on WDEL at higher pressures. In more recent research, Yacoubi et al. (2012) reported that, while wind speed only influenced WDEL at 2 bar operating pressure; when the pressure was increased to 3 bar, RH also conditioned WDEL. These results contradict what observed in the current research, where the relation between RH and WDEL was only significant ( $p < 0.05$ ) for pressure 4.2 bar and not for operating pressure 6 bar. Yan et al. (2010) observed that droplet evaporation rates were more sensitive to

droplet diameter for diameters lower than 2 mm, while for diameters higher than 2 mm droplet evaporation was more sensitive to RH. This fact may explain the significant correlation observed between RH and WDEL at lower pressure. However, this relation needs to be studied in more detail as results presented by Yan et al. (2010) were also based on a modelling approach.

The WDEL model developed in this work is presented as a valid predictor of the application efficiency. However, more research must be conducted to improve the predictions of WDEL in golf rotor sprinklers under more contrasted conditions. Further research should include tests under a range of higher wind speeds (greater than  $4 \text{ m s}^{-1}$ ), and a more extensive range of values of operating pressure, nozzle sizes, relative humidity and temperature.

#### Model performance

The similitude parameters resulting from the calibration show that the irrigation model developed in this research can successfully simulate the irrigated wetted area of a single sprinkler under windy conditions. The spatial variability of the water distribution (RMSE and MAE) presented a higher error. However, the application of the model for the prediction of CU showed good correlation. In previous research, Montero et al. (2001) obtained better accuracy in the predictions of single sprinkler spatial distribution patterns than those obtained in the current research. This variability may be caused by limitations derived from the theoretical basis of the model applied to a golf rotor sprinkler, as well as to limitations of the experimental tests. In the same research, authors presented an average absolute error of the Christiansen's Uniformity Coefficient (CU) of 3.0%, which was no far from the average error obtained in current research, 4.3%. Similar errors in the prediction of CU were found in other investigations that modelled irrigation based on ballistics theory (Dechmi et al., 2004b; Playán et al., 2006; Yacoubi et al., 2010; Sanchez et al., 2011). The predictions from these researchers presented a uniform distribution of the errors. In contrast, the simulated CU in current research tended to be overestimated (Figure 5.23), which indicates some bias in the model performance. The model predicted with high accuracy the average irrigation rates ( $\text{mm h}^{-1}$ ), presenting a coefficient of

determination  $R^2 = 0.98$ . These results indicate that the model could be used to estimate irrigation rates and, to a lesser extent, the CU on greens accurately.

Some possible sources of error in the prediction of CU have been identified. One reason that increased RMSE and MAE might be the theoretical approach of the droplets distribution used to determine drop diameters generated by the studied sprinkler (von Bernuth and Gilley, 1984). Droplet size distribution depends on the design of the nozzle and operating pressure (Kohl, 1974), being the nozzle the most influential in sprinklers (Carrión et al., 2001b). In the current research, the nozzles coupled within the sprinkler RainBird 751 consists of a central circular-grooved hole, which provides the main jet, plus two additional lateral holes on each side (Figure 5.28).



**Figure 5.28** Nozzles #28 (white) and #40 (orange) used in the sprinkler RainBird 751

The generation of the main jet can be appreciated in Figure 5.29. The main jet is generated in the central hole of the sprinkler, while the lateral holes deliver water to the first metres along the radial curve. It is likely that the complexity in the shape of this nozzle altered the droplet size distribution pattern. However, measurements to characterise the droplet diameters on at each side of the radial curve were not carried out.



**Figure 5.29** Jet formation in the RainBird 751 sprinkler fitted with the nozzle #28.

Evidence on the impact of the nozzle shape on water distribution was reported by Li et al. (1994). These authors compared the droplet size distribution between circular and squared nozzle shapes. They concluded that, at a given distance, the mean droplet sizes were larger in squared nozzles than in circular nozzles, but circular nozzles provided the largest average droplet size at the outer perimeter of their pattern. Based on those findings, Li and Kawano (1995) also reported that the modification of the drag coefficient  $C$  for non-circular sprinklers might be necessary. In the calibration of SIRIAS model, Montero et al. (2001) reported higher errors in simulations when impact sprinklers with double nozzle and non-circular shapes, especially operating at low pressure. Kincaid et al. (1996) also proposed an empirical model that permitted to establish a relationship between the drop diameter and the discharge of a given sprinkler, nozzle diameter and operating pressure. This model was successfully used in recent research, where ballistics theory was applied to simulate irrigation of spray plate sprinklers in central pivots (Ouazaa et al., 2014). The application of the concepts

presented in those investigations could improve the characterisation of the drop size distribution provided by the nozzles #28 and #40 of the sprinkler RainBird 750. However, the conceptual basis of the model developed in the current research characterised the distributions of drop sizes based only on the operating pressure, and not on the discharge rate or nozzle shape and diameter. More investigation is required to characterise drop diameters along the radial curve for multiple-hole nozzles and determine its impact on drop size.

Improvements in the estimation of droplet size distribution could be achieved by knowing the exact area of each nozzle hole and by using traditional methods of droplet size distribution measurements using flour containers (Li et al., 1994), low-speed photography methods (Bautista-Capetillo et al., 2012), or other optical methods (Félix-félix et al., 2017). That data might be useful to determine the discharge coefficient (C) of each nozzle hole. By using inverse modelling approach, it could be possible to estimate the initial droplet velocity, and modifying of the discharge coefficient as proposed by Li and Kawano (1995). Improvements in the water droplet distributions would benefit the estimated WDEL along the radial curve, as evaporation losses were calculated as a function of droplet size.

Improvements in the estimation of the  $K_1$  and  $K_2$  coefficients could also be achieved by conducting solid-set irrigation tests instead of only measuring the water distributed by a single sprinkler. Montero et al. (2001) observed that when they calibrated SIRIAS model for bloc tests, results of simulations coincided in a greater extent to that observed in field. Tarjuelo et al. (1999a) also found that irrigation uniformity as slightly higher when calculated from block irrigation tests, than when was calculated by overlapping data from sprinkler irrigation tests. This difference was higher when wind speed increased. Indeed, Dechmi et al. (2003b, 2004b), Playán et al. (2006) and Yacoubi et al. (2010) used data from solid-set irrigation tests for estimating the  $K_1$  and  $K_2$  parameters. However, in this research, it was not possible to conduct solid-set irrigation due to the limited volume of water for each test ( $1.5 \text{ m}^3$ ), and the high-water flow required to operate the sprinkler RainBird 751 SERIES ( $3.8$  to  $6.5 \text{ m}^3 \text{ h}^{-1}$  each).



## 6 SIMULATING TURFGRASS GROWTH, WATER BALANCE AND LEACHING: STICS CROP MODEL SENSITIVITY ANALYSIS, CALIBRATION AND PERFORMANCE EVALUATION

This chapter evaluates the STICS crop growth model for simulating turfgrass dry matter production (DMP), the water balance and nitrogen (N) leaching risks. A sensitivity analysis, calibration and validation of the STICS model was undertaken to evaluate the suitability of the model to simulate turfgrass under different irrigation strategies.

### 6.1 METHODOLOGY

The individual steps in this methodology are summarised in Figure 6.1. In the first step, the STICS model was pre-parameterised and model assumptions made regarding climate, soil and plant management. The sensitivity of a number of input parameters on crop model output variance was then assessed. The results from the sensitivity analysis were used to determine the most relevant parameters for this study. The parameter values were estimated in the calibration step using data from two studies conducted in Norway. The model was then validated and evaluated by comparing the simulated clippings, water balance and leaching with field measurements reported in the research literature. Finally, the model behaviour and outputs were critically evaluated and limitations and opportunities for improvement identified.

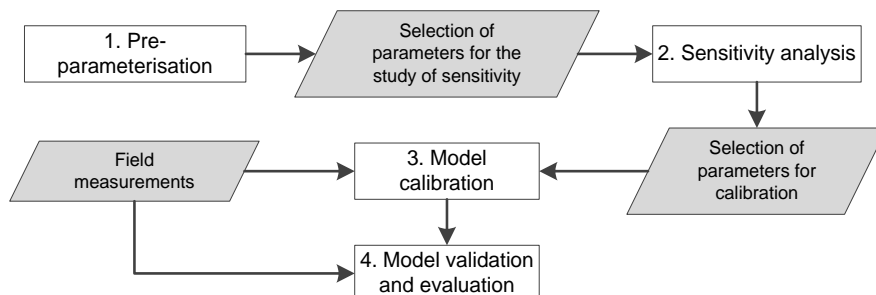


**Figure 6.1** Flowchart showing steps for model sensitivity analysis, calibration, validation and evaluation of STICS crop growth model for turfgrass.

### 6.1.1 Study site and field data

The raw data from two studies were used for the STICS model calibration, validation and evaluation. The first study was conducted by Chen et al. (2018) and referred to as *Study 1*. The second earlier study was carried out by Espevig and Aamlid (2012) and referred to as *Study 2*. Both studies were conducted at the NIBIO Turfgrass Research Centre, Landvik, Norway (58°20'N, 8°32'E, 12 m.a.s.l.). Located on the Norwegian south coast, the experimental site has a moderate summer temperature and a relatively high annual precipitation. Historical daily time-step data from 1987 for a weather station located at the study site was accessed from the NIBIO Agrometeorological Service (<http://lmt.bioforsk.no>).

Figure 6.2 shows the average monthly rainfall, reference evapotranspiration (ETo) and temperature for Landvik from 1997 to 2016. The highest monthly rainfall occurs from October to January, and then declines from February to July. In August and September, rainfall is generally higher than in the previous months. The ETo in Landvik is close to zero during the winter months, increasing steadily from March until reaching a maximum in June and July. From August to October, the average monthly ETo values drop steadily. The only months when average monthly ETo exceeds average rainfall is June and July, but differences between the two variables are small (June) and not statistically significant (July,  $p>0.05$ ).

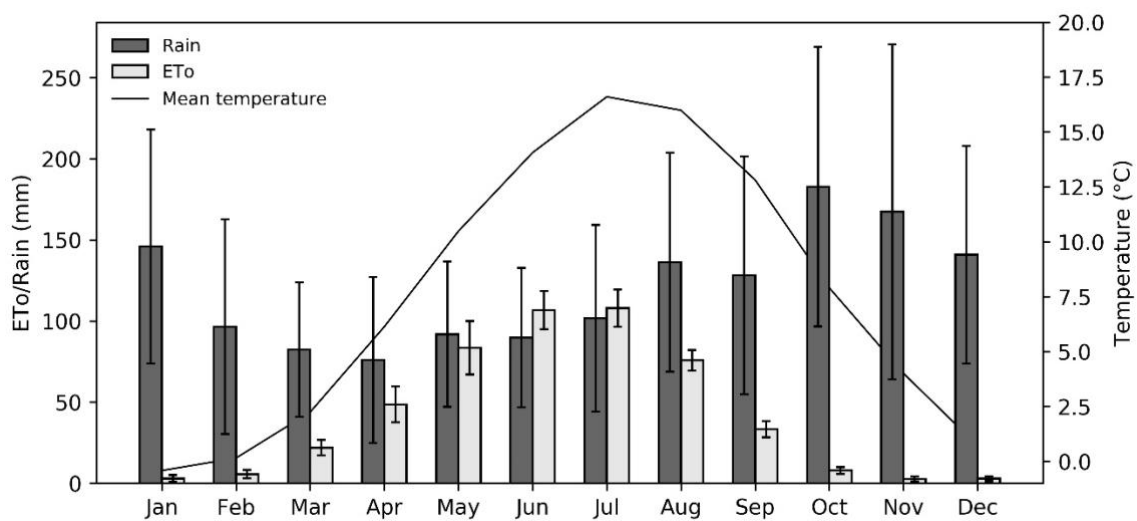


**Figure 6.2** Average monthly rainfall, reference evapotranspiration (ETo) and temperature for Landvik from 1997 to 2016. Error bars represent the standard deviation.

### Study 1: Irrigation strategies on red fescue

This dataset came from a three-year research trial conducted between 2013 and 2015 that investigated the effects of different irrigation strategies on red fescue (*Festuca rubra* L.) water use, growth rate and turf quality, among other factors. red fescue is characterised by having a lower need for pesticides, fertilisers and irrigation than other species used on greens such as annual bluegrass (*Poa annua* L.) or bentgrasses (*Agrostis* sp.). Because of these characteristics, red fescue might be considered a *low input species*, and may support more sustainable management golf greens (Aamlid et al., 2015).

The turfgrass was established on a sand-based rootzone following recommendations from the USGA (2004) under a rainout-shelter. The volumetric soil water content (VSWC) at field capacity (FC) was determined to 20% (v/v), corresponding to 40 mm of water. The soil organic content was  $43.0 \pm 1.7 \text{ g kg}^{-1}$  and  $13.8 \pm 0.5 \text{ g kg}^{-1}$  at 0-2 cm and 2-4 cm, respectively. The bulk density was  $1.55 \text{ g cm}^{-3}$  and soil pH 6.2. The green was mowed to 5 mm height three times a week. Every two weeks, clippings were collected and weighed, and the growth rate ( $\text{g m}^{-2} \text{ day}^{-1}$ ) calculated based on the dry weight gained since the last measurement. Liquid fertilisers were applied weekly corresponding to a seasonal rate of  $11.0 \text{ g N m}^{-2}$  across all treatments.

The irrigation treatments were applied between August and September in 2013, May and September in 2014 and May and August in 2015. The datasets from three irrigation treatments were used for calibrating and validating the STICS model, referred to as *treatment 1*, *2* and *3*. In *treatment 1*, irrigation was applied to FC once per week. In *treatment 2*, deficit irrigation was applied to 60% of FC content three times per week. In *treatment 3*, irrigation was applied as in *treatment 2*, plus irrigation to FC every other week from August 2013 to August 2014, changing from August 2014 to August 2015 to deficit irrigation at 60% of FC once per week. Data from a fourth treatment, where irrigation was applied to FC three times per week, was not used in this study as the reported water consumption in that treatment reported crop coefficients ( $K_c$ ) that were above 2.5, and considered to be unrepresentative of typical average water consumption on

golf greens (Romero and Dukes, 2016). The amount of irrigation applied was based on the water depletion in soil. The volumetric soil water content (VSWC, %v/v) was measured with a Time Domain Reflectometer probe (TDR) at 0 to 0.2 m depth. Table 6.1 summarises the irrigation applied in each treatment and year.

**Table 6.1** Penman-Monteith ETo and irrigation applied (mm) by treatment and year (*Study 1*).

Year	Period	ETo (mm)	Irrigation applied (mm)		
			Treatment 1	Treatment 2	Treatment 3
2013	Aug-Sept	85	139	45	85
2014	May-Sept	430	520	312	351
2015	May-Aug	331	329.	220	149

*Study 2: Irrigation strategies on velvet bentgrass*

This dataset came from a three-year research study conducted between 2007 and 2009. In this research, the effects of two irrigation frequencies on green velvet bentgrass (*Agrostis canina* L.) water drainage, nutrient leaching and visual turf quality were studied. Velvet bentgrass is known for its good performance at low N rates (Skogley, 1975) needing less irrigation water (DaCosta and Huang, 2006a) and exhibiting lower nitrate leaching (Paré et al., 2006) risks than other turf species.

Two rootzone compositions were studied: straight sand, and sand amended with 20% v/v garden compost. Here only datasets from the first tests (straight sand) were used because this was considered to be representative of a typical green rootzone. The rootzone composition followed recommendations from USGA (2004) and was constructed within stainless steel lysimeters that facilitated the collection of drainage for water analysis. The volumetric soil water content at FC was determined to be 18.9% at a depth of 13-50 mm and 10.8% at a depth of 150-187 mm. The average bulk density was 1.57 g cm<sup>-3</sup> and the ignition loss 0.54%. The green mowing height was between 3 to 4.5 mm with cutting three times a week. Between 21 August and 1 October 2007, all plots received 4.5 g N m<sup>-2</sup>. In 2008 and 2009, 19.2 and 13 g N m<sup>-2</sup> were applied, respectively. Fertilizers were applied every two weeks mostly in inorganic granular form.

Irrigation treatments were conducted between August and September in 2007 and May and September in 2008 and 2009. Irrigation treatments were either light

and frequent (*treatment 4*) or deep and infrequent irrigation (*treatment 5*). In *treatment 4*, 5 mm was applied when the accumulated pan evaporation (Epan) exceeded 5 mm. In *treatment 5*, 10 mm was applied when the cumulative pan evaporation exceeded 10 mm. Accumulated water deficits for each of the four treatments were calculated five days per week using daily rainfall and values from pan evaporation. The measured pan evaporation, rainfall and irrigation applied each year and each treatment is shown in Table 6.2.

**Table 6.2** Pan evaporation, rainfall and irrigation applied (mm) in *Study 2*

Year	Period	Pan evaporation (mm)	Rainfall (mm)	Irrigation applied (mm)	
				Treatment 4	Treatment 5
2007	Aug-Sept	78	195	50.0	45.0
2008	May-Sept	330	599	226.4	185.0
2009	May-Sept	302	129*	223.3	206.0

\*rainfall in 2009 is only accounted for May and June. From July to September 2009, treatments were conducted under rain-out shelter

### 6.1.2 Model selection for simulating turfgrass performance

In order to evaluate the effect of a range of irrigation system and management strategies on turfgrass, four crop models were reviewed. These were CropSyst, DAYCENT, DNDC and the STICS model. Despite the wide variety of models applied to grasslands, and for the sake of simplicity, only the most relevant models capable to simulate plant development, water balance, and leaching were considered. The models reviewed were composed by sub-modules that, at least, were able to simulate the effect of management practices on crop development, water and nitrogen balance:

- (i) Crop development module which simulates the effect of water applications, nitrogen fertilization and biomass removal on growth
- (ii) Water budget module which allows the estimation of the water balance in the soil given the water inputs (rain and irrigation) and water outputs (plant water consumption, drainage and runoff).
- (iii) Environmental module which simulates nitrogen losses through leaching. To achieve this, the module estimates the nitrogen balance in the crop system. Nitrogen balance includes the fate of N in the nitrogen cycle: plant uptake, leaching and soil immobilization.

- (iv) Management practices which allow the model inputs irrigation, nitrogen fertilisation and crop cut.

None of the four models reviewed were specifically designed for turfgrass. They simulate crop biomass variation and water and N balances in the soil-plant system. Although they represent different approaches (STICS and CropSyst are crop-oriented models while DNDC and DayCent are environmental models), they are all capable of producing similar outputs. Table 6.3 summarizes the main features of each model.

**Table 6.3.** Selected crop models and main features

Model	Perennial cycle	Used in turfgrass	Start established	Crop Growth/DMP	Turf Quality	Cutting simulation	Root development	Irrigation	Water balance	Leaching	N budget	Manual quality 1-5	GUI	Complexity 1-5
CROPSYST	✓	-	✓	✓	-	✓	✓	✓	✓	✓	✓	4	✓	4
DAYCENT	✓	✓	-	✓	-	✓	-	✓	✓	✓	✓	2	-	3
DNDC	-	✓	-	✓	-	✓	-	✓	✓	✓	✓	3	✓	3
STICS	✓	-	✓	✓	-	✓	✓	✓	✓	✓	✓	5	✓	4

In recent research, Sansoulet et al. (2014) compared the STICS, DNDC and DayCent models for wheat grown under Canadian weather conditions. The authors concluded that the three models were able to provide accurate results under average weather and fertilization conditions. However, when there were heavy rains or low fertilization rates were applied, STICS and DNDC models provided the most accurate predictions.

In this research, it was considered that the model should provide a graphical user interface (GUI) to provide a gentle learning curve. The DayCent model was the only model among the four crop models that did not have any GUI application. For this reason, and although it was previously used for turfgrass simulation (Zhang et al., 2013b), the DayCent model was discarded for this research.

Although STICS and CropSyst need a significant amount of more data for parameterization (especially in relation to plant characteristics), they also allow the user to modify a greater number of parameters than the DNDC and DayCent

models. This is a big advantage for this research due to specific characteristics of golf greens and turf management. Thus, due to wider possibilities for parameterising STICS and CropSyst models, the DNDC model was also discarded.

STICS and CropSyst offer similar features: robustness, large possibilities to parameterize different crops, detailed user manuals and an excellent GUI. However, the main reasons why STICS was selected were: (i) the possibility of applying multiple crop cuts within the same season, adapting the crop height to short mowing characteristics in turfgrass systems, (ii) a greater number and more recent publications on the application of the model in grassland research (Ruget et al., 2009; Durand et al., 2010; Shili-Touzi et al., 2010; Jégo et al., 2013; Constantin et al., 2015); (iii) excellent documentation, access to the source code, and equations involved in the model; and (iv) an active research community, which offer training and provided valuable support during the research.

### **6.1.3 STICS model overview**

The crop model selected for simulating turfgrass water balance, growth and leaching was STICS [Simulateur mulTIdisciplinaire pour les Cultures Standard, Brisson et al. (2002, 2003)]. The STICS model computes plant development on a daily basis time-steps and considering one dimension. Its input variables relate to climate (radiation, minimum and maximum temperatures, rainfall, reference evapotranspiration and possibly wind and humidity), soil, plant system and management practices. Its output variables relate plant development relative to quantity and quality, and environmental impacts relative to drainage and nitrogen leaching. The STICS model is divided into sub-modules, each dealing with specific crop system mechanisms but inter-related. These sub-modules are: (i) *phasic development*, (ii) *shoot growth*, (iii) *root growth*, (iv) *yield formation*, (v) *microclimate*, (vi) *management and crop environment*, (vii) *water balance*, (viii) *nitrogen transformations*, and (ix) transfer of heat, water and nitrates. Below are described the sub-modules affecting the processes simulated in this research; further information on the model is given in Brisson et al. (2008).

### Phenological stages

The STICS model phenological stages are used for simulating plant development and growth dynamics. These phenological stages determine the rate of development of leaf area index (LAI,  $\text{m}^2 \text{m}^{-2}$ ) and root development, as well as the harvested organs filling. The phenological stages comprise the different successive stages between plant germination and maturity and are specific to each species and variety. The STICS model computes the evolution within phenological stages and changes in their state over the simulation time based on the sum of degree-days. For the simulation of turfgrass, only two phenological stages were considered: *ilev*, which is the phenological stage coinciding with the plant emergence, and *iamf*, which coincides with the maximum acceleration of leaf growth and end of the juvenile phase. However, the STICS model also simulates other phenological stages such as germination (*iger*), maximum leaf area index and end of leaf growth (*ilax*) or physiological maturity of fruits (*imat*). The acceleration or deceleration of the evolution of the phenological stages is also subject to stresses such as temperature, water and/or nitrogen stresses.

### Shoot growth

The STICS model simulates shoot growth as a function of the LAI and its daily development based on phenological stage and the Beer's law analogy. Therefore, there is a direct relationship between LAI and daily growth. LAI evolves through various phases: growth, stability and senescence. The leaf growth rate, given by the variable  $\text{delta}i_{dev}$  (in  $\text{m}^2 \text{plant}^{-1} \text{degree-day}^{-1}$ ) is described by a logistic curve of development units, whose inflexion point coincides with the end of the juvenile phase (*iamf*). For the simulation of turfgrass, the automatic cuts coincided with the *iamf*, i.e., with the inflexion point of this logistic curve. The total LAI is then calculated by multiplying the daily leaf growth rate value by the effective crop temperature, the planting density, and the water and N stress indices. The total aboveground biomass is then calculated as the sum of the leaf growth rate by the plant radiation interception.

### Plant stresses



In STICS, leaf growth rate and evolution within plant phenological stages are affected by stress indices. These stress indices vary between 0 and 1, and delay phenological stages development, accelerate leaf senescence, slow down leaf growth rates and decrease radiation use efficiency and plant transpiration. These indices are a function of stress state variables, which are calculated based on the soil water available for plant transpiration (water stress index), N source/sink ratio available for plant uptake (N nutrition stress index) and optimum temperature for plant stress (suboptimal stress indices) (Brisson et al., 2008). When stress indices reach a critical level for plant development, values of  $\Delta t_{dev}$  are multiplied by the stress indices, reducing then leaf growth rate and aboveground biomass accumulation.

### Water balance

In STICS, the water balance has a two purposes: to estimate soil water content, plant water uptake and drainage (which drives leaching) and water stress indices. The variables used to compute water balance are water inputs (irrigation, precipitation) and water outputs (evapotranspiration). The evapotranspiration values are constructed based on the Penman-Monteith reference evapotranspiration equation (Allen et al., 1998), which are affected by the water stress index. Water that exceeds the maximum soil water holding capacity is lost through the profile as drainage.

### Nitrogen transformations

In STICS, the nitrogen transformations are computed considering the main processes affecting the available mineral nitrogen for plant uptake in soil (mineralisation, immobilisation, nitrification, volatilisation, denitrification and leaching). Nitrogen mineralisation is produced as a function of three sources of organic matter: humified organic matter ( $nhumt$ ), crop residues ( $res$ ) and the microbial biomass ( $dcbio$ ) growing on them. The humified organic matter is mineralised up to a soil depth called  $profhum$ , and the potential rate at which it is mineralised is mainly given by the N organic content in the first layer of soil ( $Norg$ ) and the potential mineralisation rates ( $fmin$ ). In this research, parameters of N mineralisation were calibrated and validated for leaching; however, due to lack of

data, processes such as nitrification, volatilisation, denitrification have been ignored.

### Management and crop environment

The STICS model allows for several management actions. Three of them had a direct impact on this research: water applications, N applications and cuts. The amounts of water applied can be entered from an irrigation calendar or calculated by the model. In the latter case, the model automatically calculates water inputs to satisfy water requirements when a given threshold of water stress index is achieved. Irrigation is then estimated to replenish the soil water reserve to FC without exceeding the maximum dose defined by the irrigation system. Similarly, N fertilisation can be applied by calendar or calculated automatically by the model according to the plant N requirements. The automatic fertiliser applications are driven by the plant N uptake requirements, which are driven at the same time by the plant growth and mineral N available in the soil. Eight different N fertilisation forms can be selected, with which varying in N use efficiency and the fraction of the N fertiliser applied unavailable for the plant because it is either immobilised in soil by microbial activity, denitrified or volatilized.

Forage crops (of which turfgrass can also be included) can be cut using three methods. The first consists of an automatic cut calculation: as soon as the crop reaches a given phenological stage; it is cut at a pre-defined height given by the parameter *hautcopuedefault* and transformed into biomass using the *coefmshautp* conversion parameter. The second method consists of cuts based on defined dates at a determined cutting height; leaving in the field with a given LAI, biomass and fertilisation. The third method consists of cutting by imposing physiological dates, with cutting dates defined by cumulative development units (Brisson et al., 2008).

#### 6.1.4 STICS model pre-parameterisation and assumptions

A step called *pre-parameterisation* was carried out before conducting the sensitivity analysis and parameter calibration for the STICS model to simulate turfgrass growth. This aimed to understand the model and set those parameters that allowed STICS to be as “stable” as possible when simulating a specific crop such as turfgrass. Stable simulations are meant as those simulations finished without errors in calculations or meaningless outcomes. It is important to highlight that the aim at this stage was not to find the optimum values for parameters to minimise the error between field observations and simulations. Finding the optimum values of a selected number of parameters was addressed during the calibration phase.

Firstly, a number of key modelling and parameter assumptions were defined:

- 1) Turfgrass was assumed to be a perennial forage crop.
- 2) Turfgrass must be maintained at the vegetative stage (juvenile phase) during the simulation period, i.e., between the stages of leaf emergence (*lev*) and maximum LAI expansion (*amf*). This was achieved by returning to the *lev* phase after each cut. Under this assumption, the plant was not allowed to start the reproductive stage, and hence parameters that drive the development of fruit organs were ignored.
- 3) Due to the high infiltration rates in sand-based greens, no capillarity rise was assumed; any water that exceeded FC was assumed to be lost as drainage. Due to the high soil infiltration capacity, no runoff was assumed.
- 4) Rooting density and structure remained unaltered during the simulation period, as no data was available to compare the evolution of a simulated rooting system.
- 5) Simulations were initiated with model start on the first day of each year; however, model evaluation and quality assessment of model outputs used the period May to September. These dates were selected as they correspond to the period when turfgrass is irrigated in Scandinavian countries. Also, data available to compare model outputs against measurements were limited to these dates.

- 6) Planting density was fixed at 4000 plants m<sup>-2</sup>, which corresponds to the maximum value with impact on the STICS model plant inter-competition. Higher values of plant density do not impact on the model output. Although plant and shoot density in turfgrass is usually reported as a score based on visual observation (Aamlid and Molteberg, 2011), it is worth recognising that regular mowing of turfgrass can increase the shoot density substantially compared with ungrazed grasslands, with up to 6.6 × 10<sup>6</sup> shoots per m<sup>2</sup> in a green (Beard, 1973).
- 7) Some cultural practices from the experimental site were not simulated, including soil aeration, vertical cutting, topdressing or the exact number of mowing events (set as automatic cuts in the model simulations).

Following these modelling assumptions, some parameters were set to reproduce similar conditions to those reported in the study site (Espevig and Aamlid, 2012; Chen et al., 2018). Setting some plant parameters based on assumptions also aimed to reproduce plant characteristics and reduce the number of parameters to be studied to avoid over-parameterisation (Dumont et al., 2014). Parameters related to the site conditions were local climate conditions and green soil characteristics. The plant parameters used were based on the default plant files “grass”, “Tall fescue” and “Ryegrass” from the STICS plants database. Despite the similarities between turfgrass for golf and forage grass, it was necessary to modify some plant parameters to better represent turfgrass growth. Table 6.4 summarises the description of STICS parameters assumed for turfgrass simulations, as well as their values and comparison with default values from other forage crops.

**Table 6.4** Initial assumptions of plant parameter values used in the pre-parameterisation of turfgrass, compared against default values for forage crops tall fescue, ryegrass, and grass provided in STICS.

Parameter	Description	Unit	Turfgrass for golf	Tall Fescue	Ryegrass	Grass
Phenological development						
tdmin	Minimum temperature below which development stops	°C	0	0	4.6	0
tdmax	Maximum temperature above which development stops	°C	25	30	38	25
Leaves development						
phyllotherme	Thermal duration between the apparition of two successive leaves on the main stem	°C day <sup>-1</sup>	150	200	180	200
bdens	Minimal density above which interplant competition starts	m <sup>-2</sup>	15	7	7	200
hautbase	Basal height of crop	M	0.0001	0.02	0	0.02
hautmax	Maximum height of crop	m	0.04	0.3	1	0.3
tcxstop	Temperature beyond which foliar growth stops	°C	30	100	100	30
tcmmin	Minimum temperature at which growth ceases	°C	5	0	4.6	0
tcmmax	Maximum temperature at which growth ceases	°C	20	40	38	25
ratiosen	Fraction of senescent biomass (relative to total biomass)	-	0.1	0	0.5	0.8
Shoot biomass growth						
temin	Minimum temperature for development	°C	0	0	4.6	0
temax	Maximal temperature above which plant growth stops	°C	30	40	38	25
teopt	Optimal temperature (1/2) for plant growth	°C	15	24	15	15.27
teoptbis	Optimal temperature (2/2) for plant growth	°C	20	24	20	25
efcroijuv	Maximum radiation use efficiency during the juvenile phase	g MJ <sup>-1</sup>	1	2	3.14	2.5
remobres	Fraction of daily remobilisable C reserves	-	0.02	0.2	0.02	0.05
coefmshaut	Ratio biomass/ useful height cut of crops	-	30	25	0.25	25
Partitioning biomass to organs						
tigefeuil	Ratio stem (structural part)/leaf	-	0	0.1	0.5	0.35
Roots						
zpenite	Depth at which root density is 50% of the surface root density (reference profile)	cm	10	25.5	25.12	25.5
Cultivar parameters						
stamflax	Cumulative thermal time between the stages AMF	-	10000	5000	1580	5000
adens	Interplant competition parameter	-	-0.7	0	-0.1964	-0.5
durvieF	Maximal lifespan of an adult leaf expressed in summation of Q10=2 (2**(T-Tbase))	-	120	100	140	77.539
General model parameters for STICS simulations						
			Turfgrass for golf	Default STICS		
khaut	Extinction coefficient connecting LAI to crop height	-	0.044	0.7		

To enable simulation of low cutting heights, different parameters were modified compared to the default values included in the STICS parameter option. The parameters (i) *extinction connecting of leaf area index to crop height (Khaut)*, (ii) *maximum height of crop (Hautmax, in m)* and (iii) *basal height of crop (Hautbase, in m)* were fixed at 0.044, 0.04 m, and 0.0001 m, respectively. These values enabled the simulated plants to grow evenly and at the typical short height of

turfgrass for golf. The relation between those parameters and crop height is explained by the STICS equation [ $Hauteur_i = Hautmax[1 - \exp(-K_{haut} \times LA_i)] + Hautbase$ ], where  $Hauteur_i$  is the crop height at the day  $i$ , in metres; and  $LA_i$  is leaf area index on the day  $i$ , in  $m^2$  of leaf per  $m^2$  of soil.

Rooting depth was fixed and maintained at a maximum depth of 0.2 m. This was the same for both Studies 1 and 2. The option of root density was considered to have a standard profile, with density being reduced by 50% in the 0.1 to 0.2 m soil horizon, given by the variable  $zpen$  in STICS. The soil parameters used were based on the soil characteristics reported in the studies. The clay content ( $argi$ ) was fixed at 3% due to the sandy characteristics of the rootzone in greens.

The starting leaf area index ( $lai0$ ) was fixed at  $3 m^2 m^{-2}$ , the starting aerial biomass ( $masec0$ ) was  $0.5 t ha^{-1}$  and perennial plant reserves ( $resperenne0$ )  $2 t ha^{-1}$ . Irrigation and fertilisation inputs were set to match those reported in each treatment and study. The automatic cut option was selected, with cuts at 0.005 m when the phenological stage *end of the juvenile phase* ( $amf$ ) was reached.

### 6.1.5 Sensitivity analysis

A sensitivity analysis was conducted with three objectives. The first was to explore and evaluate the model behaviour for the study conditions described above. The second was to identify the contribution of a number of selected input parameters to model output variance. Finally, based on the sensitivity analysis, the third objective was to select those parameters that needed to be accurately estimated at the calibration stage.

The sensitivity analysis followed five steps as shown in Figure 6.3. Firstly, the criteria to select the parameters for the sensitivity analysis was based on the implications of those parameters in the model equations (Brisson et al., 2008) related with the model outcomes relevant to this research (1). The STICS model was then run  $n$  times, each time for a different combination of input parameters (2,3). After running the simulations, the sensitivity indexes for the contribution of each input parameter over the output variance were estimated (4). From these results, the parameters to be calibrated were selected (5). The sensitivity analysis

was conducted using the eFAST algorithm (Saltelli et al., 1999), implemented within the OptimiStics software (Buis et al., 2011; Wallach et al., 2011).

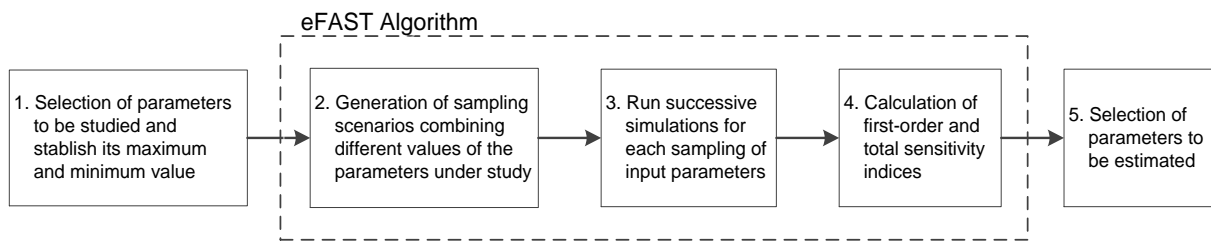


**Figure 6.3** Sequential steps followed as part of the STICS sensitivity analysis

### Selection of parameters for sensitivity analysis

The selected output parameters of particular interest to this research were those relating to evapotranspiration, drainage, water stress indexes, dry matter production and nitrogen leaching. Table 6.5 summarises the parameters included in the sensitivity analysis, and the ranges of uncertainty studied for each parameter. The choice of parameters was based on the impacts of each parameter in the STICS modelling equations, as described by Brisson et al. (2008). Parameters were also selected based on their impact on the model outcomes observed during the pre-parameterisation stage. The uncertainty ranges for each parameter were determined based on typical values found in the literature for turfgrass species. When no data was found for a given parameter, the boundaries used were the default values as recommended in the STICS model.

**Table 6.5** Parameters selected for sensitivity analysis and uncertainty ranges used for sensitivity sampling

Module	Parameter	Description	Unit	Uncertainty range	
Water balance	extin	Extinction coefficient of photosynthetic active radiation in the canopy	-	0.1	1
	q <sub>0</sub>	Cumulative soil evaporation above which evaporation rate is decreased	mm	1	50
	beta	Parameter of increase of maximal transpiration when a water stress occurs	-	1	2
	psisto	Potential of stomatal closing (absolute value)	bar	1	25
	psiturg	Potential of the beginning of decrease of the cellular extension (absolute value)	bar	1	15
	rayon	Average root radius	cm	0.005	0.07
	lvopt	Root length density (RLD) above which water and N uptake are maximum and independent of RLD	cm.cm-3	0.02	1
	psihucc	Soil water potential corresponding to field capacity	MPa	-0.05	-0.01
	rapsenturg	Threshold soil water content active to simulate water senescence stress as a proportion of the turgor stress	-	0.5	1.5
	tustressmin	Water stress index (min(turfac, inns)) below which there is an extra LAI senescence	-	0.3	1
kmax	Maximum crop coefficient for water requirements	-	1	2	
Dry matter production	vclaimax	ULAI at the inflexion point of the function DELTAI=f(ULAI)	SD	2	3
	udclaimax	ULAI from which the rate of leaf growth decreases	SD	1	3
	dclaimax	Maximum rate of the setting up of LAI	m <sup>2</sup> leaf plant <sup>-1</sup> degree-d <sup>-1</sup>	5x10 <sup>-5</sup>	5x10 <sup>-4</sup>
	extin	Extinction coefficient of photosynthetic active radiation in the canopy	-	0.01	1
	tcmax	Maximum temperature at which growth ceases	degree C	20	30
	tcmin	Minimum temperature at which growth ceases	degree C	5	15
	tcxstop	Temperature beyond which foliar growth stops	degree C	25	30
psiturg	Potential of the beginning of decrease of the cellular extension (absolute value)	bar	1	15	
Nitrogen leaching	profhum	Maximum soil depth with biological activity	cm	0	20
	fmin1	Relative potential mineralization rate	d <sup>-1</sup>	0	1
	fmin2	Parameter defining the effect of clay on the potential mineralisation rate	-	0	1
	hminm	Relative water content (fraction of field capacity) below which mineralisation rate is nil	-	0.1	1
	hoptm	Relative water content (fraction of field capacity) below which mineralisation rate is maximum	-	0.1	1
	orgeng	Maximal amount of fertiliser N that can be immobilized in the soil	-	0	1
	deneng	Maximal amount of fertiliser N that can be immobilised in the soil	-	0	1
	voleng	Maximal fraction of mineral fertiliser that can be volatilized	-	0	1
	difN	Diffusion coefficient of nitrate N in soil at field capacity	cm <sup>2</sup> d <sup>-1</sup>	0.01	0.1
	Norg	Soil organic N content in the first soil layer (supposed constant down to the depth profhum)	% dry soil	0.05	0.5
	lvopt	Root length density (RLD) above which water and N uptake are maximum and	cm cm <sup>-3</sup>	0.2	1
	epc	Thickness of each soil layer	cm	1	1000
	epd	Thickness of mixing cells in each soil layer ( = 2 * dispersion length)	cm	1	50
Concseuil	Minimum concentration of HNO <sub>3</sub> in soil	kg ha <sup>-1</sup> mm <sup>-1</sup>	0	0.5	

The sensitivity analysis was conducted for three different modules: *water balance*, *dry matter production* and *nitrogen leaching*. Each module was split into



two sub-modules: *non-water limiting conditions* and *water limiting conditions*; these were achieved using two different irrigation levels. To ensure non-water limiting the value of irrigation efficiency (*effirr*) was set at 2.0. This value ensured that the soil was refilled beyond FC. For the water limiting treatment, the parameter *effirr* was set at 0.3 to ensure that irrigation was applied with deficit. In the *water balance* and *dry matter production* modules, the simulations were run using the same conditions as those in *Study 1* in 2014 and *treatment 1*, namely, irrigation to FC once per week. In the *nitrogen leaching* module, the same conditions as used in *Study 2* in 2008 and *treatment 4* were used. The method for setting the two different irrigation scenarios was the same as for the other two sub-modules. It is important to highlight that the aim of the sensitivity analysis was not to obtain a specific result, but rather to understand the contribution of the uncertainty of selected input parameters on the variance of selected output parameters.

#### *eFAST algorithm*

Steps 2 to 4 shown in Figure 6.3 were conducted using the extended Fourier amplitude sensitivity test (eFAST) algorithm (Saltelli et al., 1999), implemented within the OptimiStics software (Buis et al., 2011; Wallach et al., 2011). The principle of eFAST is that if the response of the model outcome  $\hat{Y}$  is sensitive to a given model input parameter  $Z_i$ , then  $\hat{Y}$  and  $Z_i$  should vary simultaneously over a scenario  $k$  (Monod et al., 2006). With the eFAST method, the sensitivity of  $\hat{Y}$  variance to  $Z_i$  is quantified by estimating a sensitivity index for a series of frequencies. If the parameter  $Z_i$  has a strong influence on  $\hat{Y}$ , then the index takes high values for the frequency  $\omega = \omega_i$ . The frequency  $\omega$  is that at which  $Z_i$  comes back to its starting value after taking different values between the maximum and minimum uncertainty range. The eFAST algorithm follows two differentiated steps. Firstly, an input parameter sampling is generated with  $k$  different combinations of parameters  $Z_i$ ; and secondly, the outputs from the simulation for each  $k$  sampling scenario are used to calculate the sensitivity indexes.

### eFAST sampling method

The eFAST method was selected because of its efficiency on the generation of different combinations of input parameters. In this method, all the input parameters are assumed to be quantitative and are normalised in order to have their domain of variation between 1 and 0 (Monod et al., 2006). The values of the input parameters were selected systematically along a search trajectory which is specifically designed to explore the input space. During the design of the sampling scheme, a frequency  $\omega_i$  is associated to each parameter  $Z_i$ . The position (or value) of  $Z_i$  on each sampling  $k$  scenario is given by  $z_{i,k}$ , which is determined using the following equation:

$$z_{i,k} = \frac{1}{2} + \frac{1}{\pi} \arcsin(\sin(\omega_i s + \varphi_i))$$

where  $\varphi_i$  is a random variable between 0 and  $2\pi$  to randomise the starting point of  $z_{i,k}$ , and  $s$  is a vector given by the equation:

$$s = -\pi + \frac{2k-1}{N} \pi$$

where  $N$  is the number of samples.

Figure 6.4 shows an example of the sample obtained for a single variable, with a sample size 100 and a frequency  $\omega_i = 5$

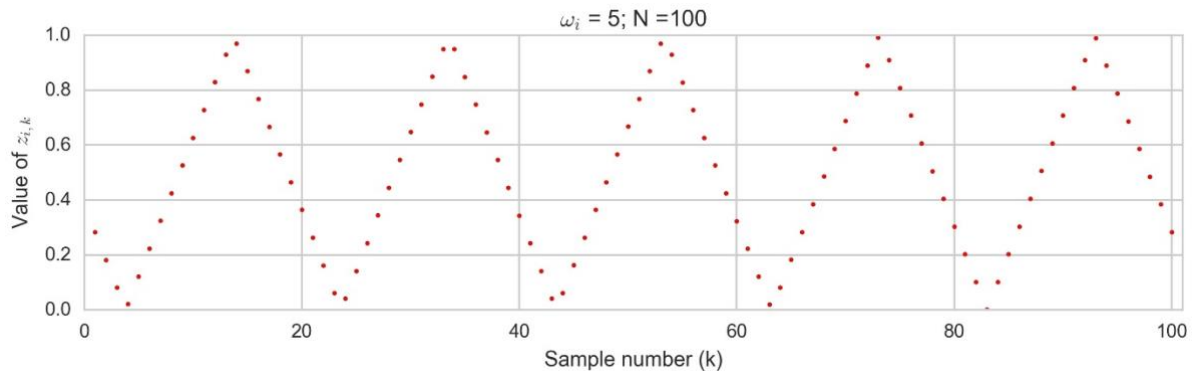


**Figure 6.4** Illustration of the eFAST sampling for one input parameter  $Z_i$ ,  $\omega_i=5$  and  $N=100$  samples

The eFAST method requires separate sets of simulations for each input parameter  $Z_i$ . For creating the sampling of various input parameters, a frequency  $\omega_j$  that satisfies  $\omega_j < \omega_i$  is associated for each input parameter other than  $Z_i$ . This

process is repeated for each parameter included in the sensitivity analysis. This is shown in Figure 6.5 for two input parameters  $Z_1$  and  $Z_2$ , and  $\omega_i=40$  and 800 samples per parameter. When  $Z_1$  was studied, the  $\omega_j$  associated to  $Z_2$  was equal to 2. When  $Z_2$  was studied new set of simulations were created, with the  $\omega_j$  associated to the  $Z_1$  equal to 1. This process was repeated for each  $Z_i$ .

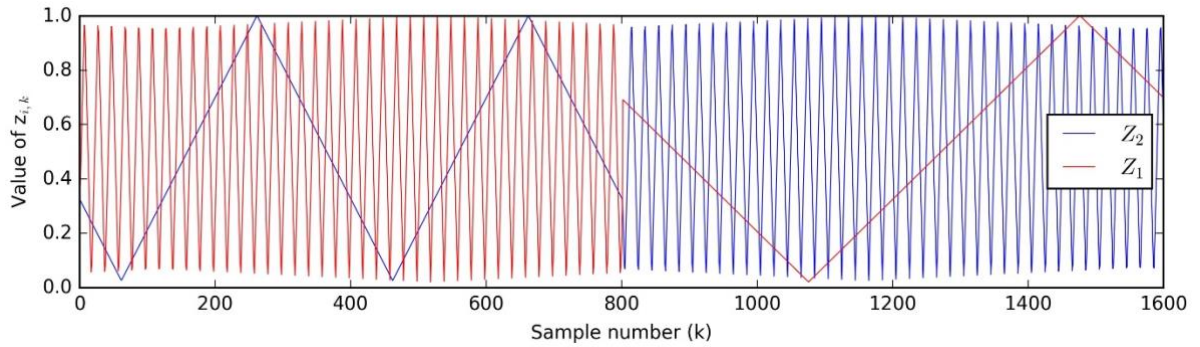


**Figure 6.5** Illustration of the eFAST sampling for two input parameters, with  $\omega_i=40$  and 800 samples per parameter

#### eFAST sensitivity indexes estimation

The eFAST method allows estimation of the first-order and total sensitivity indices (Saltelli et al., 1999). Those indices represent the proportion of the output variance as explained by the value adopted by each parameter. In addition to the efficient generation of combinations of input parameters, the eFAST sensitivity estimation method has the advantage of being global (the effect of one input parameter is evaluated on average as affected by the variation of other parameters) and model-free (no assumptions considered on model behaviour) (Monod et al., 2006).

The first order sensitivity index  $S_i$  is useful for measuring the average influence of an individual parameter  $Z_i$  on the model output, but it takes no account of the interaction effects involving  $Z_i$  with other studied parameters. It is estimated by:

$$S_i = \sum_{p=1}^M S[p\omega_i]$$

Where  $S$  is the variability associated with a frequency  $\omega_i$ , and  $M$  is the number of harmonics taken into account. The value of  $\omega_i$  corresponds to the largest frequency, related to the study of the sensitivity of  $Z_i$ , and that satisfies the

expression  $\omega_i \geq 2M \max(\omega_j)$ ; where  $\max(\omega_j)$  is the largest frequency associated with a parameter other than  $Z_i$ .

The scalar  $S_{[\omega]}$  is considered as the proportion of variability of  $f(z_{k,1}, z_{k,2}, \dots, z_{k,n})$  associated with frequency  $\omega$ .  $S_{[\omega]}$  is equal to  $D_{[\omega]} / (\sum D_{[\omega]})$ , where  $D_{[\omega]}$  is the spectral component (or variability) of  $\hat{Y}$  at the frequency  $\omega$ . In the case of having  $n$   $z$  components and  $k$  sampling scenarios,  $D_{[\omega]}$  is divided in components associated to each  $\omega$  from 1 to  $N-1$  as:

$$D_{[\omega]} = A_{\omega}^2 + B_{\omega}^2$$

Where

$$A_{\omega} = \frac{1}{2\pi} \sum_{k=1}^N f(z_{k,1}, z_{k,2}, \dots, z_{k,n}) \cos(\omega s_k)$$

$$B_{\omega} = \frac{1}{2\pi} \sum_{k=1}^N f(z_{k,1}, z_{k,2}, \dots, z_{k,n}) \sin(\omega s_k)$$

The total sensitivity index  $TS_i$  is the sum of all the factorial indices of  $Z_i$  and was estimated by:

$$TS_i = 1 - \sum_{\omega=1}^{M \max(\omega_j)} S_{[\omega]}$$

Since all the frequencies lower than  $M \max(\omega_j)$  correspond to the factorial terms not involving  $Z_i$ .

In the sensitivity analysis of the STICS model, the eFAST method required separate tests of simulations for each input parameter  $Z_i$  of interest, multiplying the total number of simulations (and computing time) by the number of  $Z_i$  parameters studied. The number of simulations for each parameter was specified first, and then the algorithm selected the largest integer of  $\omega_i$  that satisfied  $2M\omega_i + 1 \leq N$ ; and those  $\omega_j$  that satisfied  $\omega_j \geq 2M \max(\omega_j)$ . In this research, the number of simulations specified per parameter was fixed at 2000, and the number of harmonics  $M$  was 4.

## 6.1.6 Model calibration

### Selection of parameters

The estimation of values for the model parameters that reduce the errors between the model outcomes and measured data is critical in model calibration (Flénet et al., 2004). Ideally, a model should be calibrated for as many variables as possible. However, in complex non-linear models like STICS this is unviable in terms of computational time, as it might involve numerical problems, lower the efficiency of the parameter calibration and might overfit the results of the model to the measured data (Wallach et al., 2011). In this research, the parameters to be estimated were selected based on the results from the sensitivity analysis. The criteria for selection consisted of choosing those parameters (i) with a larger influence on the model output variance, (ii) and those that were not able to be estimated either based on field data or from the literature. In this case, the value of parameters was estimated with the method described below, as previously applied in STICS and implemented in the OptimiStics software (Buis et al., 2011).

The model calibration was conducted with the aim of finding the value of the parameters that resulted in the best fit between the measured and the simulated model outcomes. This process was conducted separately using datasets from both *Study 1* and 2. In *Study 1*, the calibration aimed to find the value of the parameters that reduced the error between simulated and measured gravimetric soil water content given by the variable *HR(1)*; and drainage given by the variable *drain*. The targeted value of drainage was zero, as it was assumed that during the *Study 1* no drainage occurred. The optimum values of the parameters determined for the water balance were fixed, and then a second set of input parameters were calibrated for the prediction of the accumulated dry matter in clippings, given by the parameter *rendementsec*.

For *Study 2*, parameters obtained for biomass production in clippings in *Study 1* was used. The data compared was the accumulated water drainage in mm (*draff*) and accumulated leaching in  $\text{g NO}_3^- \text{-N m}^{-2}$  (*Q/es*). The same process as used for *Study 1* was adopted: firstly, the parameters for the water balance were determined and fixed in the plant parameter file. In a second step, the parameters

of the N balance were determined. In the calibration of parameters for *Study 2*, for the best combination of inputs that predicted  $HR(1)$  close to FC were sought. Parameters of turf growth obtained for *Study 1* were considered. In both studies, the calibration process sought values of input parameters that simulated one automatic cut ( $numcoupe=1$ ) before the 1<sup>st</sup> May in each year, and 12 cuts before the end of the simulation. Table 6.6 shows the input variables and observed data used in the parameter calibration phase. The steps followed in the parameter calibration are also described.

**Table 6.6** Steps, parameters and datasets used in the parameter calibration phase

Step	Name step	Parameters optimised	Observed data	Study	Treatment	Year
1	Water balance	$kmax, extin, q0, psisto$	$HR(1), drain^*, numcoupe^*$	1	1,2,3	2014
2	Biomass production in clippings	$vlaimax, udlaimax, psiturg, stlevamf$	$HR(1), rendementsec, numcoupe^*$	1	1,2,3	2014
3	Water balance	$kmax, extin, q0, psisto$	$drat, HR(1)^*, numcoupe^*$	2	4,5	2008
4	Nitrogen leaching	$Norg, profhum, fmin1, hminm$	$drat, Qles, HR(1)^*, numcoupe$	2	4,5	2008

\*Imposed values / not measured in field

The selection of 2014 in *Study 1*, and 2008 in *Study 2* for model calibration was due to those years having more measurements during the irrigation period between May and September. Data from the other years were used for model validation, as shown in Table 6.7.

**Table 6.7** Datasets and years used for model calibration and validation

		Validation	Calibration	Validation
<b>Study 1</b>	Year	2013	2014	2015
	Months	August and September	May to September	May to August
	Treatment 1			
	Treatment 2 Treatment 3			
<b>Study 2</b>	Year	2013	2014	2015
	Months	August and September	May to September	May to August
	Treatment 4 Treatment 5			

### Simplex method for parameter calibration

The Nelder-Mead Simplex algorithm (or *Simplex algorithm*) was used for the calibration (or optimisation) of parameters. This method was implemented within the OptimiStics software. The Simplex algorithm imposes boundaries on the value of the estimated parameters, and then creates a pattern search that compares function values at the three vertices of a triangle, which represent different values of a given parameter. When applied to the estimation of parameters in the STICS model, the worst vertex is the one that creates the largest error between simulated and field observations, and is rejected and replaced by a new vertex in successive steps. The triangle itself has  $N$  dimensions, with the Simplex algorithm finding the minimum of a function with  $N$  variables, which corresponds to the  $N$  input STICS variables that were being optimised. This process generates a sequence of triangles with different shapes, and at each step, the size of the triangle is reduced until its minimum area is found. At each iteration, the new point follows a series of steps for reflecting, expanding or contracting the triangle along the line joining the worse vertex with the centroid of the remaining vertices. If a better point is not found, then the best vertex is retained with the best parameter value, and the other two vertices of the triangle are shrunk towards that value. More information on the process and illustrative examples of the method can be found at Nocedal and Wright (2007).

One of the advantages of using OptimiStics software is that it allows the calibration of multiple input parameters simultaneously, taking into account various measurements over time from different treatments and years. OptimiStics estimates the value of each parameter  $\theta$  following the best combination of parameters to optimise the goodness of fit, using the equation proposed by Wallach et al. (2001):

$$\hat{\theta} = \arg_{\theta} \min \prod_j \left\{ \left( \frac{1}{N_j} \right) \sum_i \left[ \left( \frac{1}{n_{ij}} \right) \sum_k (Y_{ijk} - f_{jk}(X_i; \theta))^2 \right] \right\}^{N_j/2}$$

Where  $\hat{\theta}$  is the estimated parameter,  $Y_{ijk}$  is the measured value for the  $k^{\text{th}}$  time point of the  $j^{\text{th}}$  response variable in the  $i^{\text{th}}$  plot;  $f_{jk}(X_i; \theta)$  is the corresponding model

prediction;  $N_j$  is the number of plots with response  $j$ ; and  $n_{ij}$  is the number of measurements of response  $j$  in plot  $i$ .

For the simplex algorithm in OptimiStics, it was necessary to specify the number of input variables to be optimised and their maximum and minimum uncertainty boundaries; the output variables from simulations to be compared against field measurements; and the observed values of those variables. The algorithm generates random starting points for each input parameter between the specified boundaries. The values of the parameters were then adjusted for each iteration, seeking a combination of parameters that minimised the sum of squared errors between the simulated and measured data.

The iterations finish based on two criteria: either when the number of iterations reaches a maximum predefined number; or when the goodness-of-fit of the model does not improve, and the estimated parameter values become stable. This process is repeated  $n$  times. The number of repetitions is chosen by the user, generating new random starting values of the input parameters. The more starting points used, the less risk of missing the model optimum. However, the main reported limiting factor for the number of repetitions is computing time (Wallach et al., 2011). In this study, the number of repetitions of the method per module was set at 10, the maximum number of iterations per repetition was set at 400, and the maximum number of function evaluations per repetition was set at 1000.

### **6.1.7 Model evaluation**

Performance evaluation of the model was conducted for the calibration and validation datasets of each study. For *Study 1*, the predicted and measured values of soil water content ( $HR(1)$ ) and cumulative dry matter in clippings ( $rendementsec$ ) were compared. Data from 2014 was used for model calibration, and data from 2013 and 2015 then used for model validation. For *Study 2*, model evaluation was conducted for the cumulative water drainage ( $drat$ ) and cumulative leaching ( $Q/es$ ). The dataset used for calibration corresponding to 2008, with data for 2007 and 2009 used for model validation.



The statistical methods used for evaluation of model performance were:

Model efficiency (EF) with an optimal value of 1.0:

$$EF=1-\frac{\sum_{i=1}^n (P_i-O_i)^2}{\sum_{i=1}^n (O_i-\bar{O})^2}$$

Where  $n$  is the number of measurements,  $O_i$  is the measured value,  $\bar{O}$  the mean of the measured values and  $P_i$  the value simulated by the model. Values of model efficiency greater than 0.6 are generally assumed to reflect an efficient model (Jégo et al., 2013).

Mean bias error (MBE) with an optimal value of 0 and its relative value in percentage (MBE %):

$$MBE=\frac{1}{n}\sum_{i=1}^n (O_i-P_i)$$

$$MBE(\%)=\left(\frac{MBE}{\bar{O}}\right)\times 100$$

The MBE (%) indicates the percentage (%) error, but also provides information on the extent to which the model tends to either over- or under-estimate its prediction.

Root mean square error (RMSE) with an optimal value of 0 and its relative value in percentage (RMSE %):

$$RMSE=\sqrt{\frac{1}{n}\sum_{i=1}^n (O_i-P_i)^2}$$

$$RMSE(\%)=\left(\frac{RMSE}{\bar{O}}\right)\times 100$$

Jamieson et al. (1991) considered the accuracy of simulations excellent when  $RMSE(\%)$  values were  $\leq 10\%$ , good when  $10\% < RMSE\% \leq 20\%$ , fair when  $20\% < RMSE\% \leq 30\%$ , and poor when  $RMSE\% > 30\%$ .

## 6.2 RESULTS

### 6.2.1 Sensitivity analysis

The sensitivity analysis was undertaken to study the contribution of the input parameters shown in Table 6.5 to the variance of a number of model outputs. Those output variables were related to the water balance, biomass removal and N leaching; all under non-water limiting and water limiting application conditions. Only the most relevant results from the sensitivity analysis are presented here for clarity. The sensitivity indexes included in this section show only the six input parameters with the greatest contribution to output variability. The results presented are the first order and total sensitivity indexes at Julian day 273, which corresponds to 30<sup>th</sup> September and the end of the simulation period.

#### Sensitivity indexes of the input parameters relating to the water balance

The first sensitivity analysis studied the influence of 11 explanatory variables (Table 6.5) on the water balance. Figure 6.6 shows the sensitivity indexes on cumulative actual evapotranspiration variance for turfgrass simulations under non-water limiting and water limiting irrigation conditions. When the sensitivity analysis was conducted under non-water limiting conditions, the variables including maximum crop coefficient ( $k_{max}$ ), cumulative evaporation at the end of maximum evaporation phase ( $q_0$ ), and extinction coefficient of photosynthetic active radiation ( $extin$ ) showed a strong influence on actual evapotranspiration ( $cet$ ) variance. Those three explanatory variables also had a great influence on the general water balance components such as water drainage ( $drat$ ), soil water content ( $HR(1)$ ), soil evaporation ( $ces$ ) and plant transpiration ( $cep$ ).

The total sensitivity index of  $k_{max}$  on  $cet$  variance did not differ from the first order index under non-water limiting conditions, with  $k_{max}$  associated with 42.8% of the total  $cet$  variance. This suggests that the influence of  $k_{max}$  on  $cet$  variance was largely independent of other input parameters. The first order and total sensitivity indexes for  $q_0$  were 0.13 and 0.36, and for  $extin$  were 0.05 and 0.22, respectively. The greater difference between first order and total indexes for  $q_0$  and  $extin$  shows that the influence of those two parameters on  $cet$  variance

depends to a large extent on the variation of other input parameters. Under water limiting conditions (Figure 6.6b), the *extin* coefficient showed the greatest contribution to *cet* variance, with a first order index of 0.49 and total index of 0.72. This shows that under water limiting conditions, *extin* increases its influence on actual evapotranspiration when compared with non-water limiting conditions, to the detriment of *kmax* and *q0* sensitivity.

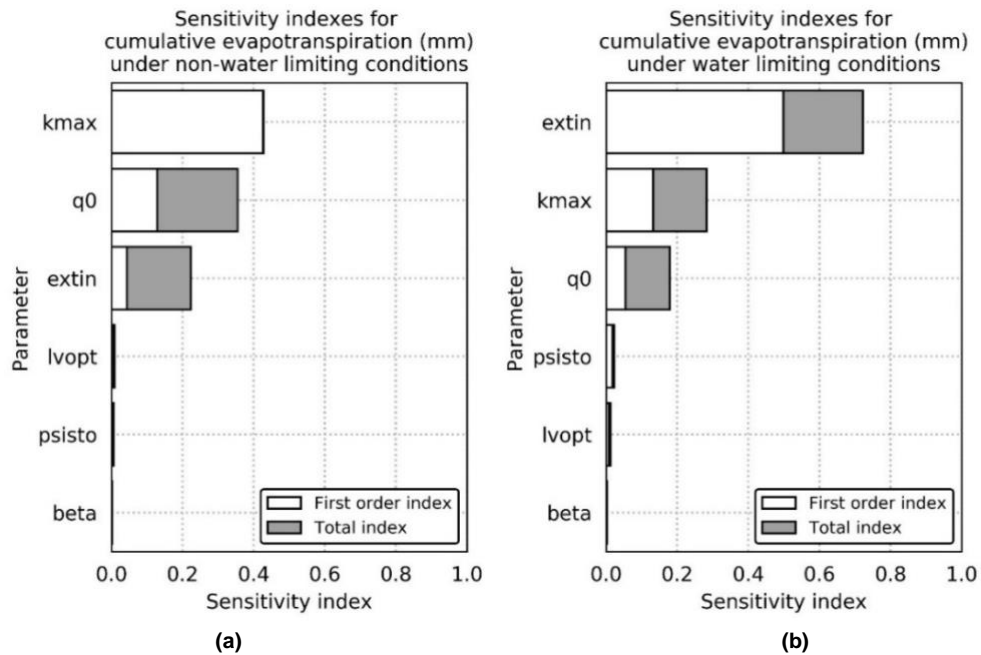


**Figure 6.6** First order and total sensitivity indexes for cumulative evapotranspiration (*cet*) at the end of the simulation period (30<sup>th</sup> Sept), under non-water limiting (a) and water limiting conditions (b) conditions.

The sensitivity indexes reported here correspond to the end of the simulation period (30<sup>th</sup> September). However, these indexes might also vary during the simulation period. The reason for choosing this date was to simplify the outputs from the sensitivity analysis, as the overall research focuses on the outputs at the end of the simulation period, rather than during the season. However, looking at the sensitivity indexes on a particular period might be useful when studying the impact of extreme weather events on model outcomes, or to gain a deeper understanding of model behaviour. For example, Figure 6.7 shows the sensitivity indexes *kmax*, *extin*, and *q0* from Figure 6.6, but on a daily basis from May until the end of September. The sensitivity indexes varied during the season and followed different paths when comparing non-water limiting and water limiting conditions. For instance, the total sensitivity indexes on 1<sup>st</sup> July under non-water

limiting conditions for  $k_{max}$ ,  $extin$  and  $q_0$  were, 0.26, 0.34 and 0.51, respectively; whereas under water limiting conditions the same indexes were: 0.19, 0.78 and 0.23. In contrast, on 30<sup>th</sup> September, the same indexes were 0.43, 0.22, 0.35 for non-water limiting conditions; and 0.31, 0.69, 0.18 for limiting water conditions. This highlights the importance of the timing at which the sensitivity indexes are considered.

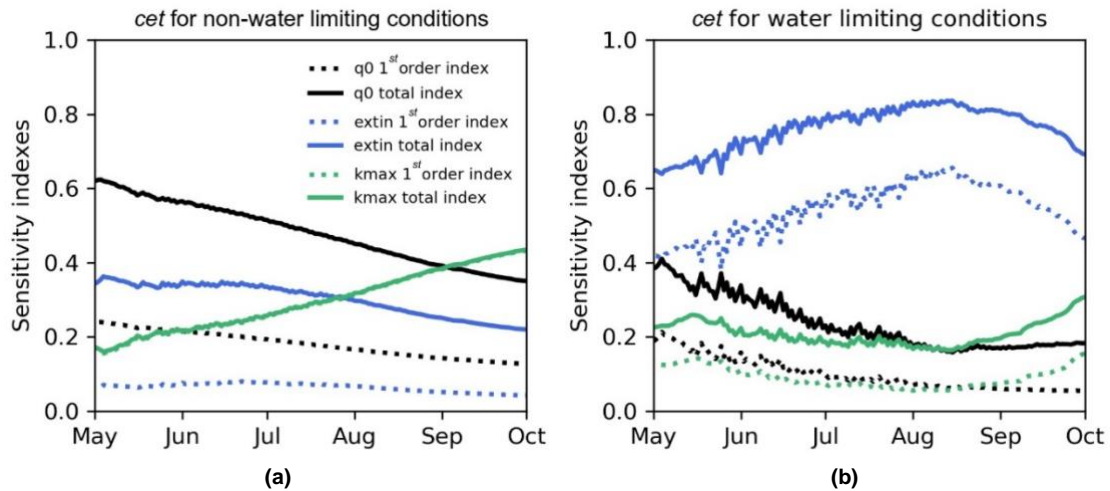


**Figure 6.7** Evolution of the first order and total sensitivity indexes for three input parameters on cumulative evapotranspiration ( $ce_t$ ) over the simulation period for (a) non-water and (b) water limiting conditions

The stomatic water stress index on day  $i$  ( $swfac$ ) was another output of relevance to this research. Its importance relies on that this parameter indicates the water stress of the plant due to lack of water in the soil. As a consequence of the variation in  $swfac$  on a given day  $i$ , the radiation use efficiency and plant transpiration are affected. In this sensitivity analysis are presented the results for the average  $swfac$ , named in STICS as  $swfac1moy$ . Figure 6.8 shows the six input parameters with the greatest contribution to  $swfac1moy$  variance. Under non-water limiting conditions (Figure 6.8a), the absolute value of the potential of stomatal closure ( $psisto$ ) was the input parameter with the highest first order (0.58) and total sensitivity indexes (0.70). After  $psisto$ , the parameters with a high sensitivity indexes on  $swfac1moy$  were ( $extin$ ) (1<sup>st</sup> order: 0.38, total: 0.52) and the optimum root density for water and N uptake ( $lvopt$ ) (1<sup>st</sup> order: 0.11, total: 0.18). In contrast, the input parameters with a greater influence on  $swfac1moy$  when irrigation was limited (Figure 6.8b) were  $k_{max}$  (1<sup>st</sup> order: 0.45, total: 0.65),  $extin$

(1<sup>st</sup> order: 0.17, total: 0.47), and  $q_0$  (1<sup>st</sup> order: 0.10, total: 0.23), being similar to cumulative actual evapotranspiration.

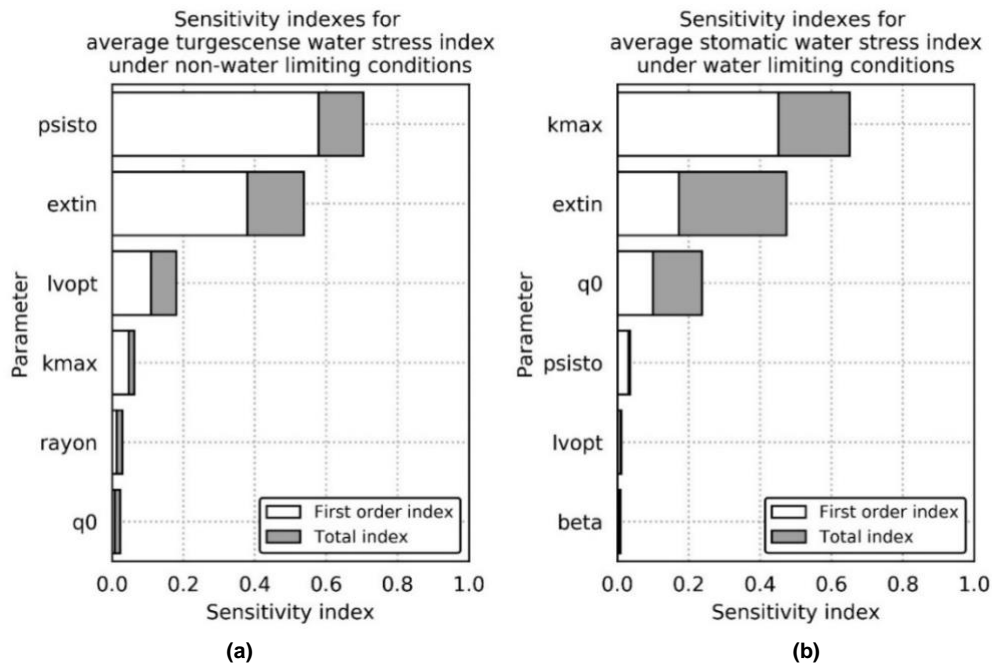


**Figure 6.8** First order and total sensitivity indexes for average stomatic water stress index ( $swfac1moy$ ) at the of the simulation period (30th Sept), under non-limiting (a) and limiting water (b) conditions.

### Sensitivity indexes of input parameters relating to biomass in clippings

The second sensitivity analysis was undertaken to understand the contribution of seven input parameters (Table 6.5) to the variance of a number of outputs relating to dry matter production. Figure 6.9a shows the results of the sensitivity analysis for the accumulated dry biomass removal ( $rendementsec$ ) under non-water limiting conditions. The parameters studied were related with the  $\Delta i_{dev}$  curve, which describes the the LAI growth rate ( $m^2 \text{ plant}^{-1} \text{ degree-day}^{-1}$ ) as a logistic curve. At the end of the simulation period, the parameter *inflexion point of the function  $\Delta i_{dev}$*  ( $vlaimax$ ) showed the greatest contribution to  $rendementsec$  variance, with a first order index of 0.36 and total sensitivity index of 0.57. This parameter indicates the point at which the increment of leaf growth rate is reduced, i.e., the derivative of the  $\Delta i_{dev}$  function reaches its maximum. Further details of the  $\Delta i_{dev}$  function are given in Brison et al. (2008). The parameter  $vlaimax$  also influences the growth rate when the end of the juvenile phase is reached ( $amf$ ), and hence an automatic cut event occurs.

The second parameter with a large contribution to clipping weight was the point of the  $\text{delta}_{dev}$  curve at which the daily leaf decreases, given by the variable  $\text{udlaimax}$ . For non-water limiting conditions, the first order and total sensitivity indexes of  $\text{udlaimax}$  were 0.14 and 0.33, respectively. The maximum rate of  $\text{delta}_{dev}$  ( $\text{dlaimax}$ ) and the minimum temperature for leaf expansion ( $\text{tcm}$ ) had a similar influence on  $\text{rendementsec}$  variance, being their first order sensitivity index close to 0.08 and their total index approximately 0.14. Figure 6.9b shows the results of the sensitivity analysis under limited water conditions. It can be observed that for the parameters studied there were little differences in their contribution to output variability when compared with the sensitivity indexes obtained under well-watered conditions (Figure 6.9a).

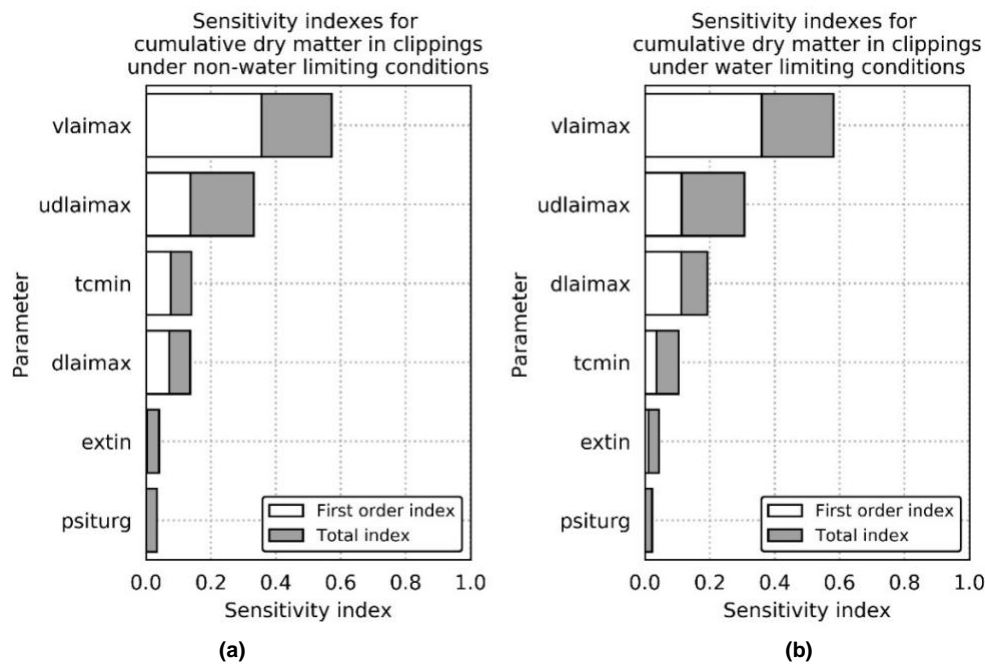


**Figure 6.9** First order and total sensitivity indexes for the cumulative dry matter in clippings ( $\text{rendementsec}$ ) at the end of the simulation period (30th Sept), under (a) non-water limiting and (b) water limiting conditions.

#### Sensitivity indexes of input parameters in relation to nitrogen balance

Figure 6.10 shows the sensitivity analysis on the outputs of cumulative nitrate leaching ( $Q_{les}$ ) and average N nutrition index ( $\text{inn1moy}$ ) at the end of the simulation period. Here only the results of the sensitivity analysis for non-water limiting conditions are shown little differences were found in the sensitivity indexes of for the irrigation regimes. A reason for that was that rainfall was the main responsible for N leaching, and not the irrigation applied in each irrigation

treatment. Thus, whether for non-limiting water or limiting water irrigation treatments, the impact of the different parameters on  $Q_{les}$  and  $inn1moy$  was similar as the main driver of leaching was rainfall and not the irrigation level.

Among the 13 variables studied in the sensitivity analysis of cumulative leaching, two parameters showed the highest contribution to leaching variance. The parameter with the greater contribution to leaching variability was the thickness of the active layer for mineralisation  $profhum$ , with a 1<sup>st</sup> order sensitivity index of 0.44 and total index of 0.59. The second parameter was the soil organic N content  $Norg$ , with a 1<sup>st</sup> order sensitivity index of 0.38 and total index of 0.53. Both parameters are related to the amount of N mineralised in the soil, which is available to be mobilised up to the plant and lost through leaching. Regarding the average N nutrition index, which is an indication of N stress in the plant,  $profhum$  was also found to be the parameter with the highest sensitivity. The 1<sup>st</sup> order sensitivity index of  $profhum$  was 0.62, and total sensitivity index was 0.73. The contribution of  $profhum$  to plant N stress and leaching demonstrates the importance of the mineralisation process in the model simulations, i.e., mineral N availability.

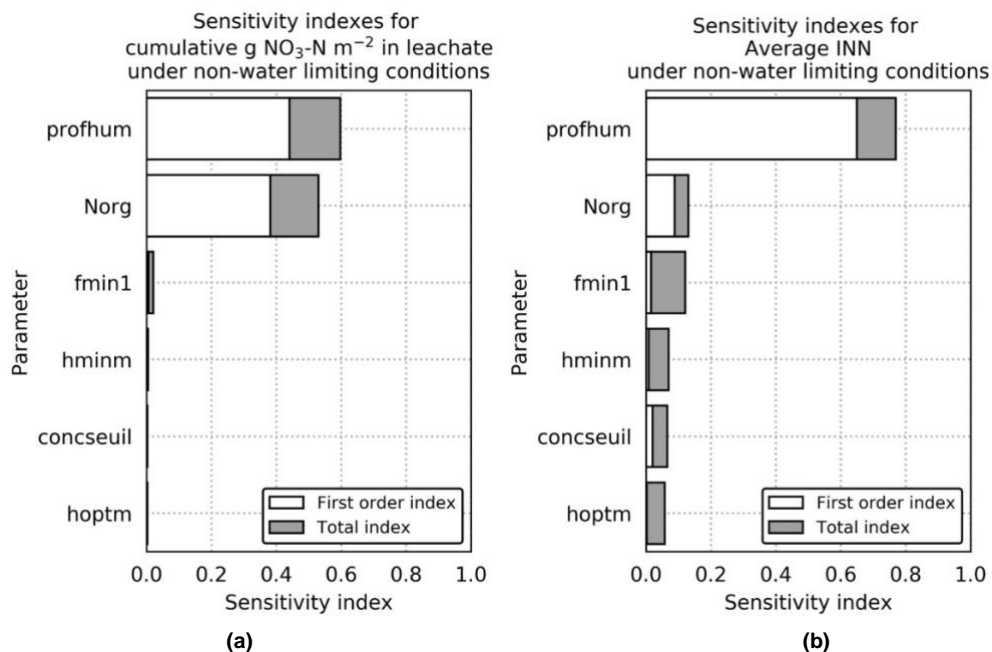


**Figure 6.10** First order and total sensitivity indexes for the cumulative NO<sub>3</sub><sup>-</sup>N in leaching ( $Q_{les}$ ) (a); and average nitrogen nutrition index ( $inn1moy$ ) (b) at the end of the simulation period (30th Sept), under non-water limiting conditions.

## 6.2.2 Model calibration

The model calibration was carried out for the measured data from *Study 1* and *Study 2* and parameters with higher sensitivity in the model outcome, described in Table 6.6. Despite the high sensitivity of the input parameter *dlaimax* on the output *rendementsec* variability, it was opted to set the value of *dlaimax* to  $3.5 \times 10^{-4} \text{ m}^{-2} \text{ leaf plant}^{-1} \text{ degree day}^{-1}$ . This decision was taken to avoid the high multicollinearity observed with the parameters *udlaimax*, *vlaimax* when simulating biomass production, which would have compromised the process of model calibration. At the end of the calibration step, the parameters determined for dry matter production for *Study 1*, leaching for *Study 2*, and water balance for both datasets were pulled together in a STICS plant file. For the dataset from *Study 1*, the first step of the model calibration aimed to find the values of the parameters *kmax*, *q0*, *extin* and *psisto* with the lowest error in the prediction of the soil moisture (*HR(1)*) as measured in field in 2014. The second step of the model calibration aimed to find the values of *udlaimax*, *vlaimax*, *psiturg* and *stlevamf* with the lowest error in the prediction of dry matter in clippings (*rendementsec*) as measured in 2014. For the dataset from *Study 2*, same values of *udlaimax*, *vlaimax*, *psiturg* and *stlevamf* than in *Study 1* were used. The first step in the model calibration aimed to estimate the optimum values of *kmax*, *q0*, *extin*, *psisto* for the prediction of the accumulated drainage during the season (*drat*) and the water content after each irrigation event (*HR(1)*), assuming that irrigation events always led to FC. The second step of the calibration for the dataset from *Study 2* aimed to estimate the values of the input parameters *Norg*, *profhum*, *fmin1* and *hminm* that predicted with the lowest error the accumulated leaching (*Qles*).

### Study 1

The results of the model calibration are presented in Table 6.8. The calibration of the water balance module showed high variability in the parameters for each repetition of the parameter calibration, as indicated by the high standard deviation for each parameter. The optimum value for *extin* was 0.19, which differed considerably from the mean optimised value 0.84, corresponding to the maximum boundary established before starting the calibration module. The *kmax* and *q0*



parameters showed less relative difference with respect to the mean value of the optimised parameter. The optimum *kmax* value was 1.30 with a mean of 1.53, and the *q0* was set at 6.8 with a mean of 9.6. The optimum *psisto* value was found to be 14, with a mean 11.2 and standard deviation of 6.7. This high variability might be explained by the high collinearity between *psisto* and *extin* parameters in the optimum solution, with a Pearson's correlation  $r=0.63$ .

**Table 6.8** Results from the parameter calibration for the water balance and biomass production modules in *Study 1*

Module	Water balance module				Biomass production in clippings module			
Parameter	<i>extin</i>	<i>kmax</i>	<i>q0</i>	<i>psisto</i>	<i>vlaimax</i>	<i>udlaimax</i>	<i>psiturg</i>	<i>stlevamf</i>
Optimum value	0.19	1.30	6.8	14.0	2.0	2.39	8.8	229.1
mean	0.84	1.53	9.6	11.2	2.14	2.47	7.8	223.65
std	0.31	0.34	6.9	6.7	0.34	0.35	4.7	53.8
Inf	0.1	1	1	1	2	1	1	100
Sup	1	2	50	25	3	3	15	300

The second step in the calibration process considered the parameters *vlaimax*, *udlaimax*, *psiturg*, and *stlevamf* for the prediction of the accumulated dry matter production in clippings given by the output variable *rendementsec*. Before launching the calibration of these parameters, values of *extin*, *kmax*, *q0* and *psisto* obtained in the previous step were set in the parameters file. The optimum values of *vlaimax*, *udlaimax* and *psiturg* given by the *Simplex* algorithm were 2.0, 2.39 and 8.8, respectively, while their means were 2.14, 2.47 and 7.8. The value of the optimum parameter *stlevamf* was 229.1.

### Study 2

Table 6.9 shows the results of the parameter calibration for the dataset of *Study 2* for the water balance and N balance modules.

**Table 6.9** Results from the parameter calibration for the water balance and leaching modules for *Study 2*

Module	Water balance module				N leaching module			
Parameter	<i>extin</i>	<i>kmax</i>	<i>q0</i>	<i>psisto</i>	<i>Norg</i>	<i>fmin1</i>	<i>profhum</i>	<i>hminm</i>
Optimum value	0.10	1.1	5.5	8.8	0.05	0.0015	7.5	0.84
mean	0.82	1.1	9.9	3.5	0.084	0.00045	7.9	0.64
st. deviation	0.37	0	2.4	5.8	0.079	0.00030	6.98	0.27
Inf	0.1	1	1	1	0.05	0	0	0.1
Sup	1	2	50	25	0.2	1	20	1

With reference to the water balance calibration module for *Study 2*, the optimum value of *kmax* found by the simplex algorithm after ten repetitions was 1.1, close to the minimum value of the boundaries imposed on *kmax*. The optimum value of *q0* was 5.5, with a mean of all estimated parameters of 9.9; the optimum value of *psisto* was 8.8, with an average 3.5 when the best parameter values from all repetitions were considered. The optimum value of *extin* was 0.1 which differed considerably when compared with the mean of 0.82. During the iterations of the simplex algorithm, the estimated values presented high variation. An explanation for that high variability might be its strong correlation to other parameters (-0.89 with *psisto*, 0.56 with *q0*, and -0.58 with *kmax*). This increased the variance in the optimum values of *q0* and *psisto* because their estimation also depended on the value of the *extin* coefficient, which might be an indicator of multicollinearity. To avoid this, a possible solution could be to set the extinction coefficient to have more independence in the estimation of the other parameters.

The values of the parameters involved in the N balance (Table 6.9) were *Norg*=0.05, *profhum*=7.5, *hminm*=0.84, and *fmin1*=0.0015. The thickness of the active layer for mineralisation *profhum* showed similar optimum and mean values during parameter calibration. The other parameters showed significant variation in their optimum values. This fact might be explained because of the complexity of the calculations involved in the equations related to the N balance in the STICS model, offering multiple combinations of values of parameters that lead to similar predictions of NO<sub>3</sub><sup>-</sup>-N leaching. Coinciding with the sensitivity analysis results, the parameters *profhum* and *Norg* resulted in the highest influence on leaching, with a strong, negative correlation coefficient in their optimum values (-0.70). This suggests that the deeper the *profhum*, the *Norg* value needs to be lower to compensate for the increase in leaching produced by higher *profhum*.

### **6.2.3 Model evaluation**

The STICS model was calibrated and validated for the water balance and dry matter production in clippings for red fescue, and the water balance and leaching in velvet bentgrass. In the model evaluation step, the calibration parameters were pooled in the same file. Thus, there were used values of the water balance from

*Study 1* and 2; the dry matter production parameters from *Study 1*, and nitrogen leaching parameters from *Study 2*. Simulations were then run for each year, fertilisation rate and soil characteristics for each study. In both cases, simulations assumed a mowing height of 5 mm to replicate the typical conditions on a golf green. The results from each simulation were evaluated against field observations from each study and treatment. Overall, the model predicted the soil water content, actual evapotranspiration, and accumulated biomass in clippings *Study 1* and water drainage measured in *Study 2* with an acceptable degree of error. Model simulation of leaching in *Study 2* showed an acceptable error in the calibration step, while higher errors were obtained during the validation stage.

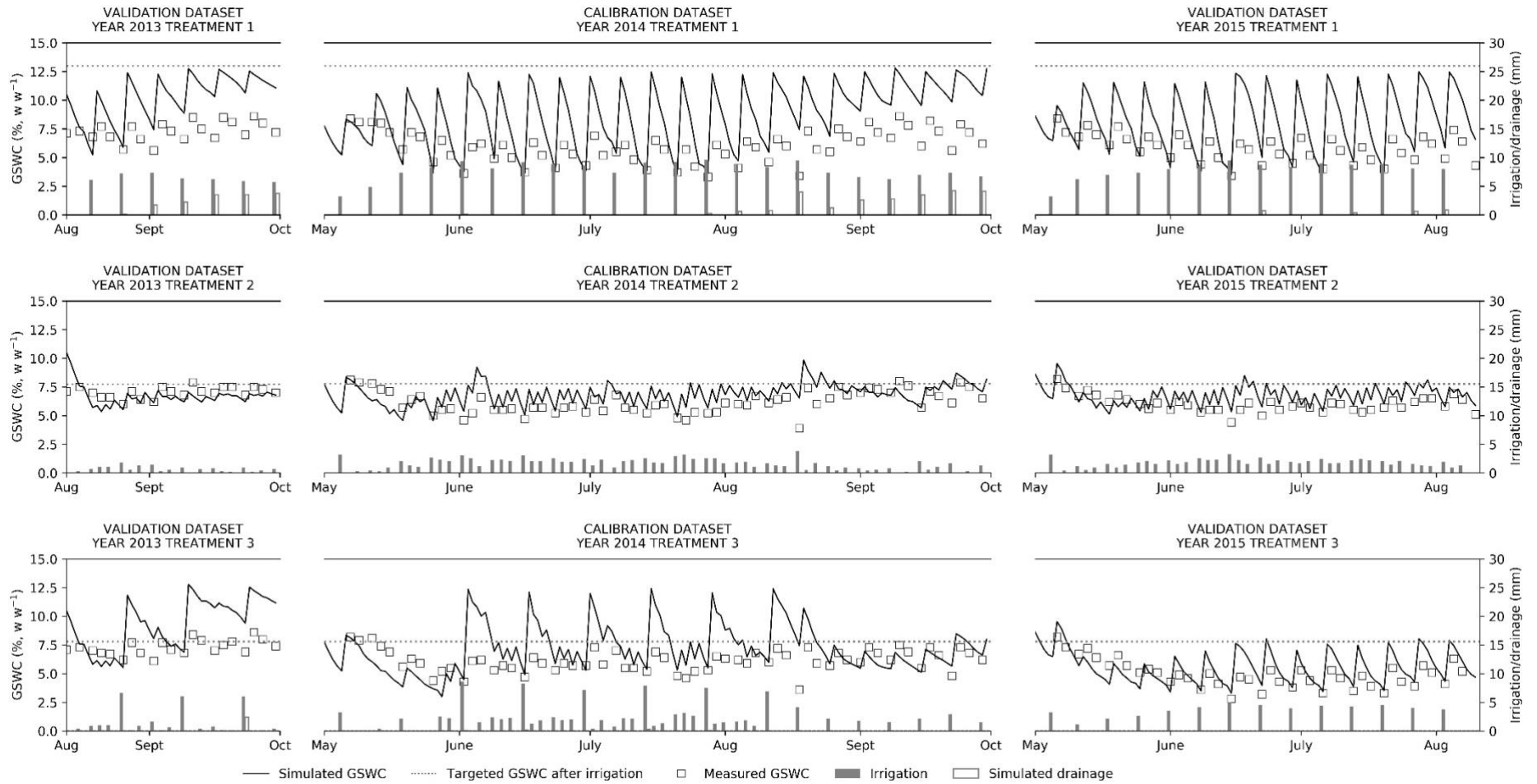
#### *Study 1. Water balance*

Table 6.10 summarises the model performance statistics of the prediction of the gravimetric soil water content (GSWC) for *treatments 1, 2* and 3 in the calibration and validation dataset. For the calibration dataset, the MBE of the gravimetric soil water content (GSWC) tended to be slightly positive, with relative MBE ranging between 2.37 and 7.33%, which confirms a slight under-estimation of the turfgrass evapotranspiration between irrigation intervals. Regarding the validation dataset, *treatment 2* (deficit irrigation three times per week) showed the best model performance, with excellent relative RMSE (8.88%) and a very low MBE. For *treatments 1* and 3, the simulated GSWC tended to be over-estimated (relative MBE 4.34 and 10.34%), with model performance considered good in *treatment 1* (RMSE 13.41%) and fair in *treatment 3* (23.1%). In any case, the relative RMSE was not above 30% for any dataset, values above which the model simulation is considered poor (Jamieson et al., 1991).

**Table 6.10** Number of measurements (n), mean bias error (MBE) and root mean square error (RMSE) for prediction of gravimetric soil water content (GSWC, % w w<sup>-1</sup>) for the calibration and validation datasets in *Study 1*.

<b>Calibration dataset (2014)</b>					
<b>Treatment</b>	<b>n</b>	<b>MBE (% w w<sup>-1</sup>)</b>	<b>MBE (%)</b>	<b>RMSE (% w w<sup>-1</sup>)</b>	<b>RMSE (%)</b>
1	21	0.95	7.33	2	15.42
2	41	0.39	4.99	0.71	9.14
3	21	0.22	2.37	1.18	13.01
<b>Validation dataset (2013 and 2015)</b>					
<b>Treatment</b>	<b>n</b>	<b>MBE (% w w<sup>-1</sup>)</b>	<b>MBE (%)</b>	<b>RMSE (% w w<sup>-1</sup>)</b>	<b>RMSE (%)</b>
1	20	0.56	4.34	1.73	13.41
2	60	-0.07	-0.94	0.69	8.88
3	31	0.86	10.34	1.92	23.1

Figure 6.11 shows the trend in simulated versus measured GSWC in *Study 1* between 2013 and 2015. When irrigation was applied back to field capacity in *treatment 1*, the model tended to predict the GSWC accurately in June, July and August. However, it can be seen that STICS slightly underestimated the GSWC in May and showed a poor prediction of GSWC during September. A similar trend followed in the deficit irrigation treatments, but the differences during May and September were less significant.



**Figure 6.11** STICS simulated and measured gravimetric soil water content (GSWC, % w w<sup>-1</sup>), irrigation applied and simulated drainage for 2013 (validation), 2014 (calibration) and 2015 (validation) for Treatments 1 to 3.

### Study 1. Dry matter production in clippings

The model evaluation for DMP in clippings was carried out by comparing the STICS model simulations with field measurements of clippings, calculated by aggregating the daily plant development ( $\text{g m}^{-2} \text{ day}^{-1}$ ) (*rendementsec*) at the end of each month. Measurements and results from simulations were compared in two ways, (i) the results from individual months were compared, and (ii) the values of the aggregated DMP across the season were compared. Those two comparisons aimed to evaluate the capability of STICS to predict monthly growth and cumulative growth at the end of the season. This analysis was repeated for drainage and leaching.

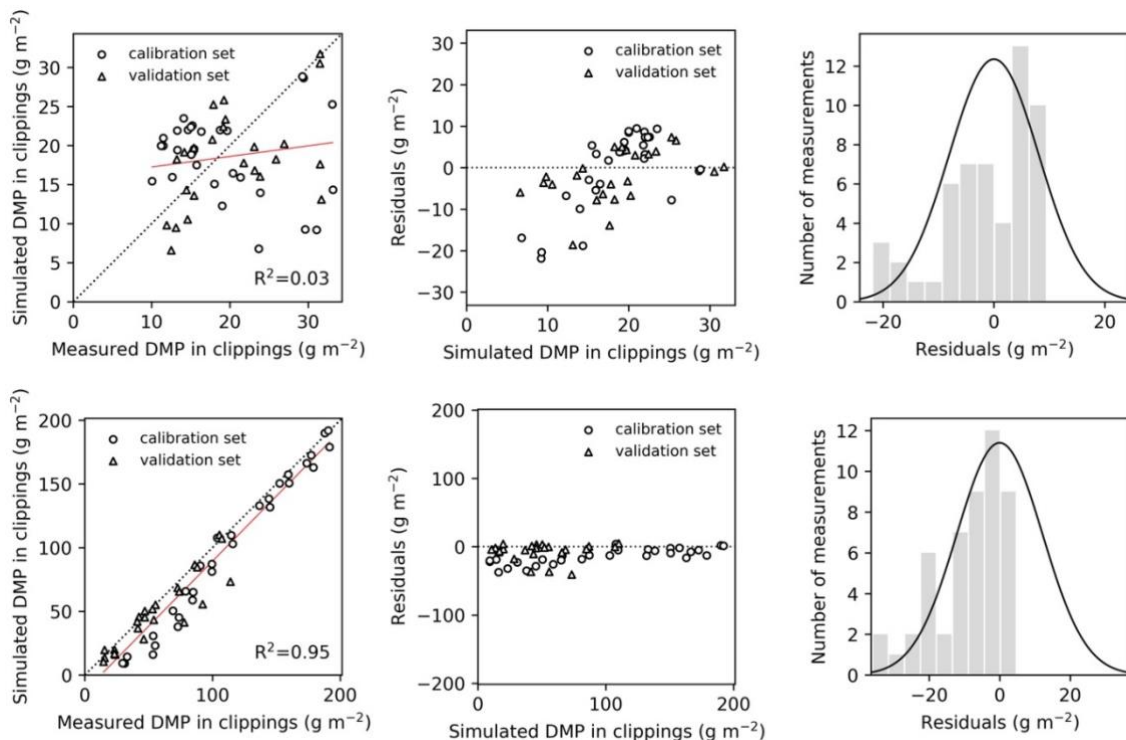
Table 6.11 summarises the model evaluation statistics for DMP in clippings. Overall, the model predicted the cumulated clippings reasonably well, with RMSE ranging between 10.5 and 18.5% for the calibration dataset, and 6.8 to 38.5% for the validation dataset. When monthly clippings were compared, the high RMSE obtained indicates a poor model prediction of clippings on shorter intervals.

**Table 6.11** Number of measurements (n), mean bias error (MBE) and root mean square error (RMSE) in the prediction of the dry matter production in clippings ( $\text{g m}^{-2}$ ) for the calibration (2014) and validation (2013, 2015) datasets in *Study 1*.

Calibration dataset (2014)						
Treatment	n	ME (%)	MBE ( $\text{g m}^{-2}$ )	MBE (%)	RMSE ( $\text{g m}^{-2}$ )	RMSE (%)
1 (monthly)	5	-70.2	0.73	1.93	13.7	35.95
2 (monthly)	5	-225.34	0.33	0.85	16.76	43.46
3 (monthly)	5	-343.75	-2.51	-6.47	18.4	47.45
1 (accumulated)	11	94.97	-6.8	-5.94	11.96	10.45
2 (accumulated)	11	90.53	-13.04	-10.94	16.62	13.94
3 (accumulated)	11	83.88	-20.24	-16.96	22.08	18.5
Validation dataset (2013 and 2015)						
Treatment	n	ME (%)	MBE ( $\text{g m}^{-2}$ )	MBE (%)	RMSE ( $\text{g m}^{-2}$ )	RMSE (%)
1 (monthly)	6	90.07	2.56	11.52	4.71	21.21
2 (monthly)	6	92.79	0.41	1.84	4.09	18.4
3 (monthly)	6	64.52	-4.1	-17.6	9.8	42.12
1 (accumulated)	9	98.14	0.54	0.98	3.73	6.78
2 (accumulated)	9	92.14	-6.51	-11.78	7.85	14.21
3 (accumulated)	9	49.64	-14.89	-26.44	21.66	38.47

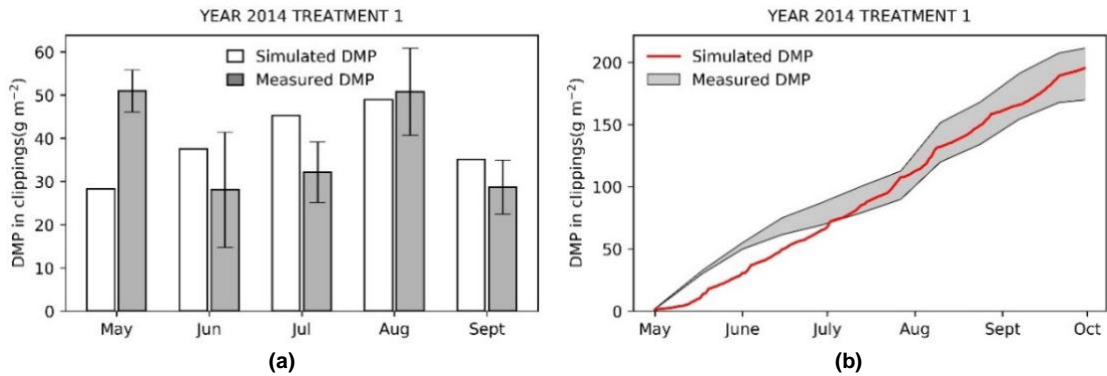
A comparison between the simulated and measured data for individual clipping events and accumulated in each simulated year is shown in Figure 6.12. For individual events (top panel Figure 6.12), a poor correlation between simulated and measured clipping weight is evident, with a coefficient of determination  $R^2=0.03$ . Analysis of the residuals shows a normal distribution of the errors, indicating compensation between months where clippings were over-estimated and months where they were under-estimated. This error compensation also explains the overall very good prediction of the cumulated DMP in each simulation year, with an  $R^2=0.95$  (lower panel Figure 6.12).

The analysis of residuals against simulated dry matter in clippings shows how the most extreme residuals were obtained for the lowest values of simulated clipping weight (corresponding to May 2014). In this case, the distribution of the residuals tended to be negative, indicating an overall under-estimation of accumulated clippings, which matches with the negative relative MBE (-5.94 to -16.96% for calibration, and 0.98 to -26.44% for validation).



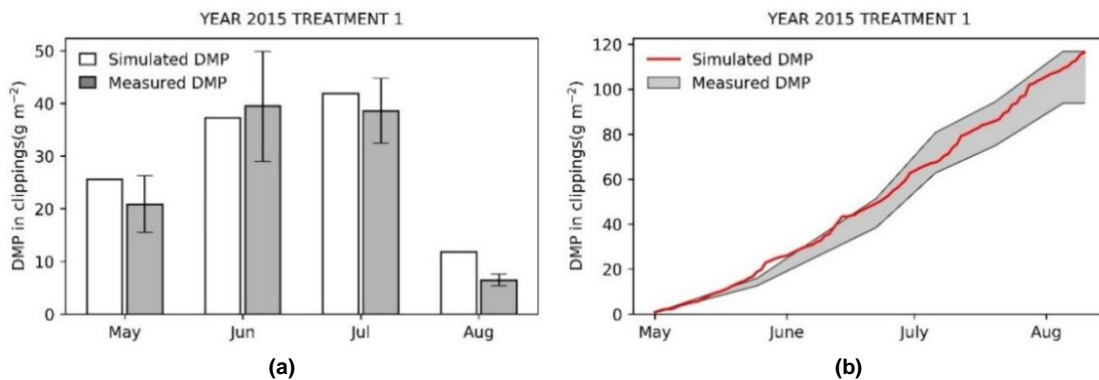
**Figure 6.12** Comparison of simulated versus measured dry matter production (DMP) in clippings (left panel), analysis of the residuals against DMP simulation (centre panel), and distribution of the residuals (right panel). The upper panel corresponds to individual observation events ( $n=54$ ), and lower panel represents the accumulated DMP in each simulated year ( $n=54$ ).

Figure 6.13 shows the prediction of monthly and accumulated dry matter in clippings for *treatment 1* in 2014 (calibration). An under-estimation in dry matter production in May is evident, while in the two following months, the simulation of the weight of the clippings was over-estimated. However, the total accumulated biomass of clippings showed a similar trend between the simulation and measurement (Figure 6.13 right panel).



**Figure 6.13** Comparison between simulated and measured monthly accumulated dry matter production (DMP) in clippings (a) and accumulated DMP (b) for 2014 (calibration) and *treatment 1*.

In contrast to Figure 6.13, the left panel in Figure 6.14 shows a good prediction of monthly accumulated DMP in *treatment 1* for 2015. This resulted in a more accurate prediction of the cumulative clipping weight (right panel).



**Figure 6.14** Comparison between simulated and measured monthly accumulated dry matter production (DMP) in clippings (a) and accumulated DMP in the simulated period (b), for 2015 (validation) and *treatment 1*.

Figure 6.15 shows the simulation of clipping weight (*treatment 3* in 2015), when irrigation was applied at 60% of field capacity once per week. Monthly growth was under-estimated between May and July, resulting in an overall poor prediction of cumulative clippings weight. This is reflected in the low ME (49%) for the



validation dataset from *treatment 3*, the negative relative MBE, -26.4%, and a high relative RMSE, 38.5%.

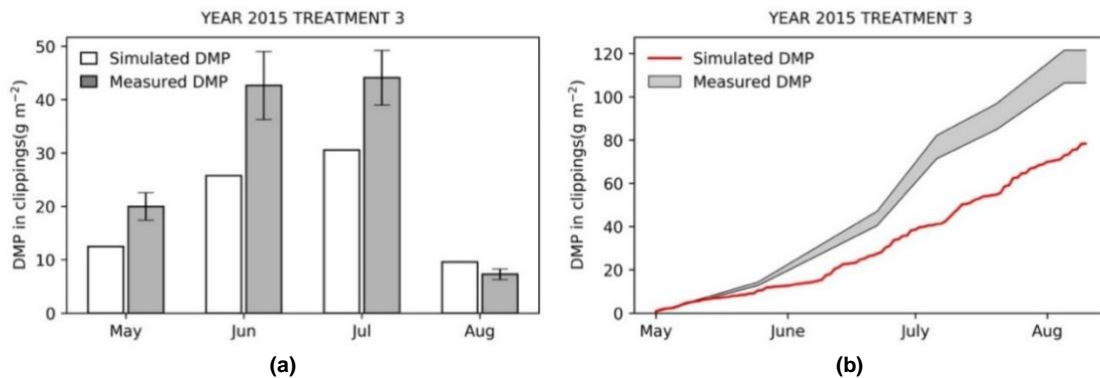


**Figure 6.15** Comparison between simulated and measured monthly accumulated dry matter production (DMP) in clippings (a) and accumulated DMP in the simulated period (b), for 2015 and *treatment 3*.

Figure 6.16 compares the simulated and measured cumulative dry matter production in clippings at the end of each treatment. In general, the prediction is excellent, confirming that the STICS model is suitable for simulating cumulative clippings at the end of the year. The outlier in Figure 6.16 corresponds to the example shown in Figure 6.15.

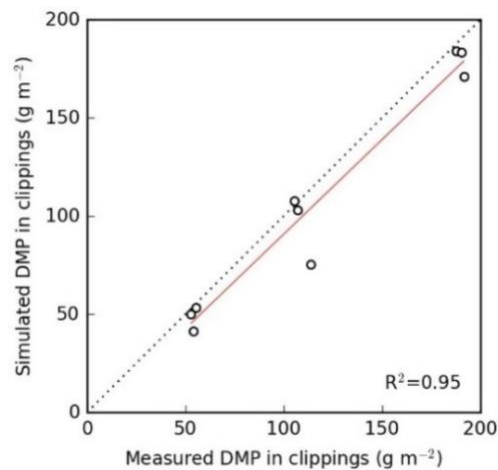


**Figure 6.16** Comparison between simulated and measured cumulative dry matter production (DMP) in clippings at the end of each treatment in 2013, 2014 and 2015.

### Study 2. Water balance

Since the estimation of irrigation in *Study 2* was based on water evaporated from a pan and not from soil water content measurements, model evaluation for the water balance was based on drainage. In simulations, drainage was considered as the water exceeding field capacity content in the soil, and therefore over-

irrigation or heavy rain events led to water losses through drainage. Imprecisions in the estimation of the plant actual evapotranspiration will then lead to inaccurate estimation of soil water content and simulated drainage. To gain a better understanding of the modelled results for drainage, the trend in simulated soil water content for *Study 2* are shown in Figure 6.17. Overall, the STICS model tended to predict higher water consumption for light-frequent irrigation (*treatment 4*) than for deep-infrequent irrigation (*treatment 5*), resulting on a lower average soil water content and water drained in more frequent irrigations.

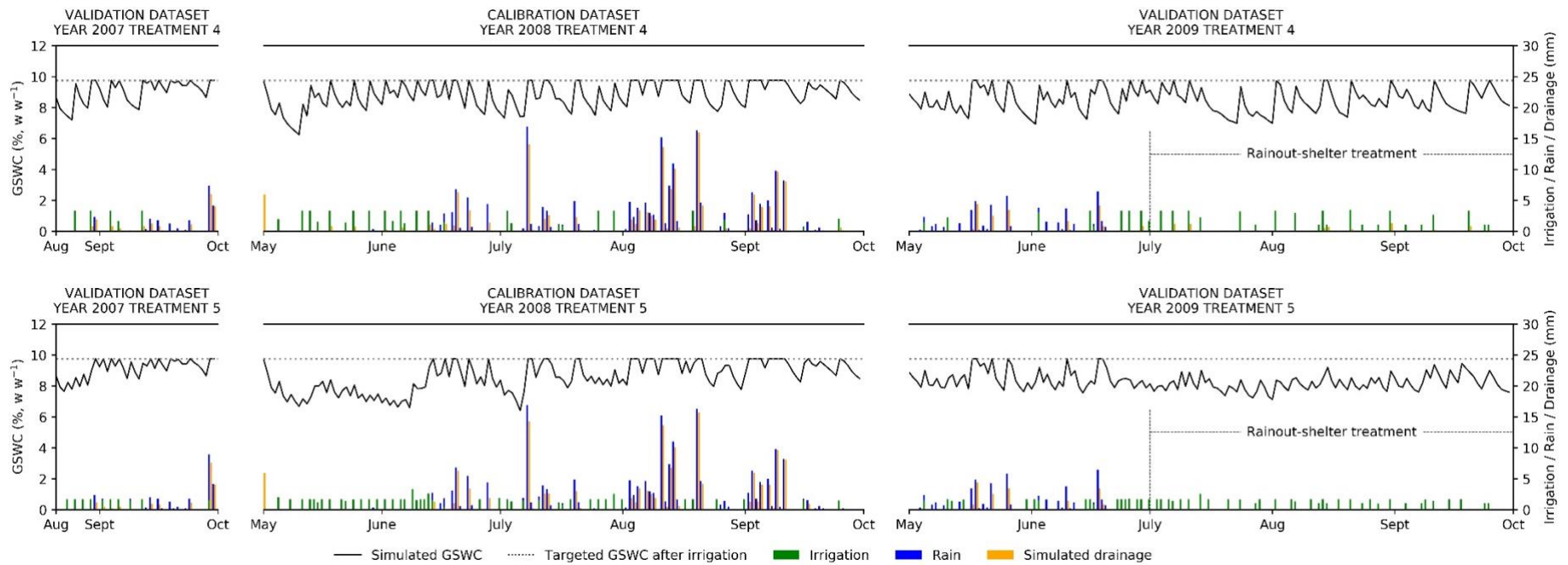


**Figure 6.17** Simulated gravimetric (GSWC, % w w<sup>-1</sup>) soil water content, irrigation applied, rainfall and drainage from 2007 to 2009 for treatments 4 and 5.

The results from the model evaluation for the prediction of monthly and accumulated drainage are shown in Table 6.12. The ME for the prediction of drainage was above 60% in all cases, showing an acceptable efficiency of the model. There were observed differences between *treatment 4* (light and frequent irrigation) and *treatment 5* (deep and infrequent irrigation). For *treatment 4*, the model tended to under-estimate drainage, as shown by the negative values of MBE. In contrast, in *treatment 5* drainage was over-estimated, resulting in a positive MBE. This trend was followed by both calibration and validation datasets. These results match with those shown in Figure 6.17, where water consumption tended to be higher in *treatment 4* than in *treatment 5*, which led to a quicker fill of the maximum soil water content, and hence more simulated drainage in deep-infrequent irrigation events.

The relative RMSE for the accumulated drainage during the simulation period also showed differences between treatments. Whilst for the calibration dataset the *treatment 4* showed good model performance with relative RMSE of 10.2%, in *treatment 5* this value was 34.2%. Conversely, in years 2007 and 2009, the relative RMSE of the cumulative drainage was higher for *treatment 4* (36.2%) than in *treatment 5* (12.3%).

**Table 6.12** Number of measurements (n), mean bias error (MBE) and root mean square error (RMSE) in the prediction of the monthly and annual drainage for the calibration (2008) and validation (2007, 2009) datasets in *Study 1*.

		<b>Calibration dataset (2008)</b>				
<b>Treatment</b>	<b>n</b>	<b>ME (%)</b>	<b>MBE (mm)</b>	<b>MBE (%)</b>	<b>RMSE (mm)</b>	<b>RMSE (%)</b>
4 (monthly)	5	85.9	-8.4	-8.7	25.2	26.1
5 (monthly)	5	88.1	12.6	16.5	21.1	27.6
4 (accumulated)	5	98.7	-4.9	-2.5	20.5	10.2
5 (accumulated)	5	86.7	48.1	31.2	52.7	34.2
		<b>Validation dataset (2007 and 2009)</b>				
<b>Treatment</b>	<b>n</b>	<b>ME (%)</b>	<b>MBE (mm)</b>	<b>MBE (%)</b>	<b>RMSE (mm)</b>	<b>RMSE (%)</b>
4 (monthly)	4	68.98	-10.6	-29.48	15.5	43.15
5 (monthly)	4	86.11	2.97	12.25	7.54	31.05
4 (accumulated)	4	68.77	-25.2	-29.64	30.8	36.24
5 (accumulated)	4	96.35	5.57	9.46	7.21	12.25

When the results from all datasets are combined and compared against measurements (Figure 6.18), good correlation for both the monthly ( $R^2=0.91$ ) and accumulated ( $R^2=0.96$ ) periods are obtained. The residuals showed a normal distribution.

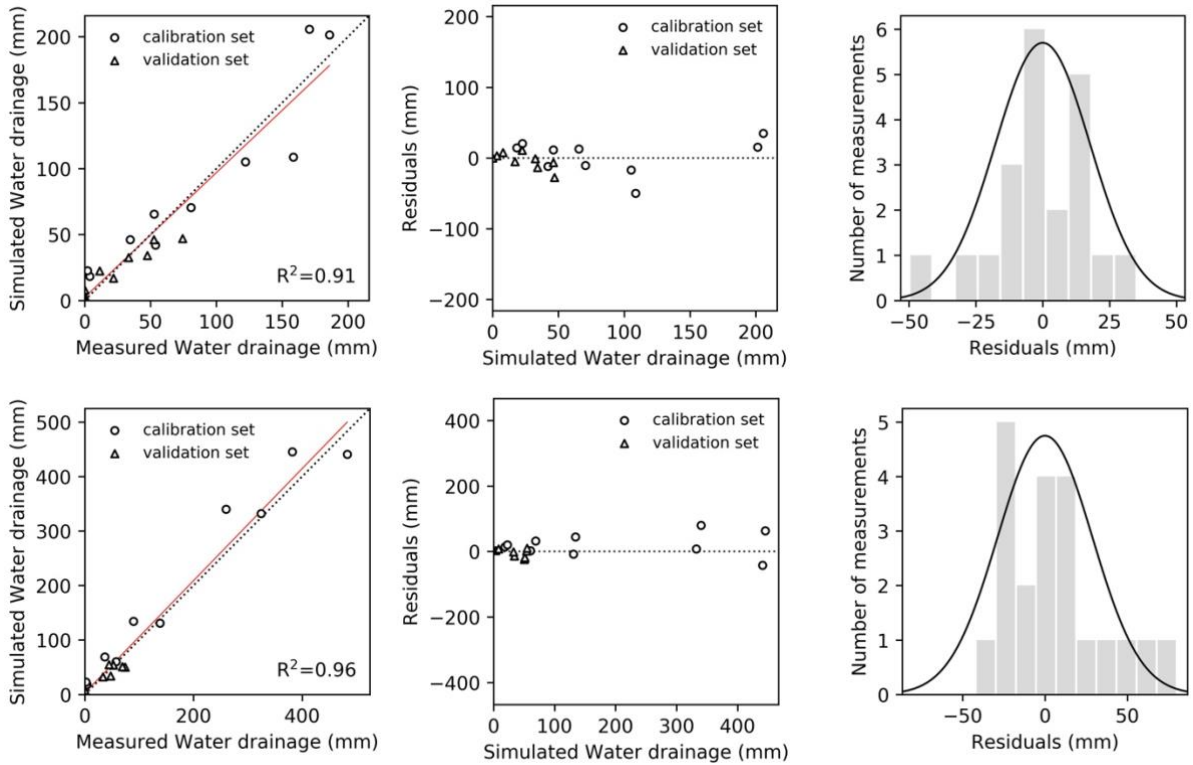


**Figure 6.18** Comparison of measured against simulated water drainage (left panel), analysis of the residuals against drainage simulation (centre panel) and distribution of the residuals (right panel). The upper graphs correspond to monthly measurement events ( $n=21$ ), and lower graphs represent the accumulated drainage in each simulated year ( $n=21$ ).

### Study 2. Nitrogen leaching

The model evaluation of STICS for leaching prediction is shown in Table 6.13. The model efficiency and relative RMSE showed strong differences between the calibration and validation datasets. For calibration, an acceptable ME was observed, but the relative RMSE was greater than 30%. When the amount of leaching was accounted as cumulative leaching during the simulation period, the model evaluation showed a very good model efficiency for both *treatment 4* and *5* (96.2 and 96.7%, respectively), and low relative RMSE (15.61 and 13.77%, respectively). When the validation dataset was tested, the values obtained differed between treatments noticeably. For individual monthly measurements, the results of the model evaluation were unacceptable. However, when the model

evaluation was carried out for the cumulative leaching during the simulated season, the *treatment 5* presented an acceptable model efficiency (77.9%) and fair quality in simulations based on the relative RMSE (27.64%). The errors observed in the validation step of *treatment 4* describe a poor prediction of the leaching. These differences might be explained because of the differences in the magnitude of the values between the amount of nitrogen leached in the calibration and validation dataset (Figure 6.20). Thus, one might also assume that the prediction of leaching is more accurate when larger quantities of leachate were measured. Further data is required for testing the model in different years.

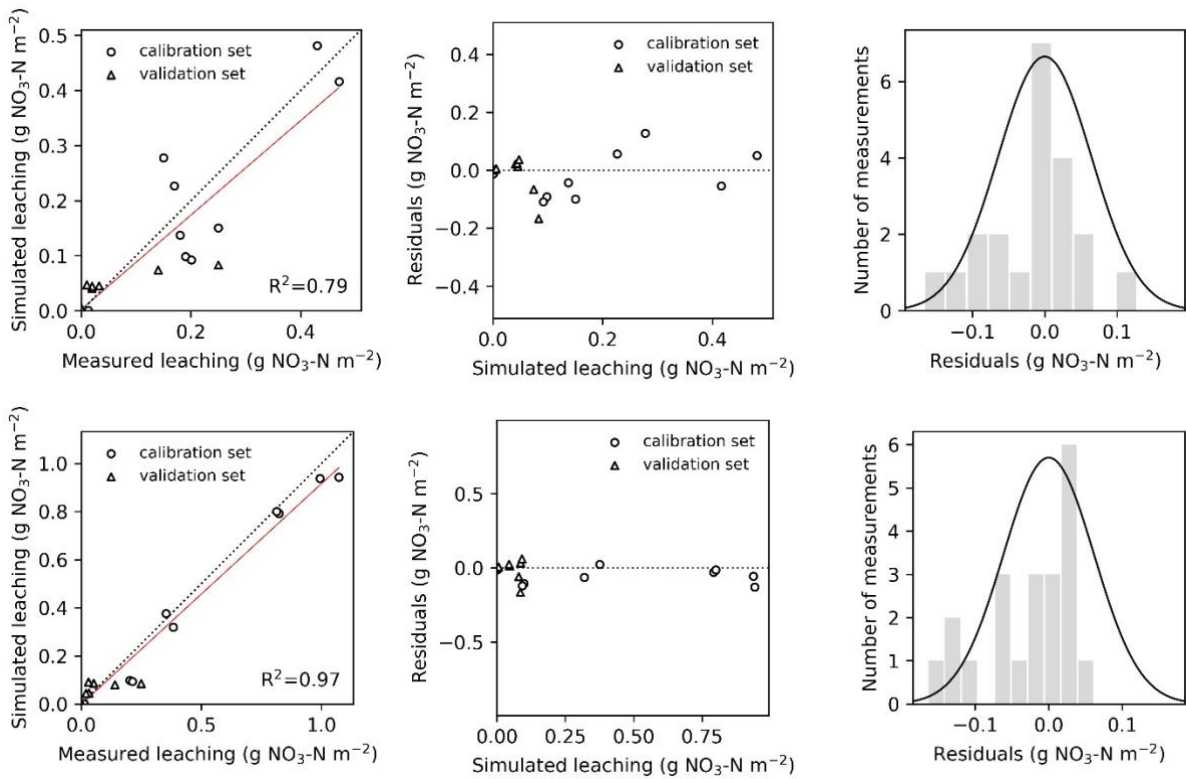
**Table 6.13** Number of measurements (n), model efficiency (ME), mean bias error (MBE) and root mean square error (RMSE) in the prediction of the monthly and annual leaching for the calibrated and validated datasets in *Study 2*.

<b>Calibration dataset (2008)</b>						
<b>Treatment</b>	<b>n</b>	<b>ME (%)</b>	<b>MBE (g NO<sub>3</sub><sup>-</sup>-N m<sup>2</sup>)</b>	<b>MBE (%)</b>	<b>RMSE (g NO<sub>3</sub><sup>-</sup>-N m<sup>2</sup>)</b>	<b>RMSE (%)</b>
4 (monthly)	5	66.38	-0.03	-12.15	0.09	40.44
5 (monthly)	5	78	-0.01	-5.61	0.06	31.54
4 (cumulative)	5	96.2	-0.05	-10.38	0.08	15.61
5 (cumulative)	5	96.71	-0.05	-11	0.07	13.77

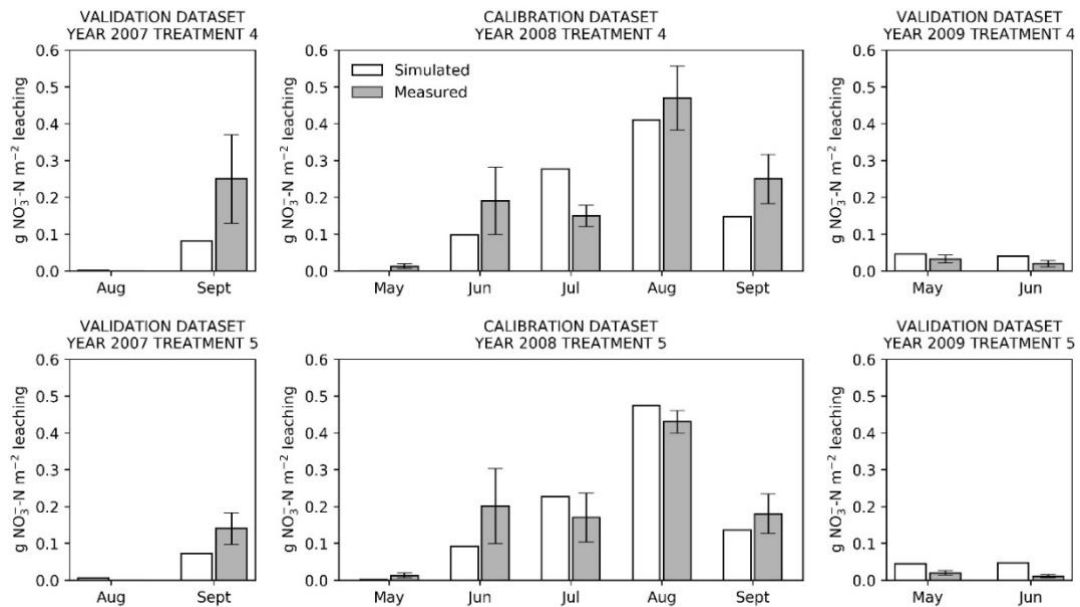
  

<b>Validation dataset (2007 and 2009)</b>						
<b>Treatment</b>	<b>n</b>	<b>ME (%)</b>	<b>MBE (g NO<sub>3</sub><sup>-</sup>-N m<sup>2</sup>)</b>	<b>MBE (%)</b>	<b>RMSE (g NO<sub>3</sub><sup>-</sup>-N m<sup>2</sup>)</b>	<b>RMSE (%)</b>
4 (monthly)	4	35.11	-0.03	-42.03	0.08	108.21
5 (monthly)	4	54.44	0	3.61	0.04	90.02
4 (cumulative)	4	-7.91	-0.11	-52.06	0.13	60.68
5 (cumulative)	4	77.64	-0.02	-16.06	0.03	27.64

In the analysis of the residuals shown in Figure 6.19 (centre panels) the highest relative error was observed for lower simulated leaching amounts. The distribution of the residuals of the simulation of cumulative leachate (Figure 6.19 lower-right panel) was slightly skewed to the left (negative), showing a general under-estimation of nitrogen lost through leaching. This corresponded with the negative relatives MBE for the evaluation of the cumulative leaching, ranging between -10.38 and -52.06%.



**Figure 6.19** Comparison of measured and simulated leaching (left panels), analysis of the residuals against leaching simulation (centre panels), and distribution of the residuals (right graphs). The upper graphs correspond to monthly measurement events (n=21), and lower graphs represent the cumulative leaching in each simulated year (n=21).



**Figure 6.20** Monthly simulated and measured leaching (g NO<sub>3</sub>-N m<sup>-2</sup>) in 2013, 2014 and 2015 for treatments 4 and 5.

## 6.3 DISCUSSION

In this section the results from the STICS model evaluation for simulating turfgrass are discussed. The model strengths and limitations are discussed for the water balance, dry matter production and nitrogen clippings component; and the results for each compared with previous research. Finally, areas for improvement in the STICS model and methodology developed in this research are described.

### 6.3.1 Performance evaluation of STICS model for turfgrass

#### Water balance

The water balance was simulated for different irrigation regimes. For *Study 1*, STICS simulated the differences in soil water depletion between irrigation events for different irrigation treatments with an acceptable level of accuracy. When irrigation was applied to FC, STICS simulated a higher water depletion than for the deficit irrigation treatments. This reduction in water consumption was produced when the soil water content was lower than the threshold given by the model output variable *testomate*. The variable *testomate* relates to the daily water content (% w/w) above wilting point, below which actual evapotranspiration (ET<sub>a</sub>) is reduced, and water stress occurs. In STICS, the threshold of soil water content at which plant transpiration is reduced is not a static variable, hence its value varied throughout the simulation period. On average, the threshold *testomate* was  $8.02 \pm 1.3\%$  (w/w) for *Study 1*. This value explains the lower water consumption in the deficit irrigation treatments (irrigated to a GSWC of 7.9%) compared with the irrigation back to FC treatment.

The prediction of the soil water content in the third treatment in *Study 1*, between August 2013 and August 2014 presented inaccuracies in the prediction of GSWC after irrigating back to FC. In this treatment, irrigation was applied at 60% FC three times per week, plus one irrigation to FC every other week. The observed values of soil water content after irrigation back to FC were noticeably lower than those simulated by the STICS model. Thus, field measurements of water content seemed to decrease rapidly when irrigated back to FC until arriving at a certain



point, after which water consumption was reduced. In STICS simulations, this depletion was less pronounced. One option to recreate this in the STICS model simulations would be to increase the maximum crop coefficient value ( $k_{max}$ ), which would directly affect water consumption after irrigation back to field capacity. However, the values that should be used would exceed  $k_{max} > 2$ , leading to an unrealistic estimation of the typical crop coefficients in turfgrass (Romero and Dukes, 2016; Colmer and Barton, 2017). Also, the use of higher  $k_{max}$  would compromise the overall robustness of the results for water consumption when simulating different irrigation strategies.

In *Study 2*, the average GSWC at which evapotranspiration decreased was  $5.03 \pm 0.95\%$  (w/w), which did not influence water consumption in *treatment 4* and *5*. However, the simulation outputs showed that deep-infrequent irrigation (*treatment 4*) tended to result in lower evapotranspiration, leading to a quicker replenishment of the soil water content and therefore increasing the water drained. This fact led to the occurrence of drainage in simulations between July and September 2009 in that treatment (17 mm drained over 146 mm applied). During the same period, no drainage was measured in field due to the use of a rain-out shelter. Although irrigation produced some drainage, it was observed that the main responsible for drainage was rainfall, and not irrigation.

Considering the predictions of water content at different time steps during the year, simulations in *Study 1* under-estimated the water consumption in September when irrigation was applied to FC. During September, the STICS model computed a reduction in actual evapotranspiration compared with the previous months. In contrast, field measurements reported that the reduction in plant water consumption was moderate. Consequently, when same water as applied in field trials during September was applied in simulations, the STICS model computed an excess of water in the soil, leading to some drainage after irrigation. This was repeated in the simulations for 2013 and 2014. In 2015, the data from *Study 1* ended in August so it was not possible to compare model outputs with field measurements. An explanation for the reduced soil water depletion during September is that the water depletion in the soil depends on the

*actual evapotranspiration (ET<sub>a</sub>)*. In STICS, *ET<sub>a</sub>* is linked with reference evapotranspiration (*ET<sub>o</sub>*). For the local climatic conditions at Landvik, the *ET<sub>o</sub>* in September usually experiences a marked decline due to a large reduction in global radiation (up to 50% compared with August). No parametric solution was found to reduce the error for *HR(1)* in September without compromising the water balance in previous months. Despite these limitations, the STICS model simulated the water balance in turfgrass with a reasonable degree of accuracy and is considered appropriate for estimating the water balance on golf greens under Northern European climate conditions. However, some improvements are required in the parameters/equations to improve estimation of soil water depletion after irrigating back to field capacity.

#### *Dry matter production in clippings*

Regarding the simulation of DMP in clippings the simulated results from the output parameter *harvested dry biomass (rendementsec)* showed an overall good prediction compared against measurements from *Study 1*. The lowest errors were obtained when predicting the cumulative *DMP* at the end of each simulation period, as showed in Figure 6.16. The prediction of monthly accumulated dry matter in clippings was better for the validation dataset (2013 and 2015) compared to the calibration dataset (2014). The *DMP* measured in *Study 1* during May 2014 was nearly 50 g m<sup>-2</sup> across all treatments. In contrast, the simulated *DMP* for the same period ranged between 13 and 27 g m<sup>-2</sup>. The lower clipping weight for simulations during May can be explained due to shoot growth, which mainly depends on the radiation intercepted by the plant (*raint<sub>(n)</sub>*), but also in the reserves mobilised for plant growth as given by the variable *deltaremobil*. The calculations for *deltaremobil* are provided in Brisson et al. (2008). One of the primary drivers to quantify this variable is the daily foliage growth (*deltai*) which is linked with temperature. The lower temperature and, to a lesser extent, global radiation in May compared to summer months seems to be responsible for the lower simulated values of dry matter in 2014. Conversely, in 2015, the prediction of simulated *DMP* was closely correlated with field observations during May. Before drawing any conclusion about the simulation errors in May 2014, more field observations from different years should be tested

in the model. The errors could be derived from errors inherent from treatments in a given year, but also due to a need to improve the STICS model equations to predict the accelerated growth characteristic from cool-season turfgrasses during the early spring (Fry and Huang, 2004).

The STICS model also tended to under-estimate (-33%) DMP when the severe deficit irrigation was applied in 2015 (*treatment 3*). An explanation for the under-estimation was that the reduction in DMP measured for deficit irrigation treatments during *Study 1* did not show high variability compared with measurements for higher irrigation rates. The model calibration would benefit from the use of data from treatments where irrigation is applied at more severe deficit irrigation. The reduction of turfgrass growth in response to deficit irrigation varied between investigations, species and climatic conditions, being more sensitive in general to irrigation applied below 50% ETo (Short and Colmer, 2007; Su et al., 2007). However, the reduction in clipping weight for red fescue could be lower than for other species because of the characteristic drought tolerance of fine fescues (Emmons, 2008) and low ETo in Nordic countries.

As mentioned previously, one of the main attributes of turfgrass is its frequent and short mowing. Mowing is usually done on a daily basis with cutting heights ranging between 2.5 and 6.4 mm (Emmons, 2008). Despite the encouraging results from the STICS simulation of clippings, it was necessary to account for them as accumulated clipping weight for a lower total number of cuts events than those that would occur in the reality. When trying to reproduce the mowing frequency by specifying the mowing calendar in the STICS model management options, the model returned errors. Under frequent mowing, the simulated turfgrass presented a cessation of development and leaf extension at a certain point, and the model did not finish the simulations. An explanation for that is that the prescribed short and frequent mowing (5 mm three times per week) produced incongruity in the model equations. For this reason, it was opted to activate the automatic cuts option.

Other researchers have used STICS for simulating forage crops with one or more cuts during the cropping season (Ruget et al., 2009; Durand et al., 2010; Jégo et

al., 2013); but did not use such frequent cuts as is characteristic of turfgrass for golf. However, Jégo et al. (2013) also reported inaccuracies in STICS simulation for regrowth period after cutting timothy grass, which highlights the difficulties of reproducing plant development and recovery after a cut. Results from recent research conducted by Pérez-Ortolá et al. (2016) also reported inaccuracies when trying to predict in the DMP of tall fescue for individual cuts using the DNDC model, showing less variability when the DMP was accounted annually. These results are consistent with those obtained in this research.

In another study on simulation of turfgrass systems using the DAYCENT model, Zhang et al. (2013b) considered mowing as harvest events, leaving 336.6 g m<sup>-2</sup> after each cut but without specifying the frequency in clipping removal. Qian et al. (2003) also estimated dry matter production in turfgrass using the CENTURY model, and considering a weekly removal of 4% of the total aboveground biomass. For both studies conducted on turfgrass, dry matter in clippings was reported as the cumulated biomass at the end of each simulation year. Modifying the STICS model to allow cuts based on a fraction of the aerial biomass rather than the crop height could simplify the process of mowing events, especially for short cutting heights as used on golf greens. In this context, there is a need to improve STICS to better simulate short mowing heights.

In this research, turf cuts were assumed to be given automatically at 0.005 m when the phenological stage *end of the juvenile phase (amf)* was achieved. Under this configuration, the cut events were delayed if the total aerial biomass was less than the parameter *minimum value of aerial biomass required to make a cut (mscoupemini)*, which was set at 0.1 t ha<sup>-1</sup>. Cuts depend on phenological stage, which is driven by the accumulation of degree days<sup>-1</sup>. This fact indicates that temperature was the primary determinant of cut events, assuming that there was not nitrogen or water deficit. After each cut, the phenological stage of the plant returned to emergence (*lev*), and the plant growth rate slowed because of the lower leaf expansion at *lev* stage. For example, Figure 6.21 shows how, after each cutting event, the expansion of the leaf area index followed an exponential trend. This trend is given by the daily increase of the green leaf index function

( $\Delta LAI_{dev}$ ) which relates the phasic development with a daily increase in foliar area. As the phenological stage was reinitiated after each cut, there was a high sensitivity in the parameters  $dLAI_{max}$  and  $uLAI_{max}$  involved in the shape of the logistic function  $\Delta LAI_{dev}$ . It was also observed that during months with higher temperatures, the increase in leaf area index ( $LAI$ ) showed a steeper slope. A detailed explanation of the  $\Delta LAI_{dev}$  function is given in Brisson et al. (2008).

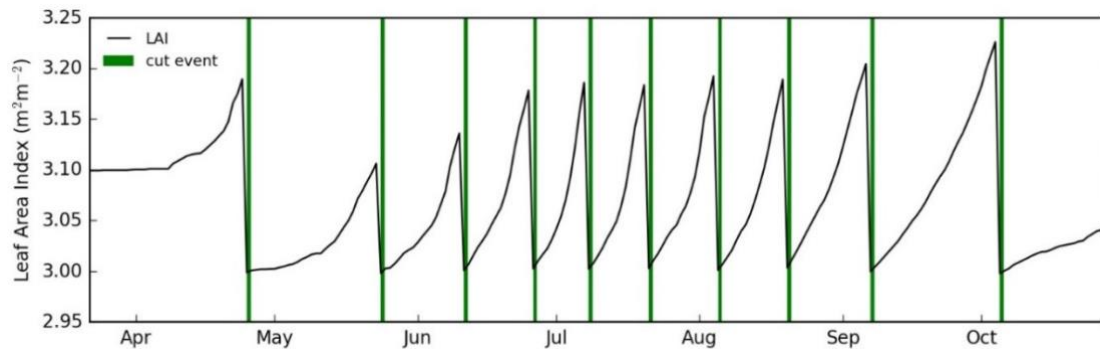


**Figure 6.21** Simulated daily variation in  $LAI(t)$  for turfgrass using the STICS model.

In addition to the cut events, simulating the short mowing height in terms of  $LAI$  and the equilibrium between plant “height-biomass- $LAI$ ” was challenging. Each cut led to a reduction in  $LAI$ , and hence its evolution was interrupted continuously by cuts (Figure 6.21). This decrease in  $LAI$  is related to the difference in crop height before and after cutting, linked through the extinction coefficient connecting  $LAI$  to crop height ( $khaut$ ). Despite the importance of  $LAI$  in the STICS model, particularly in relation to those processes involving shoot growth and radiation interception, no data of  $LAI$  was available to use in this research. Very few references were found with specific values for turfgrass  $LAI$  in the literature (i.e. Short and Colmer (2007), Goldsby (2013), and An et al. (2015)), where reported values of  $LAI$  ranging from 1 to 5  $m^2 m^{-2}$ . This lack of  $LAI$  data is mainly due to two reasons. Firstly, the traditional methods for determining  $LAI$  are destructive. Turfgrass on golf greens is generally sowed one year in advance of use and then maintained as a perennial plant. Destroying plots during the research period would be expensive. Secondly, the measurement of the foliar area is a time-consuming task because of the small and numerous leaves that make up the turfgrass canopies. Due to the lack of  $LAI$  data, the approach adopted in this research was to select those parameters in the pre-

parameterisation that maintained the *LAI* as constant as possible during the simulated cycle. Nevertheless, having field observations of *LAI* would significantly help to improve the parameter optimisation, the simulations and general model behaviour.

### Leaching and nitrogen balance

The prediction of leaching in *Study 2* showed higher variability during the validation step compared to the other output variables. While the errors observed in the predictions for 2009 were associated with inaccuracies of the STICS model in simulating low values of leaching, the under-estimate in leaching for August and September 2007 (Figure 6.20) was probably associated to the recent establishment of the trial plots in June that year, as reported by the authors in *Study 2* (Espevig and Aamlid, 2012). These observations coincided with results from similar studies (Barton et al., 2009; Telenko et al., 2015) who associated higher leaching in newly established turfgrass with lower rates of nitrogen immobilised.

A significant positive correlation was observed between simulated drainage and leaching. Events with greater water drained carried greater amount of nitrate leaching. This has been reported in previous turfgrass studies (Morton et al., 1988; Shuman, 2002b; Barton et al., 2006a). Due to the strong relationship between drainage and leaching, one can assume that failure in the prediction of the plant water consumption, which can lead to under-estimate or over-estimate in drainage, will result in errors in the prediction of nitrate losses through leaching. Nonetheless, as shown in Chapter 4, drainage is not the only explanatory variable for total nitrate leaching, and their values will vary between sites, thatch layer and management conditions.

Despite variations in nitrogen leaching being predicted, it is worth commenting the need of some improvements in the simulation of turfgrass and more experimental data are required to simulate the nitrogen balance adequately. For instance, the nitrogen concentration in clippings in *treatment 4* in 2008 averaged 1.21% g N/g dry biomass, accounting for a total of 3.12 g N m<sup>-2</sup>. This figure is lower than that reported by Ericsson et al. (2012c) who reported average nitrogen

in clippings in fine leaf fescues, ranging from 2 to 5.9% of dry matter. Thus, considering this value of nitrogen concentration in leaves, the simulated nitrogen lost in clippings should have ranged between 5.16 and 15.2 g N m<sup>-2</sup>, which assumes the 26 to 80% of the total amount of nitrogen applied in that year. Although no data was available of nitrogen concentration in leaves, the results obtained suggest that the calibration of the parameters involved in the STICS nitrogen dilution function (Brisson et al., 2008) will be necessary for correct simulation of the nitrogen uptake. Improvements in the prediction of nitrogen concentration in leaves and the nitrogen demanded by turfgrass would improve the assessment of the whole nitrogen balance in future research.

Due to the low biomass of the verdure (biomass left in the field after cutting) and apparent low nitrogen concentration in leaves, the values of the parameters used in the model tended to compensate for the low nitrogen plant uptake by increasing the amount of nitrogen immobilised in the soil. For instance, in *treatment 4* in 2008, the simulated nitrogen immobilisation was up to the 39% of the total nitrogen applications. This proportion does not match what might be expected in turfgrass systems (Shi et al., 2006) and a more exhaustive study on nitrogen balance in greens under Scandinavian climate conditions is required to gain deeper insights.

### **6.3.2 Model limitations and opportunities for improvement**

The STICS model was calibrated for the simulation of soil water depletion and DMP using dataset from *Study 1*; and drainage and leaching with data from *Study 2*. Overall, the model accurately predicted soil water content, the accumulated clipping weight, water drainage during most the simulation period; and to a lesser extent, nitrate leaching. However, the model has a number of limitations which need to be recognised. The main limitation was the instability of the model in simulations due to the short mowing height. On many occasions, this stopped plant development before ending the simulated period, or, in some cases, the model did not finish its simulation due to an error in the calculations. These errors appeared when the cut events were imposed “by calendar” instead of using the “automatic cuts” option. Thus, the only option possible that would provide stability

to the simulations was by activating the *automatic cuts* option, which was driven by the phenological stage. Conditions that delayed the development of the plant phenology, such as temperature or stresses, affected then the number of cuts and overall model behaviour. The use of automatic cuts on a plant maintained at 5 mm height led to a general feeling of “lack of control” in the model behaviour and, sometimes, to unpredictable responses in the results. In this line, big efforts were made to parameterise the model in a stable, robust and reliable way for the simulation of the output variables under study.

The use of the automatic cut option and the low plant height decreased the quality of the sensitivity analysis and the parameter calibration steps. In the sensitivity analysis, because the sensitivity indexes might be influenced by the impact of some parameters on the stability of the model behaviour rather than in the output parameter studied itself. In the calibration phase, because of the simplex algorithm did not only look for the best combination of parameters that returns the lowest error in soil moisture, dry matter production, drainage or leaching; but also was conditioned by the imposition accounting one automatic cut during April and at least 12 automatic cuts at the end of October. Then, the imposed condition of matching the number of cuts might have compromised the value of the parameters calibrated and the quality of the approach adopted.

Another limitation encountered in the simulation of turfgrass for greens was the coherence and meaning of some outcomes of the plant system itself. Although the dry matter production in clippings appeared to be correct, it was found that the selected combination of parameter values led to an unbalanced distribution of the aerial dry biomass. On average, the aboveground biomass left after cuts was 159 kg ha<sup>-1</sup>. These values differed severely from other reported in the literature for turfgrass. For instance, Su et al. (2007) reported measurements of above ground biomass ranging from 3,633 and 9,436 kg ha<sup>-1</sup>. Although in that case the species were *Poa pratensis* L., *Festuca arundinacea* Schreb., and *Poa arachnifera* Torr., and were mowed at 65 mm, the difference of magnitude between the simulated aboveground weight and the one from the example provides evidence to infer that the simulated aerial dry biomass weight (*masec*)



after clipping should be higher. Despite these differences, the value of the *masec* after each cut did not affect any of the outputs in this research. However, it should be borne in mind for future applications of the model. Also, the model did not consider the variations in tillering and rooting during the simulated months, nor the variations in the thickness of the thatch-mat layer.

Leaching and nitrogen balance processes also require further analysis, data collection and parameter improvement. Since the robustness of STICS model permitted the calibration of some parameters for simulating nitrate leaching, more work is needed to assess the whole nitrogen balance. In addition to an improvement on the aboveground plant nitrogen concentration and nitrogen uptake, it would be required a more in-depth study of the mineralisation rates, ammonia volatilisation, N<sub>2</sub>O emissions and nitrogen immobilisation. However, due the major challenge and complexity that suppose nitrogen transformations in turfgrass managed under golf green conditions, these topics should be treated in deeper and more specific studies on the turfgrass nitrogen balance. Further research should study the nitrogen balance and consider the actions that golf green rootzone is subjected to, such as regular vertical mowing, aeration and sand amendments. The aim of these operations is not only to avoid compaction and maintain a good drainage level and surface firmness for better playability, but also to control the organic matter content (Gaussoin et al., 2013). Thus, the continued and systematic modification of the soil properties, characterised by a rapid organic matter content increase (with occurrence in the *profhum* layer in STICS model), along with periodic reductions of organic matter produced by those operations, can be a major challenge in the accurate simulation of the nitrogen cycle in greens; as most of these actions are driven by human decisions and turfgrass management philosophy.

Finally, another important limitation was the lack of data for model calibration and validation. This limitation should be considered as a methodological limitation and not as a model limitation. A larger number of parameters measured in *Study 1* and *2* would have substantially improved the model set up. As reported previously, having measurements of LAI in verdure and clippings would be

particularly beneficial to estimate more accurately the relationships between turfgrass height, growth rates and water consumption. In *Study 2*, because of the high sensitivity observed of the N content in soil on leaching variance, measurements of N soil content would have also been beneficial. In summary, the measurement of the following parameters would benefit the calibration of turfgrass for simulations using STICS: LAI at different dates, dry matter in the aboveground part of the plant during all the cycle, and nitrogen content not only in leaching, but also in soil, clippings and verdure. Data from additional studies conducted on turfgrass in a similar climatic region and for similar species would be beneficial to improve the calibration and validation of the model and avoid over-parameterisation in favour of robustness in the simulations.

## **7 DEVELOPING AN INTEGRATED MODELLING FRAMEWORK TO SIMULATE IMPACTS OF IRRIGATION HETEROGENEITY ON TURFGRASS**

This chapter presents the BalliSTICS model, an integrated modelling approach to assess the impacts of irrigation heterogeneity and strategy on turfgrass agronomy and leaching. The computer program consisted of coupling the ballistics-based model to simulate irrigation system performance across a golf green (Chapter 5), with a biophysical crop growth model (STICS) (Chapter 6). The algorithms, sub-model linkages and how the various datasets were manipulated, including the simulation options and model outputs, are described. A set of scenarios were defined to evaluate model performance under contrasting conditions combining different irrigation system configurations, scheduling strategies and weather conditions.

### **7.1 DESCRIPTION OF MODELLING FRAMEWORK**

The BalliSTICS model was developed and used to address the research aim of this thesis: *to understand and assess the relationships between irrigation management and turfgrass water use, soil water availability, dry matter production, drainage and nitrate leaching in golf greens under Northern European climate conditions*. This integrative model framework was designed to simulate the impacts of irrigation heterogeneity and irrigation strategies on turfgrass. BalliSTICS model allows the quantification and evaluation of a range of scenarios representing a variety of irrigation system design, irrigation climatic conditions, climate years and irrigation scheduling practices on turfgrass agronomy and leaching. The model framework involved the coupling of a deterministic water application model based on ballistics theory (Fukui et al., 1980; Seginer et al., 1991; Carrión et al., 2001b; Playán et al., 2006); with the STICS model developed by Brisson et al. (2002, 2003) and calibrated for turfgrass. The modelling framework, referred to as BalliSTICS, has been developed in Python (Rossum, 1995). It executes the two sub-models separately but in a synchronised fashion,

exchanging data for each iteration. The two models within in the BalliSTICS model and linkages between them are summarised below.

*Ballistic simulation of irrigation heterogeneity*

The first sub-model, written in MATLAB (MathWorks, 2014), simulates irrigation application across a golf green. The model equations and simulation steps are described in detail in Chapter 5. This model allows the study of the impacts of contrasting sprinkler set-ups, green shape and wind conditions on irrigation system performance. The main output from the irrigation model is a dataset that can be used to describe irrigation rates (IR, mm h<sup>-1</sup>) and the spatial variability of irrigation across a green. In order to link the spatial variability of water with the second sub-model (STICS), the IR (mm h<sup>-1</sup>) data was aggregated to produce a cumulative distribution function (CDF). The CDF can be expressed as the integral of the probability density function of the IR at a given point:

$$CDF(IR) = \int_{-\infty}^{IR} f(t) dt$$

From each simulation, the IR corresponding to the accumulated probabilities of  $p=0.1, 0.3, 0.5, 0.7$  and  $0.9$  of the CDF were used as an input into the STICS model. These probabilities were chosen to ensure that the different areas of the green that receive different IR are adequately represented, but limited so as to not compromise the computing time in simulations.

To obtain the values corresponding to the irrigation depth or irrigation rate for each probability (IR<sub>p</sub>), the inverse function of the CDF was used:

$$IR_p(\text{mm h}^{-1}) = CDF^{-1}(p)$$

Considering that the targeted irrigation depth (TID, mm) was the mean irrigation depth represented by  $p = 0.5$  in the CDF under zero wind conditions, the irrigation calculated for each  $p$  value in the CDF was:

$$AID_p = \frac{IR_p}{IR_{ws=0}} TID$$

where  $AID_p$  is actual irrigation depth applied at a given  $p$  in the CDF, in mm; and  $IR_{ws=0}$  is the IR for  $p = 0.5$  when wind speed is zero, in  $\text{mm h}^{-1}$ .

Figure 7.1a shows an example water distribution on a golf green and expressed as a cumulative distribution function (CDF) in Figure 7.1b. The irrigation depths for probabilities  $p = 0.1, 0.3, 0.5, 0.7$  and  $0.9$  were, respectively, 11.5, 13.8, 15.7, 17.9 and 21.5  $\text{mm h}^{-1}$ .

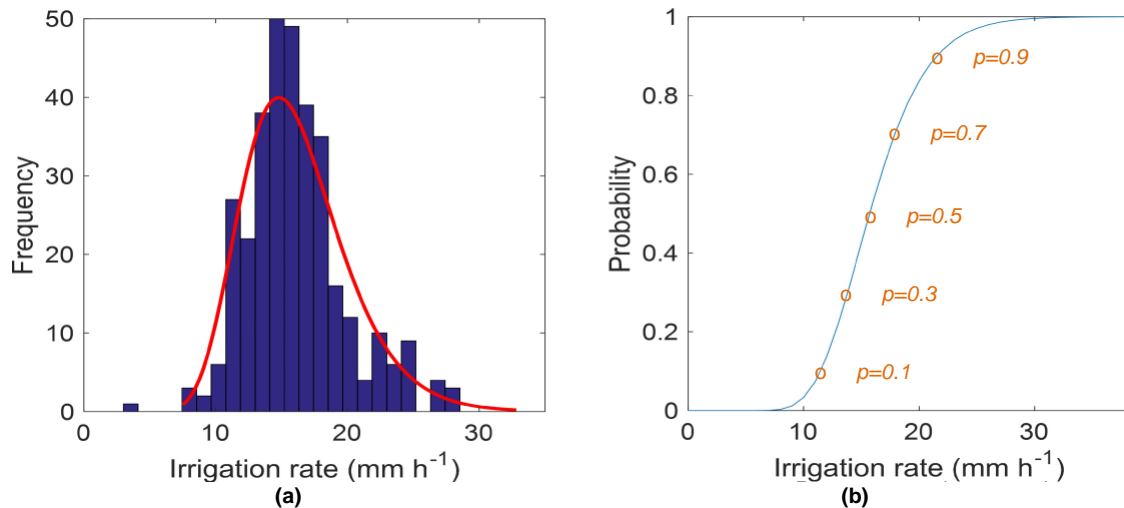


**Figure 7.1** Example of water distribution on a golf green, with a wind speed of  $3 \text{ m s}^{-1}$ . (a) Histogram showing the distribution of irrigation rate. The red line corresponds to the lognormal distribution. (b) Cumulative distribution function (CDF) of irrigation rate

### Simulating turfgrass agronomy

In this research, the STICS model was used for simulating turfgrass water balance, growth and the potential environmental risks derived from different irrigation strategies and climate years. Here turfgrass agronomy refers to a set of water balance components (inputs and outputs of water in the rootzone and variation in soil water content) and the dry biomass produced as clippings. Regarding environmental impacts, the model provides output data on drainage and nitrate losses through leaching.

Although the STICS model can provide output on a daily time-step, when STICS was used within the BalliSTICS model, it provided results as a seasonal aggregated or average, depending on the output variable. This decision was taken due to the very large number of simulations carried out by BalliSTICS. Storing daily output files from all simulations would generate very large files. In addition, the STICS model for turfgrass (Chapter 6) showed better accuracy when

the results were analysed at the end of each season. Table 7.1 summarises the output variables, as well as the method used to calculate the seasonal value for each variable.

**Table 7.1** Output variables from STICS used for the assessment of turfgrass growth and performance

<b>Component</b>		<b>Daily STICS output variable</b>	<b>Seasonal value</b>
Water balance	et	Daily actual plant evapotranspiration (mm)	Aggregated
	etm	Daily maximum plant evapotranspiration (mm)	Aggregated
	airg(n)	Daily irrigated applied (mm)	Aggregated
	resmes	Soil water on the measurement depth (mm)	Averaged
	resrac	Available water content (mm)	Averaged
	HR	Water content of the soil horizon 1 (% w/w)	Averaged
	drain	Daily amount of water drained (mm)	Aggregated
DMP in clippings	dltams(n)	Daily growth rate of the plant ( $t\ ha^{-1}\ d^{-1}$ )	Aggregated
	rendementsec	Dry biomass of harvested organs ( $t\ ha^{-1}$ )	Aggregated
N leaching	lessiv	Daily nitrate leached ( $g\ NO_3^{-1}\ N\ m^{-2}$ )	Aggregated

*Integrated model framework (BalliSTICS model)*

The development of the BalliSTICS model approach was developed to evaluate the impacts of irrigation management on greens under typical Northern European environmental conditions, where supplemental irrigation is applied during periods of low rainfall and during the warmest months to maintain healthy, actively growing turfgrass, playability conditions, and to improve fertiliser uptake and solubility. In the BalliSTICS model, only water for replenishing the soil water deficit due to a lack of rainfall was considered, rather than application of water for other agronomic or management purposes.

Table 7.2 summarises the input options available for BalliSTICS model, and how they affect the simulation of irrigation uniformity or the STICS model.

**Table 7.2** Options available in BalliSTICS and their relation to each sub-model

Options	Sub-model	
	Irrig. model	STICS
Sprinkler model and set-up	x	
Green shape	x	
Sprinkler position	x	
Wind conditions (fixed or variable)	x	x
Climatic conditions (year selection)	x	x
Multi-year simulation (on/off)	x	x
Irrigation depth		x
Irrigation frequency		x
Irrigation method (IS <sub>AVE</sub> , IS <sub>DRIEST</sub> )		x
Rain (on/off)		x

Before running the BalliSTICS model, the user must select the sprinkler set-up (model, nozzle size and operating pressure), green shape, number and position of sprinklers, and wind speed and direction (fixed or variable). The number of years to be simulated which are linked to a daily climatic database must also be selected. If preferred, the user can choose ‘no rainfall’. The user also needs to define the irrigation strategy (depth based on ET<sub>p</sub> and irrigation frequency) and scheduling method (section 7.4).

The BalliSTICS outputs include a wide range of variables relating to irrigation system performance, including IR and CU; turfgrass agronomy, including actual evapotranspiration (ET<sub>a</sub>) and dry matter production in clippings (DMP); or environmental impacts, including nitrate leaching. The relationship between input and output variables and sub-models is shown in Figure 7.2.

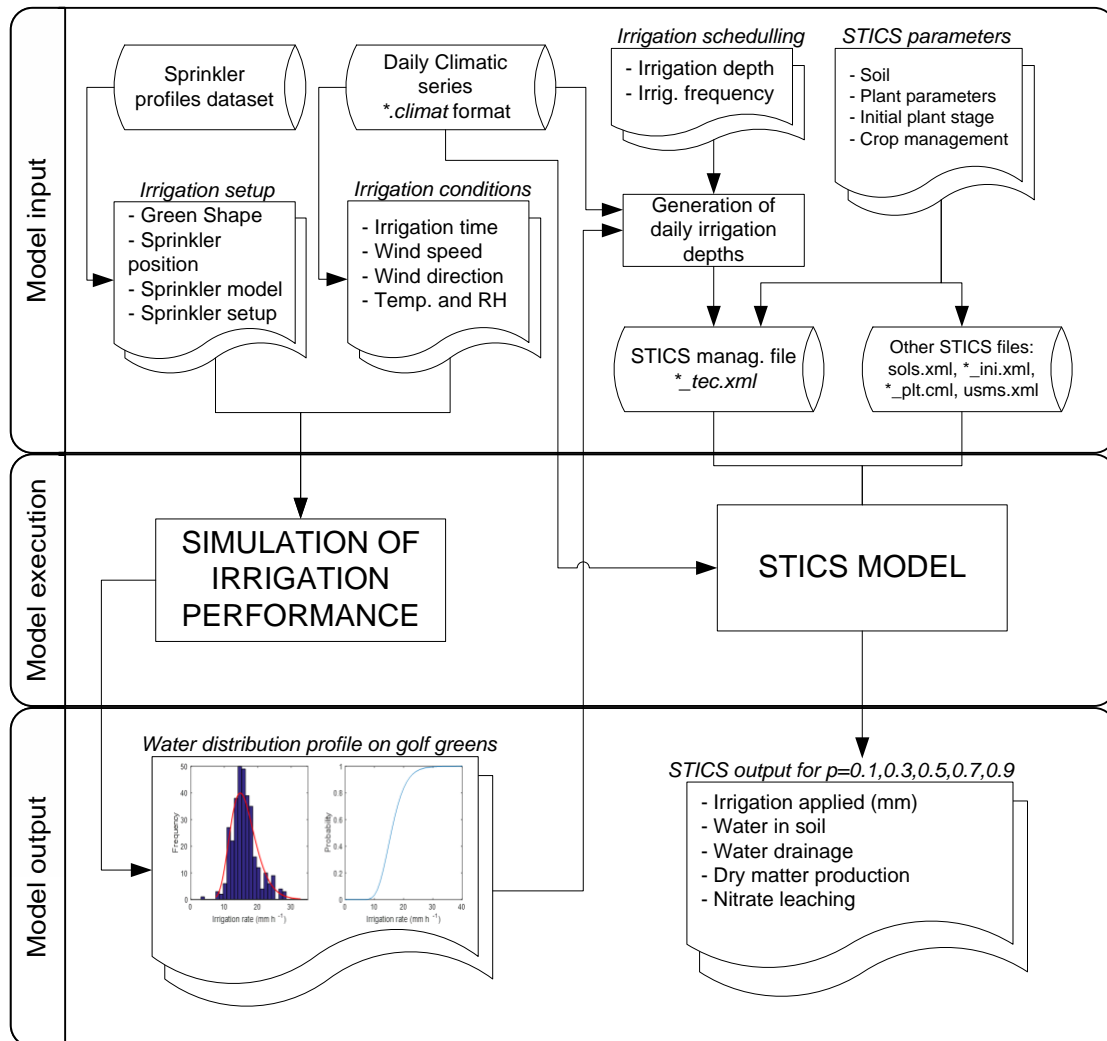


**Figure 7.2** Flowchart summarising the BalliSTICS model links, inputs and outputs

The individual steps executed within the BalliSTICS model are shown in Figure 7.3. In the first step (Box 1) the simulation of irrigation performance is conducted according to the selected green shape, sprinkler position, sprinkler model, nozzle size, operating pressure and climatic conditions. The  $IR_p$  corresponding to the probabilities  $p = 0.1, 0.3, 0.5, 0.7$  and  $0.9$  of the CDF of the simulated irrigation are then used for generating different annual irrigation application profiles, which are used to calculate  $AID_p$  to launch the STICS model.



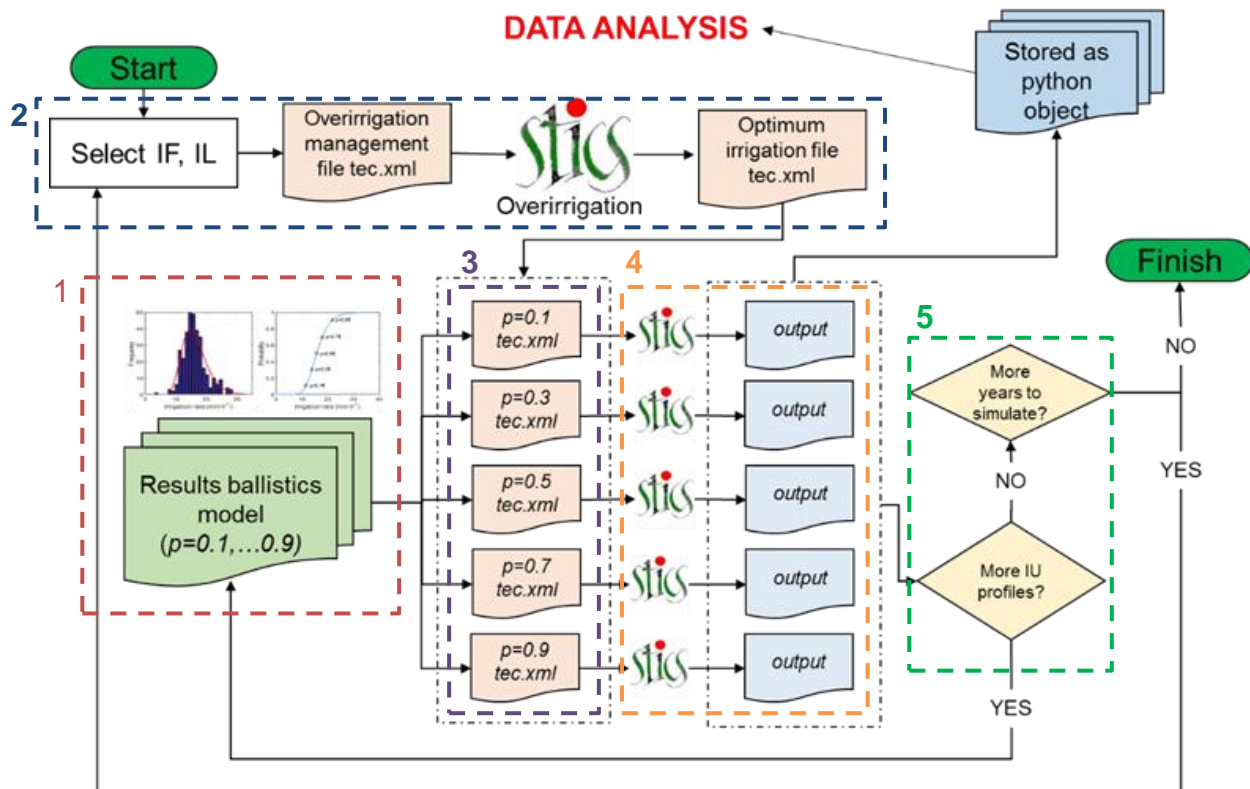


Figure 7.3 Steps followed by the BalliSTICS model

In the second step (Box 2), the irrigation needs for a given year and scheduling strategy (frequency and depth) are calculated. This step was carried out by BalliSTICS, as using STICS alone does not allow irrigation needs to be calculated based on irrigation frequency or depth strategy (ET<sub>p</sub>). The calculation follows three steps. Firstly, a simulation is launched ensuring that the soil water content exceeds field capacity. This is achieved by modifying the STICS management file (\*\_tec.xml). The BalliSTICS model modifies the values of irrigation to 50 mm per irrigation event. Secondly, the STICS model is then executed, and the optimum irrigation to field capacity is corrected for each *i* day, using the following expression:

```

if  $D_{\text{overirrigation}_i} - \text{DRAIN}_{\text{overirrigation}_i} > 0$  then
     $D_i = (D_{\text{overirrigation}_i} - \text{DRAIN}_{\text{overirrigation}_i}) \times \text{deficit level}$ 
else if  $D_{\text{overirrigation}_i} - \text{DRAIN}_{\text{overirrigation}_i} \leq 0$  then
     $D_i = 0$ 
  
```

where  $D_{\text{overirrigation}_i}$  is the over-irrigation applied in the first phase of the calculation of the optimum water application for day *i*, in mm;  $\text{DRAIN}_{\text{overirrigation}_i}$  is the simulated drainage produced by the over-irrigation on day *i*; *deficit level*

corresponds to the level of irrigation applied regarding the field capacity content, where 1 is equal to field capacity (1.0 ETp), in mm; and  $D_i$  is the new calculated irrigation applied, in mm. In the second conditional statement, no irrigation is applied because drainage exceeds irrigation. This occurs when water excess is due to rainfall and therefore there is no need for irrigation.

In the next step (Box 3) the irrigation received by each area of the golf green is calculated, based on the percentage of variation between the irrigation rates for  $p$  in the CDF, and the targeted water application. For each  $p$ , the water applied is calculated with the  $AID_p$  equation. The new irrigation values ( $AID_p$ ) are then modified within the STICS management files (\* *tec.xml*) corresponding to the simulation of each  $p$  in the CDF.

In the next step (Box 4) STICS is run in parallel for the five \*\_*tec.xml* files corresponding to each point on the CDF. The data from the outputs of each  $p$  simulation are then transformed to accumulated seasonal values, and stored for subsequent data analysis. All steps in boxes 1 to 4 are repeated where there are additional irrigation profiles (Box 5). When a new year is simulated, the BalliSTICS model modifies the year of simulation in the STICS *Unit of Simulation* file (*usms.xml*) to ensure that appropriate weather data are used.

In order to address the research aim of this thesis, the BalliSTICS model was applied following three steps. Firstly, the impacts of sprinkler set-up, green shape and wind conditions on irrigation heterogeneity and irrigation rates were assessed. Secondly, the impacts of irrigation strategy on turfgrass agronomy and the environment were assessed. Finally, the impacts of irrigation management on turfgrass agronomy and environment were simulated.

## **7.2 MODEL APPLICATION - SIMULATED IRRIGATION SYSTEM PERFORMANCE**

### **7.2.1 Methodology**

The irrigation model (Chapter 5) was used to assess the implications of irrigation design and wind on irrigation performance. Irrigation performance was assessed by quantifying irrigation rates (IR, mm h<sup>-1</sup>) and the Christiansen Uniformity

Coefficient (CU%). Nine representative golf greens were defined using the shape and sprinkler positions derived from the field evaluations (Annex-2). The main characteristics of each green are shown in Table 7.3. These greens varied in shape and size from 305 to 467 m<sup>2</sup>. No slope was considered in simulations.

**Table 7.3** Golf greens characteristics used in simulations

id	Golf Club	Green	Area (m <sup>2</sup> )	Length (m)	Width (m)	Shape	Number of Sprinklers
1	Furesø	F9	467	31	16	Irregular	5
2	Furesø	H9	327	23	16	Triangular	5
3	Furesø	H7	452	27	19	Oval	5
4	Furesø	P9	429	45	9.5	Elongated	6
5	Furesø	H3	377	30	16	Elongated	5
6	Oslo GK	9	380	29	17	Oval	4
7	Oslo GK	17	376	23	20	Circular	4
8	Oslo GK	18	340	23	20	Oval	4
9	Ashford	13	305	27	12	Oval	4

For each green, irrigation was simulated 1,760 times, combining different sprinkler set-ups, sprinkler spacings, and changes in wind speed and wind direction (Table 7.4). In total, 15,840 simulations were completed.

**Table 7.4** Summary of BalliSTICS simulations to assess irrigation heterogeneity impacts on golf greens

	Sprinkler set-up	Sprinkler spacing (m)	Wind speed (m s <sup>-1</sup> )	Wind direction (degree)	Green shapes	Total
Min	-	-3	0	0	-	-
Max	-	3	5	315	-	-
Interval	-	1.5	0.5	45	-	-
<b>Total</b>	<b>4</b>	<b>5</b>	<b>11</b>	<b>8</b>	<b>9</b>	<b>15,840</b>

- **Sprinkler set-up:** This refers to the combination of nozzle size and operating pressure. The sprinkler model assumed was the RainBird 751 SERIES. Four set-ups were simulated: nozzle size #28 operating at 4.2 and 6.0 bar and nozzle size #40 operating at 4.2 and 6.0 bar.
- **Sprinkler spacing:** Five combinations of sprinkler spacing were simulated for each green. In first instance, the original sprinkler positions were considered. Four other spacings were then derived by moving the sprinklers 1.5 and 3 m towards (-1.5 m and -3 m displacement), and 1.5 and 3 m away from the centre of gravity of the green. Figure 7.4 shows an example of sprinkler displacement on “Furesø F9”.

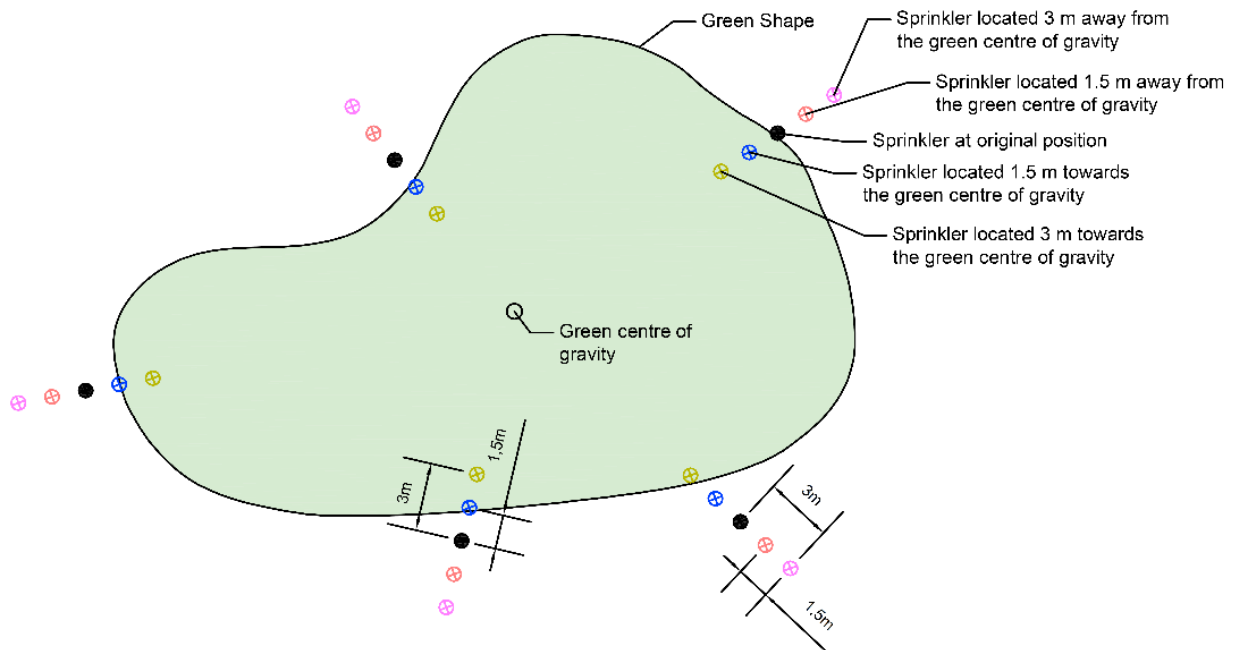


**Figure 7.4** Example of the combinations of sprinkler locations on green “Furesø F9”.

- **Wind speed:** Irrigation was simulated for wind speeds from 0 to 5 m s<sup>-1</sup> at 0.5 m s<sup>-1</sup> intervals.
- **Wind direction:** Wind direction was applied from 0 to 315 degrees, with 45 degree intervals.

The irrigation model was configured to generate a 2.5 m grid of virtual catchcans. The smallest droplet diameter considered was 0.2 mm, with increments of 0.05 mm. The rotation of the sprinklers from 0 to 360 degrees assumed 10-degree increments.

## 7.2.2 Results

The key findings relating irrigation performance to (i) sprinkler set-up, (ii) sprinkler spacing, (iii) wind speed, and (iv) wind direction and green shape are summarised below.

Impacts of sprinkler set-up on irrigation performance

Table 7.5 shows the IR and CU for the combination of two nozzle sizes and two operating pressures. These values correspond to simulations where sprinklers were in their original position and irrigating under ‘no-wind’ conditions. The irrigation model outputs confirmed that sprinkler set-up influences the IR. A larger nozzle size and higher operating pressure increased the sprinkler discharge rate ( $L h^{-1}$ ), which as expected impacts on the IR. The IR for a given sprinkler set-up varied between greens, as each green varied in shape, the number of sprinklers and sprinkler location.

**Table 7.5** Irrigation rate (IR,  $mm h^{-1}$ ) and CU (%) under ‘no-wind’ conditions and original sprinkler location, for each sprinkler set-up and simulated green.

Nozzle size		# 28				# 40			
Pressure (bar)		4.2		6.0		4.2		6.0	
	N. spr.	IR (mm)	CU (%)	IR (mm)	CU (%)	IR (mm)	CU (%)	IR (mm)	CU (%)
Furesø F9	5	11.7	79.7	12.8	76.4	15.4	76.5	17.4	77.1
Furesø H9	5	14.2	79.7	15.7	77.8	18.2	79.0	20.7	78.1
Furesø H7	5	10.9	78.9	12.0	77.6	15.0	76.6	16.9	78.3
Furesø P9	6	12.3	79.9	13.8	77.8	15.6	78.3	18.0	79.4
Furesø H3	4	10.9	80.0	12.0	75.8	14.0	77.2	15.9	77.3
Oslo G9	4	10.9	80.6	12.0	75.5	14.4	77.1	16.1	77.4
Oslo G17	4	10.3	80.3	11.2	76.3	14.0	75.7	15.7	74.9
Oslo G18	4	11.0	80.4	12.1	77.4	14.7	79.4	16.5	80.1
Ashford	4	12.1	80.3	13.4	79.8	15.3	77.2	17.5	78.9
<b>Average</b>		<b>11.6</b>	<b>80.0</b>	<b>12.8</b>	<b>77.2</b>	<b>15.2</b>	<b>77.4</b>	<b>17.2</b>	<b>77.9</b>

N.spr: number of sprinklers

Under ‘no-wind’ conditions, the CU values were slightly higher for the lowest operating pressure and smallest nozzle. The minor differences might be attributable to different green shapes, sprinkler location on each green and the unique wetted pattern and radial leg curve characteristic of each sprinkler set-up.

Impacts of sprinkler spacing on irrigation performance

Table 7.6 shows the IR and CU for different sprinkler locations. Values represent the average IR and CU of the four sprinkler set-ups under ‘no-wind’ conditions. The IR inside the greens decreased markedly as the distance between sprinklers was larger. On average, by moving the sprinklers 1.5 m away from the green

centre of gravity led to a reduction in IR of 13.8 ( $\pm 3$ )<sup>5</sup>%. This highlights the impact of sprinkler location and spacing when determining the IR.

Regarding the impacts of reduced sprinkler spacing on CU, no statistically significant differences ( $p > 0.05$ ) were obtained between the original sprinkler position and shorter spacings. In contrast, assuming larger distances between sprinklers resulted in a significant reduction in CU; 2.0 ( $\pm 0.9$ )% lower when sprinklers were located 1.5 m further apart from its original position, and 4.0 ( $\pm 1.4$ )% when they were moved 3 m further apart.

**Table 7.6** Irrigation rate (IR, mm h<sup>-1</sup>), and CU (%) under 'no-wind' conditions for different sprinkler locations

Spr. location relative to original position	IR (mm h <sup>-1</sup> )					CU (%)				
	-3	-1.5	0	1.5	3	-3	-1.5	0	1.5	3
Furesø F9	18.1	16.3	14.3	12.3	10.5	77.3	77.4	77.4	76.2	74.4
Furesø H9	21.8	19.5	17.2	15.0	12.7	80.0	79.6	78.6	77.6	77.0
Furesø H7	18.0	15.9	13.7	11.6	9.6	79.4	79.0	77.9	75.1	71.9
Furesø P9	17.7	16.4	14.9	13.4	11.8	75.1	78.4	78.9	78.2	74.2
Furesø H3	16.4	14.9	13.2	11.4	9.7	77.8	78.3	77.6	74.5	73.7
Oslo G9	16.7	15.1	13.3	11.5	9.7	79.3	78.4	77.7	74.9	73.6
Oslo G17	16.7	14.8	12.8	10.8	9.0	78.0	78.2	76.8	75.5	72.8
Oslo G18	17.4	15.5	13.5	11.5	9.5	78.8	78.8	79.4	76.3	73.3
Ashford	18.0	16.3	14.6	12.5	10.7	79.0	78.5	79.1	76.8	76.5
<b>Average</b>	<b>17.9</b>	<b>16.1</b>	<b>14.2</b>	<b>12.2</b>	<b>10.4</b>	<b>78.3</b>	<b>78.5</b>	<b>78.2</b>	<b>76.1</b>	<b>74.2</b>

#### Combined impacts of sprinkler set-up and spacing on irrigation performance

The relationship between sprinkler set-up, sprinkler spacing, and IR are shown in Figure 7.5. The variability within each boxplot was produced by the green shape and, to a lesser extent, by wind speed and direction. Although sprinkler set-up impacted on IR, the sprinkler displacements had a greater impact on IR.

<sup>5</sup> Values in brackets correspond to standard deviation

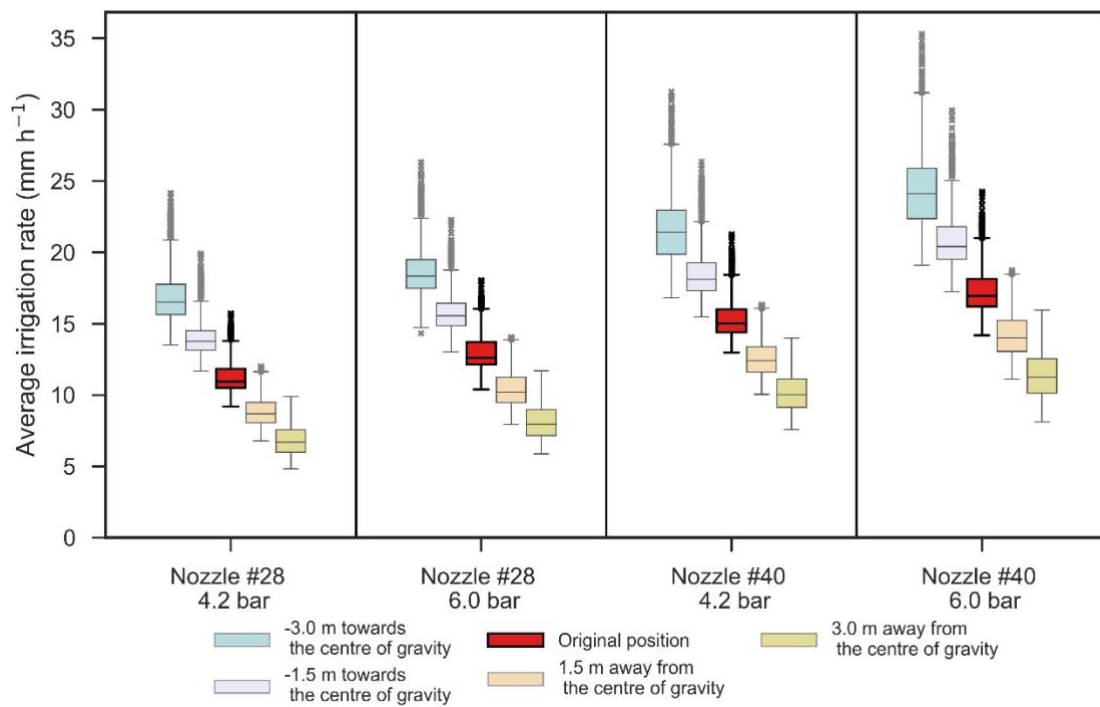


**Figure 7.5** Modelled relationship between sprinkler set-up, sprinkler spacing and average irrigation rate.

Figure 7.6 shows the variation in CU as influenced by different sprinkler spacings and set-ups.

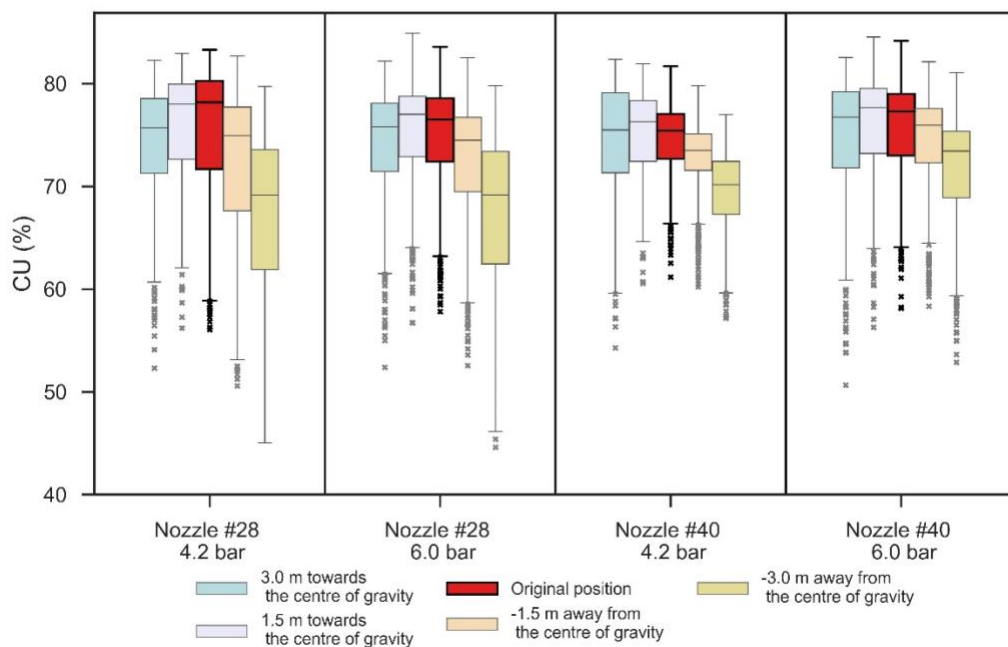


**Figure 7.6** Relationship between sprinkler set-up, sprinkler spacing and average irrigation rate. Variation in each boxplot is due to wind speed, wind direction and green shape.

For IR, sprinkler spacing had greater impact on CU than sprinkler set-up. However, differences were only evident when sprinklers were located further from their original position. In these cases, the use of a smaller nozzle size (#28) resulted in greater CU variation as affected by wind and green shape. This is associated with the wetted radius characteristic from each nozzle. Thus, when sprinklers were located at large spacings, the largest nozzle was able to deliver water at longer distances. This alleviated the negative impacts of large sprinkler spacings on CU. For instance, when simulations were run with the sprinklers in their original position, no difference in average CU was obtained between sprinkler set-up with the largest irrigated radius (nozzle #40; 6.0 bar) and with the shortest radius (nozzle #28; 4.2 bar). In contrast, when the sprinklers were located 3 m further from their original position, average CU was 4.6% higher for the set-up with the larger (#40) nozzle. Thus, when sprinklers are placed at larger spacings, it is advisable to use larger nozzles. The use of higher or lower pressures (within the studied range) did not impact on CU values at any sprinkler spacing.

#### *Impacts of wind speed on irrigation performance*

Figure 7.7 shows the percentage variation in average IR under different wind speeds when sprinkler spacing varied. It is observed that wind speed affected differently IR depending on sprinkler spacing. For simulations using the original sprinkler location on greens, no significant differences were found between IR and wind speed ( $p>0.05$ ). Conversely, at closer sprinkler spacings, increases in wind speed raised IR up to 19.1%. Conversely, when the sprinklers were moved away from their original position, wind speeds reduced the IR within the green area by up to 21.3%.



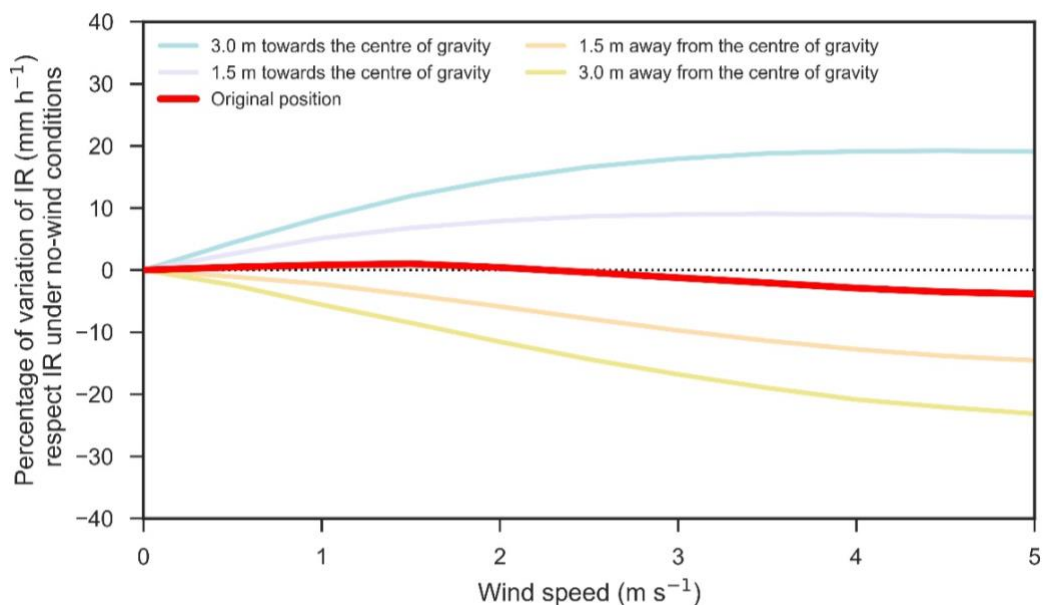


**Figure 7.7** Percentage variation in irrigation rate (IR) with respect to irrigation under no wind conditions for different wind speeds and sprinkler location.

The response of different spacings on IR was due to the wind speed which reduced the wetted area provided by each sprinkler. When sprinklers were located at shorter spacings, the reduction in wetted area resulted in a greater proportion of water falling inside the green, which increased the IR. In contrast, when the sprinklers were located farther from their original position, the reduction in wetted area resulted in a lower percentage of water falling inside the green. This finding highlights the fact that locating sprinklers near the green surroundings (as they were in the “original” position for simulations), or by choosing the optimum sprinkler location, can reduce the impacts of wind on IR.

Figure 7.8 shows the relationship between wind speed and CU depending on sprinkler set-up (Figure 7.8a) and location (Figure 7.8b). When wind speeds were equal or greater than 2.5 m s<sup>-1</sup>, the CU values decreased linearly as wind speed increased. For wind speeds below 2 m s<sup>-1</sup>, the CU remained almost constant.

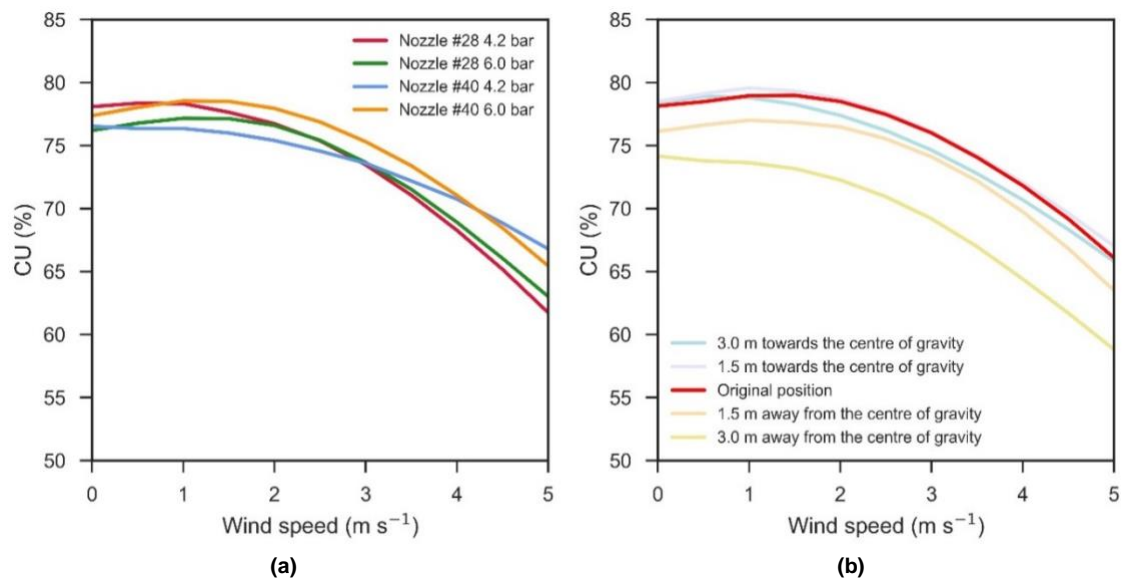


**Figure 7.8** Average values of the simulated Christiansen's Uniformity Coefficient (CU, %) for wind speed from 0 to 5 m s<sup>-1</sup> considering (a) sprinkler set-up and (b) sprinkler displacement

No marked differences were observed between sprinkler set-up and variation in CU for different wind speeds (Figure 7.8a). The most relevant difference was observed for the highest wind speed, for which the largest nozzle resulted in 3.9% higher CU. As reported above, an explanation for this is that the larger nozzle resulted in larger wetted areas. Regarding sprinkler location (Figure 7.8b), the largest spacing (3 m away from original sprinkler location) resulted in higher sensitivity of CU to low wind speeds. For wind speeds above 2.5 m s<sup>-1</sup>, all the sprinkler spacings showed a similar steep decline in CU. However, the largest spacings always resulted in the lowest CU.

#### Impacts of wind direction and green shape on irrigation performance

Figure 7.9 shows, for each green, the modelled impacts of wind speed and wind direction on CU, assuming wind directions were at 45-degree intervals and the wind speed was 5 m s<sup>-1</sup>. The variability within each boxplot reflects the different sprinkler positions and set-up. Greens with the highest sensitivity to wind direction were those which were most elongated in shape ("Green P9" and "Green H3" from Furesø GK). Differences in CU due to wind direction and green shape were only evident when the wind speed was equal or greater than 3 m s<sup>-1</sup>.

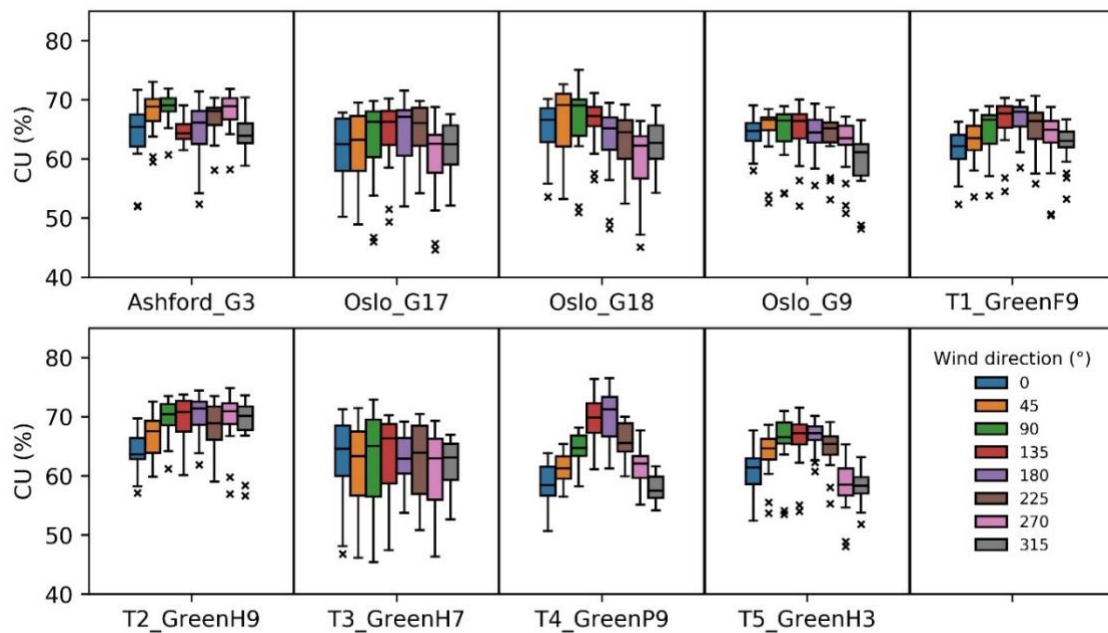


**Figure 7.9** Modelled variation in CU (%) due to wind direction and wind speed  $5 \text{ m s}^{-1}$  for each simulated green

The impacts of wind direction on CU might also be influenced by the original position of the sprinklers on the green; further research is required to understand if changes in sprinkler position help to reduce the impacts of wind direction on CU.

### 7.2.3 Discussion

The irrigation model outcomes showed the contribution of different factors on CU and IR. Overall, the results highlighted that the design of the irrigation system plays a crucial role in defining the actual IR and CU. Sprinkler location and set-up must be considered carefully when defining the irrigation strategy, as it can only be followed precisely by applying irrigation adequately. Likewise, an adequate irrigation can only be achieved by knowing the system IR. The main factors which influence system performance are discussed below.

#### Sprinkler set-up – Operating pressure

Surprisingly, the irrigation model outputs did not show a relationship between CU and different operating pressure, even under high wind speeds. This contradicts what is found in the literature, where it is reported that CU is less affected by wind at lower pressures (Darko et al., 2017). Tarjuelo et al. (1999b) reported that when

irrigation is applied under high wind and high pressure (4 to 4.8 bar) conditions using impact sprinklers, this leads to lower CU values than under similar wind conditions but with low pressure (<3 bar). In recent research, Sheikhesmaeili et al. (2016) observed that when the wind speed increases above  $4 \text{ m s}^{-1}$ , CU was more affected by operating pressure at 5 bar (CU = 66%) than 4.5 bar (CU = 73%). Dukes (2006) also reported higher irrigation uniformities in a linear move irrigation system at lower pressures as the wind speed increased. Conversely, Vories and von Bernuth (1986) concluded that although lower operating pressures led to less sensitivity of irrigation to wind, CU was generally not compromised.

In this research, the weak relationship between operating pressure and CU can be explained by two reasons. Firstly, golf rotor sprinklers generally deliver better uniformities than conventional impact sprinklers (Demirel and Sener, 2009). This could have led to the reduced influence of sprinkler set-up on CU at different wind speeds. Secondly, the range of pressures studied (4.2 and 6.0 bar) might not be sufficiently different to show CU differences under windy conditions. Further field tests under more contrasting conditions of operating pressure and wind would be useful.

In contrast, the operating pressure had a greater impact on the IR and discharge efficiency. This was reflected in the WDEL model in Chapter 5. Although a hydraulic analysis of the water distribution network was beyond the scope of this research, variations in pressure in the system will lead to fluctuations in the sprinkler operating pressure (Daccache et al., 2010). In those cases, the discharge efficiency (given by WDEL), IR and irrigation adequacy might be compromised. Zhang et al. (2013a) reported that CU was usually slightly lower when pressure fluctuations were considered in a simulated pipe network. However, it is not clear how these fluctuations would affect the CU in rotor sprinklers due to the weak relationship between pressure and CU obtained in the results of current research.

### *Sprinkler set-up – Nozzle size*

The nozzle size had a slight impact on CU, and it only was observed when wind speed was higher than  $3 \text{ m s}^{-1}$  and/or large sprinkler spacings were used. Under those conditions, the largest nozzle resulted in a higher CU. Thus, larger nozzles could be recommended for windy areas and/or when the sprinkler spacings are wide. This observation coincides with findings from Vories and von Bernuth (1986) who reported that when sprinkler spacing was enlarged, the use of smaller nozzles presented lower CU. Conversely, Sanchez et al. (2011) did not find a relationship between nozzle size and CU, with changes in CU being attributable to pressure and wind. Stambouli et al. (2014) obtained similar results, reporting that the nozzle size had a greater influence on the amount of water delivered by the sprinkler.

The simulations in this study showed that the nozzle (and operating pressure) had a high impact on IR, and therefore on the flow rate demanded by the sprinkler system. Thus, the selection of nozzle size should be driven by the capacity of the pumping station to deliver a given flow/pressure. A sprinkler set-up and spacing that provides a higher IR can be advantageous for golf since it requires a shorter set time, which is relevant as the entire turfed area needs to be irrigated in a short period so as to not interfere with play. However, a high IR might be inconvenient when soil infiltration rates are low, as this might lead to localised waterlogging and surface runoff, particularly on 'push up' clay based greens.

### *Sprinkler spacing*

The spacing between sprinklers was the most important factor affecting CU and IR. These results coincide with Montero et al. (2004). Larger distances between sprinklers resulted in a dramatic drop in CU and IR. A decline in CU when sprinklers are spaced further apart has been previously reported by various authors [e.g. (Tarjuelo et al., 1999b; Kara et al., 2008; Faria et al., 2012)]. Zhang et al. (2013a) observed that spacing had greater impact on CU than pressure variation and topography.

It is difficult to recommend an optimum irrigation spacing for greens, as their unique shape usually constrains the location and spacing of the pop-up

sprinklers. However, the results from the simulations highlighted that by not locating the sprinklers in an optimum spacing (i) CU values can be compromised, and (ii) under windy conditions, the IR on greens will be exposed to variations. The model developed in this research could be used to identify the best combination of sprinklers (number, set-up and location), facilitating the evaluation and design of irrigation systems in golf courses.

#### Wind speed

Wind speed above  $2.5 \text{ m s}^{-1}$  resulted in a dramatic reduction in CU values. These results coincide with results reported in previous research [e.g. (Dechmi et al., 2003a; Dukes, 2006; Faria et al., 2015)] that suggest that irrigation should be avoided when wind speeds exceed  $2 \text{ m s}^{-1}$ . For wind speeds above  $2.5 \text{ m s}^{-1}$ , all the sprinkler spacings modelled showed a similar steep decline in CU. These results are consistent with Dwomoh (2013), who reported that under high wind conditions, decreasing the sprinkler spacing could not significantly prevent a decrease in CU. In contrast, other investigations suggested that closer sprinkler spacings can mitigate the impact of wind on CU (Mateos, 1998; Playán et al., 2006; Sheikhesmaeili et al., 2016).

In this research, the fact that shorter distances between sprinklers did not improve CU under windy conditions could also be explained by the *edge effect*. This occurs when there is a lack of sprinkler overlap at the field boundaries (Zhang et al., 2013a). On greens, all the sprinklers are located at the “field boundaries”, i.e., there is a side of their wetted area that is not overlapped by a nearby sprinkler. Under windy conditions, the edge effect contributed to a decrease in CU even at close sprinkler spacings.

#### Wind direction and green shape

At high wind speeds, the CU varied more on greens with an irregular shape depending on wind direction. However, wind direction was less related to CU than wind speed and sprinkler location. To date, the study on the impact of wind direction on CU has been limited to agricultural sprinklers. For example, Tarjuelo et al. (1992) reported that wind direction did not affect significantly CU for sprinkler spacings of  $18 \times 18 \text{ m}$ . Conversely, in other investigations where the spacing was

not square (e.g. 12 × 18 m and 15 × 18 m), it was reported that CU varied depending on wind direction (Vories and von Bernuth, 1986; Mateos, 1998). The irrigation model developed in this study could be used to define the optimum sprinkler location and/or irregular green shapes and orientation to minimise any reduction in CU due to a dominant wind direction.

## **7.3 MODEL APPLICATION – SIMULATED IMPACTS OF IRRIGATION STRATEGY ON TURFGRASS AGRONOMY**

### **7.3.1 Methodology**

The second component within the BalliSTICS model, the STICS model, was used to quantify the impacts of irrigation strategy on turfgrass agronomy. Model outcomes to define turfgrass agronomy in response to irrigation strategy were: irrigation need (mm), actual evapotranspiration (ET<sub>a</sub>, mm), seasonal available water content (SAWC, mm), dry matter production in clippings (DMP, g m<sup>-2</sup>), drainage (mm) and leaching (g NO<sub>3</sub><sup>-</sup>-N L<sup>-1</sup>). In these simulations, a perfectly uniform irrigation (CU 100%) was considered. Irrigation strategy was assessed through irrigation depth and irrigation frequency.

- **Irrigation depth (ET<sub>p</sub> rate)** was calculated based on the potential evapotranspiration (mm) since the last irrigation event. In this research, the irrigation required to achieve ET<sub>p</sub> was assumed as the irrigation needs to reach field capacity, and expressed as 1.0 ET<sub>p</sub>. The remaining irrigation depth strategies were expressed as a proportion of ET<sub>p</sub>. For instance, for 0.6 ET<sub>p</sub> strategy, the irrigation applied was a 60% of irrigation needed for 1.0 ET<sub>p</sub> depth strategy. Irrigation strategies below 1.0 ET<sub>p</sub> was referred to as deficit irrigation. In contrast, in 1.5 ET<sub>p</sub> irrigation depth, irrigation was a 150% relative to 1.0 ET<sub>p</sub> depth strategy.
- **Irrigation frequency** was expressed as the number of irrigation events per week.

Table 7.7 shows the simulations run by the BalliSTICS model, combining: (i) irrigation depth strategies from 0 ET<sub>p</sub> (rainfed) to 1.5 ET<sub>p</sub>; (ii) irrigation frequency 1, 2, 3 and 7 events per week; (iii) weather data from 1997 to 2016 at Landvik

weather station; and (iv) simulations with and without rainfall. This last option aimed to understand the influence of rainfall on the impacts of the different irrigation strategies.

**Table 7.7** Number of simulations of turfgrass agronomy for perfect irrigation uniformity

<b>Variable</b>	<b>Alternatives</b>	<b>Total</b>
ETp rate	0 to 1.5, at 0.1 intervals	16
Irrigation frequency	1, 2, 3 and 7 irrigations per week	4
Simulation period	1997 to 2016	20
Rainfall	Yes / No	2
<b>Total</b>		<b>2560</b>

The simulations were run using the plant parameters estimated in Chapter 6 for water balance and biomass production in clippings in *Study 1*, and nitrogen leaching in *Study 2*, which are presented in Annex-4. The soil was assumed to be 0.2 m depth and constructed following the USGA (2004) specifications. The volumetric soil water content (VSWC) at FC was determined to 20% (v/v), corresponding to 40 mm water, from which 22.4 mm were available for the plant (difference between FC and permanent wilting point water content). The bulk density was 1.55 g cm<sup>-3</sup>. Clippings were removed automatically. The fertilisation was applied every week corresponding to a seasonal rate of 15.0 g N m<sup>-2</sup>.

### **7.3.2 Results**

#### *Modelled impacts of irrigation strategy on irrigation needs*

Irrigation needs based on the ETp varied for each year and irrigation strategy. Figure 7.10 shows the simulated irrigation applied for strategies designed to apply 0.3, 0.6, 1.0 and 1.5 ETp. The variability within each boxplot is explained by the variability in irrigation needs between years and, to a lesser extent, irrigation frequencies.



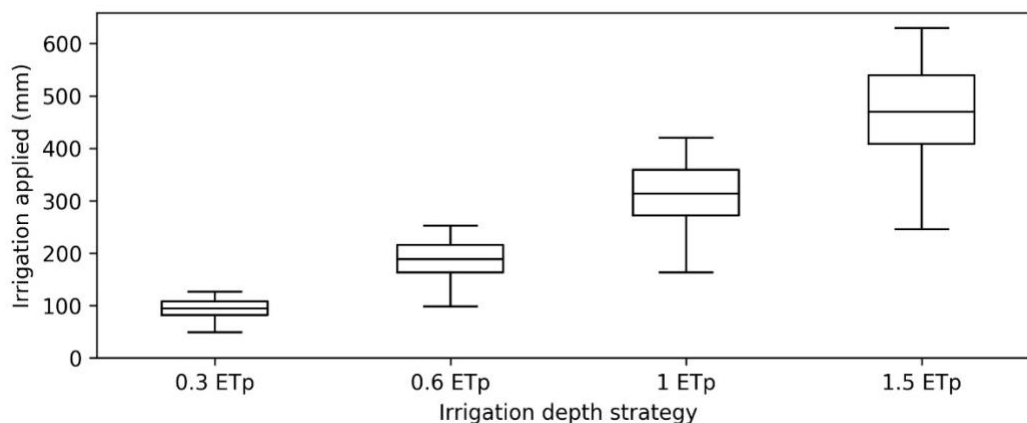


**Figure 7.10** Boxplots showing irrigation applied (mm) between May and September for each irrigation depth strategy (ETp). Each boxplot is representative of different years and irrigation frequencies.

The average application between 1997 and 2016 for 1.0 ETp irrigation strategy was 312 ( $\pm 59$ ) mm. The average irrigation need was 250 ( $\pm 46$ ) mm for 1.0 ETp once per week; while daily irrigations increased the average irrigation needs to 358 ( $\pm 46$ ) mm. The difference in irrigation needs between irrigation frequencies was likely to be due to two main factors. Firstly, longer intervals between irrigation events increases the chance that plants will receive water from rainfall between individual events. In these instances, the supplementary irrigation needs are reduced because the soil is replenished by rainfall. Secondly, the STICS model computes a higher evapotranspiration when the soil water content is closer to field capacity, while plant water evapotranspiration is reduced when the soil water content decreases. Thus, when irrigation was applied more frequently, the soil water content was closer to field capacity more often, and therefore water consumption was higher.

Table 7.8 shows the average irrigation needs, ETo and rainfall between May and September for the 1.0 ETp strategy. There is a strong correlation between modelled irrigation needs and ETo ( $R^2=0.78$ ). The correlation between irrigation needs and number of rainfall events was  $R^2=0.48$  and for irrigation needs and seasonal rainfall  $R^2=0.26$ . The strong influence of rainfall events on irrigation needs compared with seasonal rainfall suggests that a few heavy rain events during a season will not be reflected in a substantial reduction of irrigation needs because most water is not stored in the soil. This is accentuated on greens where

there is a low water storage capacity due to the characteristic shallow, sandy soil of these areas.

**Table 7.8** Ranked Summer irrigation needs (mm) for a 1.0 ETp strategy, ETo, May to September rainfall and number of rainfall events between 1997-2016. Numbers in brackets are standard deviation for different irrigation frequencies.

<b>Year</b>	<b>Irrigation need mm</b>	<b>ETo mm</b>	<b>Rainfall mm</b>	<b>Rainfall events</b>
2016	234(±46)	338	472	52
2011	238(±55)	382	784	70
1998	250(±41)	363	589	59
1999	275(±30)	376	778	74
2002	282(±37)	394	492	60
2007	290(±61)	409	620	53
2013	299(±57)	411	601	50
2015	301(±42)	410	830	68
2005	301(±43)	403	448	63
2000	305(±39)	391	583	61
2012	306(±57)	403	494	53
2009	312(±64)	437	552	58
2003	315(±39)	398	488	55
2001	342(±33)	415	424	48
2008	356(±58)	449	582	48
2010	360(±52)	425	374	40
2004	363(±38)	425	556	50
1997	368(±27)	433	356	46
2006	369(±46)	451	452	47
2014	377(±48)	441	482	46
<b>Average</b>	<b>312</b>	<b>408</b>	<b>548</b>	<b>55</b>

Figure 7.11 shows actual water use by turfgrass (actual evapotranspiration, ETa) depending on the total amount of water applied (mm) for all simulated irrigation strategies and years (Table 7.7). The results are split between outputs from simulations including rainfall, and outputs assuming “no-rainfall”.

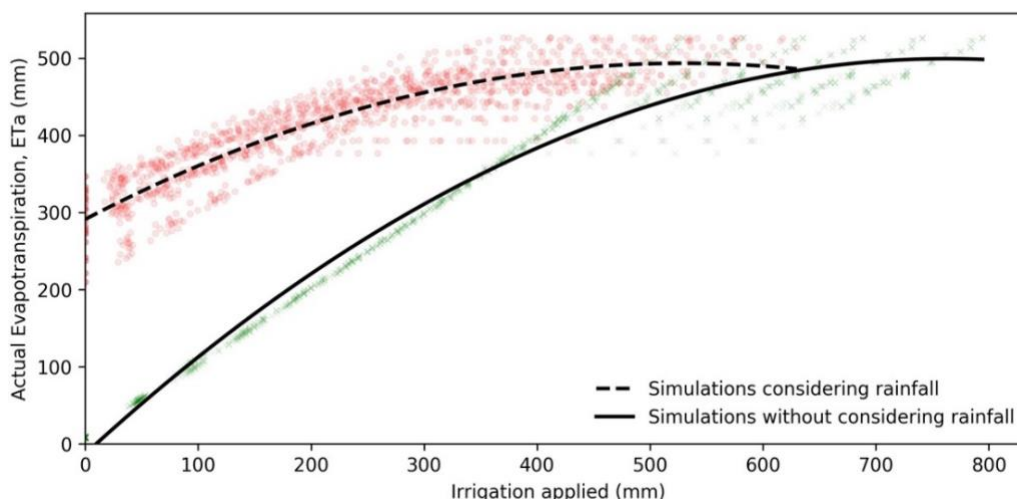


**Figure 7.11** Comparison between irrigation needs and ETa by the plant for simulations considering rainfall (red dots, dashed line) and no rainfall (green dots, continuous line).

For simulations considering rainfall, a gradual increment in supplementary water application led to a general increase in ETa. However, the ratio  $[\Delta ETa/\Delta Irrigation]$  was lower than 1, meaning that not all the irrigation applied was used by the plant. Conversely, for simulations assuming “no-rainfall”, the relationship between irrigation and ETa was linear ( $[\Delta ETa/\Delta Irrigation] = 1$ ) until ETa reached its maximum, where extra water applications did not lead to an increase in ETa. In simulations considering rainfall, the maximum ETa was achieved for lower irrigation amounts (and lower ETp strategy) than in the ‘no-rainfall’ cases. The weaker correlation between irrigation and ETa for simulations with rainfall shows that rainfall might be a source of uncertainty in the prediction of the most efficient irrigation strategy, as water needs on turfgrass for an irrigation strategy will vary depending on the climatic year.

#### Modelled impacts of irrigation strategy on average seasonal available water content

The soil water content (SWC) varied between different irrigation strategies and years. In this section results from the average seasonal available water content (SAWC, mm), i.e. the water depth stored between field capacity and the wilting point are presented in the first 0.2 m of soil. Figure 7.12 shows the results of the SAWC for different irrigation strategies and years. The variability within each boxplot is affected by irrigation frequency and year. The SAWC increased linearly from rainfed to field capacity irrigation strategy (1.0 ETp). From this point

onwards, increments in ETp strategy did not alter the SAWC. This was due to excess water beyond field capacity being lost to drainage. Considering all years, the average SAWC for the rainfed treatment was 10.4( $\pm$ 1.8) mm, 12.2( $\pm$ 1.8) mm for 0.3 ETp, 15.3( $\pm$ 1.5) mm for 0.6ETp, and 20.4( $\pm$ 0.3) mm for 1.0 ETp.

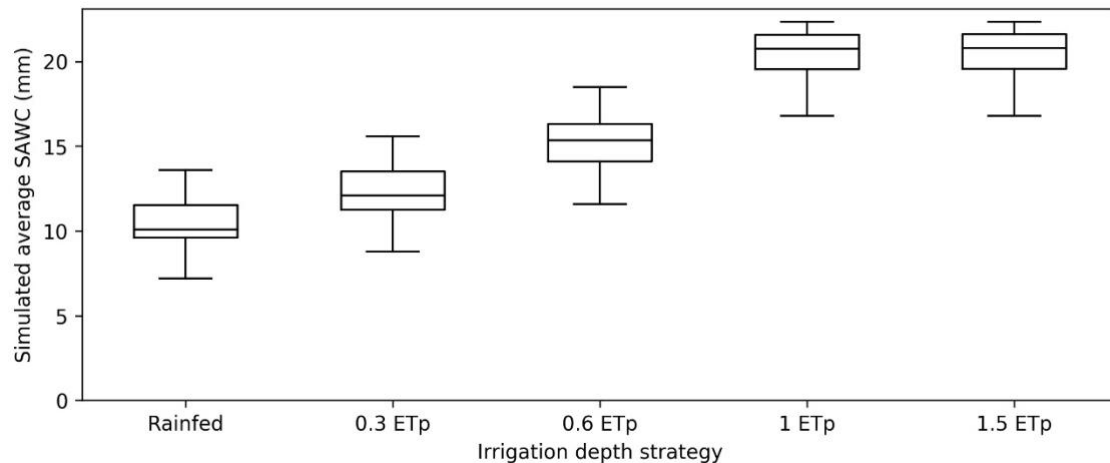


**Figure 7.12** Boxplots of seasonal available water content (SAWC, mm) between May to September for different irrigation depth strategy. Each boxplot is representative of different years and irrigation frequencies.

Regarding the impacts of irrigation frequency, the Tuckey HSD analysis ( $\alpha=0.05$ ) showed a statistical difference between irrigation frequencies of 1 and 7 irrigations per week on SAWC for treatments of 0.6 ETp and above. For irrigation strategies above 0.7 ETp, the analysis showed statistical differences between 1 and 3, and 2 and 7 irrigations per week. For 0.9 ETp or higher, the average SAWC was significantly different between all the irrigation frequencies. However, the irrigation depth strategy (ETp) resulted in a greater impact on SAWC than irrigation frequency.

The outputs from STICS simulations highlight the importance of rainfall on SAWC, especially for deficit irrigation strategies. For “no-rainfall” and deficit irrigation conditions, the soil water content never returned to field capacity. In contrast, rainfall appears to have a “restarting effect” on soil water content for deficit irrigation treatments, refilling the soil water content to field capacity after rainfall. This can alleviate the negative impacts of severe deficit irrigation; however, it can also negatively impact on turf management when specifically trying to follow a deficit irrigation strategy. This is relevant in red fescue

management, where frequent irrigation to field capacity might lead to an increase of invasion of annual bluegrass (*Poa annua* L.) and moss (Calvache et al., 2017; Chen et al., 2018).

Modelled impacts of irrigation strategy on drainage

The STICS model was used to study the relationships between irrigation strategy and drainage. For the simulated greens, drainage represented water that moved below the root-zone when the FC in in the first 0.2 m soil depth. Because of the high sand proportion, porosity, and saturated hydraulic conductivity of the USGA (2004) rootzone construction, no runoff was considered in simulations, and therefore any excess water was lost through drainage.

Figure 7.13 shows the relationship between accumulated drainage and rainfall for each simulated year. Rainfall explained 78% of the drainage variability. For the area studied, drainage will always occur irrespective of the amount of supplemental irrigation applied.

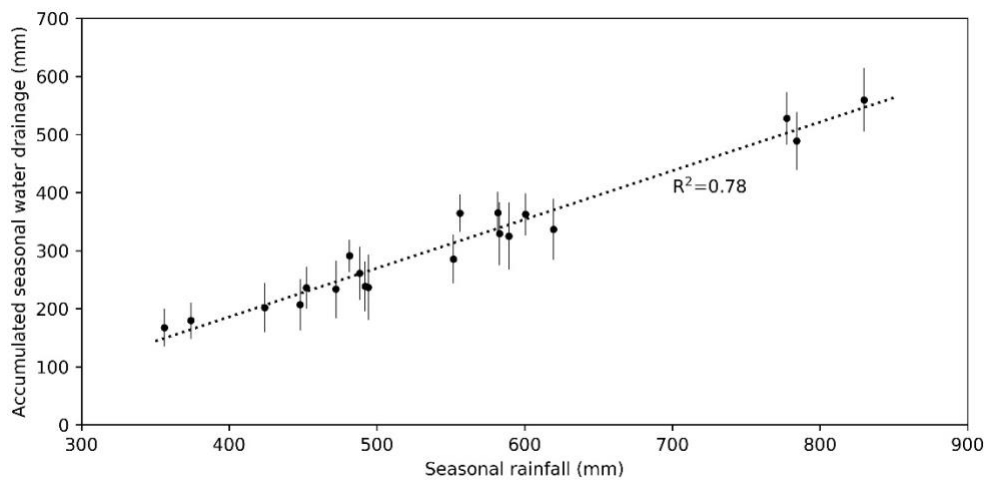


**Figure 7.13** Accumulated drainage between May and September for irrigation strategies from 0 to 1.0 ETp and irrigation frequencies of 1, 2, 3 and 7 irrigation events per week. Each dot represents the average drainage for all irrigation treatments within each year (1997 to 2016). Error lines represent the standard deviation within each year.

Figure 7.14 shows the variation in drainage for different irrigation strategies. Although irrigation had a lower influence on drainage than rainfall, larger and more frequent irrigation also contributed to increase drainage. For irrigation strategies below 1.0 ETp, the simulated drainage increased slightly as ETp increased. For irrigation beyond 1.0 ETp strategy, drainage increased linearly

with total irrigation applied. For the 20 simulated years, the average increase in drainage with respect to rainfed treatments (0 ETp) was 14.2( $\pm$ 8.1)% for 0.3 ETp irrigation level, 28.5 ( $\pm$ 13.6)% for 0.6 ETp, 61.9( $\pm$ 25.2)% for 1.0 ETp and 135.7( $\pm$ 57.0)% for 1.5 ETp.

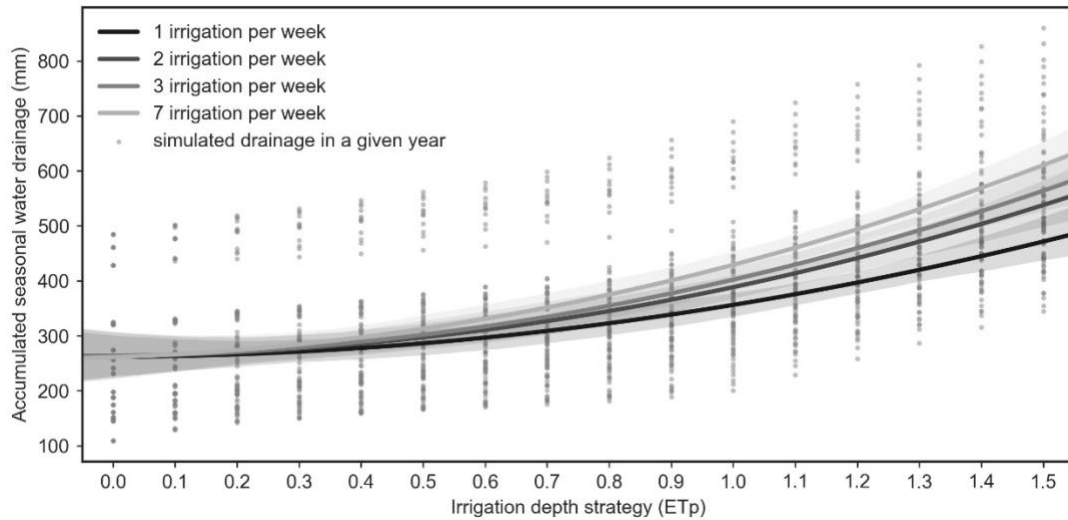


**Figure 7.14** Curve fitting of the simulated drainage in relation to irrigation amount and frequency between 1997 and 2016. Grey envelope shows the 95% confidence interval of the regression curve. Dots represent the results of individual simulations

Irrigation frequency had a smaller impact on drainage than irrigation depth strategy. Indeed, the Tuckey HSD analysis only showed statistically significant differences between irrigation frequency and drainage for weekly and daily intervals, and irrigation depth strategies greater than 1.2 ETp.

#### Modelled impacts of irrigation strategy on dry matter production of clippings

Figure 7.15 shows the relationship between irrigation strategy and DMP clippings. Variability within boxplots correspond to the effects of different years and irrigation frequency. It is observed that only irrigation below 0.6 ETp significantly reduced DMP. Above this level, the variation in DMP was not significant. The rainfed treatments (0 ETp) resulted in the lowest DMP with an average of 179 g m<sup>-2</sup>. The accumulated DMP then increased with irrigation depth strategy levelling at 0.6 ETp. At 0.6 ETp, the incremental rate of DMP with respect to irrigation was reduced until it reached a maximum at 1.0 ETp, with an average DMP of 238 g m<sup>-2</sup>. The values of DMP for this irrigation depth varied depending on irrigation frequency, ranging between 217 g m<sup>-2</sup>, irrigating once per week, and 269 g m<sup>-2</sup>,

when irrigation was applied on a daily basis. From 1.0 ETp to 1.5 ETp, the DMP decreased slightly but not significantly, dropping by on average 3%.

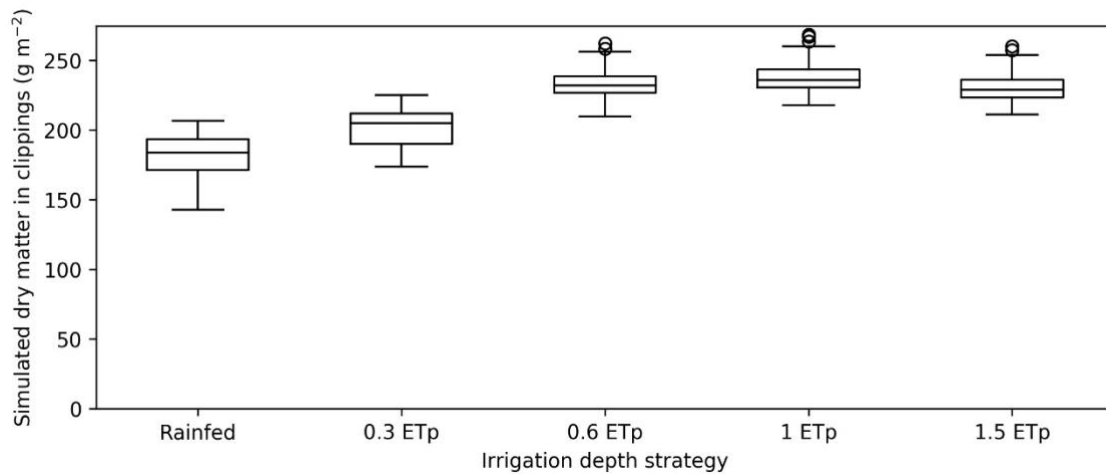


**Figure 7.15** Boxplots showing accumulated dry matter production in clippings (DMP,  $\text{g m}^{-2}$ ) between May and September for different ETp treatments. Each boxplot is representative of different years and irrigation frequencies.

Irrigation frequency was shown to have a lower impact on DMP than irrigation depth strategy. When the results of the different irrigation frequency treatments were compared, the Tuckey HSD analysis only showed a significant difference between one irrigation per week treatments with 2, 3 and 7 irrigations per week, from 0.5 ETp onwards. That difference was greater as the proportion of ETp applied was higher.

Figure 7.16 shows the simulated DMP for all irrigation treatments for rainfall and no rainfall simulations. In simulations where rainfall was excluded, very little DMP was produced at very low irrigations. As the irrigation applied increased, the ratio of  $\Delta\text{DMP}/\Delta\text{irrigation}$  also increased rapidly until reaching its maximum, approximately at 300 mm for the region studied. From that point, the DMP at the end of the simulated period remained almost constant regardless the increase of irrigation applied. Conversely, treatments considering rainfall resulted in DMP regardless the water applied. These results highlight that, for the study location, rainfall reduces considerably the impacts of high deficit irrigation on reduced DMP at the end of the season. Due to the characteristic high rainfall in humid climates, a moderate deficit irrigation strategy (0.6 ETp) seems to be sufficient to avoid a reduction in DMP due to plant water stress.

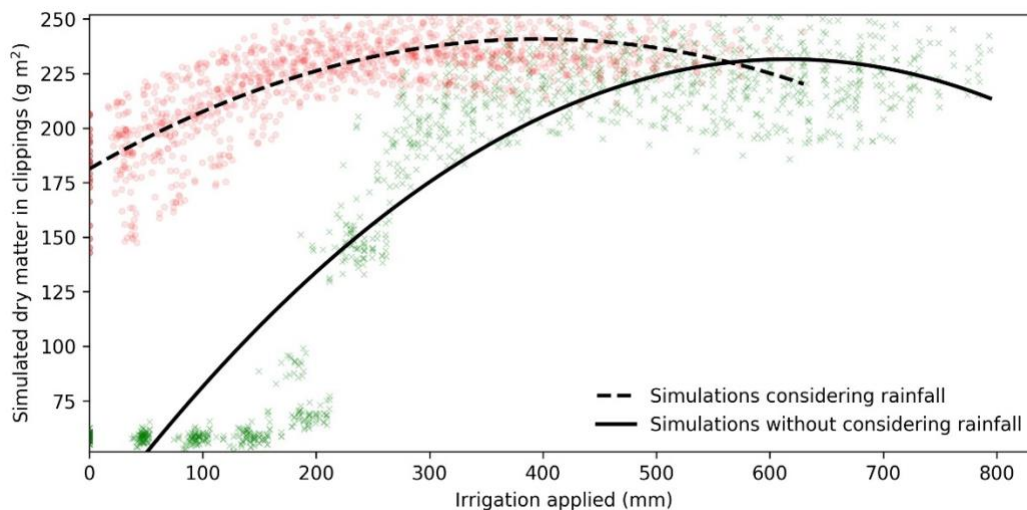


**Figure 7.16** Comparison between irrigation needs and simulated DMP in clippings for simulations considering rainfall (red dots, dashed line), and no rainfall (green dots, continuous line).

The small reduction in DMP for irrigation beyond field capacity is likely to be due to an increase in drainage. This produced an increase in leaching and subsequent reduction of nitrogen available in the soil for plant growth. This phenomenon is developed in more detail below.

#### Modelled impacts of irrigation strategy on leaching

The simulated nitrate leaching fluctuated between years and irrigation strategy, varying from 0.45 to 1.91 ( $\text{g NO}_3^- \text{-N m}^{-2}$ ). The greater variation in leaching was observed between years. This indicates that leaching was more closely related to annual (climatic) conditions. The close relationship between years and leaching is explained because of the relationship between drainage and leaching. As shown in Figure 7.14, drainage varied depending rainfall during that given year. Thus, the high rainfall characteristic in the study location, and consequent drainage, was the main variable affecting leaching.

Within a given year, irrigation strategy also affected leaching. Figure 7.17 shows the simulated leaching for different ETp strategies and irrigation frequencies. It is observed that, on average, the minimum leaching was achieved at irrigation depth strategies comprised between 0.6 and 1.0 ETp. Irrigation strategies below 0.6 ETp or above 1.0 ETp generally resulted in higher levels of leaching. Thus, two sources of leaching as affected by irrigation strategy were identified: (i)



leaching associated with over-irrigation (beyond 1.0 ETp), and (ii) leaching associated with severe deficit irrigation.

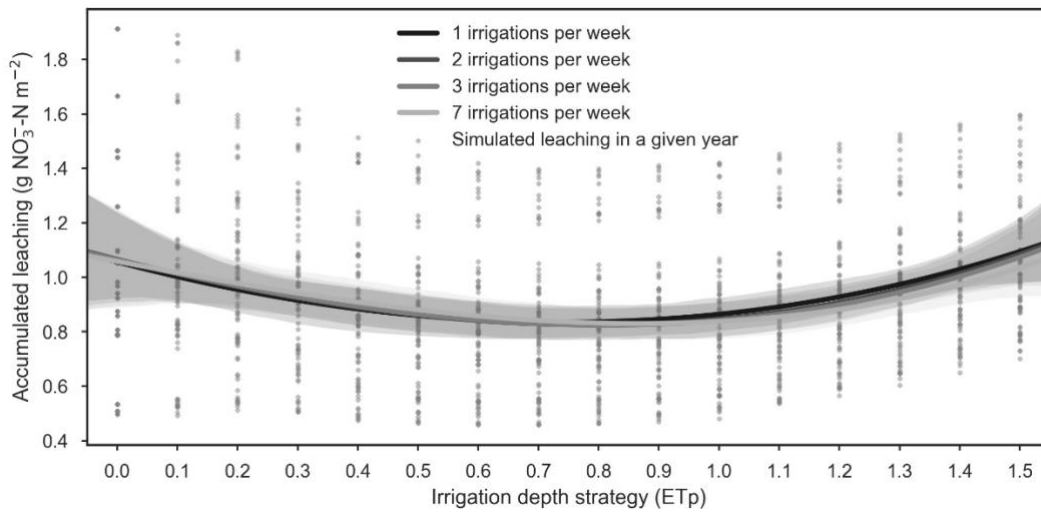


**Figure 7.17** Curve fitting of the simulated leaching in relation to irrigation level and irrigation frequency during the period 1997-2016. Grey area behind lines show the 95% confidence interval of the regression curve. Dots represent the results of individual simulations

The increase in leaching associated with over-irrigation resulted from an increase in drainage due to irrigation beyond field capacity. At these ETp rates, the relationship between drainage and leaching for over-irrigation treatments was linear ( $R^2=0.95$ ). An increase of the irrigation depth strategy from 1.0 ETp to 1.5 ETp resulted on an average increase of a 40.2% in drainage and a 23.9% in leaching. In contrast, leaching associated with irrigation rates below 0.6 ETp appeared in most simulated years, even though drainage was lower than for higher irrigation rates. The increase in leaching at low irrigation ETp rates was attributed to a reduction in DMP. As shown previously, the STICS model predicted a reduction in DMP for low ETp strategy when water became the limiting factor for leaf extension. In STICS, the water stress level (variable *TURFAC*) is linearly related with delays in plant development and the reduction of leaf growth. Lower growth rates imply a reduction of the plant nitrogen demand (*DEMAND(I)*), leaving more soluble nitrogen in the soil available to leach with drainage. Following this assumption, the adoption of a high deficit irrigation strategy during drought periods might increase the soluble nitrogen in the soil due to reduced plant nitrogen demand. Under these conditions, a high rainfall event might trigger an increase in nitrate losses in leaching.

Figure 7.18 shows the relationship between leaching and DMP for different irrigation strategies. For the lowest DMP (which coincides with the lowest ET<sub>p</sub> rates), leaching was higher than for higher ET<sub>p</sub> strategy. The increase of ET<sub>p</sub> strategy was accompanied by higher DMP and lower leaching. This reduction in leaching was associated to higher plant nitrogen uptake, in detriment of the nitrogen available in the soil. Irrigation beyond this optimum point resulted in a noticeable increase of leaching due to drainage. This increase in leaching was also reflected in a slight reduction in DMP, related to the lower availability of nitrogen in the soil.

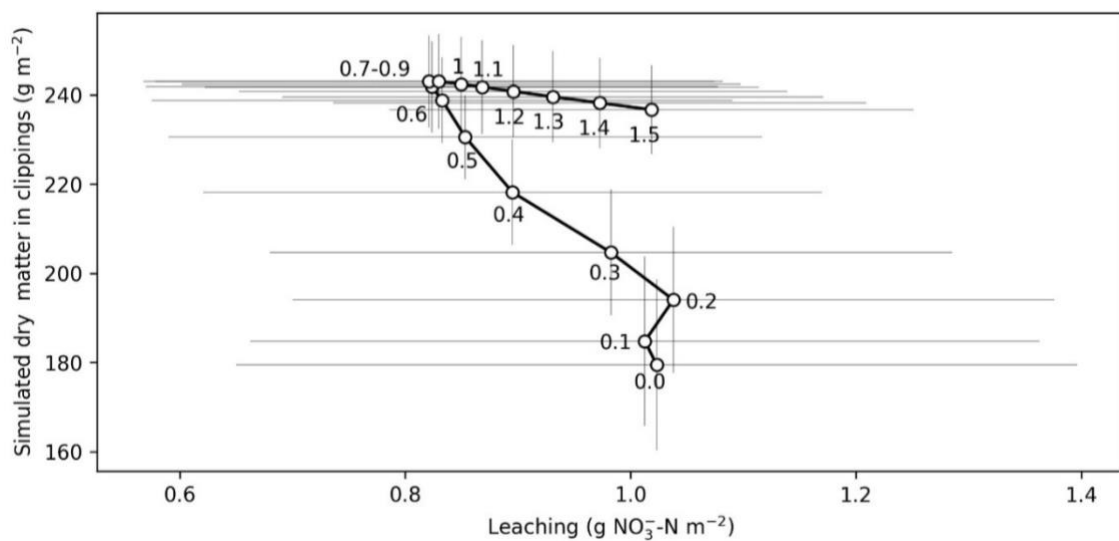


**Figure 7.18** Relationship between leaching and dry matter in clippings according to ET<sub>p</sub> strategy between 1997 and 2016. Numbers correspond to ET<sub>p</sub> strategy and error bars represent the standard deviation of each variable

It is worth noting that the STICS model was not calibrated with data that showed the relationship between reduced DMP and increased leaching at low irrigation levels. In addition, datasets for calibration for DMP and leaching came from different studies. Thus, the results from this relationship should be considered as “conceptual”. However, these findings are fairly consistent with data reported in previous research (Gómez-Armayones et al., 2018).

No year or treatment showed values of average nitrogen concentration in drainage higher than 10 mg NO<sub>3</sub>-N L<sup>-1</sup> which is defined by the United States Environmental Protection Agency (USEPA, 2018) as the limit for drinking water. The average yearly nitrate concentration in leaching for all simulations was 2.7 (±0.9) mg NO<sub>3</sub>-N L<sup>-1</sup>. The maximum nitrate concentrations (8.9 mg NO<sub>3</sub>-N L<sup>-1</sup>)

were obtained for low irrigation rates and years with the lower summer rainfall (and drainage), while the lowest concentration was obtained for over-irrigation treatments. Although over-irrigation tended to increase leaching, the higher drainage observed in those cases reduced considerably the amount of leaching per volume of water in drainage.

### **7.3.3 Discussion**

The results from the STICS model showed that under perfect irrigation uniformity moderate deficit irrigation (0.6 ETp) was the most appropriate strategy. At 0.6 ETp, the water use, drainage and leaching were reduced considerably with respect to higher ETp rates, but with minor impacts on DMP. By spreading the irrigation events, irrigation needs (and therefore water use) also decreased. However, irrigation frequency had less influence than ETp rate on turfgrass development. A recommended irrigation frequency might vary depending on rainfall and other agronomic aspects including root development, weed infestation (especially *Poa annua* and moss (Chen et al., 2018)), the time available for irrigation and time of year. However, these factors were not considered in the model simulations. Jordan et al. (2003) recommended increasing the irrigation frequency during periods when precipitation was limited and turf growth was dependent on irrigation. In this research, each simulation used the same irrigation strategy throughout the season, and further work is required to model the implications of changing irrigation strategy across the season.

#### *Dry matter production in clippings*

The similar growth rates between 0.6 and 1.0 ETp irrigation was due to rainfall (548 ( $\pm$ 130) mm) which supplied sufficient water to buffer the effects of the moderate deficit irrigation on plant water stress and DMP. Although a slight reduction in SAWC when using 0.6 ETp was observed, it was not sufficient to produce a significant impact on DMP. These results suggest that by maintaining the soil water content at moderate deficit levels might be desirable to reduce water use, while maintaining an actively growing turfgrass. In contrast, severe deficit irrigation (0.3 ETp) led to a notable reduction in DMP.

However, DMP response to deficit irrigation presented some variation from one year to another depending on rainfall. During dry years, the irrigation strategy showed a stronger influence on DMP. Fontanier et al. (2017) observed that in a year with high rainfall, deficit irrigation treatments did not lead to reductions in turfgrass quality. Jordan et al. (2003) also reported that bentgrass species did not show significant differences between irrigation frequencies (from daily irrigations to every four days) during periods with frequent rainfall. The STICS model outputs did not simulate turfgrass quality. However, previous researchers observed that a reduction of turfgrass quality due to irrigation shortage is accompanied by a reduction in DMP (Qian and Fry, 1996; Bañuelos et al., 2011; Candogan et al., 2014, 2015; Telenko et al., 2015). As shown in Chapter 4, the threshold at which a reduction in turf growth negatively affect turfgrass quality will vary depending on the location, turf species and management practices. For this reason, it was not possible to provide an estimate of turfgrass quality based on the STICS outputs, and further research is required to quantify impacts on turfgrass quality. In recent research, Wilkerson et al. (2015) developed a model to simulate turfgrass quality as a function of deficit irrigation. However, this model does not take into account variations in DMP. Improvements in the model by Wilkerson et al. (2015) could be implemented within STICS to evaluate the decline in turf quality as influenced by a reduction in irrigation and DMP.

### *Nitrogen fate*

A moderate reduction in turfgrass growth might be desirable in terms of reducing the level of turfgrass maintenance and thickness and organic matter content in the thatch layer (Gaussoin et al., 2013), which has direct implications for playability. However, an excessive reduction in DMP due to water shortage can not only reduce turfgrass quality, but will also decrease the plant N uptake (Barton et al., 2006a; Paré et al., 2006; Paulino-Paulino et al., 2008; Wu et al., 2010). In this research, a reduction in DMP led to a surplus of N in the soil as it was not used by the plants. Under these conditions, rainfall events tended to saturate the soil, leading to drainage and nitrate leaching. This phenomenon is of special interest in golf greens since they are constructed mainly from sand, with a shallow depth, low organic matter content and low moisture retention (Shuman, 2001;

Bigelow et al., 2013; Frank et al., 2013). It is important to recognise that this relationship was obtained from STICS model calibrated with two separate datasets, one relating DMP and another relating leaching. Nonetheless, findings from the systematic review (Chapter 4) are consistent with suggestions based on the BalliSTICS outputs.

Previous research has shown an increase in leaching with reduced DMP in turfgrass due to different factors such as plant dormancy (Barton et al., 2009), to recently established turfgrass (Barton et al., 2006a), to the ability of some turfgrass species to develop deeper roots (Bowman et al., 1998; Paré et al., 2006) and to the influence of cold stress or disease injury (Telenko et al., 2015). However, no literature reports on the increased likelihood of leaching due to reduced DMP as a response to severe deficit irrigation followed by heavy rainfall events. This is important for turf irrigation in humid regions and, as stated above, further research is needed to validate the modelled results in field.

Recently, a new approach to define fertilisation based on turfgrass growth potential and soil nutrient content known as *Minimum Levels for Sustainable Nutrition Soil Guidelines* (MLSN) is gaining popularity within the golf industry (Woods, 2013; PaceTurf, 2014). This approach suggests that N fertilisation should be driven considering the soil N content and the DMP rate. Growth-driven fertilisation could not only reduce the N applications (Woods, 2016), but also reduce the environmental risks associated with leaching. Ericsson et al. (2012b) suggested that turfgrass N fertilisation could be driven by solar radiation and temperature, two of the factors more closely related with plant growth rates (Jones and Rotenberg, 2011). In the current study, the same fertiliser rates (weekly application adding up to  $15.0 \text{ g N m}^{-2} \text{ year}^{-1}$ ) was used in simulations for all irrigation treatments. However, by adopting a fertilisation driven by DMP instead of by fixed schedule would probably have reduced the nitrate leaching for severe deficit irrigation treatments, where DMP (and N plant demand) was lower. Thus, it is worth suggesting that a reduction in DMP produced by water shortage should be accompanied by a reduction in fertiliser applications to reduce the leaching risk. This highlights the importance of establishing an adequate balance

between irrigation and the fertilisation strategy in humid regions, where drainage and associated leaching will always occur due to high rainfall.

Indeed, in the studied location rainfall was responsible for most of drainage and leaching. This is important as it might differ from drier regions where irrigation might have more impact on drainage and leaching due to: (i) its higher proportion as an input in comparison to rainfall, and (ii) the higher irrigation needs. The relationship between rainfall and leaching in turfgrass has been previously reported in the literature. Shaddox et al. (2016a) found a higher risk of leaching from rain during winter and early spring, when active turf growth was minimal, and soil moisture tended to be higher because of lower evapotranspiration rates. Erickson et al. (2010) reported a strong correlation between annual nitrate leaching and precipitation. The same authors concluded that sod installation when rainfall was frequent resulted in increased nutrient leaching losses and should be avoided if possible. Fontanier et al. (2017) found that deficit irrigation treatments in St. Augustinegrass under high fertilisation rates resulted in higher nitrate concentrations in runoff after heavy rainfall events. However, these authors focused on nitrate runoff rather than leaching and did not assess its relationship with DMP. Morton et al. (1988) reported that under high soil water conditions due to frequent and heavily irrigated turf, rainfall could result in significant leaching losses. These results are consistent with the STICS model outputs, which showed that rainfall on under or over-irrigated turf might lead to increased leaching. For humid regions it is therefore recommended that soil moisture conditions should be maintained at adequate levels that ensure a non-stressed, actively growing turfgrass; but without excessive soil moisture; which reduce water use and consequent drainage and leaching risk. In the current research, this was achieved by following a moderate deficit irrigation strategy.

The modelled annual concentrations of nitrate did not exceed the threshold for nitrate in drinking water ( $10 \text{ mg NO}_3\text{-N L}^{-1}$ ) (USEPA, 2018). These results are consistent with previous studies on turfgrass for golf (Quiroga-Garza et al., 2001; Carey et al., 2012) which reported that nitrate leaching in turfgrass rarely exceeds the USEPA limits for drinking water. For Landvik the modelled nitrate

concentrations tended to be around ten times lower than the USEPA limit, which was influenced by the high levels of drainage. Thus, N losses could be more critical because of decreased N application efficiency (N used by plant per unit of N applied) and economic losses rather than because of an actual risk to the environment or to human health due to excess of nitrate limit for drinking water.

Conceptual relationship between irrigation, drainage, DMP and leaching

Figure 7.19 summarises a conceptual relationship between irrigation depth, drainage, DMP, nitrate leaching, and the DMP/nitrate leaching rate based on the outputs from the modelled simulations. For clarity, the scale of all variables shown on in the y-axis have been normalised, from 0 to 1, where 0 is the minimum and 1 the maximum value for each parameter. Irrigation frequency is not shown as its impact on turfgrass performance was lower than for irrigation depth.

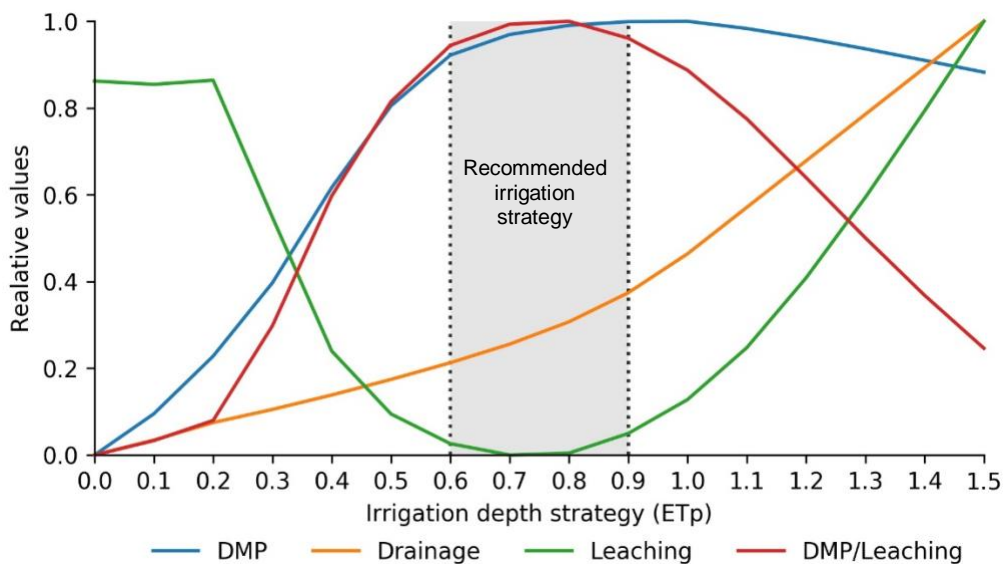


**Figure 7.19** Conceptual relationship between dry matter production (DMP), drainage, leaching and DMP/leaching rates for different irrigation depth strategies (ETp) under Northern European climate conditions.

It is observed that the most efficient irrigation strategy was one where irrigation was applied between 0.6 and 0.9 ETp. Between these irrigation depth strategies were the most efficient relationship between DMP and leaching (*DMP/Leaching*); while drainage was notably lower than at higher irrigation depths. Irrigating between 0.5 and 0.6 ETp slightly reduced the total water applied and drainage, but also reduced the *DMP/Leaching relationship*. It is important to highlight that these relationships are based on modelling and therefore are considered as being

“conceptual” relationships relevant to regions with a similar climate to the location studied, and might not be representative in drier regions.

## **7.4 MODEL APPLICATION – SIMULATED IMPACTS OF IRRIGATION MANAGEMENT ON TURFGRASS AGRONOMY**

### **7.4.1 Methodology**

The third block of simulations involved the application of the BalliSTICS model to study the impacts of irrigation management on the turfgrass system. In this section, the term *irrigation management* was assessed as the combination of irrigation system performance, strategy and scheduling method. A total of 1760 irrigation heterogeneity profiles in the form of cumulative distribution function (CDF) were used, for a reference green (“Furesø F9”). To reduce the number of simulations and computing time, the number of irrigation treatments were reduced to 3 (0.3, 0.6 and 1.0 ET<sub>p</sub>), two irrigation frequencies (one and three irrigations per week), plus a rainfed treatment. The number of years simulated was reduced from 20 to 3 to reflect a typical ‘average’, ‘dry’ and ‘wet’ year. For the average year, data for 2012 was used with summer rainfall of 494 mm between May and September. For the dry year, 1997 was used, with rainfall 356 mm. Finally, the wet year used climate data from 2011, then the rainfall was 782 mm. The simulations were also run for a hypothetical year assuming no rainfall, but weather conditions experienced in 1997. A third scheduling approach was included in this block of simulations. This was linked to irrigation heterogeneity, and referred to as *scheduling method*. The two approaches are:

- **IS<sub>AVE</sub> scheduling method.** This assumed application of an average amount of water corresponding to  $p = 0.5$  in the CDF.
- **IS<sub>DRIEST</sub> scheduling method.** This assumed the application of the water requirement in the driest area, corresponding to  $p = 0.1$  in the CDF. The justification of this scheduling method was because, in practice, many golf courses base their irrigation schedule based on the dry spots (Huck and Zoldoske, 2006).



To simplify the analysis, the BalliSTICS model outputs were grouped according to irrigation uniformity:  $CU > 80\%$ ,  $70\% < CU < 80\%$ ,  $60\% < CU < 70\%$ , and  $CU < 60\%$ .

The number of simulations and combinations of irrigation strategies, irrigation profiles, irrigation methods and rainfall patterns are summarised in Table 7.9.

**Table 7.9** Number of simulations of turfgrass agronomy regarding different irrigation strategies, different irrigation heterogeneity profiles and rain patterns

Irrigation depth	Irrigation frequency	Irrigation heterogeneity profiles	Rain patterns	Total
<b>Based on IS<sub>AVE</sub> scheduling method</b>				
Field capacity – 1.0 ET <sub>p</sub>	3 per week	1760	4	7008
	1 per week	1760	4	7008
Moderate deficit irrigation – 0.6 ET <sub>p</sub>	3 per week	1760	4	7008
	1 per week	1760	4	7008
High deficit irrigation – 0.3 ET <sub>p</sub>	3 per week	1760	4	7008
	1 per week	1760	4	7008
<b>Based on IS<sub>DRIEST</sub> scheduling method</b>				
Field capacity - 1 ET <sub>p</sub>	3 per week	1760	4	7008
	1 per week	1760	4	7008
Moderate deficit irrigation – 0.6 ET <sub>p</sub>	3 per week	1760	4	7008
	1 per week	1760	4	7008
High deficit irrigation – 0.3 ET <sub>p</sub>	3 per week	1760	4	7008
	1 per week	1760	4	7008
Rainfed	-	-	4	4
<b>Total</b>				<b>84100</b>

Finally, the BalliSTICS model was used to assess the differences in turfgrass agronomy when irrigation is applied at different times of the day. Some studies have reported differences in wind, relative humidity and temperature between day and night (Playán et al., 2005; Yacoubi et al., 2010; Sadeghi et al., 2017), which might impact on golf course irrigation performance. Simulations were therefore conducted considering the variation in wind speed for different time-slots of day. For this, hourly wind speed, temperature and relative humidity data from the weather station at Landvik were used.

## 7.4.2 Results

Results from the BalliSTICS model showing the impacts of irrigation management (irrigation heterogeneity, strategy and scheduling method) on turfgrass are summarised below.

### Modelled impacts of irrigation management on water applied on greens

Figure 7.20 shows the variation of water applied inside the green ( $p=0.1$  to  $0.9$  of the CDF) with respect to simulations where perfect uniformity was assumed as affected by non-uniform irrigation and irrigation scheduling ( $IS_{AVE}$  and  $IS_{DRIEST}$ ).

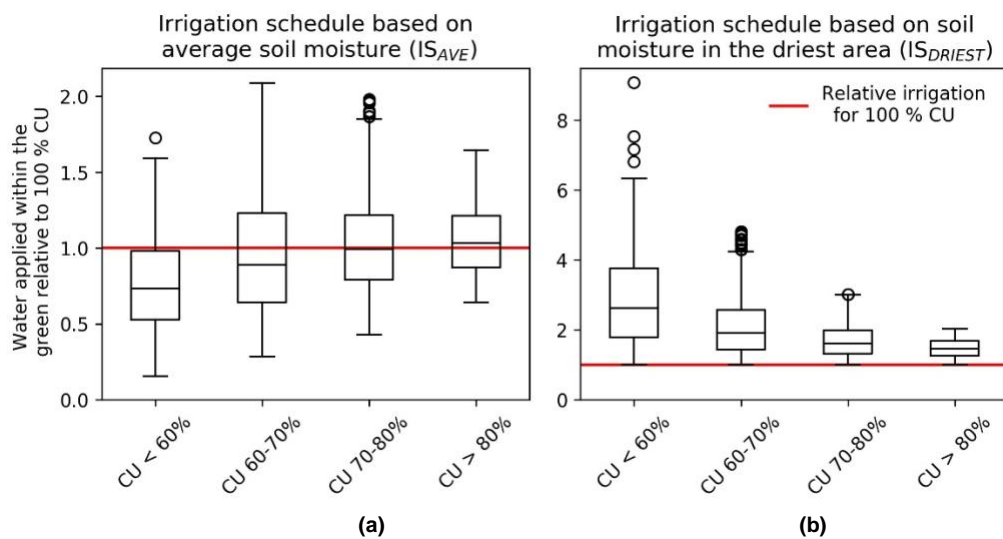


**Figure 7.20** Variation in water applied inside the green with respect to 100 % CU as affected by non-uniform irrigation for (a)  $IS_{AVE}$  and (b)  $IS_{DRIEST}$  scheduling methods

When irrigation was scheduled based on  $IS_{AVE}$  (Figure 7.20a), the water applied inside the green decreased as CU was lower. For CU > 70%, the average water applied was similar to irrigation events with 100% CU. In contrast, when CU was lower than 60%, the average water falling inside the green was a 24% lower than for 100% CU. An explanation for this is that irrigation profiles with lower CU correspond to events where the distance between sprinklers was larger, and wind speeds were higher. As shown in section 7.3, the combination of those two factors not only resulted in a marked reduction in CU but also in the IR ( $\text{mm h}^{-1}$ ) on the green.

Irrigation scheduled based on the driest area ( $IS_{DRIEST}$ , Figure 7.20b) led to a notable rise of water applied inside the green (and therefore water use) as CU

values were lower. For  $CU < 60\%$ , the water applied was almost three times greater than for  $CU 100\%$ . While  $IS_{DRIEST}$  ensures that all the green receives, at least, the water required when following given irrigation strategy ( $ET_p$ ), this scheduling method penalised low  $CU$  with an excessive water use. Based on these results, it is worth suggesting  $IS_{AVE}$  as the most adequate scheduling method, highlighting the relevance of adopting this scheduling in non-uniform irrigation to reduce the water used by irrigation.

#### Modelled impacts of irrigation management on seasonal available water content

Irrigation heterogeneity, strategy and scheduling method impacted on the seasonal available water content (SAWC). Figure 7.21 shows the simulated SAWC when irrigation was calculated based on  $IS_{AVE}$ . When no rainfall was considered in simulations, lower  $CU$  led to a decrease of SAWC; as well as to a higher SAWC variability across the green (Figure 7.21a). In contrast, simulations considering rainfall resulted in higher, less variable SAWC. This was more evident as the year was wetter.

Figure 7.22 shows the BalliSTICS model outcomes for  $IS_{DRIEST}$  scheduling method. Compared with  $IS_{AVE}$ ,  $IS_{DRIEST}$  led to higher values of SAWC. For an irrigation strategy equal or above  $0.6 ET_p$ , lower  $CU$  values resulted in less SAWC variability. The explanation for this relies on that the  $IS_{DRIEST}$  scheduling method tended to apply water in excess, which brought larger areas across the green to field capacity. However, the lower variability in SAWC produced by  $IS_{DRIEST}$  was penalised with a dramatic increase in water lost through drainage.

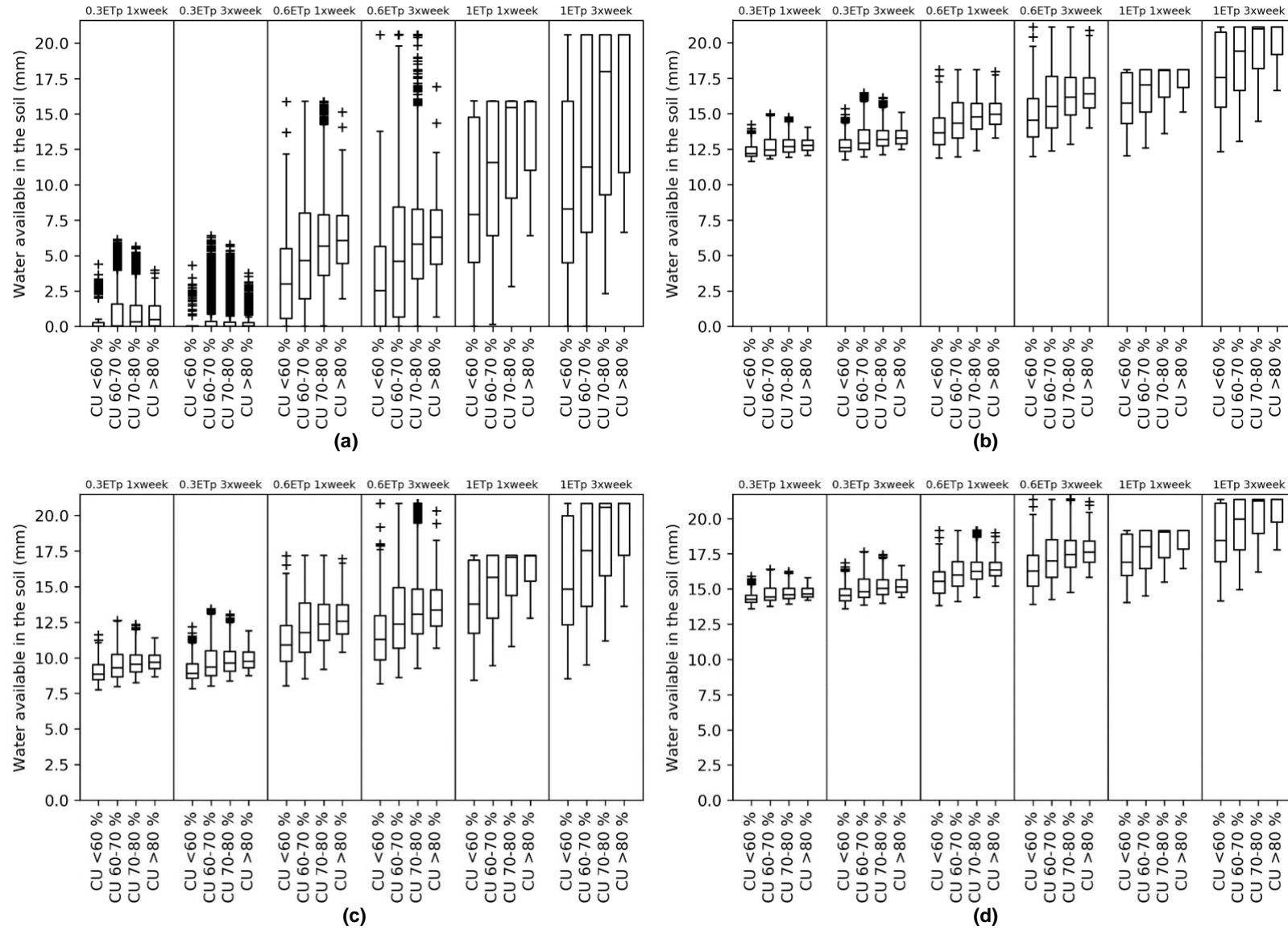


**Figure 7.21** Seasonal available water content (SAWC) across the green for different irrigation strategies and irrigation heterogeneities when using the ISAVE scheduling method. (a) No rain; (b) Average year; (c) Dry year; (d) Wet year.

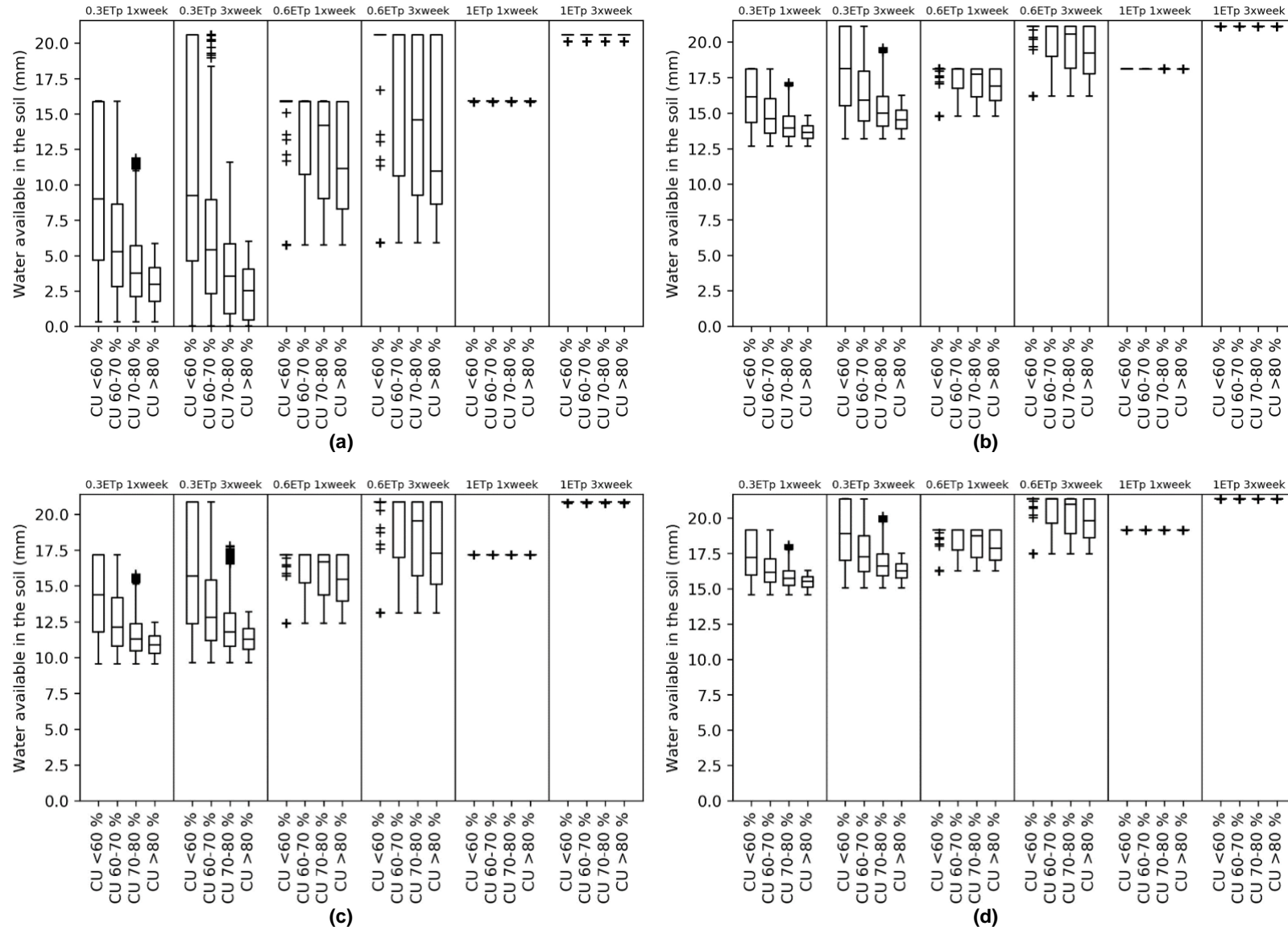


**Figure 7.22** Seasonal available water content (SAWC) across the green for different irrigation strategies and irrigation heterogeneities when using the IS<sub>DRIEST</sub> scheduling method. (a) No rain; (b) Average year; (c) Dry year; (d) Wet year

The results from the BallISTICS model showed that regardless the irrigation strategy and CU, rainfall reduced SAWC variability across the green. This is due to the “restarting effect” of rain over SAWC. Thus, after heavy rainfall events, the soil water content across the green reached FC resulting in a perfectly uniform SAWC even when the irrigation CU was poor.

Table 7.10 shows an example of the simulated SAWC uniformity ( $CU_{SAWC}$ ) across a green for two contrasting irrigation uniformities: (i) high CU (82%); and (ii) low CU (50%). The  $CU_{SAWC}$  was calculated daily using the Christiansen’s Uniformity Coefficient equation. Results for different irrigation strategies (ETp and frequency), scheduling method ( $IS_{AVE}$  and  $IS_{DRIEST}$ ) and climate year are compared.

**Table 7.10** Average SAWC uniformity ( $CU_{SAWC}$ ,%) for high irrigation CU (82%) and low irrigation CU (50%), rain patterns and irrigation scheduling methods

Rain Pattern	Average year (2012)		Dry year (1997)		Wet year (2011)	
Irrigation CU	High	Low	High	Low	High	Low
<b>Irrigation strategy</b>	<b>Scheduling method <math>IS_{AVE}</math></b>					
0.3 ETp 1 per Week	89.0	81.3	75.6	57.0	86.4	81.1
0.6 ETp 1 per Week	90.9	78.6	85.2	61.0	93.7	81.1
1.0 ETp 1 per Week	93.1	80.6	88.2	66.1	94.0	84.1
0.3 ETp 3 per Week	84.9	77.4	71.0	55.1	86.4	80.0
0.6 ETp 3 per Week	89.6	74.1	84.4	57.6	92.3	78.8
1 ETp 3 per Week	92.2	77.2	85.5	63.6	93.8	81.7
<b>Irrigation strategy</b>	<b>Scheduling method <math>IS_{DRIEST}</math></b>					
0.3 ETp 1 per Week	91.0	87.6	84.0	80.1	91.3	90.1
0.6 ETp 1 per Week	90.8	92.5	83.9	87.8	92.4	94.1
1.0 ETp 1 per Week	100.0	99.9	100.0	99.9	100.0	100.0
0.3 ETp 3 per Week	88.1	85.6	81.6	77.4	90.6	88.5
0.6 ETp 3 per Week	89.5	91.5	81.6	86.1	91.6	93.4
1.0 ETp 3 per Week	99.9	99.9	99.9	99.9	100.0	100.0

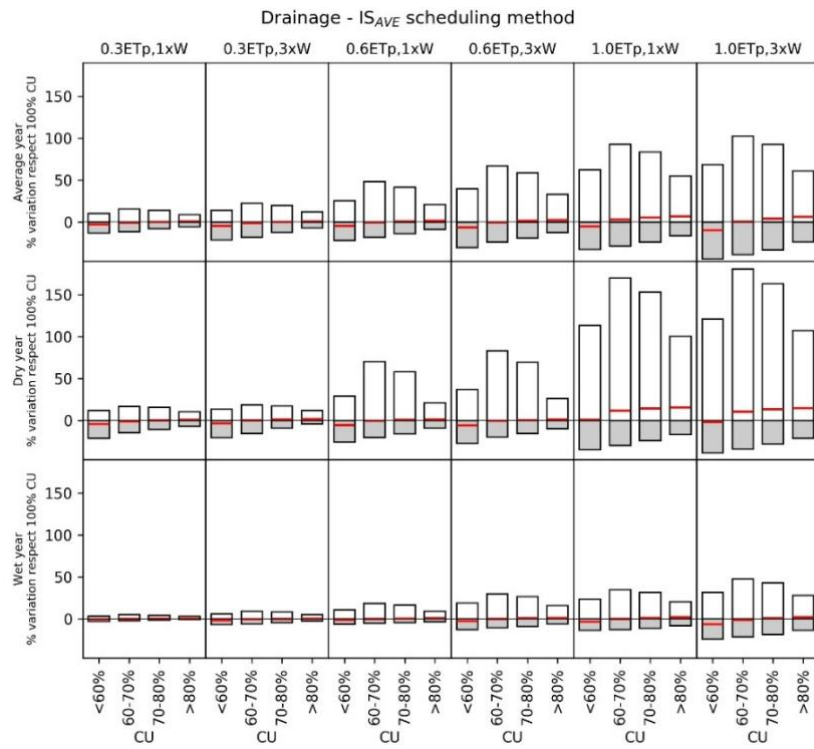
It can be observed that in almost all cases,  $CU_{SAWC}$  was higher than irrigation CU (Table 7.10). The difference between  $CU_{SAWC}$  and CU increased as the year was wetter. For instance, when using the  $IS_{AVE}$  scheduling method and irrigation CU was 50%,  $SAWC_{CU}$  was a 10.1 ( $\pm 4.2$ )% higher than CU during the dry year; a 28.2 ( $\pm 2.6$ )% higher during the average year; and 31.1 ( $\pm 1.78$ )% higher during the wet year. This highlights the implications of the “restarting effect” of rainfall on buffering the impacts of low CU on  $CU_{SAWC}$ . The use of the  $IS_{DRIEST}$  scheduling method resulted in higher  $CU_{SAWC}$  not only because of the rain, but also because more area on the green was irrigated back to field capacity. A high  $CU_{SAWC}$  might

create an incorrect perception of good scheduling practices and good irrigation system performance. For this reason,  $CU_{SAWC}$  values must be considered carefully, as they might be related to rainfall events and/or an excess of water use, and not reflect the adequacy of irrigation applications or the actual irrigation uniformity of the system.

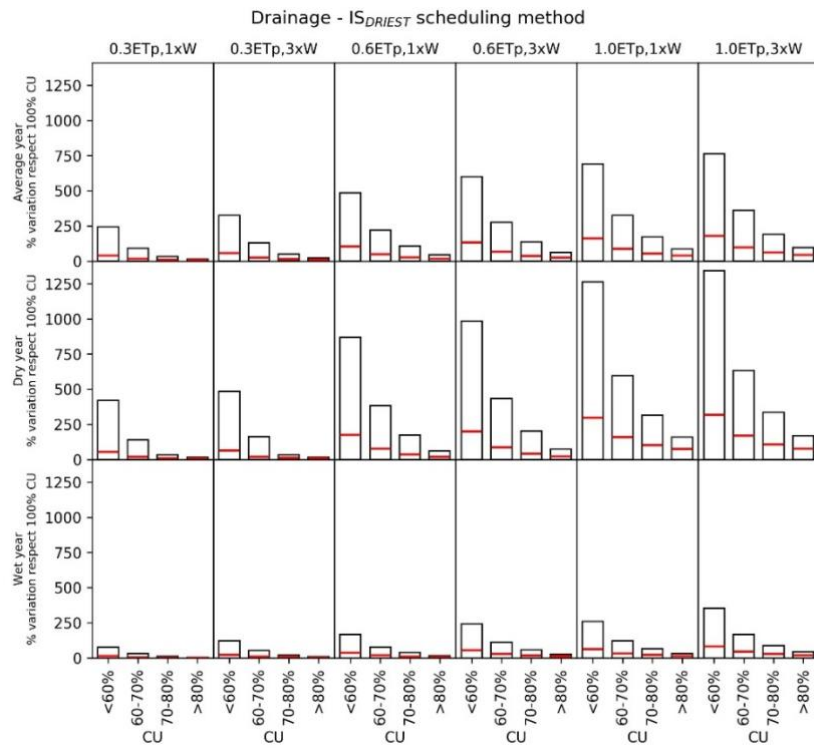
#### Modelled impacts of irrigation management on drainage

Figure 7.23 shows the percentage of variation of drainage with respect to simulated irrigation assuming 100% CU. When using the  $IS_{AVE}$  scheduling method (Figure 7.23a), non-uniform irrigation had little impact on the average drainage with respect to 100% CU. The percentage of drainage variability was higher for the 1.0 ETp strategy and dry year. However, it is worth mentioning that the greatest amount of drainage (mm considering the whole green) was obtained during the wet year. This is explained because, for the study area, rainfall has a greater influence on drainage than irrigation heterogeneity.

The  $IS_{DRIEST}$  scheduling method always led to an increase of drainage (Figure 7.23b). For  $CU > 80\%$  and deficit irrigation, differences in drainage respect CU 100% were moderate. However, as CU decreased and the irrigation strategy was closer to 1.0 ETp, the average drainage and variability across the green increased dramatically. For the  $IS_{DRIEST}$ , irrigation treatments with higher drainage matched with those that showed lower SAWC variability. However, when excess water was applied due to poor CU, the high  $SAWC_{CU}$  was obtained at the cost of excessive drainage.



(a)



(b)

**Figure 7.23** Variation in drainage across the green with respect to perfect irrigation uniformity, for different climate years, irrigation strategies and irrigation uniformities. Red lines indicate the average values across the green. (a) IS<sub>AVE</sub> scheduling method. (b) IS<sub>DRIEST</sub> scheduling method



Modelled impacts of irrigation management on dry matter production in clippings

The simulated dry matter production in clippings (DMP) was less affected by non-uniform irrigation and scheduling method than SAWC, drainage and leaching. Figure 7.24 shows the variability of DMP for different climate years and irrigation strategies when  $IS_{AVE}$  was adopted. The variability of DMP across the green as affected by CU was more evident during the dry year than during the average and wet years. This variability increased as ETp depth strategy was lower. For average and wet years, the DMP did not present marked differences between irrigation strategies (ETp and frequency). In contrast, when “no-rainfall” was considered, higher variation in DMP was observed. This was exacerbated at low CU. These results highlight the fact that rainfall in Landvik had greater impact than low CU on the seasonal DMP.

Figure 7.25 shows the results when  $IS_{DRIEST}$  was used. The excess of water applied when following this scheduling method resulted in less DMP variability than when using the  $IS_{AVE}$  scheduling. The use of  $IS_{DRIEST}$  and irrigation strategies 0.6 and 1.0 ETp resulted in a slight decrease in DMP as CU was lower. This is explained due to higher drainage and leaching produced by over-irrigation. Although this reduction was small (16% for CU < 60%, 1.0 ETp 3 times per week), these findings suggest that an inadequate irrigation scheduling coupled with low CU might not only lead to a reduction in DMP on the areas that receive less water due to water stress, but also in areas that receive more water due to a reduction of N available for plant growth.

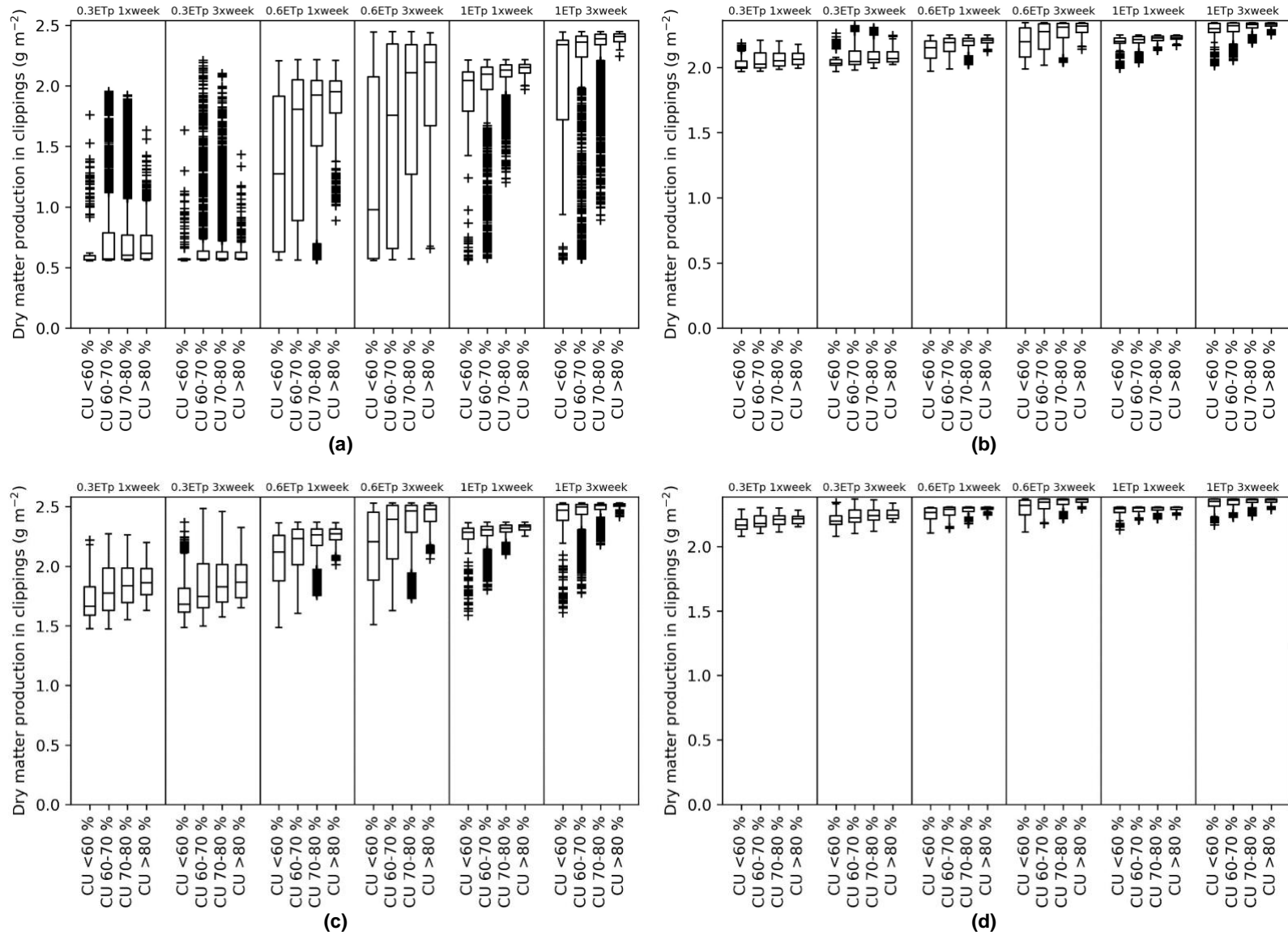


**Figure 7.24** Dry matter production in clippings across the green for different irrigation strategies and irrigation heterogeneities when using the IS<sub>AVE</sub> scheduling method. (a) No rain; (b) Average year; (c) Dry year; (d) Wet year

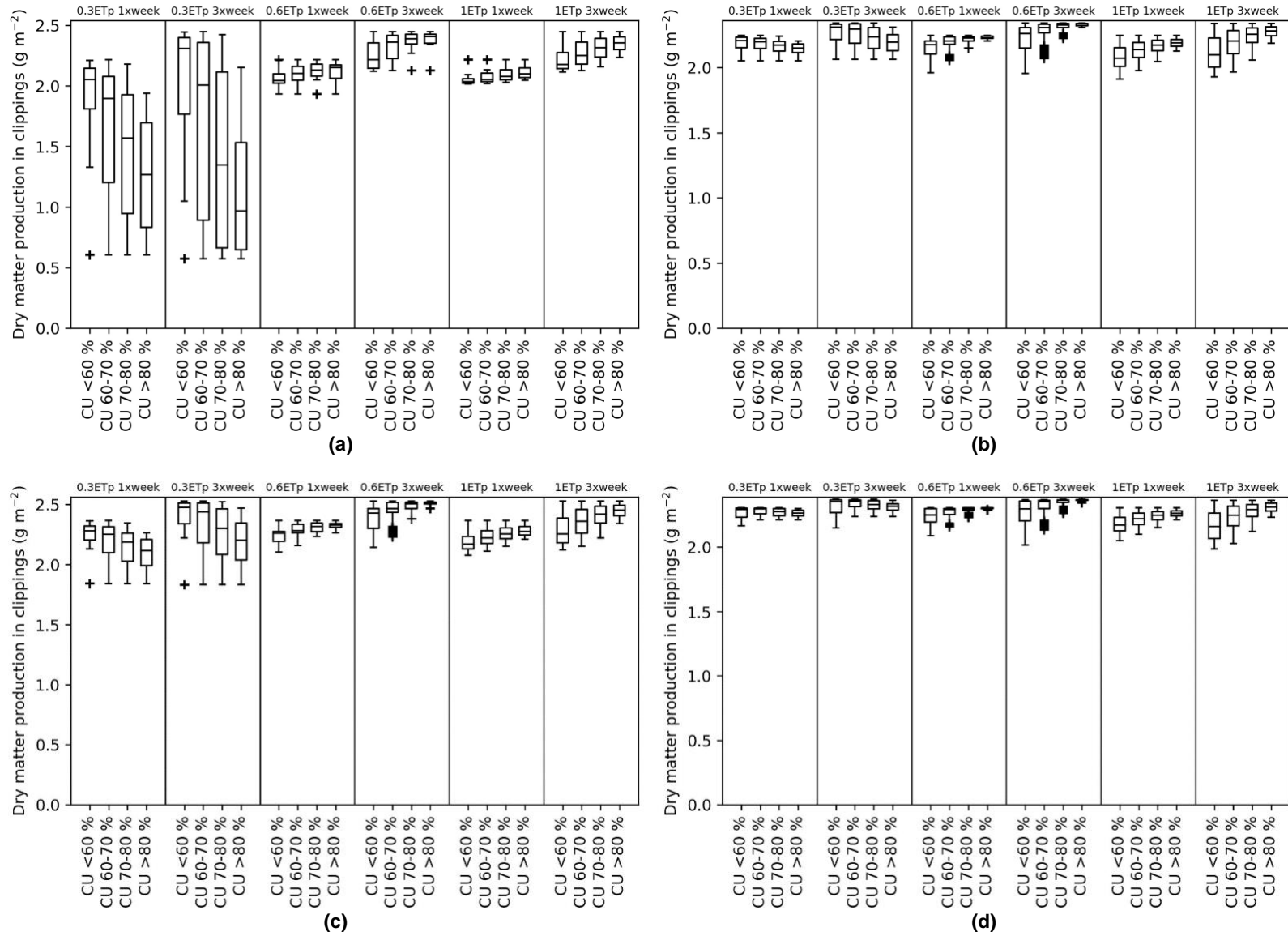


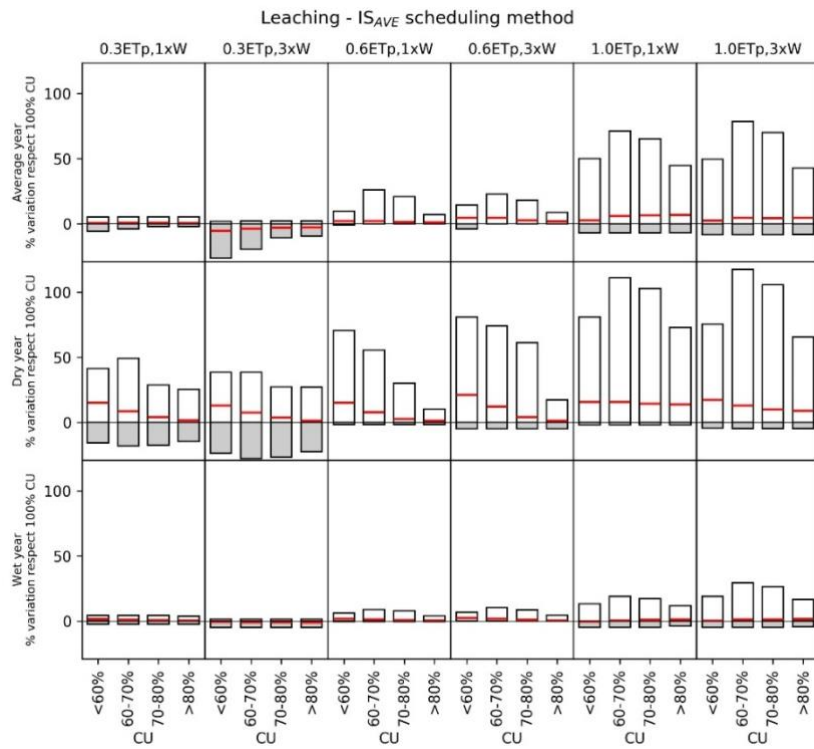
**Figure 7.25** Dry matter production in clippings across the green for different irrigation strategies and irrigation heterogeneities when using the IS<sub>DRIEST</sub> scheduling method. (a) No rain; (b) Average year; (c) Dry year; (d) Wet year

### Modelled impacts of irrigation management on nitrate leaching

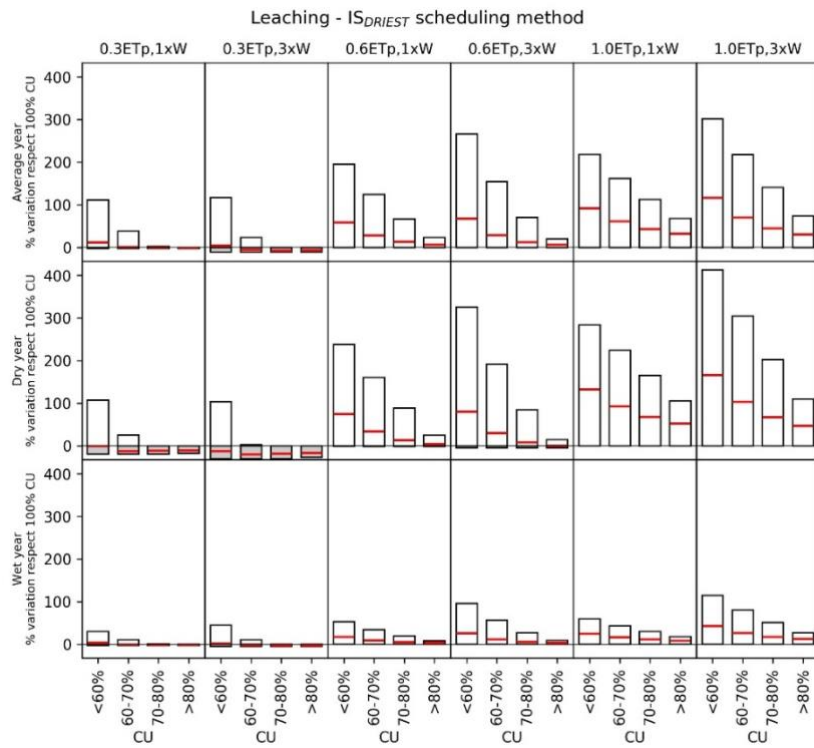
The BalliSTICS model outputs showed that non-uniform irrigation impacts differently on leaching depending on irrigation strategy, scheduling method and climate year. Figure 7.26a presents the variation of nitrate leaching as affected by non-uniform irrigation and when the IS<sub>AVE</sub> was used. During the dry year, irrigation strategy and CU had a significant impact on average leaching (red lines in Figure 7.26). In that year, the higher leaching for 0.3 ET<sub>p</sub> strategy was obtained in those areas that received the least amount of water ( $p=0.1$  and  $0.3$  in the CDF). This is explained because turfgrass was more exposed to water stress, leading to a reduction in DMP and subsequent increase of leaching. The increase in leaching at 0.6 ET<sub>p</sub> and low CU during the dry year was associated to (i) a reduction of DMP in the area that received less water ( $p=0.1$  in the CDF) and (ii) an increase of drainage in areas that received more water ( $p=0.9$  in the CDF). When irrigation strategy was 1.0 ET<sub>p</sub>, the increase in average leaching was a result of drainage. During average and wet years, non-uniform irrigation had little impact on average leaching.

Figure 18b shows the variation in leaching when adopting the IS<sub>DRIEST</sub> scheduling method. In that case, high deficit irrigation strategy (0.3 ET<sub>p</sub>) resulted in minor variability of nitrate leaching. Conversely, for 0.6 and 1.0 ET<sub>p</sub> strategies, average leaching and variability of leaching across the green increased dramatically as CU was lower and the year was drier. In all cases, the increase of leaching was related to drainage produced by excessive irrigation when using the IS<sub>DRIEST</sub> scheduling method.

The results presented in Figure 7.26 highlight the importance of adopting an adequate irrigation schedule method not only to reduce water use, but to mitigate leaching. While non-uniform irrigation presented a moderate impact on leaching when IS<sub>AVE</sub> scheduling method was adopted; the use of the IS<sub>DRIEST</sub> exacerbated the negative effects of CU on leaching. Thus, the use of irrigation schedule based on the dry spots, like the IS<sub>DRIEST</sub> schedule method should be avoided and, if used, should be limited to irrigation systems with excellent CU (> 80%) and for deficit irrigation strategies.



(a)



(b)

**Figure 7.26** Variation rate of nitrate leaching respect perfect irrigation uniformity, for different climate years, irrigation strategies and irrigation uniformities. Red lines indicate the average values across the green. (a)  $IS_{AVE}$  scheduling method. (b)  $IS_{DRIEST}$  scheduling method

The results from this section provide evidence that irrigation management affects leaching. However, it is important to bear in mind that most of the occurrence of leaching is explained due to the high rainfall characteristic in the study location. Despite that during dry years leaching showed more variation as affected by irrigation management, the absolute value of leaching ( $\text{g NO}_3^- \text{-N m}^{-2}$ ) was higher during wetter years.

The highest concentration of nitrates in leaching were obtained for the dry year for irrigation strategy 0.3 ETp, applied once per week and IS<sub>AVE</sub> scheduling method, with nitrate concentration  $5 (\pm 1.1) \text{ mg NO}_3^- \text{-N L}^{-1}$ . For this treatment, CU < 60% increased nitrate concentration by 21.1% with respect to CU 100%. However, the limit of the USEPA (2018) for drinking water ( $10 \text{ mg NO}_3^- \text{-N L}^{-1}$ ) was not exceeded even for the lowest CU values. The impact of non-uniform irrigation on nitrate concentration in leaching for average and wet years was non-significant.

#### **7.4.2.1 Impacts of irrigation time on turfgrass**

The impacts of irrigation at different times of the day on turfgrass agronomy were studied. Figure 7.27 shows the hourly wind speed at Landvik depending on the month for the period 1997-2006. During winter months (November to March), average wind speed tended to remain stable during all day, with a slight increase at midday. During these months the average wind speed between 1997 and 2016 was  $1.63 \text{ m s}^{-1}$ , with a standard deviation of  $1.56 \text{ m s}^{-1}$ . The average wind speed during summer months (May to September) varied during the day. During the night-time and early morning, the average wind speeds were lower, showing a steady increase during late morning and reaching a maximum between 13.00 hrs and 15.00 hrs.

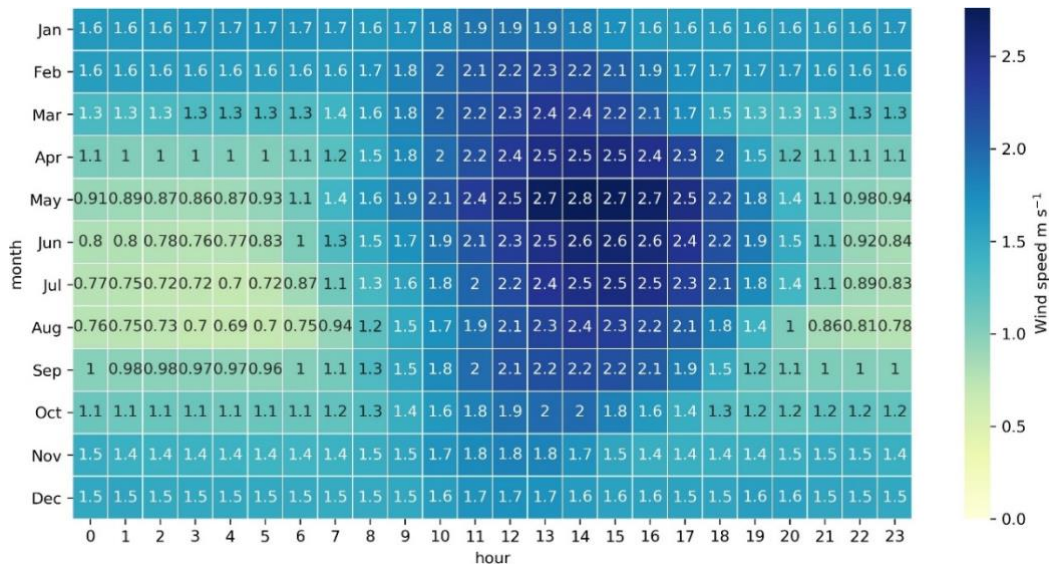


**Figure 7.27** Hourly wind speed, averaged by month, recorded at Landvik between 1997 and 2016

Due to the variability of wind within the day during the months under study (May to September), wind speeds were grouped into five time-slots. The highest contrast in wind speeds was observed between *morning* (4-7 a.m., with average wind speed  $0.94(\pm 0.9) \text{ m s}^{-1}$ ), and *afternoon* (12 to 15 p.m., with average wind speed  $2.54 (\pm 1.2) \text{ m s}^{-1}$ ). The BallISTICS model was then used to simulate turfgrass responses to *morning* and *afternoon* irrigation, as these the two time-slots presented the most contrasted climate conditions with impact on irrigation performance (wind and relative humidity).

### Impacts of irrigation time on CU

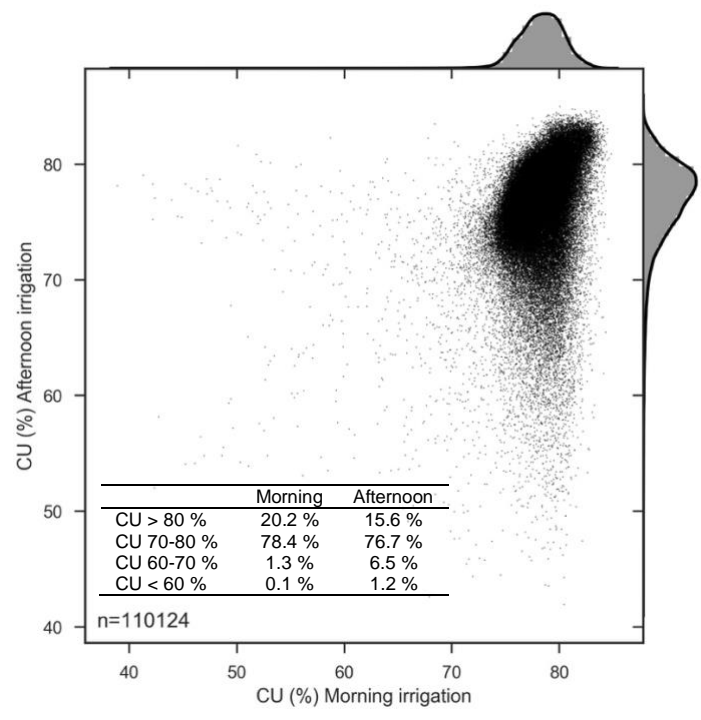
The simulation of irrigation was run combining (i) daily wind speed, wind direction, relative humidity and temperature measured in each time-slot; (ii) the nine green shapes used in section 7.3; and (iii) the four sprinkler set-ups calibrated for the sprinkler model. The sprinklers location respected their “original” position on each green.

Figure 7.28 shows the comparison of daily CU between *morning* and *afternoon* irrigation from 1997 to 2016. The results show little differences in average CU between morning (CU  $78.3 (\pm 2.3)\%$ ), and afternoon irrigation (CU  $76.4 (\pm 4.1)\%$ ). These results highlight the fact that differences in wind speed between both time-slots at Landvik are not enough differentiated to cause a remarkable reduction in

seasonal CU. Although the likelihood of an irrigation event with low CU is higher during afternoon irrigation, these episodes can be considered isolated eventualities.

Impacts of irrigation time on turfgrass agronomy

The BallISTICS model was used to quantify impacts of irrigation management on turfgrass considering the daily variation of CU presented above. The model outcomes did not show significant differences between morning and afternoon irrigation for any strategy or schedule method. These results are explained due to (i) the similitude between average CU in both time-slots, and (ii) the influence of rain in buffering the impacts of irrigation heterogeneity.



**Figure 7.28** Comparison of the simulated daily Christiansen’s Uniformity Coefficients (CU, %) for morning and afternoon irrigation in from May to September between 1997 and 2006 at Landvik

Impacts of irrigation time on WDEL

Figure 7.29 shows a comparison of wind drift and evaporation losses (WDEL) between morning and afternoon irrigation operating at 4.2 and 6.0 bar. The predictions of WDEL were based on the model equation determined in Chapter 5. Overall, it is observed that the WDEL was lower during morning irrigation. These differences are explained because of the higher relative humidity (RH)



measured in the morning 85.3 ( $\pm 11.6$ )%, with respect to RH in the afternoon 67.6 ( $\pm 18.5$ )%. In this research, variations in WDEL resulted in a higher volume of water use to compensate the reduction of the discharge efficiency as affected by WDEL. Thus, afternoon irrigation resulted in an average increase of water use of 3.8%.

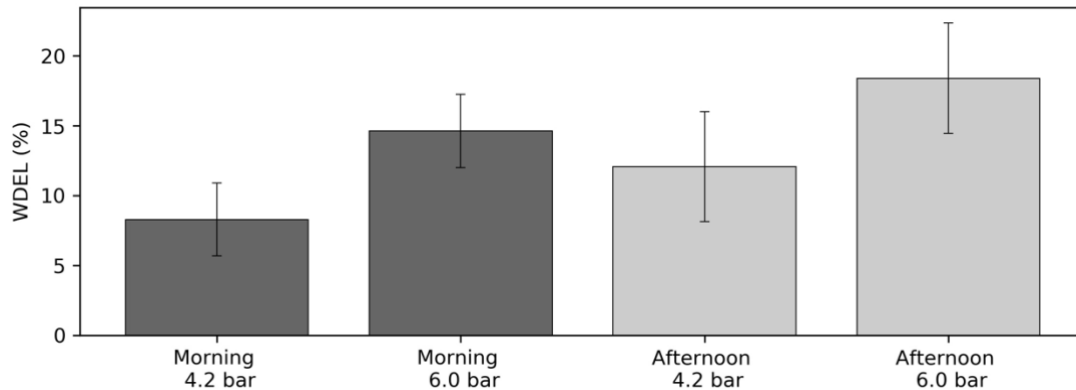


**Figure 7.29** Simulated wind drift and evaporation losses (WDEL) for morning and afternoon irrigations and operating pressures 4.2 and 6.0 bar

In summary, the results from the BalliSTICS model suggest that, in the study location, the choice of the time-slot for irrigating should be driven by other factors rather than the risk of having a low seasonal CU. Obviously, irrigation events with wind speeds above  $2.5 \text{ m s}^{-1}$  will result in a decrease of CU, which is more likely to happen during the afternoon. Also, the choice of morning irrigation can be more appropriate because the lower WDEL at that time-slot. This will result in a slight reduction in water use and/or in more adequate water application.

### 7.4.3 Discussion

The integrated modelling approach developed in this study provided evidence on the impacts of irrigation management (uniformity, strategy and scheduling method) on DMP, water balance and leaching. The key findings arising from its application demonstrated that:

- i) In humid climates, irrigation strategy has a more direct impact than irrigation heterogeneity on turfgrass agronomy;
- ii) The impacts of non-uniform irrigation varied depending on the irrigation strategy, irrigation scheduling method, and variable under study (water applied, SAWC, DMP, drainage or leaching);

- iii) When irrigation is scheduled based on the average soil water needs across the green ( $IS_{AVE}$ ), irrigation heterogeneity had an impact on the *variability* of SAWC, DMP, drainage and leaching across the green. However, in most cases their average values within the green were similar to those obtained for perfect irrigation uniformity scenario. In contrast, irrigation scheduling based on  $IS_{DRIEST}$  increased not only the variability of the model outcomes variables, but also their average values across the green. This highlights the fact that adequate irrigation scheduling alleviates the negative impacts of non-uniform irrigation;
- iv) The impacts of non-uniform are buffered by rainfall, which led to high uniformity in soil moisture; and
- v) In dry years, irrigation heterogeneity has a greater influence on drainage and nitrate losses, especially when excess irrigation was applied as a result of a non-adequate irrigation scheduling ( $IS_{DRIEST}$ ).

#### Irrigation scheduling method and water use

Two irrigation scheduling methods were proposed: one based on water needs in the area corresponding to  $p = 0.5$  in the CDF ( $IS_{AVE}$ ), and the other based on water needs the area that receives the least amount of water ( $p=0.1$  in the CDF,  $IS_{DRIEST}$ ), which corresponds to the driest area across the green. Compared with the  $IS_{AVE}$  method, the  $IS_{DRIEST}$  had only a minor impact on DMP. However, water use was up to 3 times higher, leading to a dramatic increase in drainage and leaching. Low CU exacerbated the negative impacts of  $IS_{DRIEST}$  in due to an excessive use of water. The use of the  $IS_{DRIEST}$  scheduling method would therefore only be recommended to use for CU values above 80% and an irrigation strategy using 0.6 ET<sub>p</sub> or lower. In addition,  $IS_{DRIEST}$  should be avoided when the CU is low or when irrigation targets moderate levels of SAWC. In summary, the  $IS_{AVE}$  provided a better balance between DMP and lower water use, drainage and leaching.

Indeed, the use of the  $IS_{DRIEST}$  schedule method might lead to a misconception of good irrigation system performance, since it resulted in a higher soil water

content uniformity ( $CU_{SAWC}$ ). According to Huck and Zoldoske (2006) most irrigation scheduling is driven by the “dry-spots”, which are areas that receive the least amount of water. These ‘dry-spots’ might coincide with the areas with the lowest turf quality (Chapter 4). Therefore, an irrigation scheduling based on turf quality instead of soil water measurements will inevitably lead to an increase in water use. In the Scandinavian golf survey (Annex-1), over three quarters (81%) of respondents based their irrigation scheduling on visual inspection of turf, while only 47% of respondents measured soil moisture. This implies that more effort is needed in improving the irrigation scheduling practices, or developing tools that can integrate visual signs of turf quality with objective assessments of soil moisture.

Under Scandinavian weather conditions, the economic impact of over-irrigating golf greens might have lower implications compared to agriculture. This is due to the low irrigated area on greens (typically 1 to 2 ha). Thus, the actions for more efficient and sustainable irrigation should focus on increasing water and nitrogen use efficiencies, while maintaining turfgrass health and quality. This may not be relevant for warmer and drier regions, where water requirements are higher and water is scarce; or for golf courses where the fairways or roughs are irrigated.

#### *Implications of rainfall on soil water content uniformity ( $CU_{SAWC}$ )*

The results from the BalliSTICS model showed that the seasonal available water content uniformity ( $CU_{SAWC}$ ) was higher than the irrigation CU. This difference was most notable at low CU, in the drier year and when irrigation was based on the IS<sub>DRIEST</sub> method. These results are consistent with previous research (Li and Kawano, 1996; Li, 1998; Li and Rao, 2001; Zocoler et al., 2013; Miller et al., 2014; Osman et al., 2014). All these authors related the higher soil moisture uniformity with the horizontal redistribution of soil water. However, water redistribution in soil was not taken into account in the BalliSTICS simulations and a higher  $CU_{SAWC}$  can only be explained by the “restarting effect” of rainfall. When heavy rainfall occurred, the soil reached field capacity resulting in 100%  $CU_{SAWC}$ . As reported above, over-irrigation applied in IS<sub>DRIEST</sub> method also had great impact on  $CU_{SAWC}$ .

This phenomenon might require further attention for irrigation management in humid climates. High rainfall rates and subsequent high  $CU_{SAWC}$  might lead to misleading understanding in terms of the actual performance of the irrigation system. The impacts of rain on  $CU_{SAWC}$  in turf were described by Kieffer and Huck (2008) who reported that rainfall prior to irrigation tests influenced on the results of the comparison between irrigation uniformity and soil moisture uniformity. In recent research, Gravalos et al. (2017) observed that under dry soil conditions, soil moisture uniformity was highly dependent on irrigation. In contrast, the authors observed that for wet soil conditions, irrigation had a little effect on soil moisture uniformity. The results from Gravalos et al. (2017) are highly consistent with the outputs from the BalliSTICS model. However, it is worth recognising that the modelling approach used did not consider other factors that might contribute to  $CU_{SAWC}$ , such as green slope, the use of wetting agents (surfactants) and/or the spatial variability of soil organic matter and soil compaction.

In this research only results of the  $CU_{SAWC}$  were presented as average seasonal values. However, it is necessary to highlight that the  $CU_{SAWC}$  varied during the season. This is important because during weeks with no rainfall, the  $CU_{SAWC}$  becomes more dependent on CU, and therefore its value can decrease considerably, even to levels that are lower than CU. In such cases, the short-term impacts of CU will be exacerbated. This might lead to occasional periods with uneven turf growth and variable turfgrass quality across the green. However, further investigation is needed to investigate the short-term impacts of CU on turfgrass.

#### *Dry matter production*

The high  $CU_{SAWC}$  produced by rainfall explained the low impact of CU on average DMP. The highest variation in DMP was observed for a dry year, using the ISAVE scheduling method under a low CU. In contrast, for average and wet years, little variation in DMP between the driest and wettest spots was observed. The model outputs for the dry year coincide with previous research conducted under drier climates (Mateos et al., 1997; Ruelle et al., 2003) where it was reported that although non-uniformity did not reduce yield, it induced spatial variations in

vegetative growth. Conversely, the low DMP variation observed in a wet year or when using the IS<sub>DRIEST</sub> schedule were consistent with findings from Sánchez et al. (2010), who reported that over-watering combined with non-uniform irrigation might not show its effect on crop yield.

#### Drainage and nitrogen leaching

Non-uniform irrigation had a great impact on drainage and leaching variability across the green, and to a lower extent, to the average values in the whole area. For the IS<sub>AVE</sub> schedule method, differences in average drainage and leaching within the green with respect to 100% CU were only evident in a dry year. However, for the IS<sub>DRIEST</sub> schedule method, low irrigation uniformities led to more than double the amount of drainage and leaching compared to 100% CU. This highlights that an inadequate irrigation schedule (IS<sub>DRIEST</sub>) coupled with low CU will lead to an increased risk of leaching. Ruelle et al. (2003) observed that nitrate leaching in corn was only affected by low CU when excess N fertilisation occurred. However, these authors stated that crop water needs, irrigation scheduling and specific water application levels had more influence on leaching than irrigation heterogeneity. Li et al. (2005) also concluded that a CU between 72 to 84% had an insignificant effect on leaching, nitrogen uptake and yield. Popova (2006) reported that during a dry year, the variation of yield loss due to non-uniform irrigation also increased the variation in drainage and nitrogen leaching. In this research, the results showed a greater impact of irrigation heterogeneity in a dry year, as well as an increased risk of nitrogen leaching derived from a low irrigation uniformity. However, the maximum total leaching across the green was accounted for the wet year and not for non-uniform irrigations, with rainfall being the main contributor to leaching.

#### Differences between morning and afternoon irrigation

The likelihood of having irrigation events with wind speeds above 2.5 m s<sup>-1</sup> and lower CU was higher during the afternoon than during the morning. However, differences in the seasonal CU between different times of the day were relatively low. Consequently, no statistically significant differences in seasonal turfgrass performance was observed between the irrigation times. These findings are

consistent with Ruelle et al. (2003) who reported that day versus night irrigation had little effect on yield and leaching. However, Cavero et al. (2008) and Yacoubi et al. (2010) reported that irrigating at night reduced both water deficit and relative yield losses. Nonetheless, these investigations were conducted under Mediterranean climate conditions where lower rainfall might increase the negative impacts of a lower CU. Given the little impact shown of irrigation time on seasonal turfgrass response, it could be recommended that the time of irrigation should be driven by other factors rather than the risk of having a lower seasonal CU. These factors include, for example, the interference of irrigation in play, the available time to irrigate different sectors of the course, or the higher risk of disease when irrigation is applied in the late evening (Vargas, 1993).

## 8 DISCUSSION

This chapter presents the key findings from the integrated modelling (Chapter 7) to address the research question “*How does irrigation management in golf greens affect turfgrass performance and the environment?*” The advantages and limitations of the integrated modelling approach are evaluated, and a new approach for improving irrigation management is proposed. Finally, areas for further research are identified.

### 8.1 IMPLICATIONS OF THE RESEARCH

The original contribution to knowledge arising from this research includes the assessment and quantification of the impacts of irrigation heterogeneity and irrigation strategies on turfgrass under northern Europe climate conditions. An applied ballistics modelling approach was developed for simulating irrigation on turfgrass, and the STICS model (Brisson et al., 2002, 2003) was calibrated and validated to simulate turfgrass growth, water balance and leaching under contrasting climatic and management conditions. Whilst other models have been previously used for simulating turfgrass growth, water balance and/or nutrient fate (Qian et al., 2003; Zhang et al., 2013b; Filipović et al., 2014; Wilkerson et al., 2015), this study represents the first research to explicitly consider irrigation system performance and irrigation strategies using an integrated modelling approach that integrates an irrigation and crop model for simulating turfgrass systems.

This thesis has demonstrated four major findings which relate irrigation with turfgrass performance for golf and the environment:

- i) Non-uniform irrigation on greens can be ameliorated by paying attention to the sprinkler position and spacing, and by irrigating when wind speeds are lower than  $2.5 \text{ m s}^{-1}$ . Although other authors have related sprinkler set-up (nozzle and operating pressure) with CU (Latif and Ahmad, 2008; Vega and Hermosin, 2014) the results reported here from the irrigation modelling did not demonstrate such a relationship. However, sprinkler set-

up has been shown to have a strong influence on IR, which needs to be considered when scheduling irrigation, being therefore critical to achieve adequate irrigation.

- ii) Under Northern European climate conditions, the choice of an irrigation strategy has a potentially higher impact on the turfgrass water balance, DMP and leaching risk than irrigation heterogeneity. A moderate deficit irrigation (0.6 ETp) strategy was shown to be the most appropriate to balance between actively growing turfgrass and reduced water use and leaching risk. However, an optimum irrigation strategy and scheduling must also be accompanied by an understanding of the actual irrigation rate of an irrigation system.
- iii) Under Northern European climate conditions, rainfall is the main contributor to water input and typically a more important determinant of drainage and leaching than the level of irrigation applied. It has been shown that rainfall increases the soil moisture uniformity; thus buffering the impacts of non-uniform irrigation. This might lead to a misconception regarding the actual uniformity of irrigation as rainfall can help to compensate for poor irrigation system performance.
- iv) Although rainfall is the main contributor to drainage and leaching, an inadequate irrigation strategy will also negatively impact on these two variables. Assuming a uniform nitrogen application policy, the modelled results showed that a severe deficit irrigation strategy reduced DMP which then led to an increased leaching risk due to lower plant N uptake. In contrast, over-irrigation led to an increased leaching risk due to excess drainage. This highlights the importance of an appropriate irrigation strategy and scheduling. Nonetheless, the relationships between increased leaching at severe deficit irrigation in humid climate has not been found in the literature, and further field research is required to prove this finding based on a modelling approach.

The approaches adopted in the current research considered a perfect knowledge of the water delivered by the irrigation system and the soil water deficit when irrigation was scheduled. However, in field conditions, the lack of consideration



of any of these components will lead to inadequate irrigation. This can be especially relevant when the irrigation decision is driven by visual inspection, based on the drier spots, or amount of irrigation applied is not considered. This can be relevant during dry periods, where the need for supplemental water applications is higher. In those cases, an inadequate irrigation scheduling will typically result in more irrigation than is actually required to replenish the soil water content. As shown in Chapters 4 and 7, this might not have an impact on turfgrass quality and DMP, and might lead to a misconception of “good irrigation practices”. However, this will lead to an inevitable excess of water use and potential leaching risk, which is difficult to quantify in field conditions. An irrigation strategy for Nordic countries should, therefore, consider four factors: (i) irrigation system performance, (ii) actual soil water content and soil water holding capacity, (iii) plant water requirements, and (iv) local weather conditions including ETo and rainfall (with impact on plant water demands); and wind speed and, to a lower extent, relative humidity (with impact on irrigation system performance).

## **8.2 INTEGRATED MODELLING APPROACH**

The integrated modelling framework developed in this thesis (BalliSTICS) couples an irrigation model with a biophysical crop model. This approach was used to study the impacts of irrigation heterogeneity and irrigation strategy on turfgrass performance and the environment. Due to the massive number of combined scenarios, such an approach could only be provided by the integrated modelling process, which would have been impractical and impossible to address using only experimental methods. The model used in this thesis falls into the category of “models as tools for research” as described by Matthews et al. (2002). However, it also has potential to be used as a decision-support tool in the evaluation of alternate irrigation system and scheduling strategies for turf management in golf.

The two models embedded within the BalliSTICS model could also be used separately. Firstly, the irrigation model could serve to analyse impacts of changes in irrigation system design. Secondly, the STICS model could be used to assess turfgrass performance and help in the definition of suitable irrigation (and

fertilisation) strategies, but their use would need improvements prior to practical application. Improvements in the model processes are proposed in Chapters 5 and 6. Additional data are also required to calibrate the models for a broader range of sprinkler models and set-ups, turf species, irrigation strategies and climate conditions. An enhanced version of the BalliSTICS model could potentially be used by the sportsturf consultancy, for studies assessing the environmental sustainability of courses, and for improving irrigation and fertiliser management practices.

### Modelling limitations

The BalliSTICS modelling approach inevitably has a number of limitations; these are described in Chapters 5 and 6, and briefly considered below in the context of the integrated approach:

1. Great care must be taken when coupling models as errors in the simulations produced in one model can be inherited by a subsequent model. There is hence a risk of introducing additional modelling uncertainty and error propagation in the results.
2. For each irrigation heterogeneity profile, the simulations were launched considering that the spatial variability of water application remained constant across the season. In practice, the areas that receive more or less water will vary during the season because of the variability in wind speed and direction, the starting position of the water jet and other factors that add uncertainty to irrigation heterogeneity prediction. The assumptions made for the simulations might have exacerbated the impacts of non-uniform irrigation.
3. The use of a pre-existing model (STICS) limited the flexibility in developing an integrated process. This made the task of determining the water requirements for different strategies under non-uniform irrigation difficult. However, the use of an existing model considerably reduced the time spent developing a new model. Despite this is introduced as a model limitation, the approach adopted in this research for determining irrigation could be implemented in future versions of the STICS model.

4. The research is limited to irrigation on greens, for one sprinkler model, and under specific climate conditions. The modelling approach adopted in this research could be widely applied to other irrigation systems, environmental conditions and crop systems. However, before the BalliSTICS model is applied to other systems, further data collection would benefit model calibration.

### **8.3 IMPLICATIONS FOR IMPROVING IRRIGATION EFFICIENCY**

The evaluation of irrigation efficiency in turfgrass is subject to interpretation and could be considered more challenging than in agriculture. In agricultural crops, irrigation efficiency is usually related to water that is beneficially used for yield production (Pereira and Marques, 2017). Its assessment might consider several factors, such as economic efficiency, water distribution efficiency or irrigation system efficiency. However, the overall evaluation of efficiency will usually relate to the yield production per unit of water used (whether at basin, network or field scale).

As reported in Chapters 4 and 7, the aim of irrigation in turfgrass was not to increase plant growth (or yield) but rather to apply just the amount of water needed to maintain a healthy, high-quality turfgrass. Some features related to turfgrass quality (and golf) such as playability, hardness, or visual aspect can be quantified. However, determining the threshold at which each variable has attained an “acceptable” level is quite arbitrary, and subject to turfgrass management philosophy, the intensity of the traffic in that area, acceptance by golf players or economic constraints given by the course budget. For example, during high-stress periods such as hot summer days or intense traffic, irrigation strategies should reflect the target use and accept there may be periods with reduced visual turfgrass quality.

Figure 8.1 presents a Venn diagram with the relationships between the different elements affecting turf irrigation management. The irrigation decision-making in turfgrass should aim to lower the amount of water needed to achieve healthy turfgrass, with reducing the environmental impacts of turfgrass management, whilst providing an excellent quality playing surface for golf. Although irrigation

system performance is not included, a poor irrigation uniformity and inadequate applications given by a lack knowledge of the IR or water requirements will lead to inadequacies in the equilibrium between the *turfgrass agronomy*, the *sustainability* and the *golf practice* components.

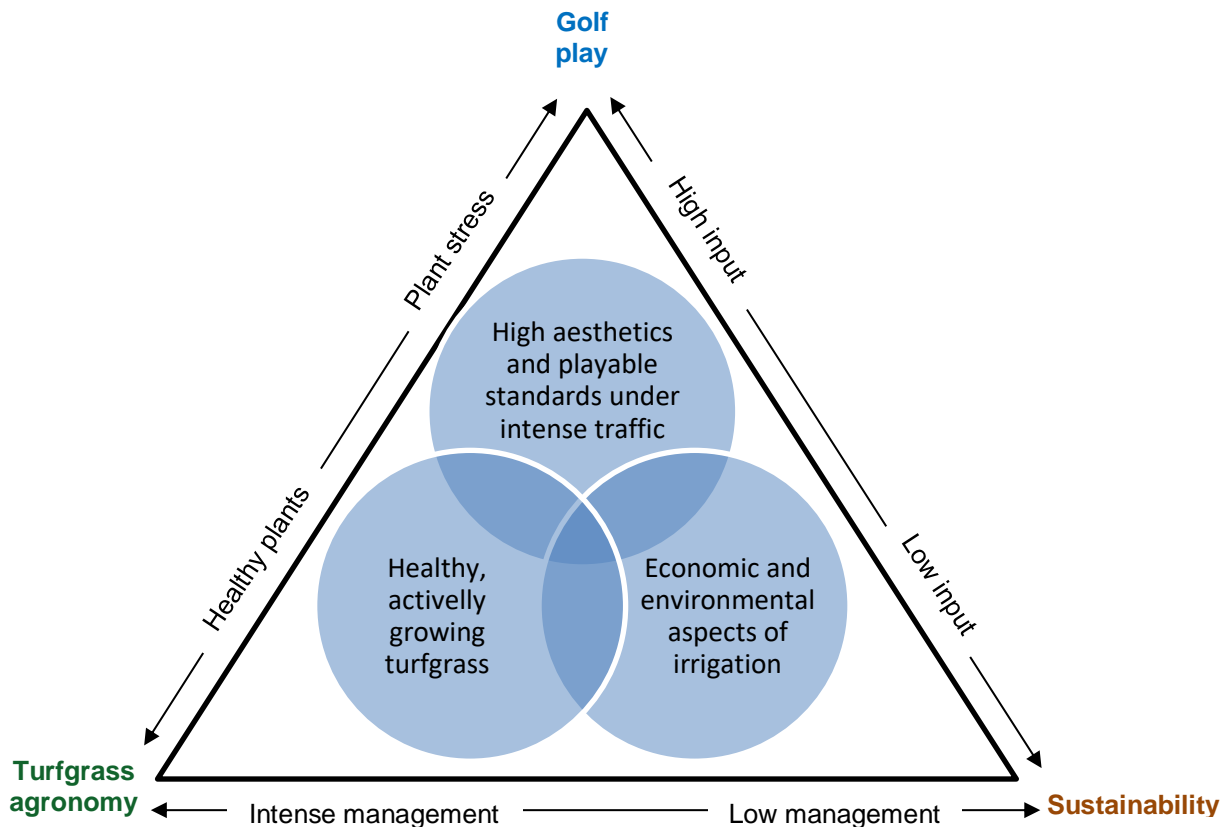


**Figure 8.1** Relationships between golf practice, agronomic and sustainability aspects in turf irrigation management

This research has focused on the relationships between irrigation and *turfgrass agronomy* (turf growth) and *sustainability* (water use and leaching). Although visual turf quality was discussed in Chapter 4, further research is required to model the relationships between irrigation with other aspects of *golf play*. This should include not only turf quality, but also other aspects such as thatch development, ball roll or surface hardness.

Increasing irrigation efficiency can not only reduce dependence on water resources (Carrow, 2006) but can also result in more even turf quality, lowered environmental risks due to reduced leaching, and more efficient use of fertilisers. As it has been observed in the results from the systematic review (Chapter 4) and the integrative modelling approach (Chapter 7), this can only be achieved by

adopting an adequate irrigation strategy and by applying the required amount of water, which requires from consideration of the irrigation system performance. Thus, based on findings from this research, efficient irrigation management must embrace the following factors:

1. **Knowledge of the system**, which is composed of the turfgrass system (soil and plant characteristics) and the irrigation system characteristics.
2. **Management practice**, which is related to irrigation decision-making considering the turfgrass, irrigation system, and weather constraints;
3. **System response**, which is described by the turfgrass response variables affected by irrigation; these are equivalent to the outputs from the BalliSTICS model.
4. **Evaluation of irrigation**, which consists of an analysis of system response as affected by irrigation management. This is implemented through an iterative process to (i) identify needs for improvement in irrigation equipment, (ii) increasing knowledge of the turfgrass system, and (iii) optimising irrigation decision-making including scheduling.

The relationships between these four components are shown in Figure 8.2. The sole use of one of these factors might lead to inefficient water applications. The proposed steps for improving irrigation efficiency are based on the results from the BalliSTICS model (Chapter 7). However, it is worth recognising that there are other factors outside the scope of the modelling approach that might also affect irrigation efficiency, including, for example, maintenance activities such as aeration, sand-capping and use of surfactants; pest and disease outbreaks; seasonal changes of soil organic matter content; and soil variability across the green due to long-term turfgrass establishment and intense traffic.

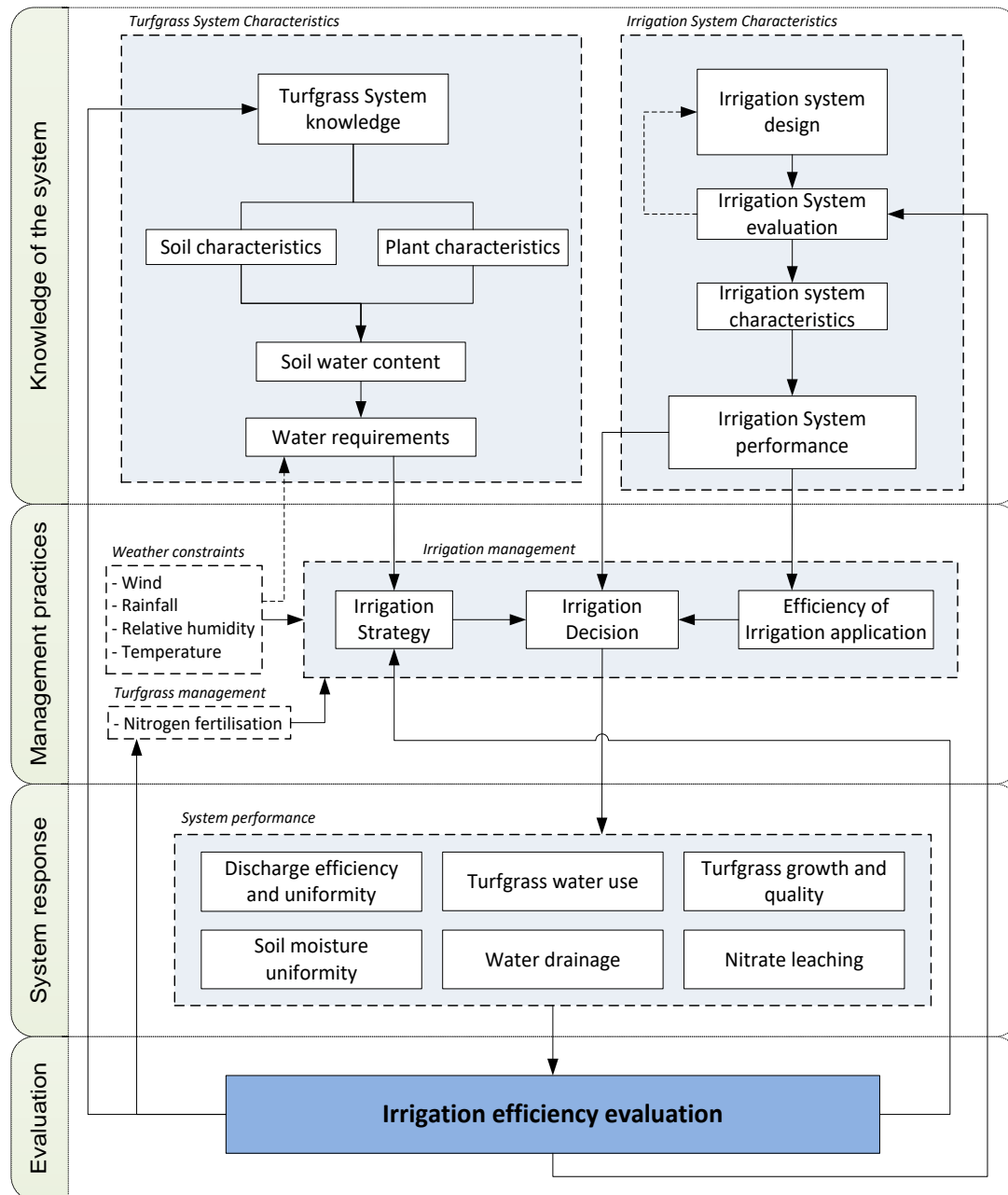


**Figure 8.2** Schematic for proposing improvements in turfgrass irrigation efficiency

The relevance of each component in achieving high irrigation efficiency are summarised below:

*Knowledge of the system*

Detailed knowledge of turfgrass and irrigation systems is the starting point for efficient irrigation. Failing to determine soil water storage capacity, plant water demand or irrigation rates provided by the irrigation system, will lead to irrigation inadequacies. The maximum soil water storage capacity is given by the field

capacity (FC) and is one of the most critical physical soil characteristics affecting irrigation management. Its importance assumes that all water applied beyond FC is lost to drainage. In the Scandinavian golf course survey (Annex-1), only 25% of respondents reported knowing the value for FC in their golf greens. Given the relevance of knowing this value, greater effort should be made to increase awareness of the understanding of the soil characteristics in greens for greenkeeping staff.

In this study, irrigation strategy (based on  $ET_p$  and irrigation frequency) was found to be a primary factor in irrigation management affecting turfgrass performance. Nonetheless, a given irrigation strategy can only be achieved by measuring or estimating the soil water status prior to irrigation, and by applying an adequate irrigation. Adequate irrigation will only be achieved by knowing the water delivered on an irrigation event (mm), for which it is necessary to understand the irrigation rates (IR) provided by the system. As it has been reported in Chapter 7, IR is highly affected by the sprinklers location and set-up. The replacement of sprinkler heads and nozzles or variation in the operating pressure will lead to changes in IR, which will trigger irrigation inadequacies. It is essential that greenkeepers know the irrigation rates, as defined by sprinkler model, nozzle size, operation pressure, and jet angle and distance between sprinklers; which tends to be unique on each part of the course due to the nature of golf course design. The irrigation model developed in this research could be used by greenkeepers to quickly estimate irrigation rates for their greens, avoiding field work required to determine water application depths. Also, it could be used to identify a poor irrigation system design or to study the impact of changes in irrigation system on irrigation rates and heterogeneity. However, manufacturers generally only provide data on their sprinklers regarding the discharge rate ( $L\ h^{-1}$ ) and wetted radius, but not the radial leg curves for each sprinkler model. This restricts the use of irrigation models based on radial leg curves. This observation coincides with previous research (Tarjuelo et al., 1999b; King et al., 2010; Sanchez et al., 2011).

### Management practices

The information on turfgrass and irrigation system characteristics should be used to drive irrigation decision-making. In the BalliSTICS model, the amount of water applied was driven by actual soil water content. The use of portable soil moisture meters such as time domain reflectometers (TDR) has become an affordable, reliable tool for measuring the soil water content (Cardenas-Lailhacar and Dukes, 2012). Measurements of the soil water content can be used to determine the water deficit in the soil quickly and estimate the irrigation requirements. Some studies have reported that irrigating using soil moisture sensors for irrigation decision-making might reduce the water use more than 50% in comparison with other irrigation scheduling methods (McCready et al., 2009; Davis et al., 2009; Cardenas-Lailhacar et al., 2010). Irrigation decision based on visual inspection could lead to imprecise irrigation. Irrigation could also be inadequate when schedules are based on a fixed time (minutes). The use of data from nearby weather stations might also help to estimate plant water requirements (given by evapotranspiration values) and avoid irrigating when rainfall or strong winds are forecast.

### System response

To evaluate irrigation efficiency, it is necessary to quantify turfgrass responses to irrigation management. Therefore, gathering data on turfgrass system response during the season is critical. The modelling approach used in this research permitted the quantification of the system response parameters. However, some of those parameters are rarely measured by green-keeping staff. In addition, turfgrass responses to irrigation practices might vary depending on the location, species and other management practices not related with irrigation (Chapter 4). There is, therefore, a need for implementing new technologies emerging from precision agriculture to automate data collection for turf. These include remote sensing tools, mobile mapping platforms and optical sensor technologies (Bell et al., 2013). These technologies might facilitate near real-time monitoring and decision-making in the future. The use of TDR's or spectral cameras can help identify "dry spots" produced by deficiencies in the irrigation system. However,



the evaluation of irrigation in humid regions needs to be considered carefully due to the influence of rainfall on soil moisture uniformity (Chapter 7). In addition, the measurement of the amount of water applied and regularly inspecting sprinkler condition and irrigation uniformity is essential.

A precise measurement of in-situ DMP is a time-consuming task mainly limited to experimental trials. Some authors proposed the measurement of the volume of fresh clippings (Woods et al., 2016) which provides an estimate of the relative DMP for a given period and can be used to drive N fertilisation. The development of tools for in-situ measurements of clippings combined with the use of unmanned aerial vehicles might be an affordable solution for automated data collection (Caturegli et al., 2016); helping to identify areas where turf is growing at higher or lower rates.

Regarding drainage and leaching on greens, these are two variables that are hardly quantifiable in real world conditions. Thus, the solution for minimising leaching is to adopt measures that minimise nitrate lost via drainage. As described in Chapter 7, adopting a moderate deficit irrigation strategy might reduce leaching. Also, as presented in Chapter 4, avoiding over-fertilisation and over-irrigation when turf growth rates are low will reduce the potential leaching risk. However, more research is required to quantify the impacts of variable irrigation strategies along with variable fertilisation, as this last point was out of the scope of the BalliSTICS model simulations. Finally, by avoiding fertilising before heavy rainfall events (which inevitably result in drainage) could also help to reduce N losses.

Improvements in the BalliSTICS model could be useful to complement in-field observations, helping to estimate *system response* variables and to identify potential nitrate losses through leaching. However, the BalliSTICS sub-models still need improvement and refining (Chapters 5 and 6), especially in the dry matter production and nitrogen balance relationships.

### Evaluation

The evaluation of the system response should aim to reach an equilibrium between *turfgrass agronomy, sustainability* and *golf practice requirements* (Figure 8.1). The data gathering process must be accompanied by an analysis and interpretation of data to evaluate and improve current irrigation practices, identify inefficiencies and provide solutions for improving efficiency. As stated previously, the evaluation of a successful irrigation might be subjected to interpretation, and will be obviously affected by other factors including site-specific characteristics, golf maintenance practices other than irrigation, or the uncontrollable occurrence of stresses such as diseases or extreme climatic events.

The process of improving irrigation efficiency is presented here as an iterative process, in which the performance of the turfgrass system is evaluated to enhance *knowledge of the system* and *general management practices*. In this research, it has been shown that an inappropriate irrigation strategy and irrigation performance will not only impact on the water distribution and DMP across a green but also might increase nitrate leaching losses and drainage. When combined with field data, tools such as BalliSTICS model could be used to detect anomalies in irrigation and turfgrass management and support improvements in irrigation efficiency.

In summary, the final aim of an iterative process must be:

- (i) to acquire and reinforce knowledge on irrigation rates and uniformity provided by each sector of the golf course;
- (ii) to improve the irrigation strategy in turfgrass given by the micro- and pedo-climate characteristic in each golf course;
- (iii) to reduce the water and energy consumption;
- (iv) to reduce the number of inputs used in the golf course, and;
- (v) to enhance the sustainability of golf course management actions while reducing potential environmental risks.

## 8.4 FURTHER RESEARCH

This research has developed and applied an integrated modelling approach which allows evaluation of the impact of different irrigation system set-up and irrigation scheduling on irrigation performance and their impacts on turfgrass growth, water balance and nitrate leaching on golf greens. Some suggested areas for further research are outlined below.

- a) The integrated model framework presented would benefit from improvements in both irrigation and STICS models.
  - a.1. *Irrigation model*: The irrigation model would benefit of improvements such as the use of sectoring sprinklers (with adjustable irrigated angle), simulation of undulations on the green and variable wind speeds and direction during an irrigation event. These improvements would require of re-programming the model algorithms to reduce computation time. Also, further research in the simulation of golf rotor sprinklers should aim to improve the simulation of water droplets generation in non-circular nozzles.
  - a.2. *STICS model*: This crop model would benefit from some improvements in the prediction of turfgrass performance before being applied to different turfgrass species. Some modifications of the processes involving biomass production at very short mowing heights, and improvements in the N balance for turfgrass needs to be implemented. More data on turfgrass under severe deficit nitrogen fate (in plant, soil, and leaching) is required to recalibrate STICS and enable the simulation of the overall nitrogen cycle in greens.
  - a.3. *Time-step in simulations*: Simulations have been conducted in a daily-step phase, but the results have been presented on a seasonal basis. It was also observed that when outcomes of the model were analysed in shorter time-steps, the precision of the predictions were reduced. Thus, improvements in the model prediction would allow a more accurate analysis in daily-time intervals.
- b) The BalliSTICS model would benefit from the implementation of new modules. For instance, the integration of a pipe network module to allow golf course

scale evaluation to study impacts of different network designs on performance, optimisation of irrigation schedules, energy consumption and the financial impact of irrigation management.

- c) This research has focused on the *turfgrass agronomy* and *sustainability* components (Figure 8.1). Future research might focus on quantifying the *golf playability* components, i.e., how irrigation management affects turf visual quality, surface hardness or ball roll. The integration of a module for estimating turfgrass quality as presented by Wilkerson et al. (2015) would be beneficial.
- d) This research has been conducted using a modelling approach. However, new research should test these findings under field conditions. There is a need of improving the understanding on the relationships between water, nitrogen balance and dry matter production. New research should also focus on embrace these three components to understand their relationships.
- e) The impacts of rainfall and its relationship with irrigation on turfgrass performance should be studied in more detail, especially in humid regions. To date, most studies have focused on exploring impacts of irrigation on turfgrass under controlled conditions. Future research is required to understand the effects of uneven, heavy rains combined with different irrigation strategies.
- f) Figure 8.2 outlines the importance of gathering site-specific data in an automatic and real-time manner. A precision agriculture approach utilising advanced sensor technology (soil, plant, and atmosphere) will need to be embraced by the turf industry. Research is needed to adapt these tools to the golf and wider sportsturf sector.
- g) Climate change will affect future temperature and precipitation patterns (Hatfield, 2017); it is thus necessary to study the impacts of these changes on turfgrass. The STICS model could be used to study the impacts of climate change on turfgrass and its implication on water use in golf courses with some of the refinements proposed above.

## 9 CONCLUSIONS

This thesis aimed to understand and assess the relationships between irrigation management and turfgrass water use, soil water availability, dry matter production, drainage and nitrate leaching in golf greens under Northern European climate conditions. By combining a review of existing knowledge with field data collection and the development and application of an integrated modelling approach, this research has produced substantive new insights and contributed to advancing our understanding of the impacts of irrigation management on sportsturf. A summary of the main conclusions, with respect to the four research objectives defined in Section 1.3, is presented below:

***Objective 1. To critically review and synthesise existing science and industry evidence on the links between irrigation management, turfgrass agronomy and environmental impacts***

A comprehensive systematic review (SR) has been undertaken of the scientific and grey literature (Chapter 4) following an internationally recognised approach (CEBC, 2010) to assess the links between irrigation management, turfgrass agronomy and environmental impact. The SR findings have been published in a high impact journal (Gómez-Armayones et al., 2018). The analysis show that visual turf quality can be maintained at moderate levels of deficit irrigation (50 – 60% of potential evapotranspiration). Although larger irrigation applications led to increases in dry matter production (DMP), N fertilisation appeared to be a more important driver of turfgrass growth. Evidence confirmed that irrigation beyond field capacity increases the risk of nitrate leaching. However, the total loss of N in leachate is influenced more by fertilisation rates, soil characteristics, turfgrass species and turfgrass growth rates than by irrigation practices alone. Despite the clear relationships between irrigation and turfgrass agronomy presented in the SR, it has also been found that the impacts of irrigation strategy vary depending on the turfgrass species, mowing height, fertilisation rates and local weather conditions.

**Objective 2.** *To develop, calibrate and validate a ballistics-based model to simulate irrigation system performance under contrasting environmental and irrigation design conditions*

This research represents the first study to apply ballistics theory to simulate the performance of irrigation for a golf rotor sprinkler. The research was split into field data collection, model development and model calibration. The model developed in this research successfully simulates the wetted area from a single sprinkler under windy conditions and, with some error, the spatial distribution in irrigation rate ( $\text{mm h}^{-1}$ ). For sprinkler overlapping, the model predicts with a high degree of accuracy the average irrigation rates, and, to a lower extent, the irrigation uniformity (CU) which tends to be slightly over-estimated. Notwithstanding these limitations, the model allows the simulation of different sprinkler set-ups, changes in sprinkler position, and irrigated area (green shape) under varying wind conditions, and is considered a novel tool for studying and understanding the impacts of irrigation design on system performance. It could also be used by greenkeepers and golf architects to evaluate irrigation performance for given designs without the need of conducting time-consuming fieldwork.

Although the model was shown to provide robust simulations of irrigation application, some areas for improvement have been identified, particularly relating to data collection and some of the modelling algorithms. Firstly, it has not been possible to collect reliable data for the characteristic radial leg curves under “no-wind” conditions in outdoor tests. This highlights the need for conducting such tests under controlled indoor conditions. Secondly, the complexity of the nozzle shape used in golf sprinklers has been identified as a potential source of error in the modelling of droplet formation and, consequently, in the uniformity assessment. Further work is needed to acquire better knowledge of the processes involved in the droplet formation and distribution for these non-circular, multi-aperture nozzles.

**Objective 3.** *To calibrate and validate a biophysical crop growth model to simulate changes in dry matter production, water use and nutrient leaching for fine turf under varying environmental conditions*

A biophysical crop model (STICS) was chosen as the most suitable model for this research. This model has been previously used in grassland and forage crop research, but this is the first research where it has been used for simulating fine turfgrass growth and development for golf course conditions.

After parameterisation and sensitivity analysis, the STICS model was calibrated and validated with experimental field data obtained from research conducted in Norway on turfgrass irrigation under typical golf management conditions. Simulations of seasonal dry matter production (clippings), water use and nutrient leaching have been undertaken with acceptable levels of modelling accuracy and goodness of fit. However, the evaluation of the model outcomes in shorter time-steps than seasonally, the model presented larger inaccuracies in the predictions. Consequently, the model use has mainly been limited to assess seasonal outcomes and responses for the variables described above.

STICS parameterisation was shown to be a complex process. Despite encouraging results, some modelling improvements have been identified. Specifically, the relationships between shallow, frequent mowing on turfgrass and leaf expansion still present a major challenge in the stability of the simulations. Further work is required to enhance the model equations to better simulate the particularities of turfgrass, such as the relationships between plant biomass, leaf area index and nitrogen balance. Data available for model calibration and validation was also limited highlighting the significant number of variables that STICS needs to be successfully calibrated. Model performance would benefit from improved data relating to irrigation, dry matter production and nitrogen fate in golf greens.

**Objective 4.** *To simulate a range of irrigation management strategies on turfgrass performance and their environmental impacts through the development of an integrated irrigation-crop modelling framework*

The development and application of the BalliSTICS model provides a useful tool to simulate the impacts of irrigation strategy and non-uniformity on turfgrass. This research demonstrates that although non-uniform irrigation affects fine turf growth, the water balance and leaching potential, the irrigation strategy is the primary component of management with impacts on turfgrass agronomy. The most appropriate irrigation strategy was one that provides moderate deficit irrigation (60% of potential evapotranspiration). Irrigation beyond field capacity not only increased water use but also the leaching risk. These results are consistent with those obtained from evidence found in the systematic review (Chapter 4). A novel finding arising from the modelling is that, assuming a pre-determined nitrogen policy, leaching increased for severe deficit irrigation, which was due to lower DMP and subsequent reduction in plant nitrogen uptake. This outlines the importance of adopting a precise irrigation strategy not only to achieve an actively growing turfgrass, but also to reduce the environmental impacts derived from turf management.

An adequate irrigation strategy can only be achieved by understanding the irrigation rates ( $\text{mm h}^{-1}$ ) provided by the system. Through the application of the irrigation model, it has been shown that changes in the sprinkler position, nozzle size and operating pressure will collectively impact on the irrigation rates. With inadequate understanding of the irrigation application rate on a golf green, it is impossible to implement an adequate irrigation strategy. This situation is exacerbated under low irrigation uniformities. In order to achieve high irrigation uniformity, sprinkler positions must be optimised for the constraints given by the green shape, and irrigation should preferably not be applied when wind speeds are equal or greater than  $2.5 \text{ m s}^{-1}$ . Surprisingly, under windy conditions, the different nozzle sizes and operating pressures had little impact on CU.

This research demonstrated that rainfall in humid climates requires special attention in turf irrigation management. The typical high precipitation rates in the



region studied in this research are the primary source of water input, reducing the irrigation requirements substantially in comparison to other more arid areas where golf irrigation is essential for fine turf survival. However, rainfall might lead to “side effects” in turf management. It has been found that rainfall is the main factor affecting drainage and leaching. In the irrigation treatments in which the DMP was reduced, leaching risk increased due to the lower N uptake and drainage following heavy rainfall. Rainfall also helps to buffer any negative impacts of non-uniform irrigation, as it helps to reduce soil moisture variation across the golf green. Although rainfall has a positive effect on turfgrass management, it could lead to turf management staff having a false sense of satisfaction with their irrigation system and its performance. It could also help to offset poor irrigation scheduling and management decisions.

The findings from this research also support existing knowledge on the increased leaching risks when N uptake in turfgrass (and therefore DMP) is low. Although the turf simulations have only considered one fertilisation strategy, the results from the simulations (Chapter 7) and systematic review (Chapter 4) provided sufficiently robust evidence that DMP should be considered as a major driver for N fertilisation. In this context, a need for future research on the relationships between deficit irrigation, DMP and nitrogen fate has been identified. Future research could assess a new hypothesis arising from this study, that *“severe deficit irrigation under humid climates leads to higher leaching risks than under moderate deficit or field capacity irrigation strategies”*.

In conclusion, through a combination of evidence synthesis, new empirical evidence and development of an integrated modelling approach, this research demonstrates that irrigation management can be improved through careful consideration of irrigation design and turfgrass agronomy practices and strategies. By selecting an appropriate sprinkler design and adopting a moderate deficit irrigation strategy, water use for golf can be reduced while still maintaining a healthy, actively growing turfgrass, which is a requirement to meet the exacting demands from players for optimum ball speed, bounce and playability. This research improves our understanding of the importance of irrigation for turfgrass

management even in humid climates. The approaches developed and findings from this research will be essential in supporting the turfgrass industry to better understand the need for developing new technological solutions for data collection and evaluating the impacts of irrigation in turfgrass, not just for golf but other sportsturf sectors. Further improvements in the BalliSTICS modelling framework will contribute to the sustainable management of turfgrass and enhancement of irrigation practices in both the golf and sportsturf sectors.

## REFERENCES

- Aamlid, T.S., A.M.D. Jensen, P.E. Rasmussen, and Kvalbein. 2015. Best management of red fescue (*Festuca rubra*) golf greens for high sustainability and playability. 2(128): 1–24.
- Aamlid, T.S., J.W. Knox, H. Riley, A. Kvalbein, and T. Pettersen. 2016. Crop Coefficients, Growth Rates and Quality of Cool-Season Turfgrasses. *J. Agron. Crop Sci.* 202(1): 69–80.
- Aamlid, T.S., A. Kvalbein, and T. Pettersen. 2012. Irrigation strategies and soil surfactant on golf course fairways. p. 1–2. *In* European Turfgrass Society Conference 'Quality Turf and Efficient Utilization of Resources'. Kristansand, Norway.
- Aamlid, T.S., and B. Molteberg. 2011. Turfgrass species and varieties for Scandinavian golf greens. *Acta Agric. Scand. Sect. B - Plant Soil Sci.* 61(2): 143–152.
- Abraham, E.M., W. a. Meyer, S. a. Bonos, and B. Huang. 2008. Differential responses of hybrid bluegrass and kentucky bluegrass to drought and heat stress. *HortScience* 43(7): 2191–2195.
- Adams, W.A., and R.J. Gibbs. 1994. *Natural Turf for Sport and Amenity*. 2nd ed. CAB International, Oxon, UK.
- Al-Ghobari, H.M., M.S. El-Marazky, A.Z. Dewidar, and M.A. Mattar. 2018. Agricultural Water Management Prediction of wind drift and evaporation losses from sprinkler irrigation using neural network and multiple regression techniques. *Agric. Water Manag.* 195: 211–221.
- Aldous, D.E. 1999. *International turf management handbook*. Inkata Press.
- Allaire-Leung, S.E., L. Wu, J.P. Mitchell, and B.L. Sanden. 2001. Nitrate leaching and soil nitrate content as affected by irrigation uniformity in a carrot field. *Agric. Water Manag.* 48(1): 37–50.
- Allen, R.G., L.S. Pereira, D. Raes, and M. Smith. 1998. Crop evapotranspiration - Guidelines for computing crop water requirements - FAO Irrigation and drainage paper 56. *Irrig. Drain.* 300(56): 300.
- An, N., A.L. Goldsby, K.P. Price, and D.J. Bremer. 2015. Using hyperspectral radiometry to predict the green leaf area index of turfgrass. *Int. J. Remote Sens.* 36(5): 1470–1483.
- ANSI/ASAE. 1985. ASAE S398.1 Procedure for Sprinkler Testing and Performance Reporting (Revised 2016). : 1–6.
- ANSI/ASAE. 1989. ASAE S436.1 Test Procedure for Determining the Uniformity of Water Distribution of Center Pivot and Lateral Move Irrigation Machines Equipped with Spray or Sprinkler Nozzles (Revised 2001). : 932–938.
- Augier, P. 1996. Contribution a l'etude et a la modelisation mecaniste-statistique de la distribution spatiale des apports d'eau sous un canon d'irrigation : application a la caracterisation des effets du vent sur l'uniformite d'arrosage.
- Aydinsakir, K., D. Buyuktas, R. Bastug, and S. Yilmaz. 2016. Evapotranspiration and quality characteristics of some bermudagrass turf cultivars under deficit irrigation. *Grassl. Sci.* 62(4): 224–232.
- Baldwin, C.M., H. Liu, L.B. McCarty, W.L. Bauerle, and J.E. Toler. 2006. Response of six bermudagrass cultivars to different irrigation intervals. *Horttechnology* 16(3): 466–470.
- Bandaranayake, W., Y.L. Qian, W.J. Parton, D.S. Ojima, and R.F. Follett. 2003. Estimation of soil organic carbon changes in turfgrass systems using the CENTURY model. *Agron. J.* 95(3): 558–563.
- Bañuelos, J.B., J.L. Walworth, P.W. Brown, and D.M. Kopec. 2011. Deficit Irrigation of Seashore Paspalum and Bermudagrass. *Agron. J.* 103(6): 1567.
- Bartlett, M.D., and I.T. James. 2011a. A model of greenhouse gas emissions from the management of turf on two golf courses. *Sci. Total Environ.* 409(23): 5137–5147.
- Bartlett, M.D., and I.T. James. 2011b. Are golf courses a source or sink of atmospheric carbon dioxide? A modelling approach. *Proc. Inst. Mech. Eng. Part P J. Sport. Eng. Technol.* 225(2): 75–83.
- Barton, L., and T.D. Colmer. 2006. Irrigation and fertiliser strategies for minimising nitrogen leaching from turfgrass. *Agric. Water Manag.* 80(1–3 SPEC. ISS.): 160–175.
- Barton, L., G.G.Y. Wan, R.P. Buck, and T.D. Colmer. 2009. Does N fertiliser regime influence N leaching and quality of different-aged turfgrass (*Pennisetum clandestinum*) stands? *Plant Soil* 316(1–2): 81–96.
- Barton, L., G.G.Y. Wan, and T.D. Colmer. 2006a. Turfgrass (*Cynodon dactylon* L.) sod production on sandy

- soils: I. Effects of irrigation and fertiliser regimes on growth and quality. *Plant Soil* 284(1–2): 129–145.
- Barton, L., G.G.Y. Wan, and T.D. Colmer. 2006b. Turfgrass (*Cynodon dactylon* L.) sod production on sandy soils: II. Effects of irrigation and fertiliser regimes on N leaching. *Plant Soil* 284(1–2): 147–164.
- Bautista-Capetillo, C., M. Zavala, and E. Playán. 2012. Kinetic energy in sprinkler irrigation: Different sources of drop diameter and velocity. *Irrig. Sci.* 30(1): 29–41.
- Beard, J.B. 1973. *Turfgrass: Science and Culture*. Prentice-Hall, Englewood Cliffs, New Jersey.
- Beard, J.B. 2000. Turfgrass benefits and the golf environment. *Fate Manag. Turfgrass Chem.* 743: 36–44.
- Beard, J.B. 2002. *Turf management for golf courses*. 2nd ed. John Wiley & Sons, Hoboken, NJ, USA, Hoboken, New Jersey.
- Beard, J.B., and R.L. Green. 1994. The Role of Turfgrasses in Environmental Protection and Their Benefits to Humans. *J. Environ. Qual.* 23(3): 452.
- Bell, G.E., J.K. Kruse, J.M. Krum, J.C. Stier, B.P. Horgan, and S.A. Bonos. 2013. The Evolution of Spectral Sensing and Advances in Precision Turfgrass Management. *In* *Turfgrass: Biology, Use, and Management*.
- Bergez, J.E., H. Raynal, M. Launay, N. Beaudoin, E. Casellas, J. Caubel, P. Chabrier, E. Coucheney, J. Dury, I. Garcia De Cortazar-Atauri, E. Justes, B. Mary, D. Ripoche, and F. Ruget. 2014. Evolution of the STICS crop model to tackle new environmental issues: New formalisms and integration in the modelling and simulation platform RECORD. *Environ. Model. Softw.* 62: 370–384.
- von Bernuth, R.D., and J.R. Gilley. 1984. sprinkler Droplet Size Distribution Estimation from Single Leg Test Data. *Trans. ASAE* 27(5): 1435–1441.
- von Bernuth, R.D., and I. Seginer. 1990. Wind considerations in sprinkler system design. p. 334–339. *In* *Third National Irrigation Symposium*. ASAE.
- Bigelow, C.A., D.J. Soldat, J.C. Stier, B.P. Horgan, and S.A. Bonos. 2013. Turfgrass Root Zones: Management, Construction Methods, Amendment Characterization, and Use. p. 383–423. *In* Stier, J.C., Horgan, B.P., Bonos, S.A. (eds.), *Turfgrass: Biology, Use, and Management*. American Society of Agronomy, Madison, WI.
- Blanco, B. 2012. Assessing the environmental impacts of sport-turf irrigation.
- Boote, K.J., J.W. Jones, and N.B. Pickering. 1996. Potential uses and limitations of crop models. *Agron. J.* 88(5): 704–716.
- Bowman, D.C., D.A. Devitt, M.C. Engelke, and T.W. Ruffy. 1998. Root architecture affects nitrate leaching from bentgrass turf. *Crop Sci.* 38(6): 1633–1639.
- Bowman, D.C.D.C., J.L. Paul, and W.B. Davis. 1989. Nitrate and ammonium uptake by nitrogen-deficient perennial ryegrass and Kentucky bluegrass turf. *J. Am. Soc. Hortic. Sci.* 114: 421–426.
- Bowman, D.C., J.L. Paul, W.B. Davis, and S.H. Nelson. 1987. Reducing Ammonia Volatilization from Kentucky Bluegrass Turf by Irrigation. *Hortscience* 22(1): 84–87.
- Branham, B. 2006. Leaching of pesticides and nitrate in turfgrasses. p. 107–120. *In* Beard, J.B., Kenna, M.P. (eds.), *Water quality and quantity issues for turfgrasses in urban landscapes*. *Counc. Agric. Sci. Technol.*, Las Vegas.
- Bremer, D.J. 2006. Nitrous Oxide Fluxes in Turfgrass. *J. Environ. Qual.* 35(5): 1678.
- Brennan, D. 2008. Factors affecting the economic benefits of sprinkler uniformity and their implications for irrigation water use. *Irrig. Sci.* 26(2): 109–119.
- Breuninger, J.M., M.S. Welterlen, B.J. Augustin, V. Cline, K. Morris, J.C. Stier, B.P. Horgan, and S.A. Bonos. 2013. *The Turfgrass Industry*.
- Brisson, N., C. Gary, E. Justes, R. Roche, B. Mary, D. Ripoche, D. Zimmer, J. Sierra, P. Bertuzzi, P. Burger, F. Bussièrre, Y.M. Cabidoche, P. Cellier, P. Debaeke, J.P. Gaudillère, C. Hénault, F. Maraux, B. Seguin, and H. Sinoquet. 2003. An overview of the crop model STICS. *Eur. J. Agron.* 18(3–4): 309–332.
- Brisson, N., M. Launay, B. Mary, and N. Beaudoin. 2008. Conceptual basis, formalisations and parameterisation of the STICS crop model.
- Brisson, N., F. Ruget, P. Gate, J. Lorgeou, B. Nicoulaud, X. Tayot, D. Plenet, M.-H. Jeuffroy, A. Bouthier, D. Ripoche, B. Mary, and E. Justes. 2002. STICS: a generic model for simulating crops and their water and nitrogen balances. II. Model validation for wheat and maize. *Agronomie* 22(1): 69–92.
- Bristow, A.W., J.C. Ryden, and D.C. Whitehead. 1987. The fate at several time intervals of 15N-labelled

- ammonium nitrate applied to an established grass sward. *J. Soil Sci.* 38(2): 245–254.
- Brown, S. 2005. Sports turf & amenity grassland management. The Crowood Press Ltd.
- Buis, S., D. Wallach, S. Guillaume, H. Varella, P. Lecharpentier, M. Launay, M. Guérif, J.-E. Bergez, E. Justes, L.R. Ahuja, and L. Ma. 2011. The STICS Crop Model and Associated Software for Analysis, Parameterization, and Evaluation. p. 395–426. *In* Methods of Introducing System Models into Agricultural Research.
- Callahan, L.M., W.L. Sanders, J.M. Parham, C.A. Harper, L.D. Lester, and E.R. McDonald. 1997. Comparative Methods of Measuring Thatch on a Creeping Bentgrass Green. *Crop Sci.* 37(1): 230.
- Calvache, S. 2014. Determinación de las necesidades de nitrógeno de un green mediante sensores remotos.
- Calvache, S., T. Espevig, T.E. Andersen, E.J. Jøner, A. Kvalbein, T. Pettersen, and T.S. Aamlid. 2017. Nitrogen, Phosphorus, Mowing Height, and Arbuscular Mycorrhiza Effects on Red Fescue and Mixed Fescue–Bentgrass Putting Greens. *Crop Sci.* 57(2): 537.
- Candogan, B.N., U. Bilgili, S. Yazgan, and E. Acikgoz. 2014. Growth and quality responses of tall fescue (*Festuca arundinacea* Schreb.) to different irrigation levels and nitrogen rates. *Turkish J. F. Crop.* 19(1): 142–152.
- Candogan, B.N., U. Bilgili, S. Yazgan, and E. Acikgoz. 2015. Irrigation Level and Nitrogen Rate Affect Evapotranspiration and Quality of Perennial Ryegrass (*Lolium perenne*). *Int. J. Agric. Biol.* 17(3): 431–439.
- Cardenas-Lailhacar, B., and M.D. Dukes. 2012. Soil moisture sensor landscape irrigation controllers: A review of multi-study results and future implications. *Trans. ASABE* 55(2): 581–590.
- Cardenas-Lailhacar, B., M.D. Dukes, and G.L. Miller. 2010. Sensor-Based Automation of Irrigation on Bermudagrass during Dry Weather Conditions. *J. Irrig. Drain. Eng.* 136(3): 184–193.
- Carey, R.O., G.J. Hochmuth, C.J. Martinez, T.H. Boyer, V.D. Nair, M.D. Dukes, G.S. Toor, A.L. Shober, J.L. Cisar, L.E. Trenholm, and J.B. Sartain. 2012. A Review of Turfgrass Fertilizer Management Practices: Implications for Urban Water Quality. *Horttechnology* 22(3): 280–291.
- Carley, D.S., D. Goodman, S. Sermons, W. Shi, D. Bowman, G. Miller, and T. Ruffy. 2011. Soil Organic Matter Accumulation in Creeping Bentgrass Greens: A Chronosequence with Implications for Management and Carbon Sequestration. *Agron. J.* 103(3): 604.
- Carrión, P., J. Montero, and J.M. Tarjuelo. 2001a. Aplicación de la simulación al diseño de los sistemas de riego por aspersión: el modelo SIRIAS. *Rev. Int. Métodos Numéricos para Cálculo y Diseño en Ing.* 17(3): 347–362.
- Carrión, P., J.M. Tarjuelo, and J. Montero. 2001b. SIRIAS: A simulation model for sprinkler irrigation. I. Description of model. *Irrig. Sci.* 20(2): 73–84.
- Carrow, R.N. 2006. Can we maintain turf to customers' satisfaction with less water? *Agric. Water Manag.* 80(1–3 SPEC. ISS.): 117–131.
- Carrow, R.N., J.M. Krum, I. Flitcroft, and van Cline. 2010. Precision turfgrass management: Challenges and field applications for mapping turfgrass soil and stress. *Precis. Agric.* 11(2): 115–134.
- Caturegli, L., M. Corniglia, M. Gaetani, N. Grossi, S. Magni, M. Migliazzi, L. Angelini, M. Mazzoncini, N. Silvestri, M. Fontanelli, M. Raffaelli, A. Peruzzi, and M. Volterrani. 2016. Unmanned Aerial Vehicle to Estimate Nitrogen Status of Turfgrasses (X Hu, Ed.). *PLoS One* 11(6): e0158268.
- Cavero, J., L. Jiménez, M. Puig, J.M. Faci, and A. Martínez-Cob. 2008. Maize growth and yield under daytime and nighttime solid-set sprinkler irrigation. *Agron. J.* 100(6): 1573–1579.
- CEBC, C. for E.-B.C. 2010. Guidelines for Systematic Reviews in Environmental Management. (May): 1–75.
- Chen, Y., T. Pettersen, A. Kvalbein, and T.S. Aamlid. 2018. Playing quality, growth rate, thatch accumulation and tolerance to moss and annual bluegrass invasion as influenced by irrigation strategies on red fescue putting greens. *J. Agron. Crop Sci.* 204(2): 185–195 Available at <http://doi.wiley.com/10.1111/jac.12246>.
- Choate, R.B. 1994. Turf irrigation manual: The complete guide to turf and landscape irrigation systems. 5th ed. Water-matic Division of TELSCO INDUSTRIES, Dallas, TX.
- Christians, N.E., A.J. Patton, and Q.D. Law. 2017. Fundamentals of turfgrass management. 5th Editio.
- Christiansen, J.E. 1942. Irrigation by Sprinkling. *Calif. Agric. Exp. Stn. Bull.*
- Cisar, J. 2012. Reducing Environmental Impacts of Fertilizers and Pesticides through Sustainable High Performance Turfgrass Systems. *Acta Hort.* 938: 105–111.

- Clemmens, A.J. 1991. Irrigation uniformity relationships for irrigation system management. *J. Irrig. Drain. Eng.* 117(5): 682–699.
- Colmer, T.D., and L. Barton. 2017. A Review of Warm-Season Turfgrass Evapotranspiration, Responses to Deficit Irrigation, and Drought Resistance. *Crop Sci.* 57(supplement1): S-98.
- Constantin, J., C. Le Bas, and E. Justes. 2015. Large-scale assessment of optimal emergence and destruction dates for cover crops to reduce nitrate leaching in temperate conditions using the STICS soil–crop model. *Eur. J. Agron.* 69: 75–87.
- D. C. Kincaid. 1996. Spraydrop Kinetic Energy from Irrigation Sprinklers. *Trans. ASAE* 39(3): 847–853.
- Daccache, A., C. Keay, R.J.A. Jones, E.K. Weatherhead, M.A. Stalham, and J.W. Knox. 2012. Climate change and land suitability for potato production in England and Wales: impacts and adaptation. *J. Agric. Sci.* 150(02): 161–177.
- Daccache, A., N. Lamaddalena, and U. Fratino. 2010. On-demand pressurized water distribution system impacts on sprinkler network design and performance. *Irrig. Sci.* 28(4): 331–339.
- DaCosta, M., and B. Huang. 2006a. Deficit irrigation effects on water use characteristics of bentgrass species. *Crop Sci.* 46(4): 1779–1786.
- DaCosta, M., and B. Huang. 2006b. Minimum Water Requirements for Creeping, Colonial, and Velvet Bentgrasses under Fairway Conditions. *Crop Sci.* 46(1): 81–89.
- DaCosta, M., B. Huang, J.C. Stier, B.P. Horgan, and S.A. Bonos. 2013. Heat-Stress Physiology and Management. *In Turfgrass: Biology, Use, and Management.*
- Darko, R.O., Y. Shouqi, L. Junping, Y. Haofang, Z. Xingye, D.R. O, Y.S. Q, J.P. Liu, H.F. Yan, and X.Y. Zhu. 2017. Overview of advances in improving uniformity and water use efficiency of sprinkler irrigation. 10: 1–15.
- Davis, S.L., M.D. Dukes, and G.L. Miller. 2009. Landscape irrigation by evapotranspiration-based irrigation controllers under dry conditions in Southwest Florida. *Agric. Water Manag.* 96(12): 1828–1836.
- Dechmi, F., E. Playán, J. Caverro, J.M. Faci, and A. Martínez-Cob. 2003a. Wind effects on solid set sprinkler irrigation depth and yield of maize [*Zea mays*]. *Irrig. Sci.* 22(2): 67–77.
- Dechmi, F., E. Playán, J. Caverro, a. Martínez-Cob, and J.M. Faci. 2004a. Coupled Crop and Solid Set Sprinkler Simulation Model. II: Model Application. *J. Irrig. Drain. Eng.* 130(6): 511–519.
- Dechmi, F., E. Playán, J. Caverro, A. Martínez-Cob, and J.M. Faci. 2004b. Coupled Crop and Solid Set Sprinkler Simulation Model. I: Model Development. *J. Irrig. Drain. Eng.* 130(6): 499–510.
- Dechmi, F., E. Playán, J.M. Faci, M. Tejero, and a. Berbero. 2003b. Analysis of an irrigation district in northeastern Spain II. Irrigation evaluation, simulation and scheduling. *Agric. Water Manag.* 61(2): 93–109.
- Dinka, M.O. 2016. Evaluating the Adequacy Performance of Sprinkler Irrigation Systems at Finchaa Sugar Cane Plantation, Eastern Wollega Zone (Ethiopia). *Irrig. Drain.* 65(4): 537–548.
- Du, H., and Z. Wang. 2009. Differential Responses of Warm-season and Cool-season Turfgrass Species to Heat Stress Associated with Antioxidant Enzyme Activity. *Reading* 134(4): 417–422.
- Dukes, M.D. 2006. Effect of wind speed and pressure on linear move irrigation system uniformity. *Appl. Eng. Agric.* 22(4): 541–548.
- Dukes, M.D., M.B. Haley, and S.A. Hanks. 2006. Sprinkler Irrigation and Soil Moisture Uniformity. p. 446–460. *In 27th Annual International Irrigation Show.*
- Dumont, B., V. Leemans, M. Mansouri, B. Bodson, J.-P. Destain, and M.-F. Destain. 2014. Parameter identification of the STICS crop model, using an accelerated formal MCMC approach. *Environ. Model. Softw.* 52: 121–135.
- Durand, J.-L., V. Gonzalez-Dugo, and F. Gastal. 2010. How much do water deficits alter the nitrogen nutrition status of forage crops? *Nutr. Cycl. Agroecosystems* 88: 231–243.
- Dwomoh, F.A., Y. Shouqi, and L. Hong. 2013. Field performance characteristics of fluidic sprinkler. *Appl. Eng. Agric.* 29(4): 529–536.
- Elansary, H.O., and K. Yessoufou. 2015. Growth regulators and mowing heights enhance the morphological and physiological performance of Seaspray turfgrass during drought conditions. *Acta Physiol. Plant.* 37(11): 1–11.
- Emmons, R.D. 2008. *Turfgrass science and management.* 4th ed. Clifton Park, NY.

- Erickson, J.E., D.M. Park, J.L. Cisar, G.H. Snyder, and A.L. Wright. 2010. Effects of sod type, irrigation, and fertilization on nitrate-nitrogen and orthophosphate-phosphorus leaching from newly established St. Augustinegrass Sod. *Crop Sci.* 50(3): 1030–1036.
- Ericsson, T., K. Blombäck, and A. Kvalbein. 2012a. Precision Fertilisation - From theory to practice. STERF.
- Ericsson, T., K. Blombäck, A. Kvalbein, and A. Neumann. 2012b. Demand-driven fertilization. Part II: Influence of demand-driven fertilization on shoot nitrogen concentration, growth rate, fructan storage and playing quality of golf turf. *Acta Agric. Scand. Sect. B Soil Plant Sci.*
- Ericsson, T., K. Blombäck, and A. Neumann. 2012c. Demand-driven fertilization. Part I: Nitrogen productivity in four high-maintenance turf grass species Tom. *Acta Agric. Scand. Sect. B - Plant Soil Sci.* 62(1): 113–121.
- Ervin, E.H., and A.J. Koski. 1998. Drought Avoidance Aspects and Crop Coefficients of Kentucky Bluegrass and Tall Fescue Turfs in the Semiarid West. *Crop Sci.* 38(3): 788.
- Espevig, T., and T.S. Aamlid. 2012. Effects of root zone composition and irrigation regime on performance of velvet bentgrass putting greens. II. Thatch, root development and playability. *Acta Agric. Scand. Sect. B Soil Plant Sci.* 62(SUPPL.1): 106–112.
- Evet, S.R., and J.A. Tolk. 2009. Can Water Use Efficiency Be Modeled Well Enough to Impact Crop Management? *Agron. J.* 101(3): 423.
- Faria, L.C., S. Beskow, A. Colombo, B.G. Nörenberg, O. Rettore Neto, and M.C. Simões. 2015. Influence of the wind on water application uniformity of a mechanical lateral move irrigation equipment using rotating plate sprinklers. *Ciência Rural* 46(1): 83–88.
- Faria, L.C., S. Beskow, A. Colombo, H.F.E. De Oliveira, and R. Esu. 2012. Modelagem dos efeitos do vento na uniformidade da irrigação por aspersão: Aspersores de tamanho médio Modelagem dos efeitos do vento na uniformidade da irrigação por aspersão: Aspersores de tamanho médio. *Rev. Bras. Eng. Agric. e Ambient.* 16(2): 133–141.
- Faria, L.C., A. Colombo, H.F.E. De Oliveira, and G. Prado. 2009. Simulação da uniformidade de aplicação de água em sistemas convencionais de irrigação operando sob diferentes condições de vento. *Engenharia Agric.* 29(1): 76.
- Feldhake, C.M., R.E. Danielson, and J.D. Butler. 1984. Turfgrass Evapotranspiration. II. Responses to Deficit Irrigation. *Agron. J.* 76(1): 90.
- Félix-félix, J.R., · H Salinas-tapia, · C Bautista-capetillo, · J García-aragón, · J Burguete, and · E Playán. 2017. A modified particle tracking velocimetry technique to characterize sprinkler irrigation drops. 35: 515–531.
- Filipović, V., G.S. Toor, G. Ondrašek, and R. Kodešová. 2014. Modeling water flow and nitrate–nitrogen transport on golf course under turfgrass. *J. Soils Sediments* 000(Epa 2010): 1847–1859.
- Flénet, F., P. Villon, and F. Ruget. 2004. Methodology of adaptation of the STICS model to a new crop: spring linseed (*Linum usitatissimum*, L.). *Agronomie* 24(6–7): 367–381.
- Fontanier, C.H., J.A. Aitkenhead-Peterson, B.G. Wherley, R.H. White, J.C. Thomas, and P. Dwyer. 2017. Deficit Irrigation and Fertility Effects on NO<sub>x</sub>–N Exports from St. Augustinegrass. *J. Environ. Qual.* 46(4): 793.
- Frank, K.W., E.A. Guertal, J.C. Stier, B.P. Horgan, and S.A. Bonos. 2013. Nitrogen Research in Turfgrass. p. 457–491. *In* Stier, J.C., Horgan, B.P., Bonos, S.A. (eds.), *Turfgrass: Biology, Use, and Management*. American Society of Agronomy, Madison, WI.
- Frank, K.W., K.M. O'Reilly, J.R. Crum, and R.N. Calhoun. 2006. The Fate of Nitrogen Applied to a Mature Kentucky Bluegrass Turf. *Crop Sci.* 46(1): 209.
- Fry, J.D., and J.D. Butler. 1989. Responses of Tall and Hard Fescue to Deficit Irrigation. *Crop Sci.* 29(6): 1536.
- Fry, J., and B. Huang. 2004. *Applied turfgrass science and physiology*. John Wiley & Sons, Hoboken, NJ, USA.
- Fu, J., and P.H. Dernoeden. 2009a. Creeping Bentgrass Putting Green Turf Responses to Two Irrigation Practices: Quality, Chlorophyll, Canopy Temperature, and Thatch–Mat. *Crop Sci.* 49(3): 1071–1078.
- Fu, J., and P.H. Dernoeden. 2009b. Creeping Bentgrass Putting Green Turf Responses to Two Summer Irrigation Practices: Rooting and Soil Temperature. *Crop Sci.* 49(3): 1063–1070.
- Fu, J., J. Fry, and B. Huang. 2004. Minimum water requirements of four turfgrasses in the transition zone. *HortScience* 39(7): 1740–1744.
- Fu, J., J. Fry, and B. Huang. 2007. Tall fescue rooting as affected by deficit irrigation. *HortScience* 42(3): 688–691.

- Fukui, Y., K. Nakanishi, and S. Okamura. 1980. Computer evaluation of sprinkler irrigation uniformity. *Irrig. Sci.* 2(1): 23–32.
- Gaussoin, R.E., W.L. Berndt, C.A. Dockrell, and R.A. Drijber. 2013. Characterization, development, and management of organic matter in turfgrass systems. p. 425–456. *In* Stier, J.C., Horgan, B.P., Bonos, S.A. (eds.), *Turfgrass: Biology, Use, and Management*. American Society of Agronomy.
- Goldsby, A.L.E.E. 2013. Establishment, drought tolerance and recovery, and canopy analysis of turfgrasses in the transition zone.
- Gómez-Armayones, C., A. Kvalbein, T.S. Aamlid, and J.W. Knox. 2018. Assessing evidence on the agronomic and environmental impacts of turfgrass irrigation management. *J. Agron. Crop Sci.* (December 2017): 1–14.
- González Perea, R., A. Daccache, J.A. Rodríguez Díaz, E. Camacho Poyato, and J.W. Knox. 2017. Modelling impacts of precision irrigation on crop yield and in-field water management. *Precis. Agric.*
- Granier, J., B. Molle, and J.M. Deumier. 2003. IRRIPARC-Part 1 : Modeling spatial water distribution under a sprinkler in windy conditions. *In* EUROPEAN REGIONAL CONFERENCE OF THE INTERNATIONAL COMMISSION ON IRRIGATION AND DRAINAGE. Montpellier.
- Gravalos, I., A. Georgiadis, D. Kateris, T. Gialamas, E. Bompolas, Z. Tsiropoulos, A. Avgoustis, and P. Xyradakis. 2017. An experimental simulation of moisture distribution and its uniformity within the soil profile under laboratory conditions. *Precis. Agric.* 18(1): 19–36.
- Graves, A., T. Hess, R. Matthews, and W. Stephens. 2002. Using models as tools in education and training. *In* *Crop-soil simulation models: applications in developing countries*.
- Guillard, K., and K.L. Kopp. 2004. Nitrogen Fertilizer Form and Associated Nitrate Leaching from Cool-Season Lawn Turf Vadose Zone Processes and Chemical Transport Nitrogen Fertilizer Form and Associated Nitrate Leaching from Cool-Season Lawn Turf. *J. Environ. Qual.* 33.
- Han, S., R.G. Evans, and M.W. Kroeger. 1994. Sprinkler distribution patterns in windy conditions. *Am. Soc. Agric. Eng. Soil Water Div.* 37(5): 1481–1489.
- Hanna, W., P. Raymer, B. Schwartz, J.C. Stier, B.P. Horgan, and S.A. Bonos. 2013. Warm-Season Grasses: Biology and Breeding. *In* *Turfgrass: Biology, Use, and Management*.
- Haro-Monteagudo, D., A. Daccache, and J. Knox. 2017. Exploring the utility of drought indicators to assess climate risks to agricultural productivity in a humid climate. *Hydrol. Res.*: nh2017010.
- Hartwiger, C. 2014. The Big Three of Putting Green Setup: Firmness, Slope, and Speed.
- Hatfield, J. 2017. Turfgrass and Climate Change. *Agron. J.* 109(4): 1708.
- Haydu, J., A. Hodges, and C. Hall. 2008. Estimating the economic impact of the US golf course industry: Challenges and solutions. *HortScience* 43(3): 759–763.
- Hejl, R.W., B.G. Wherley, R.H. White, J.C. Thomas, and C.H. Fontanier. 2016. Deficit Irrigation and Simulated Traffic on 'Tifway' Bermudagrass Summer Performance and Autumn Recovery. *Crop Sci.* 56(2): 809.
- Huang, B. 2008. Turfgrass Water Requirements and factors affecting water usage. p. 193–203. *In* *Water quality and quantity issues for turfgrasses in urban landscapes*. Counc. Agric. Sci. Technol., Las Vegas.
- Huang, B., M. DaCosta, and Y. Jiang. 2014. Research Advances in Mechanisms of Turfgrass Tolerance to Abiotic Stresses: From Physiology to Molecular Biology. *CRC. Crit. Rev. Plant Sci.* 33(2–3): 141–189.
- Huang, B., and H. Gao. 2000. Growth and carbohydrate metabolism of creeping bentgrass cultivars in response to increasing temperatures. *Crop Sci.* 40(4): 1115–1120.
- Huck, M.T., and D.F. Zoldoske. 2006. Achieving high efficiency in water application via overhead sprinkler irrigation. p. 223–241. *In* Beard, J.B., Kenna, M.P. (eds.), *Water quality and quantity issues for turfgrasses in urban landscapes*. Counc. Agric. Sci. Technol., Las Vegas, Nevada.
- Van Ittersum, M.K., K.G. Cassman, P. Grassini, J. Wolf, P. Tittonell, and Z. Hochman. 2013. Field Crops Research Yield gap analysis with local to global relevance—A review. *F. Crop. Res.* 143: 4–17.
- Jackson, S.H., and T.L. Estes. 2007. Comparison of leaching predictions based on PRZM3.12, LEACHP, and RZWQM98 using standard scenario modeling. *J. Agric. Food Chem.* 55(13): 5194–8.
- Jamieson, P.D., J.R. Porter, and D.R. Wilson. 1991. A test of the computer simulation model ARCWHEAT 1 on wheat crops grown in New Zealand. *F. Crop. Res.* 27: 337–350.
- Jégo, G., G. Bélanger, G.F. Tremblay, Q. Jing, and V.S. Baron. 2013. Calibration and performance evaluation of the STICS crop model for simulating timothy growth and nutritive value. *F. Crop. Res.* 151: 65–77.



- Jensen, M.E. 2007. Beyond irrigation efficiency. *Irrig. Sci.* 25(3): 233–245.
- Johnson, P.G. 2003. The Influence of Frequent or Infrequent Irrigation on Turfgrasses in the Cool-arid West. *USGA Turfgrass Environ. Res. Online* 2(6): 1–8.
- Jones, J.W., J.M. Antle, B. Basso, K.J. Boote, R.T. Conant, I. Foster, H.C.J. Godfray, M. Herrero, R.E. Howitt, S. Janssen, B.A. Keating, R. Munoz-Carpena, C.H. Porter, C. Rosenzweig, and T.R. Wheeler. 2017a. Brief history of agricultural systems modeling. *Agric. Syst.* 155: 240–254.
- Jones, J.W., J.M. Antle, B. Basso, K.J. Boote, R.T. Conant, I. Foster, H.C.J. Godfray, M. Herrero, R.E. Howitt, S. Janssen, B.A. Keating, R. Munoz-Carpena, C.H. Porter, C. Rosenzweig, and T.R. Wheeler. 2017b. Toward a new generation of agricultural system data, models, and knowledge products: State of agricultural systems science. *Agric. Syst.* 155: 269–288.
- Jones, H.G., and E. Rotenberg. 2011. Energy, Radiation and Temperature Regulation in Plants. *In* eLS. John Wiley & Sons, Ltd, Chichester, UK.
- Jordan, J.E., R.H. White, D.M. Vietor, T.C. Hale, J.C. Thomas, and M.C. Engelke. 2003. Effect of Irrigation Frequency on Turf Quality, Shoot Density, and Root Length Density of Five Bentgrass Cultivars. *Crop Sci.* 43(1): 282–287.
- Kara, T., E. Ekmekci, and M. Apan. 2008. Determining the uniformity coefficient and water distribution characteristics of some sprinklers. *Pakistan J. Biol. Sci.* 11(2): 214–219.
- Kaye, J.P., I.C. Burke, A.R. Mosier, and J. Pablo Guerschman. 2004. Methane and nitrous oxide fluxes from urban soils to the atmosphere. *Ecol. Appl.* 14(4): 975–981.
- Keller, J., and R.D. Bliesner. 1990. *Sprinkle and Trickle Irrigation*. AVI Book, New York.
- Kieffer, D.L., and M. Huck. 2008. A comparison of fairway distribution uniformity computed with catch can data and with soil moisture data from three sampling depths. p. 1–15. *In* 29th Annual Irrigation Show. Anaheim, CA.
- Kincaid, D., K. Solomon, and J.C. Oliphant. 1996. Drop size distributions for irrigation sprinklers. *Trans. ASAE* 39(3): 839–845.
- King, K.W., and J.C. Balogh. 1999. Modeling Evaluation of Alternative Management Practices and Reclaimed Water for Turfgrass Systems. *J. Environ. Qual.* 28(1): 187.
- King, B. a., T.W. Winward, and D.L. Bjorneberg. 2010. Laser precipitation monitor for measurement of drop size and velocity of moving spray-plate sprinklers. *Appl. Eng. Agric.* 26(2): 263–271.
- Kiniry, J.R., J.R. Williams, D.J. Major, R.C. Izaurralde, P.W. Gassman, M. Morrison, R. Bergentine, and R.P. Zentner. 1995. EPIC model parameters for cereal, oilseed, and forage crops in the northern Great Plains region. *Can. J. Plant Sci.* 75(3): 679–688.
- Knight, E.C., E.A. Guertal, and C.W. Wood. 2007. Mowing and Nitrogen Source Effects on Ammonia Volatilization from Turfgrass. *Crop Sci.* 47(4): 1628.
- Knox, J., A. Daccache, T. Hess, and D. Haro. 2016. Meta-analysis of climate impacts and uncertainty on crop yields in Europe. *Environ. Res. Lett.* 11(11): 1–10.
- Kohl, R.A. 1974. Drop Size Distribution from Medium-Sized Agricultural Sprinklers. *Trans. ASAE* 17(4): 0690–0693.
- KPMG. 2017. *Golf Participation Report for Europe 2017*.
- Krans, J. V., and K. Morris. 2007. Determining a Profile of Protocols and Standards used in the Visual Field Assessment of Turfgrasses: A Survey of National Turfgrass Evaluation Program-Sponsored University Scientists. *ats* 4(1).
- Kuiper, M.G. 1997. Application of current environmental research to golf course design, construction, and management practices. Available at <http://lib.dr.iastate.edu/rtd> (verified 30 April 2018).
- Kvalbein, A., and T.S. Aamlid. 2014. *Irrigation of turf on golf courses*. Scandinavian Turfgrass and Environment Research Foundation (STERF).
- Latif, M., and F. Ahmad. 2008. Operational Analysis of Water Application of a Sprinkler Irrigation System Installed in a Golf Course: Case Study. *J. Irrig. Drain. Eng.* 134(4): 446–453.
- Lee, S. 2014. Irrigation Frequency and Nitrogen Rates for Tall Fescue Growth. *Weed Turfgrass Sci.* 3(2): 130–136.
- Lee, D.J., A. Wollum, D.C. Bowman, C.H. Peacock, and T.W. Ruffy. 2001. Temperature effects on nitrogen mineralization in bermudagrass turf. *Int. Turfgrass Soc. Res. J.* 9.

- Leinauer, B., and D.A. Devitt. 2013. Irrigation Science and Technology. p. 1075–1131. *In* Stier, J.C., Horgan, B.P., Bonos, S.A. (eds.), *Turfgrass: Biology, Use, and Management*. American Society of Agronomy, Madison, WI.
- Leskys, A.M., D.A. Devitt, L.S. Verchick, R.L. Morris, and L.S. Verchick. 1999. Response of Tall Fescue to Saline Water as Influenced by Leaching Fractions and Irrigation Uniformity Distributions. *Agron. J.* 91(3): 409.
- Li, J. 1998. Modeling crop yield as affected by uniformity of sprinkler irrigation system. *Agric. Water Manag.* 38(2): 135–146.
- Li, J., and H. Kawano. 1995. Simulating water-drop movement from noncircular sprinkler nozzles. *J. Irrig. Drain. Eng.* 121(2): 152–158.
- Li, J., and H. Kawano. 1996. The area distribution of soil moisture under sprinkler irrigation. *Agric. Water Manag.* 32: 29–36.
- Li, J., H. Kawano, and K. Yu. 1994. Different Shaped Sprinkler Nozzles. 37(6): 1871–1878.
- Li, J., B. Li, and M. Rao. 2005. Spatial and temporal distributions of nitrogen and crop yield as affected by nonuniformity of sprinkler fertigation. *Agric. Water Manag.* 76: 160–180.
- Li, J., and M. Rao. 2001. Crop Yield as Affected by Uniformity of Sprinkler Irrigation System. *Agric. Eng. Int. CIGR J. Sci. Res. Dev.* III(4).
- Li, X., C. Zhu, J. Wang, and J. Yu. 2012. *Computer Simulation in Plant Breeding*.
- Mancino, C.F., W.A. Torello, and D.J. Wehner. 1988. Denitrification Losses from Kentucky Bluegrass Sod. *Agron. J.* 80(1): 148.
- Mantovani, E.C., F.J. Villalobos, F. Organ, and E. Fereres. 1995. Modelling the effects of sprinkler irrigation uniformity on crop yield. *Agric. Water Manag.* 27(3–4): 243–257.
- Marchione, V., and M. Fracchiolla. 2016. Performance of warm-season turfgrasses under different water regimes in the Mediterranean climate conditions of Southern Italy. *Ital. J. Agron.* 11(3): 158.
- Maroufpoor, E., A. Faryabi, H. Ghamarnia, and G. Yamin Moshrefi. 2010. Evaluation of Uniformity Coefficients for Sprinkler Irrigation Systems under Different Field Conditions in Kurdistan Province (Northwest of Iran). *Soil Water Res* 5(4): 139–145.
- Márquez-villagrana, C.B.H.H. 2013. Caracterización de las gotas emitidas por un aspersor de impacto de dos boquillas, aplicando técnica fotográfica. IV: 147–164.
- Mateos, L. 1998. Assessing whole-field uniformity of stationary sprinkler irrigation systems. *Irrig. Sci.* 18(2): 73–81.
- Mateos, L., E.C. Mantovani, and F.J. Villalobos. 1997. Cotton response to non-uniformity of conventional sprinkler irrigation. *Irrig. Sci.* 17(2): 47–52.
- MathWorks, I. 2014. *MATLAB and Statistics Toolbox Release 2014a*.
- Matthews, R.B. 2002. Introduction. *In* Matthews, R.B., Stephens, W. (eds.), *Crop-soil simulation models - Applications in Developing Countries*. CAB International.
- Matthews, R.B., W. Stephens, and T. Hess. 2002. Impacts of crop-soil models. *In* Matthews, R., Stephens, W. (eds.), *Crop-soil simulation models: applications in developing countries*. CABI, Wallingford.
- McCarty, L.B. 2005. *Best golf course management practices*. 2nd ed. Pearson Prentice Hall, Upper Saddle River, N.J.
- McCarty, L.B., M.F. Gregg, and J.E. Toler. 2007. Thatch and mat management in an established creeping bentgrass golf green. *Agron. J.* 99(6): 1530–1537.
- McClellan, T.A., R.E. Gaussoin, R.C. Shearman, C.S. Wortmann, M. Mamo, G.L. Horst, and D.B. Marx. 2009. Nutrient and chemical properties of aging golf course putting greens as impacted by soil depth and mat development. *HortScience* 44(2): 452–458.
- McCoy, E.L., and K.R. McCoy. 2009. Simulation of putting-green soil water dynamics: Implications for turfgrass water use. *Agric. Water Manag.* 96(3): 405–414.
- McCready, M.S., M.D. Dukes, and G.L. Miller. 2009. Water conservation potential of smart irrigation controllers on St. Augustinegrass. *Agric. Water Manag.* 96(11): 1623–1632.
- Mecham, B. 2004. Using Distribution Uniformity to Evaluate the Quality of a Sprinkler System. p. 379–386. *In* *Irrigation Association's 2004 International Irrigation Show*, Tampa, Fla. Irrigation Association.

- Meyer, J.L., and V.A. Gibeault. 1986. Turfgrass performance under reduced irrigation. *Calif. Agric.* (August): 19–20.
- Milesi, C., S.W. Running, C.D. Elvidge, J.B. Dietz, B.T. Tuttle, and R.R. Nemani. 2005. Mapping and Modeling the Biogeochemical Cycling of Turf Grasses in the United States. *Environ. Manage.* 36(3): 426–438.
- Miller, G.L., M.D. Dukes, N.D. Pressler, and N. Carolina. 2014. Golf course irrigation systems' distribution uniformity affects soil moisture variability. *Eur. J. Hortic. Sci.* 79(3): 135–141.
- Miltner, E.D., B.E. Branham, E.A. Paul, and P.E. Rieke. 1996. Leaching and Mass Balance of 15N-Labeled Urea Applied to a Kentucky Bluegrass Turf. *Crop Sci.* 36(6).
- Moeller, A. 2013. Irrigate for Playability and Turf Health , Not Color. *Green Sect. Rec.* 51(214701): 1–6.
- Molle, B., S. Tomas, M. Hendawi, and J. Granier. 2012. Evaporation and Wind Drift Losses During Sprinkler Irrigation Influenced By Droplet Size Distribution. *Irrig. Drain.* 61(2): 240–250.
- Monod, H., C. Naud, and D. Makowski. 2006. Uncertainty and sensitivity analysis for crop models. p. 55–99. *In* Wallach, D., Makowski, D., Jones, J.W. (eds.), *Working with Dynamic Crop Models*. Elsevier.
- Montazar, A., and M. Sadeghi. 2008. Effects of applied water and sprinkler irrigation uniformity on alfalfa growth and hay yield. *Agric. Water Manag.* 95(11): 1279–1287.
- Montero Martínez, J., R.S. Martínez, and J.M. Tarjuelo Martín-Benito. 2004. Analysis of water application cost with permanent set sprinkler irrigation systems. *Irrig. Sci.* 23(3): 103–110.
- Montero, J., J.M. Tarjuelo, and P. Carrión. 2001. SIRIAS: A simulation model for sprinkler irrigation. II. Calibration and validation of the model. *Irrig. Sci.* 20(2): 85–98.
- Montero, J., J.M. Tarjuelo, and P. Carrión. 2003. Sprinkler droplet size distribution measured with an optical spectropuviometer. *Irrig. Sci.* 22(2): 47–56.
- Morton, T.G., a. J. Gold, and W.M. Sullivan. 1988. Influence of Overwatering and Fertilization on Nitrogen Losses from Home Lawns. *J. Environ. Qual.* 17(1): 124–130.
- Nektarios, P.A., A.M. Petrovic, and T.S. Steenhuis. 2014. Nitrate and tracer leaching from aerated turfgrass profiles. *Eur. J. Hortic. Sci.* 79(3): 150–157.
- Nin, R.A. 2008. PhD Thesis: Tecnología Del Riego Por Aspersión Estacionario. Calibración Y Validación De Un Modelo De Simulación.
- Nocedal, J., and S.J. Wright. 2007. *Numerical Optimization* (T Milkosch, S Robinson, and S Resnick, Eds.). 2nd Editio. Springer.
- Odhiambo, L.O., W.L. Kranz, and D.E. Eisenhauer. 2011. *Irrigation Efficiency and Uniformity, and Crop Water Use Efficiency*. Univ. Nebraska: 8.
- Olmstead, S.M. 2014. *Climate change adaptation and water resource management: A review of the literature*.
- Osman, M., S. Bin Hassan, K. Bin, and W. Yusof. 2014. Soil moisture uniformity under low-pressure sprinkler irrigation system. *Adv. Rev. Sci. Res.* 3(1): 1–13.
- Ouazaa, S., J. Burguete, M.P. Paniagua, R. Salvador, and N. Zapata. 2014. Simulating water distribution patterns for fixed spray plate sprinkler using the ballistic theory. *Spanish J. Agric. Res.* 12(3): 850–864.
- Ouazaa, S., · J Burguete, · N Zapata, and J. Burguete. 2016. Solid-set sprinklers irrigation of field boundaries: experiments and modeling. *Irrig. Sci.* 34(34).
- PaceTurf. 2014. *Minimum Levels for Sustainable Nutrition Soil Guidelines*. Available at [https://www.paceturf.org/PTRI/Documents/1202\\_ref.pdf](https://www.paceturf.org/PTRI/Documents/1202_ref.pdf) (verified 21 March 2018).
- Pang, X.P., J. Letey, and L. Wu. 1997. Irrigation quantity and uniformity and nitrogen application effects on crop yield and nitrogen leaching. *Soil Sci. Soc. Am. J.* 61: 257–261.
- Paré, K., M.H. Chantigny, K. Carey, W.J. Johnston, and J. Dionne. 2006. Nitrogen Uptake and Leaching under Annual Bluegrass Ecotypes and Bentgrass Species. *Crop Sci.* 46(2): 847–853.
- Paulino-Paulino, J., E.W. Harmsen, D. Sotomayor-Ramírez, and L.E. Rivera. 2008. Nitrate leaching under different levels of irrigation for three turfgrasses in southern Puerto Rico. *J. Agric. Univ. Puerto Rico* 92(3–4): 135–152.
- Peacock, C.H., and A.E. Dudeck. 1984. Physiological Response of St. Augustinegrass to Irrigation Scheduling. *Agron. J.* 76(2): 275.
- Pereira, L.S. 1999. Higher performance through combined improvements in irrigation methods and scheduling: A discussion. *Agric. Water Manag.* 40(2–3): 153–169.

- Pereira, H., and R.C. Marques. 2017. An analytical review of irrigation efficiency measured using deterministic and stochastic models. *Agric. Water Manag.* 184: 28–35.
- Pérez-Ortolá, M., A. Daccache, T.M. Hess, and J.W. Knox. 2015. Simulating impacts of irrigation heterogeneity on onion (*Allium cepa* L.) yield in a humid climate. *Irrig. Sci.* 33(1): 1–14.
- Pérez Ortolá, M., A. Daccache, and J.W. Knox. 2016. Modeling irrigation and fertilizer use for chlorophyll production. *Grassl. Sci.* 62(2): 102–111.
- Persson, T., M. Höglind, A.-M. Gustavsson, M. Halling, L. Jauhiainen, O. Niemeläinen, G. Thorvaldsson, and P. Virkajärvi. 2014. Evaluation of the LINGRA timothy model under Nordic conditions. *F. Crop. Res.* 161: 87–97.
- Petrovic, A.M. 1990. The fate of nitrogenous fertilizers applied to turfgrass. *J. Environ. Qual.* 19(1): 1–14.
- Phan, C., A. Raheja, S. Bhandari, R.L. Green, and D. Do. 2017. A predictive model for turfgrass color and quality evaluation using deep learning and UAV imageries. *In Proc. SPIE 10218, Autonomous Air and Ground Sensing Systems for Agricultural Optimization and Phenotyping II.*
- Playán, E., R. Salvador, J.M. Faci, N. Zapata, A. Martínez-Cob, and I. Sánchez. 2005. Day and night wind drift and evaporation losses in sprinkler solid-sets and moving laterals. *Agric. Water Manag.* 76(Playán, E., R. Salvador, J.M. Faci, N. Zapata, A. Martínez-Cob, and I. Sánchez. 2005. Day and night wind drift and evaporation losses in sprinkler solid-sets and moving laterals. *Agric. Water Manag.* 76(3): 139–159.3): 139–159.
- Playán, E., N. Zapata, J.M. Faci, D. Tolosa, J.L. Lacueva, J. Pelegrín, R. Salvador, I. Sánchez, and A. Lafita. 2006. Assessing sprinkler irrigation uniformity using a ballistic simulation model. *Agric. Water Manag.* 84(1–2): 89–100.
- Popova, Z. 2006. Water, nitrogen and yield losses for a nonhomogeneous furrow set. *Irrig. Drain. Syst.* 20: 1–21.
- Poró, J., J.S. Ebdon, M. DaCosta, and P.W. Brown. 2016. Effects of Mowing Height of Cut and Nitrogen on FAO-56 PM Crop Coefficients for Recreational Turf in the Cool-Humid Region. *Crop Sci.* 57: 1–11.
- Qian, Y.L., W. Bandaranayake, W.J. Parton, B. Mecham, M. a Harivandi, and a R. Mosier. 2003. Long-term effects of clipping and nitrogen management in turfgrass on soil organic carbon and nitrogen dynamics: the CENTURY model simulation. *J. Environ. Qual.* 32: 1694–1700.
- Qian, Y.L., and M.C. Engelke. 1999. Performance of Five Turfgrasses under Linear Gradient Irrigation. *Hortscience* 34(5): 893–896.
- Qian, Y.L., and J.D. Fry. 1996. Irrigation frequency affects zoysiagrass rooting and plant water status. *HortScience* 31(2): 234–237.
- Qian, Y.L., and J.M. Fu. 2005. Response of creeping bentgrass to salinity and mowing management: Carbohydrate availability and ion accumulation. *HortScience* 40(7): 2170–2174.
- Quiroga-Garza, H.M., G.A. Picchioni, and M.D. Remmenga. 2001. Bermudagrass Fertilized with Slow-Release Nitrogen Sources. I. Nitrogen Uptake and Potential Leaching Losses. *J. Environ. Qual.* 30(2): 440–448.
- R&A. 2017. *Golf Around the World 2017.* : 22.
- R&A, and USGA. 2016. *Rules of Golf.*
- Regan, R. 1987. Irrigation practices: measuring sprinkler system application uniformity. *Ornam. northwest Arch.* 11(1): 10–12.
- Rey, D., C. Dionisio Pérez-Blanco, A. Escriba-Bou, C. Girard, and T.I.E. Veldkamp. 2018. Role of economic instruments in water allocation reform: lessons from Europe. *Int. J. Water Resour. Dev.*
- Richards, P.J., and E.K. Weatherhead. 1993. Prediction of Raingun Application Patterns in Windy Conditions. *J. Agric. Eng. Res.* 54(4): 281–291.
- Roberts, S.Z. 2015. The great debate. Irrigation efficiency vs. distribution uniformity? *Golf course Manag.:* 68–76.
- Rodríguez Díaz, J.A., J.W. Knox, and E.K. Weatherhead. 2007. Competing demands for irrigation water: golf and agriculture in Spain. *Irrig. Drain.* 56(5): 541–549.
- Rohatgi, A. 2017. WebPlotDigitizer. Available at <http://arohatgi.info/WebPlotDigitizer>.
- Romero, C.C., and M.D. Dukes. 2016. Review of Turfgrass Evapotranspiration and Crop Coefficients. *Trans. ASABE* 59(1): 207–223.
- Rossum, G. Van. 1995. Python tutorial. Available at <http://docs.python.org/tutorial/>.

- Ruelle, P., J.C. Mailhol, H. Quinones, and J. Granier. 2003. Using NIWASAVE to simulate impacts of irrigation heterogeneity on yield and nitrate leaching when using a travelling rain gun system in a shallow soil context in Charente (France). *Agric. Water Manag.* 63(1): 15–35.
- Ruget, F., S. Satger, F. Volaire, and F. Lelièvre. 2009. Modeling Tiller Density, Growth, and Yield of Mediterranean Perennial Grasslands with STICS. *Crop Sci.* 49(6): 2379.
- Sadeghi, S.-H., T. Peters, B. Shafii, M.Z. Amini, and C. Stöckle. 2017. Continuous variation of wind drift and evaporation losses under a linear move irrigation system. *Agric. Water Manag.* 182: 39–54.
- Saltelli, A., S. Tarantola, and K.P.-S. Chan. 1999. A Quantitative Model-Independent Method for Global Sensitivity Analysis of Model Output. *Technometrics* 41(1): 39–56.
- Salvador, R., C. Bautista-Capetillo, J. Burguete, N. Zapata, A. Serreta, and E. Playán. 2009. A photographic method for drop characterization in agricultural sprinklers. *Irrig. Sci.* 27(4): 307–317.
- Sanchez, I., J.M. Faci, and N. Zapata. 2011. The effects of pressure, nozzle diameter and meteorological conditions on the performance of agricultural impact sprinklers. *Agric. Water Manag.* 102(1): 13–24.
- Sanchez, I., N. Zapata, and J.M. Faci. 2010. Combined effect of technical, meteorological and agronomical factors on solid-set sprinkler irrigation: I. Irrigation performance and soil water recharge in alfalfa and maize. *Agric. Water Manag.* 97(10): 1571–1581.
- Sansoulet, J., E. Pattey, R. Kröbel, B. Grant, W. Smith, G. Jégo, R.L. Desjardins, N. Tremblay, and G. Tremblay. 2014. Comparing the performance of the STICS, DNDC, and DayCent models for predicting N uptake and biomass of spring wheat in Eastern Canada. *F. Crop. Res.* 156: 135–150.
- Seginer, I., D. Nir, and R.D. von Bernuth. 1991. Simulation of Wind-Distorted Sprinkler Patterns. *J. Irrig. Drain. Eng.* 117(2): 285–306.
- Shaddox, T.W., J.B. Unruh, and L.E. Trenholm. 2016a. Nitrate Leaching from Soluble Nitrogen Applied to 'Floritam' St. Augustinegrass and Common Centipedegrass during Dormancy. *Crop Sci.* 56(2): 837 Available at <https://dl.sciencesocieties.org/publications/cs/abstracts/56/2/837>.
- Shaddox, T.W., J.B. Unruh, L.E. Trenholm, P.C. McGroary, and J.L. Cisar. 2016b. Nitrogen rate required for acceptable St. Augustinegrass and associated nitrate leaching. *Crop Sci.* 56(1): 439–451.
- Shahba, M. a., M.S. Abbas, and S.F. Alshammary. 2014. Drought resistance strategies of seashore paspalum cultivars at different mowing heights. *HortScience* 49(2): 221–229.
- Sheikhesmaeili, O., J. Montero, and S. Laserna. 2016. Analysis of water application with semi-portable big size sprinkler irrigation systems in semi-arid areas. *Agric. Water Manag.* 163: 275–284.
- Shi, W., S. Muruganandam, and D. Bowman. 2006. Soil microbial biomass and nitrogen dynamics in a turfgrass chronosequence: A short-term response to turfgrass clipping addition. *Soil Biol. Biochem.* 38: 2032–2042.
- Shili-Touzi, I., S. De Tourdonnet, M. Launay, and T. Dore. 2010. Does intercropping winter wheat (*Triticum aestivum*) with red fescue (*Festuca rubra*) as a cover crop improve agronomic and environmental performance? A modeling approach. *F. Crop. Res.* 116(3): 218–229.
- Short, D.C., and T.D. Colmer. 2007. Development and use of a variable-speed lateral boom irrigation system to define water requirements of 11 turfgrass genotypes under field conditions. *Aust. J. Exp. Agric.* 47(1): 86–95.
- Shuman, L.M. 2001. Phosphate and Nitrate Movement Through Simulated Golf Greens. *Water. Air. Soil Pollut.* 129(1/4): 305–318.
- Shuman, L.M. 2002a. Phosphorus and Nitrate Nitrogen in Runoff Following Fertilizer Application to Turfgrass. *J. Environ. Qual.* 31(5): 1710–1715.
- Shuman, L.M. 2002b. Nutrient Leaching and Runoff from Golf Courses. *USGA Turfgrass Environ. Res. Online* 1(17): 1–9.
- Sinclair, T.R., A. Schreffler, B. Wherley, and M.D. Dukes. 2011. Irrigation frequency and amount effect on root extension during sod establishment of warm-season grasses. *HortScience* 46(8): 1202–1205.
- Sinclair, T.R., and N.G. Seligman. 1996. Crop Modeling: From Infancy to Maturity. *Agron. J.* 88(5): 698.
- Skogley, D.C.R. 1975. Velvet Bentgrass Putting Greens- Fertilizer and Topdressing Management. *USGA green Sect.*
- Smith, R.J., M.H. Gillies, G. Newell, and J.P. Foley. 2008. A decision support model for travelling gun irrigation machines. *Biosyst. Eng.* 100(1): 126–136.
- Soldat, D.J., B. Lowery, and W.R. Kussow. 2010. Surfactants Increase Uniformity of Soil Water Content and

- Reduce Water Repellency on Sand-Based Golf Putting Greens. *Soil Sci.* 175(3): 111–117.
- Stambouli, T., N. Zapata, and J.M. Faci. 2014. Performance of new agricultural impact sprinkler fitted with plastic nozzles. *Biosyst. Eng.* 118: 39–51.
- Stanhill, G. 1969. A Simple Instrument for the Field Measurement of Turbulent Diffusion Flux. *J. Appl. Meteorol.* 8(4): 509–513.
- Steduto, P., T.C. Hsiao, D. Raes, and E. Fereres. 2009. AquaCrop—The FAO Crop Model to Simulate Yield Response to Water: I. Concepts and Underlying Principles. *Agron. J.* 101(3): 426.
- Stier, J.C., K. Steinke, E.H. Ervin, F.R. Higginson, P.E. McMaugh, J.C. Stier, B.P. Horgan, and S.A. Bonos. 2013. Turfgrass Benefits and Issues. p. 105–145. *In* Stier, J.C., Horgan, B.P., Bonos, S.A. (eds.), *Turfgrass: Biology, Use, and Management*. American Society of Agronomy, Madison, WI.
- Strandberg, M., K. Blomba, A.M.D. Jensen, and J.W. Knox. 2012. Priorities for sustainable turfgrass management : a research and industry perspective. *Soil Plant Sci.* 62(March): 3–9.
- Su, K., D.J. Bremer, S.J. Keeley, and J.D. Fry. 2007. Effects of High Temperature and Drought on a Hybrid Bluegrass Compared with Kentucky Bluegrass and Tall Fescue. *Crop Sci.* 47(5): 2152–2161.
- Su, K., D.J. Bremer, S.J. Keeley, and J.D. Fry. 2009. Mowing and Drought Effects on a Hybrid Bluegrass compared with a Kentucky Bluegrass. *Interational Turfgrass Soc. Res. J.* 11: 871–882.
- Tanner, C.B., and W.L. Pelton. 1960. Potential evapotranspiration estimates by the approximate energy balance method of Penman. *J. Geophys. Res.* 65(10): 3391–3413.
- Tarjuelo, J.M. 2005. *El Riego por Aspersión y su Tecnología*. Mundi-Prensa S.A, Madrid, Spain.
- Tarjuelo, J.M., P. Carrión, and M. Valiente. 1994. Simulación de la distribución del riego por aspersión en condiciones de viento. *Investig. Agrar. Prod. y protección Veg.* 9(2): 255–271.
- Tarjuelo, J.M., M.V. Gómez, and J.L. Pardo. 1992. Working Conditions of Sprinkler to Optimize Application of Water. *J. Irrig. Drain. Eng.* 118(6): 895–913.
- Tarjuelo, J.M., J. Montero, F.T. Honrubia, and M.A. Calvo. 1999a. Irrigation Uniformity with Medium Size Sprinklers Part II: Influence of Wind and Other Factors on Water Distribution. *Am. Soc. Agric. Eng. Soil Water Div.* 42(3): 677–689.
- Tarjuelo, J., J. Montero, F.. Honrubia, J.. Ortiz, and J.. Ortega. 1999b. Analysis of uniformity of sprinkler irrigation in a semi-arid area. *Agric. Water Manag.* 40(2–3): 315–331.
- Telenko, D.E.P., T.W. Shaddox, J.B. Unruh, and L.E. Trenholm. 2015. Nitrate Leaching, Turf Quality, and Growth Rate of 'Floritam' St. Augustinegrass and Common Centipedegrass. *Crop Sci.* 55(3): 1320–1328.
- The MathWorks Inc. 2010. MATLAB and statistics toolbox, Release 2010b [computer software].
- Trenholm, L.E., J.B. Unruh, and J.B. Sartain. 2012. Nitrate Leaching and Turf Quality in Established 'Floritam' St. Augustinegrass and 'Empire' Zoysiagrass. *J. Environ. Qual.* 41(3): 793–799.
- Turgeon, A.J. 2008. *Turfgrass Management* (J Jones-Renger, Ed.). Pearson Prentice Hall, Upper Saddle River, New Jersey.
- USDA. 2006. *Irrigation Water Management - Conservation practice standard*.
- USEPA. 2018. Basic Information about Nitrate in Drinking Water. Available at <http://water.epa.gov/drink/contaminants/basicinformation/nitrate.cfm>.
- USGA. 2004. *USGA Recommendations For a Method of Putting Green Construction*. : 1–11.
- USGA. 2018. *Glossary of Golf Turfgrass Terms (T-W)*. Available at <https://www.usga.org/course-care/glossary-of-golf-turfgrass-terms-ac-222efb41.html> (verified 23 May 2018).
- Vargas, J.M. 1993. *Management of Turfgrass Diseases*, Second Edition.
- Vega, P.M., and L.C. Hermosin. 2014. *Auditoria de riego en campos de golf* (I Editorial, Ed.).
- Vories, E.D., and R.D. von Bernuth. 1986. Single nozzle sprinkler performance in wind. *Trans. ASABE* 29(5): 1325–1330.
- Vories, E.D., R.D. von Bernuth, and R.H. Mickelson. 1987. Simulating Sprinkler Performance in Wind. *J. Irrig. Drain. Eng.* 113(1): 119–130.
- Wallach, D., S. Buis, P. Lecharpentier, J. Bourges, P. Clastre, M. Launay, J.E. Bergez, M. Guerif, J. Soudais, and E. Justes. 2011. A package of parameter estimation methods and implementation for the STICS crop-soil model. *Environ. Model. Softw.* 26(4): 386–394.

- Wallach, D., B. Goffinet, J.-E. Bergez, P. Debaeke, D. Leenhardt, and J.-N. Aubertot. 2001. Parameter Estimation for Crop Models: A New Approach and Application to a Corn Model. *Agron. J.* 93(4): 757.
- Wallach, D., D. Makowski, J.W. Jones, and F. Brun. 2006. Working with dynamic crop models (D Wallach, D Makowski, and JW Jones, Eds.). First. Elsevier.
- Wang, W., D. Haver, and D.E. Pataki. 2014. Nitrogen budgets of urban lawns under three different management regimes in southern California. *Biogeochemistry* 121(1): 127–148.
- Wherley, B. 2011. Turfgrass Growth, Quality, and Reflective Heat Load in Response to Deficit Irrigation Practices. *In* Labeledzki, L. (ed.), *Evapotranspiration*. InTech.
- Wherley, B.G., W. Shi, D.C. Bowman, and T.W. Ruffy. 2009. Fate of N-Nitrate Applied to a Bermudagrass System: Assimilation Profiles in Different Seasons. *Crop Sci.* 49(6): 2291.
- Wilkerson, G.G., G.S. Buol, Z. Yang, C. Peacock, M.S. McCreedy, K. Steinke, and D. Chalmers. 2015. Modeling Response of Warm-Season Turfgrass to Drought and Irrigation. *Agron. J.* 107(2): 515.
- Woods, M. 2013. Using temperature to predict turfgrass growth potential (GP) and to estimate turfgrass nitrogen use.
- Woods, M. 2016. A Short Grammar of Greenkeeping. : 1–46.
- Woods, M.S., L.J. Stowell, W.D. Gelernter, and M. Woods. 2016. Minimum soil nutrient guidelines for turfgrass developed from Mehlich 3 soil test. Available at <https://peerj.com/preprints/2144.pdf> (verified 26 February 2018).
- De Wrachien, D., and G. Lorenzini. 2006. Modelling Jet Flow and Losses in Sprinkler Irrigation: Overview and Perspective of a New Approach. *Biosyst. Eng.* 94(2): 297–309.
- Wu, L., R. Green, G. Klein, J.S. Hartin, and D.W. Burger. 2010. Nitrogen Source and Rate Influence on Tall Fescue Quality and Nitrate Leaching in a Southern California Lawn. *Agron. J.* 102(1): 31–38.
- Wu, L., R. Green, M. V. Yates, P. Pacheco, and G. Klein. 2007. Nitrate Leaching in Overseeded Bermudagrass Fairways. *Crop Sci.* 47(6): 2521–2528.
- Yacoubi, S., K. Zayani, A. Slatni, and E. Playán. 2012. Assessing Sprinkler Irrigation Performance Using Field Evaluations at the Medjerda Lower Valley of Tunisia. *Engineering* 04(10): 682–691.
- Yacoubi, S., K. Zayani, N. Zapata, A. Zairi, A. Slatni, R. Salvador, and E. Playán. 2010. Day and night time sprinkler irrigated tomato: Irrigation performance and crop yield. *Biosyst. Eng.* 107(1): 25–35.
- Yan, H.J., G. Bai, J.Q. He, and Y.J. Li. 2010. Model of droplet dynamics and evaporation for sprinkler irrigation. *Biosyst. Eng.* 106(4): 440–447.
- Zapata, N., R. Salvador, J. Cavero, S. Lecina, C. López, N. Mantero, R. Anadón, and E. Playán. 2013. Field test of an automatic controller for solid-set sprinkler irrigation. *Irrig. Sci.* 31(5): 1237–1249.
- Zhang, Y. 2012. SIMULATED CARBON AND NITROGEN DYNAMICS IN TURFGRASS SYSTEMS USING THE DAYCENT MODEL Submitted (Intergovernmental Panel on Climate Change, Ed.).
- Zhang, L., G.P. Merkle, and K. Pinthong. 2013a. Assessing whole-field sprinkler irrigation application uniformity. *Irrig. Sci.* 31(2): 87–105.
- Zhang, Y., Y. Qian, B. Mecham, and W.J. Parton. 2013b. Development of Best Turfgrass Management Practices Using the DAYCENT Model. *Agron. J.* 105(4): 1151.
- Zocoler, Orsi, Lima, and Rodrigues. 2013. Variação entre a lâmina de irrigação aplicada e armazenada no solo sob condições de irrigação com baixa uniformidade de distribuição de água. *Irriga* 18(1): 171–183.





## **ANNEXES**

**Annex 1.** Survey of golf course irrigation management practices in four Nordic countries

**Annex 2.** Summary of irrigation system performance assessment in three golf courses

**Annex 3.** Results from single sprinkler field tests

**Annex 4.** STICS model parameters for turfgrass simulation

